Improved satiety signalling in obesity with a novel combination treatment of *Caralluma fimbriata* Extract and Lorcaserin

by

VENKATA BALA SAI CHAITANYA THUNUGUNTLA

In fulfilment for the award of

DOCTOR OF PHILOSOPHY

College of Health and Biomedicine

(Specialisation: Neuroscience)

Institute of Health and Sport

VU Research

December 2022

Abstract:

Being overweight and obese are risk factors for multiple chronic diseases, including hypertension, type II diabetes mellitus, and cardiovascular diseases. These factors drive the development of new treatments to control obesity. The regulation of food appetite is a critical element of energy balance in obese people. Hypothalamic neurons of the brain region play a crucial role in balancing hunger and satiety for an individual. The hypothalamus's arcuate nucleus (ARC) contains Proopiomelanocortin (POMC) neurons that mediate food satiety signalling. They express one of the serotonin receptors called 5HT2cR, which binds to the ligand serotonin to activate satiety signalling through the anorexigenic pathway. Hence, the 5HT2cR is proposed as one of the potential targets for regulating obesity and overeating disorders. Several agonists have been developed to increase the functional activity of 5HT2cR and further enhance satiety signalling. This satiety signalling is dysregulated in overeating diseases like Prader-Willi syndrome and Bardet–Biedl syndrome. Studies have shown that a succulent plant, *Caralluma fimbriata* extract (CFE), can reduce body weight and waist circumference. In addition, preliminary data on modified fibroblasts (3T3 cells) showed that CFE increased expression of the full-length 5HT2cR mRNA compared to the truncated/non-functional variant. However, the mechanism through which CFE reduces obesity remains undefined. The FDA approved the 5HT2cR-specific agonist Lorcaserin to treat obesity in 2012. However, the drug Lorcaserin has limited use for the long-term treatment of obesity due to concerns about side effects and it was withdrawn from sale in the USA in 2020.

The current study aims to investigate whether the combination of CFE and a lower dose of lorcaserin can increase 5HT2cR activation and reduce diet-induced obesity. The CFE is predicted to increase 5HT2cR expression, thereby increasing satiety signalling when activated by the specific agonist lorcaserin. The study comprises three phases; the first phase involved human SHSY5Y neuroblast cell culture as a model to study 5HT2cR expression studies in response to treatment with CFE. The treatment was carried out for 48h and 96h duration with different concentrations of CFE. In addition, these SHSY5Y cells can be differentiated from fibroblasts to mature neurons. These differentiated neurons retain the property of expressing 5HT2cR. Therefore, these neurons were treated with CFE for 48h and 96h with different concentrations (ranging from 0.1 to 50 µg /mL) of CFE. The treated cells were analysed for differential gene expression studies, including full-length (functional) and truncated 5HT2cR

expression by quantitative PCR and pilot-scale next-generation sequencing (NGS) for further metabolic analysis. The results showed a significant two-fold increase in the expression level of the 5HT2cR functional receptor in CFE-treated neurons at 25 µg /mL (1.87-fold at 48h and 2.41-fold at 96h of CFE treatments with p value 0.01 and 0.03 respectively) and at 50 µg /mL (2.84-fold at 48h and 2.54-fold at 96h of treatments with p values <0.001 and 0.02 respectively) concentrations, respectively. These results encouraged follow-up of the changes in metabolic pathways in the presence of CFE-treated neurons. The whole transcriptome analysis revealed anorexigenic genes like PCSK1 and BDNF, and 5HT2cR were upregulated. In contrast, orexigenic genes like NPY and NPY2R were down regulated. In addition, the longer (96h) CFE treatment showed a greater increase in functional 5HT2cR expression in qPCR and transcriptome analysis.

The second phase investigated the effect of combined CFE and Lorcaserin treatment in a high-fat diet (HFD) -induced obese mouse model. The study measured physiological parameters, including food and water intake and body weight changes. Since 5HT2cR activation also influences mood and behaviour, the current study included observations of behavioural changes in anxiety, depression, and exploration parameters. The six-week-old mice were housed at standard facility conditions and fed a HFD for eight weeks to induce obesity. The animal groups were divided as control diet, HFD, HFD with CFE (100mg/kg/day) treatment, HFD with Lorcaserin (5mg/kg/day), and HFD with CFE and Lorcaserin (combination: CFE+LOR) for eight weeks of treatment. The animals were measured weekly for food and water intake and body weight. The treatments of hydroethanolic extract of CFE (100mg/kg body weight (bwt) /day) and Lorcaserin (5mg/kg bwt/day) were mixed in a jelly form and given at a weight below 10% of the daily food intake of the mice. In the CFE+LOR-treated group of mice, the results showed a reduction of anxiety and depression parameters to the normal range compared to the HFD group. The explorative behaviour in the y-maze test didn't show significant variation in any parameters. The food intake was trended down in CFE and CFE+LOR groups compared to the HFD group; however, the data was not significant. On the other hand, the HFD group significantly decreased water intake compared to CFE+LOR treated group.

The animal study also measured energy expenditure by indirect calorimetry and body fat composition with EchoMRI for all the groups. The analysis revealed fat content decreased significantly in CFE and CFE+LOR treatment groups compared to the HFD group. The

Promethion indirect calorimetry and locomotor activity system was used for three days to determine energy expenditure. There was a significant increase in the overall energy expenditure of treated groups compared to HFD. The sleep cycle and daily walking percentage also improved significantly in CFE+LOR-treated mice compared to HFD and LOR-treated mice. Overall, CFE and CFE+LOR treatments protected the animals against HFD exposure and reduced body weight gain and fat deposition. The water intake during the dark cycle was significantly more in CFE and CFE+LOR groups than in HFD mice. Even though the CFE treatment group showed reduced weight gain and fat deposition, the CFE+LOR group showed better resistance to HFD. On the other hand, the LOR treatment alone did not significantly alter weight gain. In addition, obesity-related comorbidities include an increased risk of vascular endothelial dysfunction. Functional analysis of the abdominal aortic rings showed that all the treatments improved the vasodilatory response in HFD-fed mice.

In conclusion, the study used a novel combination therapy consisting of CFE and a relatively low dose of Lorcaserin to reduce food appetite and obesity. The CFE was able to increase the functional 5HT2cR expression in SHSY5Y-neurons. In HFD-induced mice, CFE and CFE+LOR treatments showed reduced food intake compared to the HFD group. In addition, the behavioural data showed reduced anxiety and depression parameters in the presence of CFE+LOR treatments compared to individual treatments of CFE or LOR alone. The study summarises that CFE alone and CFE with a low dose of Lorcaserin can reduce obesity and improve parameters of mood and vascular function in an HFD-induced model of obesity. Further research is required to confirm if this combination approach will be a potential therapy for obesity and overeating diseases with a lowered risk of possible side effects compared to Lorcaserin alone.

Doctor of Philosophy Declaration

"I, Venkata Bala Sai Chaitanya Thunuguntla, declare that the PhD thesis entitled [title of thesis] is no more than 80,000 words in length including quotes and exclusive of tables, figures, appendices, bibliography, references, and footnotes. This thesis contains no material that has been submitted previously, in whole or in part, for the award of any other academic degree or diploma. Except where otherwise indicated, this thesis is my own work". "I have conducted my research in alignment with the Australian Code for the Responsible Conduct of Research and Victoria University's Higher Degree by Research Policy and Procedures.

Date: 15-DEC-2022

ACKNOWLEDGEMENTS

It is my pleasure to mention my regards to many people who have supported me throughout the time to complete my PhD thesis. I want to start by thanking Dr Maharshi, who encouraged me to apply for a PhD scholarship VUIPRS. Then, I want to thank Prof. Jayakumar Singh, who has inspired me to undertake research activities from my undergrad time. Finally, I extend my special thanks to Prof. Prasunpriya Nayak, who trained me in animal handling and created an interest in animal behavioural studies during my master's degree.

I thank all the mentors and research colleagues Sadia, Danielle, Laura, Lauren and Kristen from Victoria University. A special thanks to all the animal facility and biosafety staff, Anne Luxford, Kelly Wilson, Stacey Lloyd and Steven Holloway (AWO), for their support and for treating me like a member of the family. I would like to convey my gratitude to Victoria University facilitates for allowing me to conduct all the cell culture and animal experiments. My special thanks to Danielle Debruin for training me in Echo-MRI, Promethion and other animal handling techniques. Finally, I would like to acknowledge Anthony Zuli's group members (Laura Gadanec and Kristen McSweeney) for their support in completing the isometric tension analysis for mouse abdominal aortic rings and Lauren Sahakian for her efforts to finish the gut motility experiments.

My PhD journey would not have been successful without my supervisors, Prof. Michael Mathai and Assoc. Prof. Puspha Sinnayah. I want to thank Puspha for her support during animal behaviour training and for giving me an opportunity to attain teaching experience. I can only express my gratitude to Michael Mathai because I don't have words to express my appreciation. I also would like to extend my thanks to my PhD panel members, Prof Andrew McAinch, Vasso Apostolopoulos and Aaron Peterson, for their suggestions and intellectual discussions during review meetings.

This acknowledgement never completes without mentioning special people, who are the world to me. My mother, Rajya Lakshmi and father, Madhusudhana Rao. Thanks, mom and dad, for showing faith, giving me the liberty to choose what I desire, and filling me with confidence and self-belief through your wonderful upbringing. I have a tough competitor in my own house, my brother Rahul who is also finishing his PhD soon, an excellent companion and partner in

crime. Missing them for the last four years due to my work busy and travel restrictions hope to see you, people, soon.

I want to dedicate my PhD thesis work to my family members, my guide Michael, and my Aussie mom Anne.

List of Abbreviations

2−ΔΔCT	Double-delta Ct
2OG	2-oxoglutarate
5HT	5-hydroxytryptamine
5HT2cR	5-hydroxytryptamine receptor 2C
7-TM	Seven-transmembrane
9-THC	Δ 9-tetrahydrocannabinoid
AA	Amino acid
ACTH	Adrenocorticotrophin
ADAR	Adenosine deaminase acting on RNA
ADCY 3	Adenylate cyclase 3
ADRB3	B-3 adrenergic receptor
AGRP	Agouti-related protein
AMRI	Albany molecular research inc.
ANOVA	Analysis of Variance
ARC	Arcuate nucleus
ARC	Animal supply recourse centre
ARC	Arcuate nucleus
ARID5B	At-rich interaction domain 5
ATP	Adenosine tri-phosphate
BAT	Brown adipose tissue
BDNF	Brain-derived neurotrophic factor
BLOOM	Behavioural Modification and Lorcaserin for Overweight and Obesity Management
BMI	Body mass index
BMR	Basal metabolic rate
CADM 1	Cell adhesion molecule 1
CADM 2	Cell adhesion molecule 2
cAMP	Cyclic adenosine monophosphate
CART	Cocaine-and amphetamine-Regulated transcript
CCK	Cholecystokinin
CFE	*Caralluma fimbriata* extract

CGRP	Calcitonin gene-related peptide
ChR2	Channelrhodopsin-2
CLIP	Corticotropin-Like Intermediate lobe Peptide
CNS	Central nervous system
CRH	Corticotropin-releasing hormone
Ct	Cycle threshold
CVD	Cardiovascular disease
DA	Dopamine
DEPC	Diethyl pyro carbonate
DF 1	Differentiation media 1
DF 2	Differentiation media 2
DGAT	Diacylglycerol transferase
DIO	Diet induced obesity
DM	Diabetes mellitus
DPP-4	Dipeptidyl peptidase-4
DSBH	Double-Stranded β--Helix
EC	Endocannabinoid
ECM	Extracellular matrix
EMO	Emodin
EOSS	Edmonton obesity staging system
EPM	Elevated plus maze
ER	Endoplasmic reticulum
FDA	Food and Drug Administration
FGF21	Fibroblast growth factor 21
FMRI	Functional magnetic resonance imaging
FST	Forced swim test
FTO	Fat mass Obesity associated
GABA	Gamma-aminobutyric acid
GHSR	Ghrelin's secretagogue receptors
GIP	Glucose-dependent Insulinotropic Polypeptide
GLP-1	Glucagon-like peptide-1
GnRH	Gonadotropin-releasing hormone
GOAT	Ghrelin O-acyltransferase

GPCRs	G-protein coupled receptor
HFD	High-fat diet
Hhcy	Hyper-homocysteinemia
HPA	Hypothalamic Pituitary Adrenal axis
IAPP	Islet amyloid polypeptide
IP 6	Inositol hexa-his-phosphate
Irx3	Iroquois homeobox 3
Irx5	Iroquois homeobox 5
KSR 2	Kinase Suppressor of Ras 2
LDL-C	Low-density lipoprotein
LEP	Leptin
LEPR	Leptin receptors
LH	Lateral hypothalamus
MC3R	Melanocortin-3-receptor
MC4R	Melanocortin-4-receptor
MCH	Melanin-concentrating hormone
mCPP	Meta-chlorophenyl-piperazine
MCRs	Melanocortin receptors
MRAP2	Melanocortin-2-receptor Accessory Protein 2
mRNA	Messenger Ribonucleic acid
MSH	Melanocyte-stimulating hormone
NAc	Nucleus accumbens
NAFLD	Non-alcoholic fatty liver disease
NCBI	National centre for biotechnology information
NEGR 1	Neuronal growth regulator 1
NPY	Neuropeptide Y
NRP2	Neuropilin 2
NTRK 2	Neurotrophic receptor tyrosine kinase 2
NTS	Nucleus tractus solitarius
OFC	Orbitofrontal cortex's
PCR	Polymerase chain reaction
PCs	Prohormone convertases
PCSK 1	Proprotein convertase subtilisin/kexin type 1

PHIP 1	Pleckstrin homology domain interacting protein
PKC	Protein kinase-c
PLC	Phospholipase C
POMC	Pro-opiomelanocortin
PPAR	Peroxisome proliferator-activated receptor
PVN	Paraventricular Nucleus of the Hypothalamus
PWS	Prader Willi syndrome
PWS	Prader-will syndrome
PYY	Pancreatic peptide YY
REE	Resting energy expenditure
RIN	RNA integrity number
RYGB	Roux-en-Y gastric bypass technique
SCT	Secretin
SCTR	Secretin receptor
SEMA 3	Semaphorin 3
SEMA 3A	Semaphorin 3 A
SERCA	Sarcoplasmic reticulum Ca^{2+}-atpase
SIM 1	Single minded homolog 1
SSRIs	Selective-serotonin reuptake inhibitors
T2D	Type 2 diabetes
TMEM	Transmembrane protein 18
TrkB	Tropomyosin receptor kinase B
TST	Tail suspension test
UCP	Uncoupling proteins
VMN	Ventromedial Nucleus
VTA	Ventral tegmental area
WAT	White adipose tissue
WHO	World Health organization
α- MSH	Alpha-Melanocyte-Stimulating Hormone

Table of Contents

Chapter 1 Literature review **1**

1.1. Genetic modulators and Obesity: 5

1.2. Leptin-Melanocortin pathway 6
1.2.1 AgRP and NPY 9
1.2.2 Ghrelin 10
1.2.3 Secretin 11
1.2.4 FTO (fat mass and obesity-associated) 11
1.2.5 NEGR1 12
1.2.6 ADCY3 13
1.2.7 TUB gene 13
1.2.8 5HT2cR 13
1.2.9 ADRB3 14
1.2.10 Pancreatic lipase 14
1.2.11 Adrenoceptor 15
1.2.12 UCP genes 15
1.2.13 DGAT 15
1.2.14 Amylin 16
1.2.15 PPAR 16

1.3 Obesity- drug development: 17

1.4 Obesity and energy expenditure: 24

1.5 Importance of 5HT2cR in satiety: 35

1.6 Behavioural changes with high calorie intake and 5HT2cR obligation: 41

1.7 Obesity and consequences in cardiac dysfunction: 45

1.8 *Caralluma fimbriata* extract (CFE) as anti-Obesity treatment 47

1.9 Significance of the Study: 52

Chapter 2 Materials and Methods **54**

2.1. Human SHSY5Y cell culture study: 55
2.1.1. SHSY5Y cell culturing: 55
2.1.2. CFE treatment to undifferentiated SHSY5Y cells: 56

2.2. Human SHSY5Y derived neuronal study: 57
2.2.1. SHSY5Y cell Differentiation to Neurons: 57
2.2.2. CFE treatment: 59

2.3. RNA Analysis 59
2.3.1. RNA Extraction 59
2.3.2. RNA Quantification 60
2.3.3. Reverse transcription of RNA samples 61
2.3.4. Primer sequences 61
2.3.5. Quantitative real-time PCR (qPCR) 62
2.3.6. Gel electrophoresis 63

2.4. Next Generation Sequencing 63
2.4.1. RNA preparation and quality check 63
2.4.2. Brief description of NGS conditions 63

2.5. High fat-induced mouse model 63
2.5.1. Parameters monitored during treatment 66
2.5.1.1. Body weight, Food, and water consumption 66
2.5.1.2. Jelly dosage 66
2.5.1.3. Echo Magnetic Resonance Imaging (Echo-MRI) 67
2.5.2. Energy expenditure by Promethion cage monitoring 68

2.5.3. Animal behavioural studies.....69
2.5.3.1. Measuring Anxiety with Elevated Plus Maze and Light and Dark box analysis.....69
2.5.3.2. Measuring Exploration behaviour by Open field and Y-maze experiments.....69
2.5.3.3. Measuring Depression with Tail Suspension and Force Swim test.....70
2.5.3.4. Quantification of behavioural parameters with Cleversys software tool.....70
2.5.4. Anaesthesia, tissue collection, and storage.....70
2.6. Statistical analysis:.....71

Chapter 3 CFE induced 5HT2cR expression in SHSY5Y derived neurons.....72

3.1 Abstract.....73

3.2 Introduction.....74

3.3 Methods.....78
RNA isolation for sequencing:.....78
Next-generation sequencing.....78
NGS analysis.....79

3.4 Results and Discussion.....80
3.4.1 CFE influence on undifferentiated SHSY5Y cells.....80
3.4.2 Differentiated SHSY5Y neuronal cells.....81

Outcomes of the study.....101

3.5 Conclusion.....102

Chapter 4 Food and water intake rate and behaviour response in CFE and Lorcaserin treated high-fat diet mice model.....103

4.1 Abstract.....104

4.2 Introduction.....105

4.3 Materials and methods:.....107
4.3.1 Animal food, water, and body weight measurement:.....107
4.3.2 Behavioural Experiments:.....108
4.3.4 Exploration behaviour:.....108
4.3.5 Open field analysis:.....108
4.3.6 Y-maze analysis:.....109
4.3.7 Anxiety and depression assessment:.....109
4.3.8 Elevated plus maze (EPM):.....109
4.3.9 Light and dark box analysis (LDB):.....110
4.3.10 Tail suspension test (TST):.....110
4.3.11 Forced swim test (FST):.....110
4.3.12 CleverSys tool conditions:.....110
4.3.13 Statistical analysis:.....111

4.4 Results and Discussion:.....111
4.4.1 Effect of CFE and Lorcaserin on body weight, food, and water intake:.....111
4.4.2 The effect of CFE and Lorcaserin on behavioural changes:.....118
4.4.3 Anxiety-like behaviour alteration assessment:.....121
4.4.4 Depression-like behaviour analysis:.....125

Outcomes of the study:.....128

4.5 Conclusion:.....128

Chapter 5 Effect of CFE and Lorcaserin on energy expenditure and vascular dysfunction in a high-fat diet-induced mice model of obesity.....129

5.1 Abstract:.....130

5.2 Introduction:.....131

5.3 Materials and Methods:.....134
5.3.1 Body composition analysis:.....134

5.3.2 Promethion cage monitoring:.....135
5.3.3 Isometric tension analysis:.....138
5.3.4 Statistical analysis:.....139
5.4 Results and Discussion:.....139
Outcomes of the study:.....153
5.5 Conclusion:.....153
Chapter 6 Overall Summary.....154
Future directions and limitations of the current study:.....158
Chapter 7 References.....160

List of Tables

Table 1.1: Body mass index range for obesity condition(Guo et al., 2016) 2
Table 1.2: Obesity staging system adopted from (Bessell et al., 2021) 3
Table 1.3: Genes associated in early-onset and severe obesity modified from (Loos and Yeo, 2021) 9
Table 1.4: Weigh loss drugs available for treatment (Daneschvar et al., 2016) 18
Table 1.5: Potential compounds for obesity treatment that can regulate appetite through AgRP and POMC neurons.. 20
Table 2.1: Selected human genes and primers, Syp38: Synaptic vesicle protein 38, GAP43: growth-associated protein 43, Akt1: Protein kinase, 5Ht2cR: serotonin receptor 2c, ExonVb: exon Vb sequence of 5Ht2cR. 61
Table 3.1: Lane and Band Volume/intensity analysis from Chemidoc™ MP of gel images of PCR products from CFE treated SHSY5Y neurons. Where, fn: functional and tr: truncated 5HT2cR. 84
Table 4.1: Bodyweight measurements during 16weeks of the study. 117

List of Figures

Figure 1.1: Schematic representation of fundamental differences in Monogenic and Polygenic Obesity classification inspired from (Loos and Yeo, 2021) 4
Figure 1.2: Different systemic factors influencing energy homeostasis (Theilade et al., 2021) 26
Figure 1.3: Conceptual representation of hypothalamic circuits in energy balance 31
Figure 1.4: Functional aspects of AgRP and POMC neurons involved (Heksch et al., 2017) 32
Figure 1.5: Schematic representation of 5HT2cR localisation and pivotal role in POMC neurons, inspired from (Stamm et al., 2017) 33
Figure 1.6: The complementary sequence of SNORD115 binding to 5HT2cR pre-mRNA in functional 5HT2cR expression, the absence of SNORD115 binding to pre-mRNA leads to lack of exon VI region and forms the truncated 5HT2cR protein (Stamm et al., 2017) 38
Figure 2.1: The illustration describes methodology according to chapter significance 55
Figure 2.2: Description of SHSY5Y cells for 5HT2cR expression with CFE treatment 55
Figure 2.3: Workflow for SHSY5Y cells treatment with CFE 56
Figure 2.4: Schematic representation of SHSY5Y differentiation media composition. Where, RA: retinoic acid, antibiotics are penicillin and streptomycin, KCl: potassium chloride, BDNF: brain-derived neurotrophic factor. 58
Figure 2.5: Microscopic visualisation (Labomed-TCM400) of SHSY5Y-derived neurons from SHSY5Y neuroblasts and at (A) 4X, (B) 20X, and (C) 40X lenses. 58
Figure 2.6: CFE treatment workflow for SHSY5Y-derived neurons 59
Figure 2.7: Schematic representation of Total RNA isolation by TRIzol extraction protocol 60
Figure 2.8: Schematic representation of principle behind Polymerase chain reaction (PCR), where (A) Reverse transcription PCR: RNA translated into cDNA copies and (B) Quantitative analysis of the desired gene of expression by qPCR assay. 62
Figure 2.9: The brief description of rodent high fat diet and control diet composition details 64
Figure 2.10: Schematic representation of animal groups with special diet induction and treatment time points 65
Figure 2.11: Schematic representation of animal study flow 65
Figure 2.12: Schematic representation of animal study flow 66
Figure 2.13: Jelly dose treatment to individual mice 67
Figure 2.14: Overview of Promethion cage monitoring system 68
Figure 3.1: The editing variants of 5HT2cR. 76
Figure 3.2: Schematic representation of the workflow for whole transcriptome analysis steps (Adilijiang et al., 2019) 79
Figure 3.3: CFE induced 5HT2cR expression visualisation from qPCR products of undifferentiated SHSY5Y cells on agarose gel: The 5HT2cR expression in both functional (at 400bp) and truncated (at 300bp) isoforms, (A) 48h and (B) 96h of the treatment period. Where L represents 100bp DNA ladder and concentrations of CFE represented over each lane representing from 0 to 50 in mg/mL. 81
Figure 3.4: The SHSY5Y derived neurons during CFE treatment: all the pictures were captured with a regular inverted microscope (Labomed-TCM400) available in the lab. The images represented are at 400x zoom. 81
Figure 3.5: CFE induced serotonin receptor expression: 5HT2cR expression in SHSY5Y neurons after (A) 48h and (B) 96h of CFE treatment; The exon Vb region (present in functional and lacks for truncated 5HT2cR) quantified after (A) 48h and (B) 96h of CFE treatment. The data represented the Mean ± SEM with n = 3 replicates from individual wells. 82
Figure 3.6: The qPCR run for Exon Vb region between control and CFE treatment 83
Figure 3.7: CFE induced 5HT2cR expression in SHSY5Y derived neurons after 48 h of treatment: The qPCR derived products were used to visualise (A) The 5HT2cR expression in both functional (at 400bp) and truncated (at 300bp) isoforms, (B) Exon Vb (at 140bp) region-specific to functional 5HT2cR visualisation at 140bp by agarose gel electrophoresis with SYBER green staining. 83
Figure 3.8: CFE induced 5HT2cR expression in SHSY5Y derived neurons after 96 h of treatment: (A) The visualisation of 5HT2cR expression levels in both functional (at 400bp) and truncated isoform (at 300bp), (B) Exon Vb (at 140bp) region-specific to functional 5HT2cR visualisation at 140bp band length on the gel. 84
Figure 3.9: Representation of Unedited and fully edited amino acid residues at 16, 158 and 160 positions of exon V region in 5HT2cR. 85

Figure 3.10: Next-generation sequencing of SHSY5Y neurons: (A) RNA intactness for NGS analysis (gel image shows 18s and 28s rRNA consistency), (B) Volcano plot of differentially-expressed genes identified between control and CFE-treated SHSY5Y neurons after 48h of treatment, (C) Volcano plot between control and CFE treated neurons after 96 h of treatment and (D) comparison of both CFE treated neurons for 48 h and 96 h. FC represents fold change in expression and FDR represents false discovery rate. 88
Figure 3.11: Enriched gene ontology (GO) representation in dot plot: The 30 GO processes with the highest gene ratios (initial group of selection) are plotted in the direction of gene ratio. The number of genes with differentially expressed gene list (which are significant) by the size of the dots in respective process, and the colour of the dots denotes the FDR cut off values. 89
Figure 3.12: Enrichment GO plot: The top 30 highly enriched GO terms (as determined by P-adjusted values) are displayed, with related terms clustered together. The size of the terms denotes the number of significant genes from the list of the significant genes, and the colour shows the p- values compared to the other established terms. 89
Figure 3.13: Enriched gene ontology (GO) representation in dot plot: The 30 (second group of interest) GO processes with the most significant gene ratios are plotted in the direction of gene ratio. The size of the dots represents the number of genes in the differentially expressed gene list associated with the GO process, and the colour of the dots represents the FDR cut off values. 90
Figure 3.14: The phylogenetic connection plot of GO represents the interlink between the top 30 pathways selected, and their inter-connection was represented with corrected p values. 90
Figure 3.15: HT2cR interaction with top differentially expressed genes involved in the dendrite communication process, the plot derived from CytoScape tool; Where brighter colour represents more significant increased and lighter colour means significantly reduced levels. 91
Figure 3.16: Differentially expressed gene cluster involved in thermogenesis process, the plot derived from CytoScape tool; brighter colour represents more significant increased and lighter colour means significantly reduced levels. 91
Figure 3.17: String network has drawn of proteins identified from upregulated anorexigenic genes after adjusted p-value by using string database. The brightness of the connecting line represents the strength of association. 92
Figure 3.18: DEG's associated with obesity and energy expenditure: The gene expression in SHSY5Y derived neurons after 25 *m*g/mL of CFE treatment for 48 h and 96 h. All the expression values are represented with adjusted p values. 93
Figure 3.19: The variants of PHIP found in obese cases and control samples of a clinical study, the diagram adopted from (Marenne et al., 2020). 93
Figure 3.20: KSR2 - AMPK mediated lipid oxidation in energy expenditure (Kim, 2010) 94
Figure 3.21: The MRAP2 signalling hypothalamic pathway illustration (Rouault et al., 2017) 96
Figure 3.22: Leptin - melanocortin pathway regulates food intake in PVN of the hypothalamus showing the influence of SH2B1 (Yazdi et al., 2015) 97
Figure 3.23: NTRK2 mediated food intake regulation signalling in the arcuate nucleus of the hypothalamus (Choquet and Meyre, 2010) 98
Figure 3.24: PRLH mouse model study illustrating the importance of food intake and body weight (Cheng et al., 2021) 100
Figure 3.25: The string database derived protein network: Overall genes concentrated in this chapter and their association with 5HT2cR. 101
Figure 4.1: Cleversys TopScan and depression analysis: (A) TopScan suit analysis for EPM and OFA (B) Y-maze and LDB analysis using TopScan suit; Depression scan suit for (C) TST, (D) FST analysis, and (E) After analysis tracking patterns from TopScan data. 111
Figure 4.2: Bodyweights during 16 weeks of the study 112
Figure 4.3: Change in growth rate during 16 weeks of the study: 113
Figure 4.4: Overall growth rate during 16 weeks of the study. 114
Figure 4.5: Water and food intake: The cumulative (A) Food and (B) Water intake represent the change in intake with respect to treatments from week 9 to week 16. The weekly (C) Food and (D) Water intake data are drawn on a line plot. 115
Figure 4.6: Open field analysis (OFA) - During exploring Centre area: The behavioural testing for exploration parameters before and after treatment with CFE and Lorcaserin. The OFA parameters included are (A) Number of entries into the centre area, (B) Distance covered in mm during centre area exploration, (C) Time spent in the centre area and (D) Number of random wall-climbing efforts attempted during exploration. 118

Figure 4.7: Open field analysis - During the exploration of the Outer area: The behavioural testing for exploration parameters before and after treatment with CFE and Lorcaserin. The OFA parameters included are (A) The number of entries into the outer area, (B) the distance covered in mm during outer area exploration, and (C) the time spent in the outer area. 119
Figure 4.8: Y-maze analysis - Centre area and known arms exploration: The behavioural testing for exploration parameters before and after treatment with CFE and Lorcaserin. The Y-maze parameters included are (A) Time spent in the outer area, (B) Distance covered in mm during centre area exploration, (C) Time spent in the known arms, and (D) Distance covered in known arms. 120
Figure 4.9: Y-maze analysis - Unknown arm exploration: The behavioural testing for exploration parameters before and after treatment with CFE and Lorcaserin. The Y-maze parameters included are (A) Number of entries into the unknown arm, (B) Time spent in the unknown arm, and (C) Distance covered in the unknown arm.. 121
Figure 4.10: Elevated plus maze analysis - to validate anxiety-like behaviour: The behavioural testing for anxiety level before and after treatment with CFE and Lorcaserin. The EPM parameters included are (A) Number of entries into the open arms, (B) Time spent in open arms, and (C) Distance covered in open arms. 123
Figure 4.11: Elevated plus maze analysis - to validate anxiety-like behaviour: The behavioural testing for anxiety level before and after treatment with CFE and Lorcaserin. The EPM parameters included are (A) Time spent in the centre area of EPM and (B) Distance covered in the EPM centre area. 123
Figure 4.12: Elevated plus maze analysis - to determine anxiety: The behavioural testing for anxiety level before and after treatment with CFE and Lorcaserin. The EPM parameters included are (A) Number of entries into the closed arms, (B) Time spent in closed arms, and (C) Distance covered in closed arms. 124
Figure 4.13: Light and dark box analysis - to validate anxiety-like behaviour: The behavioural testing for anxiety level before and after treatment with CFE and Lorcaserin. The light and dark box parameters included are (A) The Number of nose bouts in the light area, (B) the Time spent in the brighter chamber area, and (C) the Distance covered in the light area. 125
Figure 4.14: Tail suspension analysis - to determine depression behaviour: The behavioural testing for depression level before and after treatment with CFE and Lorcaserin. The tail suspension parameters included are (A) Mobility and (B) immobility duration during test time; 126
Figure 4.15: Forced swim test (FST) analysis - to determine depression level: The behavioural testing for anxiety level before and after treatment with CFE and Lorcaserin. The FST parameters included are (A) Floating time, (B) Swimming time, and (C) Struggling time. 127
Figure 5.1: EchoMRI-900 and workflow of the body composition measurement: (A) Canola oil holder for EchoMRI calibration with fat content of 35.68g, (B) The red holder is used to place the animal to measure the body composition, (C) The slot to place the animal holder into the instrument, (D) After placing the animal holder into the system, and (E) work flow of EchoMRI to measure the mice body composition. 135
Figure 5.2: Components of Promethion cage and workflow of Promethion metabolic cage monitoring: (A) Promethion cage base with gas channel, (B) and (C) cage lid with mass module inserts, (D) Different hoppers that can go with each mass module in the cage, (E) Hoppers hanging to the respective mass module, (F) Gas tubes connected to the gas channel in the cage and (G) Overall brief workflow of Promethion system handling 137
Figure 5.3: Isometric tension analysis workflow description 138
Figure 5.4: Fat content - change in fat during the treatment period (8weeks): Echo MRI based fat mass measurement difference between week 8 to week 16. 141
Figure 5.5: Fat and lean mass percentage with respect to bodyweight: (A) Fat mass percentage (B) Lean mass percentage during the 8^{th} and 16^{th} week of all the groups with respect to bodyweights by Echo MRI; 142
Figure 5.6: Energy expenditure, glucose, and lipid oxidation analysis: (A) Energy expenditure (B) Glucose oxidation and (C) Lipid oxidation during the 8^{th} and 16^{th} week of all the groups with respect to bodyweights. The glucose and lipid oxidation were calculated by estimating VO2 and VCO2 gas emission values from each cage using the Promethion system. 143
Figure 5.7: Respiratory quotient over 48hr (RQ): The VCO_2/VO_2 ratio was represented as RQ for all the groups during week 8 and week 16. 144
Figure 5.8: Promethion analysis - Dark cycle: (A) Total walking distance (B) Average speed of walking, (C) total percentage of walking, and (D) Still percentage (immobility) during 8^{th} and 16^{th} week of all the groups. 145

Figure 5.9: Promethion analysis- Dark cycle: (A) Food intake, (B) Water intake, (C) Sleep percentage, and (D) Sleep hours during the 8th and 16th week of all the groups.. 146
Figure 5.10: During Promethion run HFD fed mice making food pellets into smaller particles and the Promethion system couldn't measure exact food intake.. 147
Figure 5.11: Promethion analysis- Dark cycle: (A) Y-axis Lane crossing counts (B) X-axis Lane crossing counts, (C) Z-axis Lane crossing counts (climbing), and (D) XY- plane walking distance, during 8th and 16th week of all the groups..... 148
Figure 5.12: Promethion analysis- Interaction with hoppers: (A) Interaction with food hopper (TFODA), (B) Interaction with water hopper (TWATR), (C) Time spent in housing hopper (IHOME), during 8th and 16th week of all the groups. 149
Figure 5.13: Isometric tension analysis of abdominal aortic rings: The abdominal aortic rigs were used to measure the vasodilation pattern of HF-diet induced mice with CFE and Lorcaserin treatments. 150
Figure 5.14: Isometric tension analysis of abdominal aortic rings. 152

Chapter 1 Literature review

Obesity is linked to premature mortality and is a severe public health problem, contributing to the global non-communicable disease burden, including type 2 diabetes (T2D), cardiovascular disease (CVD), hypertension, and certain malignancies (Tabarés Seisdedos, 2017, Grant et al., 2022). Osteoarthritis and sleep apnoea are two involuntary issues that might arise from gaining weight (Parande et al., 2022). Obesity impacts infectious diseases; namely, viral infection has lately been highlighted by the finding that more obese people are hospitalised and suffer severe sickness from COVID-19 (Sattar and Valabhji, 2021, Aghili et al., 2021). In 2016, nearly 2 billion persons (39% of the world's adult population) were predicted to be overweight, with 671 million (12% of the world's adult population) having obesity, a threefold increase in obesity and overweight since 1975. Obesity is predicted to affect 1 billion adults (almost 20% of the world's population) by 2025 if current trends continue (Keramat et al., 2021).

The global upsurge in obesity among children and adults is particularly concerning; in 2016, more than 7% of children and adolescents were obese, compared to less than 1% in 1975. According to WHO statistics, Australia's combined rate of overweight/obesity in adulthood is 25% and will rise to 35% by 2025, while New Zealand's overweight rate is 40% with 16% obesity (Keramat et al., 2021, Guo et al., 2016). In addition, the death rate numbers with obesity-related comorbidities have increased over the last decade throughout the world (Montégut et al., 2021a, Geiger et al., 2021, Cominato et al., 2021, Guo et al., 2016). Overweight and obesity have become much more of a concern during the previous three decades, affecting people of all ages (Keramat et al., 2021). Obesity has traditionally been defined based on a body mass index (BMI) of >30 kg/m^2, with a BMI of 25 to 29.9 kg/m^2 defined as overweight (shown in Table 1.1).

Table 1.1: Body mass index range for obesity condition(Guo et al., 2016)

Stage description	Body Mass Index (BMI) in kg/m^2
Under weight	<18.5
Normal weight	18.5-24.9
Overweight	25.0-29.9
Obese	≥ 30.0
Obese class I	30.0-34.9
Obese class II	35.0-39.9
Obese class III	≥ 40

Table 1.2: Obesity staging system adopted from (Bessell et al., 2021)

Stage	Description	Suggested management
S0	There were no apparent obesity-related risk factors (blood pressure, serum lipids, fasting glucose, etc. are within the healthy range), No physical symptoms, No psychopathology, No functional limits and/or impairment of well-being	Factors that contribute to a rise in body weight are identified. Counselling to prevent further weight gain by incorporating a healthy diet and increased physical exercise into one's lifestyle.
S1	Obesity-related subclinical risk factors (e.g., impaired fasting glucose, elevated liver enzymes, borderline hypertension, etc.) are evident, Mild physical symptoms (e.g., dyspnoea on moderate exertion, occasional aches and pains, fatigue, etc.), Mild psychopathology, Mild functional limitations, Mild impairment of well-being	Investigation for other (non-weight-related) contributors to risk factors. More intense lifestyle interventions, including diet and exercise, prevent further weight gain. Monitoring of risk factors and health status
S2	Presence of established obesity-related chronic disease (e.g., hypertension, T2D, sleep apnoea, osteoarthritis, reflux disease, polycystic ovary syndrome, anxiety disorder, etc.), moderate limitations in activities of daily living and/or well-being	Initiation of obesity treatments, including considerations of all behavioural, pharmacological, and surgical treatment options. Close monitoring and management of comorbidities as indicated
S3	Established end-organ damage such as myocardial infarction, heart failure, diabetic complications, incapacitating osteoarthritis, significant psychopathology, significant functional limitations and/or impairment of well-being	More intensive obesity treatment, including consideration of all behavioural, pharmacological, and surgical treatment options. Aggressive management of comorbidities as indicated
S4	Severe (potentially end-stage) disabilities from obesity-related chronic diseases, severe disabling psychopathology, severe functional limitations and/or severe impairment of well-being	Aggressive obesity management as deemed feasible. Palliative measures, including pain management, occupational therapy, and psychosocial support

While increased BMI does increase the risk of various complications, this is not always linear, and the threshold at which this appears is variable. For example, certain ethnic groups develop complications associated with increased adiposity at a lower BMI (Marti and Martinez, 2004). Thus, an alternative definition of obesity as a condition in which increased adiposity impairs mental and physical health has been proposed (Shi and Burn, 2004). The Edmonton Obesity Staging System (EOSS) considers the degree of physical and psychological impairment when recommending treatment and is a stronger predictor of mortality than BMI (Table 1.2) (Sarma et al., 2021). Obesity is caused by complex interactions between hereditary and environmental variables, just like other chronic disorders like hypertension and T2D (Sarma et al., 2021).

Obesity can be classified into two categories, monogenic obesity, which is inherited in a genetic pattern, typically rare, early-onset, and severe, and involves small or large chromosomal deletions or single-gene defects; and polygenic obesity (also known as common obesity); which is caused by hundreds of polymorphisms, each of which has a minor effect (Tabarés Seisdedos, 2017, Stamm et al., 2017, Loos and Yeo, 2021) (described in Figure 1.1). Polygenic obesity has a heritability pattern like other complex characteristics and disorders. Gene discovery investigations of monogenic and polygenic obesity have converged on similar underlying biology, even though they are often thought to be two distinct kinds (Must et al., 1999, Fontaine and Barofsky, 2001).

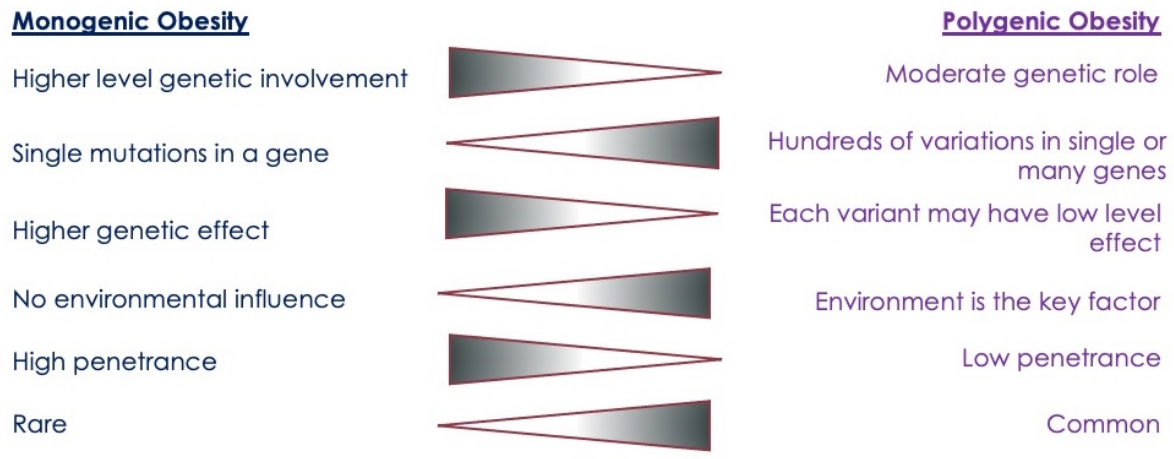

Figure 1.1: Schematic representation of fundamental differences in Monogenic and Polygenic Obesity classification inspired from (Loos and Yeo, 2021)

For both monogenic and polygenic obesity, the central nervous system (CNS) and neuronal pathways that control behavioural elements of food intake have emerged as essential drivers of

body weight (Crowley et al., 2002, Quarta et al., 2021). In addition, some of the neuroendocrine peptides like agouti-related protein (AgRP) and proopiomelanocortin (POMC) variation in the central nervous system change adipose deposition and contribute to the divergence of (Ehrhart et al., 2018, Brandt et al., 2018, Guillemot-Legris and Muccioli, 2017). Furthermore, preliminary data suggest that the manifestation of monogenic obesity-causing mutations may be impacted, at least in part, by an individual's polygenic obesity susceptibility. Bardet–Biedl syndrome and Prader–Willi syndrome are two examples of syndromic obesity(Hall et al., 2022, Tran et al., 2022b). However, it is becoming apparent that monogenic and polygenic obesity are not two different things. Instead, they exist on a range and, at least in part, share biology. For example, the MC4R, BDNF, SH2B1, POMC, LEP, LEPR, NPY, SIM1, NTRK2, PCSK1, and KSR2 genes that are identified initially for excessive and early-onset obesity in human and animal models (Lindberg and Fricker, 2021, Loos and Yeo, 2021, Wallace and Fordahl, 2021). In obesity, most of the genes implicated in the leptin-melanocortin and BDNF–TrkB signalling pathways are linked to hunger and satiety regulation (Theilade et al., 2021). While hereditary impairment of these pathways causes extreme obesity, genetic polymorphisms in or near these genes that have a more subtle effect on their expression can affect where an individual falls in the typical BMI distribution(Organization, 2020, Parande et al., 2022).

1.1. Genetic modulators and Obesity:

Excessive caloric intake, partly explained by the weakening of satiation following meal intake, is the primary reason for the lack of long-term weight loss in overweight or obese patients (Keramat et al., 2021, Montégut et al., 2021b). Many regions of the central nervous system (CNS) respond to sensory (smell, hearing, sight), endocrine (gastrointestinal hormones, leptin, insulin, etc.) and neurological (vagal afferents) inputs to control food intake (Kwon et al., 2022, Lama et al., 2022a, Li et al., 2022). Homeostatic control is mediated by specific brain areas such as the hypothalamus and the brainstem (in response to calorie deficit). Other regions (the ventral tegmental area (VTA), the nucleus accumbens (NAc), the striatum, etc.) are more engaged in non-homeostatic control of food intake, responding to motivational or reward inputs (Lindberg and Fricker, 2021, Loos and Yeo, 2021, Theilade et al., 2021). The methods used to find genes connected to obesity vary according to the type of obesity and the genotyping technology available. Advances in high-throughput genome-wide genotyping and sequencing technology and a deep understanding of the human genetic architecture have enabled a hypothesis-generating strategy to interrogate genetic variants throughout the entire genome for their function in body-weight control (Perreault, 2018). The leptin-melanocortin pathway is a

vital appetite regulation circuit, and genes expressed in the brain and CNS play a crucial role in obesity.

1.2. Leptin-Melanocortin pathway

Obesity and impaired glucose tolerance are becoming increasingly prevalent worldwide. The brain, which coordinates feeding behaviours, is home to a complex network of networks that regulate energy balance (Sainsbury et al., 1997, Hwa et al., 1999). Leptin is a 146-amino-acid protein that aids in body weight maintenance. Human white adipose tissue produces the leptin hormone. Its gene sequence is found on chromosome 7 in humans, and a lack of leptin causes obesity (Spanswick et al., 1997, Brennan and Mantzoros, 2006). As a result, blood leptin levels are proportional to body fat. This implies that blood leptin levels are proportional to body fat (Friedman and Halaas, 1998). When the leptin hormone is absent or fails to work, the brain's hypothalamus signals that fat-stored energy is being used up, causing an increase in energy consumption. Leptin works as a negative signal to manage body weight by reducing food intake and increasing energy expenditure (Khansari et al., 2020). Dexamethasone and insulin, the two main molecules implicated in the production of stored leptin, generate a twofold increase in leptin levels in the blood (Quarta et al., 2021, Friedman and Halaas, 1998). Fasted mice are given leptin, which eliminates many of the neuroendocrine effects of starvation, implying that leptin's natural biological role is to begin the starvation response (Vohra et al., 2021, Bradley and Cheatham, 1999).

Leptin receptors (LEPR) are also known as CD295and are encoded by the LEPR gene. Obesity is caused by variations in these receptors, expressed in five different forms: Ob-Ra, Ob-Rb, Ob-Rc, Ob-Rd, and Ob-Re (Friedman and Halaas, 1998). The cytokine receptor family includes LEPR, which is a single transmembrane domain. The Ob-Ra receptor is primarily responsible for assisting leptin trafficking across the blood-brain barrier. The hypothalamic receptor Ob-Rb is implicated in signalling pathways that regulate body weight (Mercer et al., 1996). The LEPRb is found on two types of neurons in the hypothalamic arcuate nucleus (ARC), one of which expresses POMC and the other of which expresses agouti-related protein (AGRP) (Spanswick et al., 1997). POMC was converted into a variety of physiologically active components by prohormone convertases (PCs), including lipotropin, endorphin, melanocortin peptides, adrenocorticotropin (ACTH), and α, β, and γ- melanocyte-stimulating hormone (MSH) (Mercer et al., 1996, Ollmann et al., 1997).

The ARC/POMC neurons regulate melanocortin signalling, which may reduce food intake (Hwa et al., 1999). In contrast, AGRP works as an endogenous MC3R antagonist to promote food intake. However, because mice with MC3R gene deletions are not obese but have a different fat-to-lean mass ratio, MC3R is less likely to be involved in food intake and more likely to be involved in nutrient partitioning. According to genetic evidence, mutations in essential melanocortin pathway genes cause hyperphagia and extreme obesity. This pathway contains many single-gene abnormalities that cause severe early-onset obesity in humans, including LEPR, POMC, AGRP, MCR4R, PCSK1, SH2B1, SIM1, PHIP, and MRAP2 (Heymsfield et al., 2014).

Leptin changes synaptic connections between neurons by stimulating classical neuropeptide receptor systems within the brain and regulating downstream functions (Chen et al., 2020). The signalling of brain-derived neurotrophic factor (BDNF) to its receptor TrkB (neurotrophic receptor tyrosine kinase) is thought to be one of the mechanisms in which this plasticity is achieved. In the CNS, BDNF is widely expressed and plays a crucial role in the neuronal formation. The BDNF related synaptic plasticity in the hippocampus is associated with learning and memory (Parande et al., 2022). Recent studies revealed that BDNF and TrkB are also involved in mammalian feeding behaviour and energy balance regulation (Wu et al., 2021). Dietary deficiency lowers BDNF production in the hypothalamic ventromedial nucleus (VMN), but leptin boosts it. In both humans and animals, genetic disruption of BDNF and TrkB causes hyperphagia and severe obesity. The BDNF in VMN is downregulated by caloric deprivation and elevated by leptin (Jansson et al., 2018). However, this regulation is indirect because only a few VMN BDNF neurons express the LEPR, and some evidence suggests an involvement in the melanocortin signalling pathway. The class 3 semaphorins (SEMA3A–G) are another set of neuronal proteins crucial in developing neural circuitry and associated with energy balancing (Loos and Yeo, 2021). SEMA3 signalling via NRP2 (neuropilin 2) receptors appears to drive the development of POMC projections from the ARC to the PVN in mouse and zebrafish (Loos and Yeo, 2021).

In a human study, 40 uncommon loss-of-function mutations in SEMA3A–G and its receptors (PLXNA1–4, NRP1 and NRP2) were significantly enriched in 982 obese people compared to 4,449 healthy people (González-Amor et al., 2020, Patel et al., 2020). Insulin, like leptin, is thought to operate as an adiposity signal, helping to manage body weight eventually and the near term. As a result, a change in plasma leptin or insulin levels is detected as an alteration in

energy homeostasis and adiposity. The brain responds by changing food intake to restore the basal fat mass level (Marti and Martinez, 2004). These long-term impacts could partly explain seasonal variations in weight and fat mass. Approaches that include a co-injection of amylin, on the other hand, are effective (Miller, 2005). Peripheral insulin acts in the hypothalamus by inhibiting NPY/AgRP/GABA neurons and activating POMC/CART neurons, both of which express the insulin receptor (Nogueiras et al., 2008). According to new research, insulin activates POMC neurons via transient receptor potential (TRPC) 5 channels. On the other hand, insulin inhibits NPY/AgRP/GABA neurons by activating K(ATP) channels, causing hyperpolarisation (Lindberg and Fricker, 2021, Montégut et al., 2021b).

There are now two obesity treatments that are genotype specific. The delivery of recombinant human leptin to leptin-deficient individuals because of mutations in the LEP gene is the paradigm of genotype-informed obesity treatment. Leptin replacement therapy has significantly reduced food intake, body weight, fat mass, and normalised endocrine function for these individuals (Loos and Yeo, 2021). Setmelanotide, a selective MC4R agonist newly approved by the FDA for uncommon monogenic obesity diseases such as LEPR, PCSK1 deficiency, and POMC deficiency, is the second genotype-informed treatment for obesity (Perreault, 2018). The overall genes influencing weight regulation are mentioned in Table 1.3.

Table 1.3: Genes associated in early-onset and severe obesity modified from (Loos and Yeo, 2021)

Gene description	Presence	Role in body-weight regulation
ADCY3 (Adenylate cyclase) Gene ID: 109	Primary cilia of cells	Disruption of primary cilia in neurons known to influence energy balance; some evidence of a specific link to the correct function of MC4R
AGRP	Neurons in the arcuate nucleus of the hypothalamus	The endogenous antagonist of MC4R, to which it binds to increase food intake
BDNF	Brain	Probably via its role in regulating neuronal synaptic plasticity
KSR2 (kinase suppressor of Ras2) Gene ID: 283455	Wide expression throughout the body	Influences both energy intake and expenditure, possibly via interaction with AMPK
LEP (leptin) Gene ID: 3952	Fat	Circulates in proportion to fat mass and turns on the neuroendocrine starvation response when circulating levels drop below a minimum threshold
LEPR, (Leptin receptor) Gene ID: 3953	The long 'signalling' form is expressed widely in the brain	Cognate receptor for leptin, mediating its downstream neuroendocrine functions
MC4R (melanocortin 4 receptor) Gene ID: 4160	Central nervous system	Binds melanocortin peptides and AGRP to mediate appetitive behaviour and autonomic output
MRAP2 (melanocortin receptor accessory protein 2) Gene ID: 112609	Wide expression throughout the body, but highest in the brain	An accessory protein that plays a role in trafficking MC4R to the cell surface
NTRK2 (neurotrophic receptor tyrosine kinase 2) Gene ID: 4915	Brain	Cognate receptor for BDNF, mediating its downstream effects on synaptic plasticity
PCSK1 (proprotein convertase subtilisin/ Kexin type 1) Gene ID: 5122	Endocrine organs, with the highest expression in the brain	Encodes one of the prohormone convertases required for processing POMC
PHIP (pleckstrin homology domain interacting protein) Gene ID: 55023	Widely expressed	Regulates transcription of *POMC*
POMC (proopiomelanocortin) Gene ID: 5443	Hypothalamus, Nucleus Tractus Solitaris, pituitary, skin, adrenal glands, and numerous other tissues	Complex pro-polypeptide that is processed into melanocortin peptides that signal to MC4R in the brain
SH2B1, SH2B (adaptor protein 1)	Widely expressed	A signalling molecule downstream of the leptin receptor
SIM1, SIM bHLH transcription factor 1 Gene ID: 6492	Hypothalamus, kidney, and fat	A transcription factor crucial for the proper development of the paraventricular nucleus and hence the appropriate expression of *MC4R*, among other genes

1.2.1 AgRP and NPY

Agouti-related peptide (AgRP) is a neuropeptide produced by AgRP/NPY neurons in the arcuate nucleus of the brain. This neuropeptide is co-expressed with Neuropeptide Y (NPY).

Its key role is to enhance hunger while decreasing energy expenditure, making it one of the most influential and long-lasting appetite stimulators (Bäckberg et al., 2004, Inui et al., 2004). The AGRP gene encodes the agouti-related peptide in humans. AgRP acts as an antagonist to melanocortin receptors, especially MC3R and MC4R. Energy expenditure, metabolism, and weight regulation are linked to these receptors. The agouti-related protein inhibits the hormone α-MSH from activating these receptors. α-MSH acts on all members of the MCR family except MC2R, whereas AGRP is more specific to MC3R and MC4R. AgRP levels are high in fasting (Shutter et al., 1997, Spanswick et al., 1997). The critical signalling point for hormones that regulate appetite is in the hypothalamus. Specifically, the arcuate nucleus (ARC) is related to anorexigenic neuropeptides such as cocaine and amphetamine-regulated transcript (CART) and POMC as appetite suppressors. Appetite stimulators include the orexigenic neuropeptides AgRP and NPY. These circulatory neurons are essential for energy balance and hunger (Heisler et al., 2006). NPY has a significant impact on food intake and body weight. The five distinct G-protein coupled receptor subtypes (Y1, Y2, Y4, Y5, and Y6) produced by NPY signals were blocked by anorexigenic hormones like insulin and leptin (Lloret Linares et al., 2011). Because there are various types of NPY receptors, it is difficult to target all five variants without causing unwanted side effects. One of the isoforms targeted to promote weight reduction and responsible for the orexigenic effects is the Y5 receptor. It is located on POMC neurons in the ARC. Melanin-concentrating hormone (MCH) is another orexigenic neuropeptide (Shi and Burn, 2004, Erondu et al., 2007) in hypothalamus. The MCH involved in downstream of leptin resistance of the lateral hypothalamic area on food intake.

1.2.2 Ghrelin

Ghrelin is a 28-amino-acid protein made from the precursor proghrelin. This appetite hormone is produced by entero-endocrine cells in the stomach, diffuses into the bloodstream, and influences feeding behaviour by blocking neurotransmitter discharge in the brain (Evans et al., 2004, Inui et al., 2004). Obese people have deficient levels of this hormone. Ghrelin is octanylated in the endoplasmic reticulum, particularly on the rough surface, by any enzyme GOAT (ghrelin O-acyltransferase), resulting in n-octanoic acid, which aids in the stimulation of appetite by raising the activity of NPY/AgRP/GABA neurons (Lall et al., 2001, Larose et al., 2001, Crowley et al., 2002). Ghrelin levels are high in persons with anorexia nervosa and people with Prader-Will syndrome (PWS). Ghrelin's interaction with GH secretagogue receptors (GHSR) or the pituitary gland's anatomical morphology (Valentino, 2012).

Individuals with Prader-Willi syndrome (PWS) (Cacciari et al., 1990) and those with EMO have reduced their pituitary size (Miller et al., 2008). Compared to sibling controls, functional connectivity during fMRI measurement is changed in PWS participants. FMRI imaging has revealed regions activated by appetite-regulating hormones such as leptin, PYY, and ghrelin food images or even increased hunger due to fasting (Chen et al., 2008, Malik et al., 2008).

1.2.3 Secretin

Secretin (SCT), a digestive peptide that regulates gastric acidity and motility, has recently been recognised as an anorexigenic peptide. Previous research on appetite regulation has yielded mixed results: appetite reduction was accomplished in mice after central and peripheral injections of SCT, accompanied by enhanced lipolysis (Theilade et al., 2021). However, these findings contradict prior findings in rats and lambs (Sekar et al., 2017). SCT-receptor-deficient mice did not change their eating habits yet were protected from HFD-induced obesity due to defective lipogenesis, which suggested a significant function in lipid metabolism regulation (Montégut et al., 2021b). The SCTR-expressing brown adipocytes promote thermogenesis and appetite-regulating effects. The effects of SCT-induced brown adipose tissue (BAT) activation on appetite and energy regulation in seven human individuals were also validated, paving the door for applying adipose tissue-based techniques for food intake reduction (Jimenez-Munoz et al., 2021).

1.2.4 FTO (fat mass and obesity-associated)

The FTO locus, which contains six genes discovered more than a decade ago, is the most studied obesity locus. However, the FTO locus gene variants have yet to be identified with convincing evidence, and the mechanisms by which the locus influences body weight have yet to be thoroughly understood (Tierney, 2001) The DSBH (double-stranded β-helix) folds of FTO protein are like those of Fe (II) and 2-oxoglutarate (2OG) oxygenase (Frayling et al., 2007). FTO localises to the nucleus in transfected cells due to nucleic acid demethylation. Intronic FTO single nucleotide polymorphisms are linked to energy homeostasis; this could be changed by changing the expression of FTO mRNA (Hess and Brüning, 2014). In mice, FTO deficiency causes a lean phenotype, whereas FTO overexpression causes increased body weight and is involved in cellular nutrition sensing. FTO binds to brain regions that govern ghrelin levels in humans and dopaminergic signalling in mice, affecting appetite, reward processing, and reward desire (Hess and Brüning, 2014). The promoter of Irx3, a gene located

0.5 Mb downstream of FTO, interacts directly with the FTO locus. Weight reduction and higher metabolic rate were observed in Irx3-deficient animals, along with browning of white adipose tissue, with no alterations in physical activity or appetite (Frayling et al., 2007, Gerken et al., 2007, Hess and Brüning, 2014). FTO disrupts the transcriptional repressor ARID5B during early adipocyte development, doubling IRX3 and IRX5 expression (Hill et al., 2012, Valsamakis et al., 2017).

TMEM18 is a poorly understood transmembrane protein that is highly conserved across species and expressed in various tissues, including multiple brain areas. TMEM18 deficiency causes mice to gain weight due to increased food intake, but Tmem18 overexpression causes food intake to decrease and weight gain to be limited (Loos and Yeo, 2021). A knockdown experiment in Drosophila melanogaster reveals that TMEM18 disrupts insulin and glucagon signalling, affecting glucose and lipid levels. Apart from these loci, many other loci are associated with obesity expressed in the central nervous system association with upstream of CADM1, CADM2 alleles, and NEGR1 (Georgescu et al., 2021, Jimenez-Munoz et al., 2021, Vohra et al., 2021). Mice lacking CADM1 or CADM2 have reduced body weight and have higher insulin sensitivity, glucose tolerance, and energy expenditure without changing their diet. Higher CADM1 or CADM2 neuronal expression, on the other hand, is linked to increased body weight. In addition, CADM1 is expressed in POMC neurons, and CADM1 loss increases the number of excitatory synapses, implying more remarkable synaptic plasticity. Furthermore, CADM2 knockout mice have higher locomotor activity and core body temperatures (Loos and Yeo, 2021).

1.2.5 NEGR1

In mice, NEGR1 absence resulted in reduced body weight, owing to a reduction in lean mass, mediated by reduced food intake. However, knocking down Negr1 expression in two other functional investigations, one in mice and the other in rats, resulted in the reverse outcome of weight gain and food intake. While it has been discovered that NEGR1 loss in mice impairs vital behaviours, the data and postulated mechanisms have not yet been fully aligned (Lindberg and Fricker, 2021, Loos and Yeo, 2021).

1.2.6 ADCY3

The ADCY3 existing loci were the first to be discovered as having a function in severe obesity. ADCY3 is an adenylate cyclase that catalyses cAMP's creation, a critical second messenger in signal transduction pathways. There is limited evidence that ADCY3 (adenylate cyclase) colocalised with MC4R at PVN neurons in cilia. These cilia are essential for energy balance and control of MC4R-expressing neurons. ADCY3 or MC4R gene deletion in these neurons may influence melanocortin signalling in mice, resulting in hyperphagia and obesity (Fernández Vázquez et al., 2018, Jansson et al., 2018, Vohra et al., 2021).

1.2.7 TUB gene

The hypothalamus has short and long transcripts of TUB gene. Late onset obesity is caused by a mutation in the TUB gene (Nies et al., 2018). The mRNA is expressed in the hypothalamus with a single base mutation causes a mature mRNA to have an intron, meaning the 44 amino acids in the c-terminal end of the protein are replaced with the 24-intron coded amino acids, resulting in increased body weight. These aberrant mRNA findings point to tubby obesity being induced (Kleyn et al., 1996).

1.2.8 5HT2cR

Serotonin 2c receptor, is a G-protein coupled receptor that belongs to the seven-transmembrane (7-TM) receptor superfamily (GPCRs) (Lee et al., 1999, Pérusse and Bouchard, 2000). GPCRs are part of a large integral membrane protein family that has over 1000 members of the human genome. The seven subtypes of serotonin receptors, 5HT1 through 5HT7, have a variety of biological functions, including modulation of mood, sleep, bowel movement, and appetite (Huang et al., 2018). Depression, anxiety, obsessive-compulsive disorder, chronic pains, obesity, eating disorders, epilepsy, and erectile dysfunction have all been linked to the 5HT2 receptor. The 5HT2 receptor family has three subtypes: 5HT2a, 5HT2b, and 5HT2c; all have similar sequences and are active in signal transduction pathways (Ryan, 2000, Vaisse et al., 2000, Tierney, 2001, Price et al., 2002). The 5HT2c receptor, which plays an essential role in metabolic processes, appears to be a promising anti-obesity target (Pérusse and Bouchard, 2000). Food signal regulation occurs through promoting the production of the agonist α--melanocyte-stimulating hormone (a-MSH) and suppressing the antagonist agouti-related peptide by activating the 5HT2c receptor (Heisler et al., 2003, Bäckberg et al., 2004).

Further, it may induce satiety by inhibiting the agouti-related peptide (AgRP) associated appetite signal. Designing a medication that targets a specific subtype of the 5HT2 receptor has proven to be extremely difficult. The therapeutic impact of fenfluramine, D-fenfluramine, and sibutramine is to improve 5HT2cR mediated satiety response (Kurebayashi et al., 2013). However, due to severe side effects including pulmonary hypertension and heart valve disease these drugs with drawn from further assessment. Only 5HT2cR deficient mice exhibit hyperphagia and obesity and acquire type 2 diabetes-like features (Garfield et al., 2016).

Furthermore, the 5HT2cR knockout mice study showed more death rate during breeding. As a result, developing a compound with high affinity for the 5HT2cRs but low affinity for the 5HT2bR was a problem throughout the drug discovery process (Miller, 2005, Heisler et al., 2006). Obesity and diabetes-related characteristics are seen in whole-brain 5HT2cR knockout mice (e.g., insulin resistance and impaired glucose tolerance) (Astrup et al., 2008, Garfield et al., 2009). These preliminary findings suggest that a 5HT2cR agonist could be used to treat obesity and type 2 diabetes and that the melanocortin system mediates both effects.

1.2.9 ADRB3

The β-3 adrenergic receptor (ADRB3) gene is found on chromosome 8 and is expressed in adipose tissue. The adipose tissue is a key component of the neuroendocrine network, and overexpression of this gene identified with obesity progression (Valentino, 2012, Misra and Verma, 2013). Many other genes, such as appetite-regulating peptides or receptors, a complex of reproduction-related genes, and a local autocrine/paracrine regulatory network, were also expressed in visceral adipose tissue (Speakman, 2013). Other than neuromodulated genes, other peripheral tissue-associated genes are also involved in obesity regulation. Recent meta-analysis study revealed ADRB3 rs4994 (Trp 64 Arg) associated polymorphism leading to overweight/obesity in both adult and children by reduced resting metabolic rate (Xie et al., 2020).

1.2.10 Pancreatic lipase

A key enzyme in the breakdown of lipids has emerged as a viable therapeutic target for obesity treatment. It is a major pancreatic enzyme that aids in the digestion of total dietary lipids (50–70%) by breaking them down to monoglycerides and fatty acids (Shi and Burn, 2004). Micelles are formed when these end products interact with bile acids, cholesterol, and lysophosphatidic

acid. After fat is absorbed by smaller intestine and deposited in adipose tissue, in the form of triglycerides. Inhibiting pancreatic lipase prevents triglyceride breakdown and so aids in the decrease of excess fat absorption (Crowley et al., 2002, Shi and Burn, 2004).

1.2.11 Adrenoceptor

The gastrointestinal tract lining contains β-3-A receptors. The protein aids adipocyte metabolism, and brown adipose tissue stimulates b3-AR in norepinephrine. In addition, activation of this receptor increases lipolysis in response to catecholamines, a class of aromatic amines with anti-obesity properties. The prevalent variation linked to reduced lipolytic activity is tryptophan replacement by arginine at position 64 (Zhang et al., 2004, Park et al., 2005). Lipid builds up in the adipose tissue as a result.

1.2.12 UCP genes

Uncoupling proteins (UCPs) are a type of carrier protein found in mitochondria's inner membrane layers. These proteins are involved in mitochondrial thermogenesis. The different members of this family include UCP1, UCP2, and UCP3. UCP1 is usually found in brown adipose tissue, UCP2 is found in any tissue, and UCP3 is found in skeletal muscle and brown adipose tissue. UCP1 and UCP2 target proton leaks in mitochondria, releasing stored energy as heat, affecting energy metabolism. These individuals are thought to be energy metabolism regulators. UCP2 and UCP3 are the most studied targets in the treatment of obesity (Zhang et al., 2004, Park et al., 2005).

1.2.13 DGAT

Triacylglycerols are neutral lipid types that are the most usual form of metabolic energy storage in eukaryotes. Triacylglycerols are three fatty acids joined by ester bonds to a glycerol backbone. The diacylglycerol transferase (DGAT) is a transmembrane protein with a molecular mass of 55kda that catalyses the final and committed step in triglyceride production. It is expressed in the liver, white adipose tissue, and other organs. The two isoforms of DGAT are DGAT1 and DGAT2. In very-low-density lipoprotein (VLDL) assembly, DGAT1 activity is seen, while DGAT2 activity is seen in steatosis (Shi and Cheng, 2009). Mice lacking DGAT1 were having increased sensitivity to insulin and resistant to obesity. The antisense oligonucleotide treatment against DGAT2 in diet-induced obese mice showed hyperlipidemia

and reduced hepatic lipogenesis and hepatic steatosis Obesity can be treated with a new pharmaceutical therapy that inhibits the action of these enzyme.

1.2.14 Amylin

Pancreatic β- cells express and release amylin, also known as- Islet amyloid polypeptide (IAPP). Calcitonin gene-related peptide (CGRP) and amylin are structurally similar. This hormone's levels are low during fasting and high after eating. Amylin, through central and peripheral processes, reduces food intake directly. Slow stomach emptying can help with food intake indirectly (Morley, 1987, Bradley and Cheatham, 1999). Supplementing with the peptides CCK (Cholecystokinin), glucagon, and bombesin causes an increase in amylin secretion, which reduces food consumption. While NPY neurons express the required components of the amylin receptor, it is still unknown what direct effect amylin has on NPY neurons (Georgescu et al., 2021). It is possible that it is inhibitory, which would explain why it is often neglected in investigations of neuron activation. Multiple factors, however, are required to reverse the fasting-induced activation of ARC neurons, implying that these first-order neurons already integrate a variety of peripheral cues, and that endogenous amylin alone may not be sufficient to prevent NPY-driven eating behaviour (Xie et al., 2021).

1.2.15 PPAR

One of the key targets in obesity treatment, the Peroxisome Proliferator-Activated Receptor (PPAR), has attracted attention in developing novel medicines (Zhang et al., 2004). Apart from obesity, this nuclear receptor plays an important function in metabolic processes such as fatty acid oxidation, hypertension, insulin resistance, and atherogenic dyslipidemia (Costet et al., 1998). The PPARs are a family of three isoforms encoded by distinct genes: PPAR γ, PPAR α, and PPARδ (Berger et al., 2005). These isoforms are ligand-regulated transcription factors whose actions are controlled via modifying gene expression. PPAR α and γ are two of the three isoforms expressed in adipose tissue that has been targeted for the treatment of obesity (Berger et al., 2005). The two major states observed in obesity are increased adipocyte number and hypertrophy, which is characterised by an increase in adipocyte volume. PPAR α maintains the energy balance in the cell by catabolizing fat. Increased fatty acid oxidation and lower plasma triglyceride levels are essential for adipose tissue growth and hyperplasia, which leads to a reduction in body weight. This idea was validated by mouse experiments that showed that a lack of PPAR α caused anomalies in plasma triglycerides and cholesterol metabolism,

eventually leading to obesity. Conversely, inhibition of PPAR-γ causes a decrease in the number of adipocytes, which leads to a reduction in fat accumulation in obesity regulation (Barish et al., 2006, Holst et al., 2009, Kim et al., 2010). The invitro studies of the differentiation of 3T3L1 pre-adipocytes to mature adipocytes showed that the 5HT2c receptor antagonist SB-242084 inhibited adipocyte differentiation (Yu et al., 2021). Further, 5HT2cR mRNA expression is increased with adipocyte differentiation. The obese models, 5HT2cR mutant (2-fold), *ob/ob* (leptin deficient-7 fold) mice and *db/db* (leptin-receptor deficient-9 fold) mice have increased PPAR-γ mRNA expression in liver tissue (Memon et al., 2000). Therefore, reduced functioning of the 5HT2c receptor is linked to increased PPAR-γ expression, adipogenesis and obesity.

1.3 Obesity- drug development:

Obesity can be avoided and reversed. Previously, preventative and treatment techniques focused on limiting energy intake and raising energy expenditure. However, most attempts and programmes have proven ineffective at a population level, necessitating a more comprehensive strategy. Rodents were widely used in a recent obesity research investigation. Mice fed a high-fat diet (HFD) for one week demonstrated altered behavioural responsiveness and molecular changes in the hypothalamus in response to leptin administration (Park et al., 2022).

Pramlintide/ Metreleptin reversed HFD-induced leptin resistance in mice (Powell and Khera, 2010). The metreleptin (MYALEPT) by AstraZeneca was approved by the FDA in 2014 for treating leptin deficiency in obese people. Another way to activate leptin is by removing the phosphate from the tyrosine activation sites of the leptin receptor, which inhibits PTP-1B and so activates leptin activity. A PTP-1B inhibitor, trodusquemine (MSI-1436, Genaera Corp., Plymouth Meeting, PA, USA), is currently in phase II clinical studies (Lantz et al., 2010).

The Y-5 antagonist (MK-0557: Whitehouse Station, NJ, USA: Merck & Co., Inc., and Shionogi (Osaka, Japan)) was evaluated. Velneperit, a Y-5 antagonist, in conjunction with an intestinal lipase inhibitor like orlistat (Erondu et al., 2007).

Elixir Pharmaceuticals, Inc. (Cambridge, MA, USA) has created a ghrelin receptor antagonist which is being tested in humans (Baggio and Drucker, 2007). In addition, the enzyme ghrelin O-acyltransferase (GOAT) levels are directly or indirectly repressing the GHRL gene the post-

translational activation is another target (Laferrere et al., 2010, Powell and Khera, 2010, Kirchner et al., 2009).

Orlistat (Orlistat, F. Hoffmann-LaRoche, Basel, Switzerland; Alli, GlaxoSmithKline plc, Brentford, UK) is a weight-loss medication. It is a lipase inhibitor that prevents triglyceride breakdown in the intestine. As a result, fat absorption is reduced (Powell and Khera, 2010). Unfortunately, this medication had gastrointestinal side effects after long-term use. Cetilistat, a lipase inhibitor (Norgine BV, Amsterdam, The Netherlands, in partnership with Takeda Pharmaceutical Co., Ltd., Osaka, Japan), has improved tolerance and is currently undergoing phase III clinical studies (Yao and MacKenzie, 2010).

Table 1.4: Weigh loss drugs available for treatment (Daneschvar et al., 2016)

Drug	Mechanism of action	Dosing	Approving bodies	Weight loss	Side effects
Orlistat	Pancreatic lipase inhibitor	60–120 mg three times daily	FDA (1999) EMA (1998)	2.9–3.4 kg/ year	Steatorrhea, faecal urgency
Phentermine/ topiramate	Sympathomimetic, appetite suppressant	3.75/23 mg 7.5/46 mg 11.25/69 mg 15/92 mg once daily	FDA (2012)	6.6–8.6 kg/ year	Insomnia, dizziness, paraesthesia
Lorcaserin	5HT2C receptor activation	10 mg twice daily	FDA (2012)	3.2–3.6 kg/ year	Headache, nausea, dizziness
Naltrexone/ bupropion	Dopamine and noradrenaline reuptake inhibitor (bupropion); Opioid receptor antagonist (naltrexone)	32 mg/360 mg 2-tablets Four times daily	FDA (2014) EMA (2015)	4.8% body weight per year	Nausea/ vomiting, headache, dizziness
Liraglutide	GLP-1 receptor agonist	3.0 mg injection once daily	FDA (2014) EMA (2015)	5.9 kg/year	Nausea, vomiting, pancreatitis

The activity of Δ 9-tetrahydrocannabinoid (9-THC), exogenous cannabinoid leads to the development of an endocannabinoid (EC) system, which includes EC ligands, receptors, and synthetic and catabolic enzymes (André and Gonthier, 2010). The EC system interacts with the hypothalamus circuit, which stimulates energy balance. As a result, the FDA rejected Rimonabant (Sanofi-Aventis, Paris, France), a CB1 receptor antagonist that caused weight reduction and reduced consumption due to psychiatric side effects (Cota et al., 2009, Holst et al., 2009). The drugs approved for weight loss in obesity were mentioned in Table 1.4.

The proglucagon gene produces an incretin hormone in the intestinal mucosa in response to meal consumption (Baggio and Drucker, 2007). The posttranslational proteolytic products of this hormone include glucagon-like peptide-1 (GLP-1) and glucose dependent insulinotropic polypeptide (GIP) (Holst et al., 2009). Dipeptidyl peptidase IV rapidly inactivates GLP-1 in the bloodstream (DPP-4). The GLP-1 analogues resistant to DPP-4 are exenatide (Amylin Pharmaceuticals, San Diego, CA and Eli Lilly & Co., Indianapolis, IN, USA) and liraglutide (Novo Nordisk, Inc., Princeton, NJ, USA). DPP-4 inhibitors such as sitagliptin (Merck & Co., Inc) and saxagliptin (Bristol Myers Squibb, New York, NY, USA) assist in raising endogenous incretin levels (Kim et al., 2010). Oxyntomodulin, a product of intestinal mucosa cells, has also suppressed appetite. TKS1225, an oxyntomodulin analogue derived from intestinal mucosal cells (Thiakis Limited, London, UK), was tested in Phase I clinical studies. Wyeth (Madison, NJ, USA), a subsidiary of Pfizer, Inc., has now bought this (New York, NY, USA) (Suzuki et al., 2010, Laferrere et al., 2010).

The FDA rejected Qnexa, a combination of phentermine and the anticonvulsant topiramate developed by Vivus, Inc. (Mountain View, CA, USA). Contrave (Orexigenic Therapeutics, Inc., La Jolla, CA, USA) is an opiate antagonist that combines naltrexone with bupropion (Greenway et al., 2009), a catecholamine reuptake inhibitor and nicotinic antagonist that targets both hypothalamic POMC neurons and the midbrain dopamine neuron reward circuit (Billes and Greenway, 2011). Empatic (Orexigen Therapeutics), a combination treatment of bupropion and the anticonvulsant zonisamide, in phase II clinical trials (Coleman and Renger, 2010, Cox et al., 2010). On the other hand, Transtech Pharma, Inc. (High Point, NC, USA) has completed phase II clinical trials with an AgRP antagonist (Yao and MacKenzie, 2010).

The combination of fenfluramine and phentermine, which releases serotonin and catecholamines, has proven to be an efficient weight-loss medication. However, Fen-Phen was taken off the market due to its adverse side effects including hypertension and cardiovascular dysfunction. Sibutramine (Abbott Laboratories), a nonselective 5HT and noradrenergic inhibitor, has been found to help people lose weight (James et al., 2010). However, this medicine has been taken off the European market due to its numerous adverse effects, the most common of which is cardiovascular disease (Yao and MacKenzie, 2010).

Tesofensine, a serotonergic reuptake inhibitor currently in phase III clinical trials (NeuroSearch A/S, Ballerup, DK), has shown efficacy in animal studies (Astrup et al., 2008). Another novel agonist, lorcaserin (Arena Pharmaceuticals, Inc., San Diego, CA, USA), has been identified to have specific agonist of 5HT2cR in obese or overweight patients with no cardiovascular issues (Pollack, 2010). Neurons expressing MCH or orexins are numerous in the hypothalamic location. The injection of an MCH-1 receptor antagonist resulted in a reduction in body weight and increased energy output. AMRI (Albany molecular research Inc, CURIA NY: recently renamed as CURIA in 2021) has started a Phase I clinical trial for an MCH-1 receptor antagonist (ALB-127158) for anti-obesity therapy (Chee et al., 2011). Actelion Pharmaceuticals, Ltd (San Francisco, CA, USA) and GlaxoSmithKline plc (Brentford, UK) completed Phase III clinical trials to treat sleeping disorders using Almorexant, an orexin-receptor antagonist. MK-4305, an orexin receptor antagonist produced by Merck & Co., Inc., targets sleep disturbances and anti-appetite effects (Cox et al., 2010, Coleman and Renger, 2010). A list of other drugs targeting satiety or appetite regulation is described in Table 1.5.

Table 1.5: Potential compounds for obesity treatment that can regulate appetite through AgRP and POMC neurons. The data has been modified from Vohra 2022 (Muhammad Sufyan Vohra 2022). where ↑- indicates increase and ↓- indicates decreased activity.

Name	Description	Mechanism	Comments
S-2367 and S-234462	Novel NPY-Y5 antagonist	↓ Body weight ↓ Food intake	S-234462 showed higher efficacy
Phenethyl isothiocyanate (PEITC)	Isothiocyanate compound found in vegetables	↑ Leptin signalling ↑ JAK-2 ↑STAT-3 ↑ POMC ↓ Food intake ↓ AgRP/NPY	PEITC prevents and improves obesity conditions
Flaxseed polysaccharide (FP)	Non-starch polysaccharides	↓ Body weight ↓ NPY ↑ GLP-1 ↓ LR ↑ AMPK signalling	FP shows promising anti-obesity effects by enhancing lipolysis, FAO, and suppressing lipogenesis
2,4-dinitrophenol (DNP)	Organic compound for uncoupling oxidative phosphorylation	↓ Food intake ↓ NPY ↑ POMC ↑ Weight loss ↑ BAT and WAT browning	DNP displays central anti-obesity action and highlights the potential role in targeting metabolic disorders
Bisphenol A (BPA)	Endocrine-disrupting agent	↑ AgRP ↑ ATF3	BPA dysregulated AgRP via involving ATF3 mechanism CBD shows anorexigenic role
Cannabidiol (CBD) and cannabigerol (CBG)	Terpenophenol isolates of *Cannabis sativa*	↑ ATF3 ↓ POMC ↓ NPY ↓ Dopamine (DA) release	LPS suppresses feeding activity

		↓ Norepinephrine (NE) synthesis	
Lipopolysaccharide (LPS)	Gram-negative bacteria membrane	↓ NPY ↓ AgRP	
Long chain fatty acids (LCFAs)		↓ POMC ↑ NPY	LCFAs in the cerebrospinal fluid exert an orexigenic role to regulate energy homeostasis
Saponin extract of Korean Red Ginseng (Rb1, Rd, Rg1, or Re)	Supplemental drug for physical and mental voiding symptoms	↓ Body ↓ Leptin ↓ Nitric oxide (NO) ↓ NPY ↑ CCK	Ginsenoside Rb1 displays an anti-obesity effect
Lorcaserin	5-HT2C receptor agonist drug	↓ NPY ↓ AgRP ↑ MC3/4 ↑ POMC ↑ CART	Lorcaserin approved as an anti-obesity drug
Naltrexone/bupropion	Opioid antagonist/anti-depressant drug	↓ NPY ↓ AgRP ↑ MC3/4 ↑ POMC ↑ CART	Approved anti-obesity drugs
α-2 adrenergic agonist clonidine (CLO)	Adrenergic agonists agent	↑ C-fos in ARC and PVN ↑ POMC ↑ Non-POMC	CLO impacts neuronal activity in ARC and induces homeostatic response via food intake
Baclofen	Muscle relaxer and an antispasmodic drug	↓ Body weight ↓ Food intake ↓ WAT ↑ Adiponectin ↓ Blood glucose and HbA1c ↓ NPY ↑ POMC	Baclofen identified as a new therapeutic agent against obesity
Peanut skin extract (PSE)	Herbal medicine to treat conditions including haemophilia and hepatic haemorrhage	↓ Body weight ↓ Food intake ↓ SREBP-1c ↓ Fatty acid synthase (FAS) ↓ AgRP/NPY ↑ Leptin signalling	PSE can be developed as functional medical food to treat metabolic associated disorders
Whole grain-like structural form (WGLSF)	Dietary fibre	↓ Body weight ↓ WAT ↓ SREBP-1C ↓ FAS ↑ AMPK signalling ↑ POMC ↓ NPY	WGLSF may increase EE and reduce body weight gain
Phloretin	Agent found in apples, pears, and other fruits	↑ Food intake Phloretin ↑ Ghrelin ↓ miR-488 and miR-103 ↑ AgRP ↑ NPY ↓ POMC	Phloretin increases feeding via ghrelin signalling
Grape-seed PAC extract (GSPE)	Bioactive food compound extract found in fruits and vegetables	↓ Food intake ↑ STAT-3 ↑ POMC ↓ Leptin resistance ↓ Hypothalamic inflammation	GSPE exerts anti-obesity effects.

		↑ SIRT-1	
Cinnamaldehyde (CIN)	Compound found in commonly used spice used in cooking	↓ Food intake ↑ TRPA1 and InsR ↓ Body weight ↑ Glucose tolerance ↑ FAO	CIN shows anti-hyperglycaemic and anti-obesity effects
Orange juice extract (OJe)	Flavonoid-rich extract of Citrus sinensis	↓ Body weight ↓ BMI ↓ Adipocytes cell size ↑ POMC ↓ NPY	OJe reduces obesity via lipolytic action and central signalling
Red grapes or cherries extract	Polyphenol-rich fruits extract	↓ Food intake ↑ EE ↑ POMC ↓ AgRP ↓ PTP1B ↑ leptin signalling	Consumption of seasonal fruits influences energy homeostasis and obesity
Green tea polyphenols (GTP)		↓ Body weight ↓ Food intake ↓ Nr3c1 ↓ AgRP ↓ IL-1β _and Ins1	GTP exerts anti-obesity effects
Evodiamine (Evo)	Alkaloidal component extract of Evodiae fructus fruit	↓ Food intake ↓ Body weight ↓ NPY ↓ AgRP	Evo shows anti-obesity actions
Anthocyanins	Secondary metabolite of flavonoids	↓ Body weight ↓ Food intake ↓ AT size ↓ NPY ↑ GABAB1 receptor	Anthocyanins have an anti-obesity effect
Ciliary neurotrophic factor (CNTF)	Interleukin-6 cytokine protein	↓ Food intake ↑ Leptin signalling ↑ JAK-2-STAT-3 pathway ↓ NPY	CNTF shows anti-obesity effects via exerting leptin-like action
RVD-hemopressin-α	N-terminally extended form of haemoglobin α _chain-derived peptide	↓ Food intake ↑ Locomotor activity ↓ POMC ↓ AgRP	RVD-hp-α _treatment shows an anorexigenic action
Liver kinase B1 (LKB1)	Serine/threonine kinase	↑ Food intake ↑ Obesity phenotype ↑ LR ↑ hypothalamic inflammation ↓ POMC	LKB1 displays significant action in regulating energy homeostasis
C1q/TNF-related protein-4 (CTRP4)	Unique secreted protein belongs to C1q adipocytokine superfamily	↓ Food intake ↑ POMC ↓ NPY ↑ STAT-3 pathway	CTRP4 may help in preventing obesity by attenuating feeding
Amyloid-beta (Aβ) peptides	Peptide found in Alzheimer's disease (AD)	↓ Leptin signalling ↑ Allosteric binding to LepR ↑ Inhibitory effects of leptin binding via STAT-3, AKT and ERK ↓ POMC	Preventing interaction of Aβ _with LepR shows improvement in both metabolic and cognitive dysfunctions in the AD condition
Liraglutide	Analogue of glucagon-like	↑ POMC ↓ AgRP/NPY ↓ AMPK signalling	Liraglutide found as a critical regulator of energy balance

	peptide- 1 (GLP-1) hormone		
Exendin-4 (EX-4)	GLP-1 receptor agonist	↓ Food intake ↓ Body weight ↑ POMC ↑ PI3K-AKT ↑ IRS-1 activity	EX-4 shows anti-obesity effects via insulin and PI3K signalling in the ARC
Mothers against decapentaplegic homolog 7 (Smad7)	SMAD family of TGFβ _superfamily of ligands	↑ POMC ↓ AKT ↓ Insulin signalling	Smad7 disrupts glucose balance in POMC neurons by reducing insulin signalling
Des-fluoro-sitagliptin (DFS)	Dipeptidyl peptidase (DPP)-4 inhibitor	↓ Body weight ↓ WAT ↑ BAT ↑ PPAR-α, PGC-1, and UCP ↑ POMC	DFS shows anti-obesity activity
Fluoxetine (FLX)	Serotonin reuptake inhibitor (SSRI) protein	↑ POMC ↓ AgRP/NPY	FLX treatment results in improved energy balance
FAM19A5	Cytokine-like protein	↑ Anorexia ↓ Body weight ↑ C-fos expression ↑ POMC ↑ Inflammatory factors	FAM19A5 found as a critical regulator in hypothalamic inflammatory responses
α7nAChR	α7 subunit of the nicotinic acetylcholine receptor	↓ Food intake ↑ POMC ↓ AgRP ↓ NPY ↑ p-AMPK ↑ JAK-2-STAT-3	α7nAChR exerts anti-obesity effects via suppressing orexigenic markers AgRP and NPY and increasing expression of anoorexigenic markers like POMC
Corticotropin-releasing factor (CRF)	Neuropeptide of hypothalamic-pituitary-adrenal system	↓ Food intake ↑ C-fos in ARC, DMN, VMN, PVN ↓ NPY-R1 ↓ NPY ↓ AgRP ↑ CRF Receptor-2	CRF shows an anorexigenic effect
Spexin (SPX)	Novel endogenous neuropeptide	↓ Food intake ↓ Body weight ↑ p-CaMK2 ↑ c-Fos expression ↓ NPY	SPX treatment reveals anti-obesity effects
Agmatine	Endogenous biogenic amine neurotransmitter	↓ Food intake ↑ Insulin level ↑ IRS-2 ↑ MC4R ↓ AgRP ↓ NPY	Agmatine displays anorexigenic effects in fish
NNC0165-1273	Modified analogue of PYY3-36 gut produced hormone	↓ Ghrelin-induced feeding ↓ Food intake ↓ Body weight ↓ AgRP/NPY ↑ NPY-Y2	Modification of PYY3-36 may be useful for the treatment of obesity
Melatonin	Circadian hormone secreted by pineal gland	↓ Food intake ↓ Body weight ↓ Visceral and subcutaneous AT ↑ POMC ↑ EE ↓ Ghrelin signalling	administration of melatonin through gelatin capsules in water showed reduced food intake in zebra fish

		↓ NPY	
Calcitonin receptor (Calcr)	Hormone produced by parafollicular cells of thyroid gland	↑ Food intake ↑ Hyperphagic obesity ↑ NPY ↑ AgRP ↑ GABA	Calcr plays a crucial role in control of feeding and energy balance via leptin
Obestatin	Peripheral hormone synthesized in GIT tract	↑ NPY/AgRP in MBH ↓ NPY in ARC and PVN ↑ POMC/CART in MBH ↑ GPR-39	Obestatin transmits nutritional signals to hypothalamic neuronal network for appetite regulation by antagonistic-anorexigenic effect
Irisin	Muscle-derived hormone acts in different organs and tissues to improve energy homeostasis	↑ CART ↑ POMC ↑ NPY ↑ BDNF	Irisin may have ability to increase the expression of anorexigenic and neurotrophic genes
Amylin	Pancreas-derived hormone co-secreted in response to a meal together with insulin	↑ POMC ↓ NPY	Amylin may act directly on POMC and NPY neurons to affect energy homeostasis
Chemerin	Recently identified adipokine	↓ Body weight ↓ AgRP ↓ Orexin A ↑ CART ↑ NPY ↓ Food intake ↑ Serotonin synthesis and release	Chemerin displays an anorexigenic effect by increasing 5-HT synthesis and release in hypothalamus
Vaspin	Visceral AT-derived serpin	↓ Food intake ↓ AgRP ↓ NPY ↑ POMC	Vaspin shows an anorexigenic effect
vBLOC® _Therapy	Intra-abdominal electrical device	↑ CCK ↑ Somatostatin ↑ Tyrosine hydroxylase ↑ AgRP/NPY ↓ CCK ↓ MC4R ↓ Insulin receptor	vBLOC therapy induces satiety via vagal signalling, and reduces food intake and body weight
Auricular electric stimulation (AES) therapy	Electric stimulation at exterior margin of the auricle	↑ Food intake ↑ POMC ↑ EE ↑ UCP-1 ↑ Tyrosine hydroxylase ↓ AgRP/NPY	AES therapy reduces weight loss via inducing WAT browning and suppressing appetite

1.4 Obesity and energy expenditure:

Energy is used to run biological functions in the human body. Total energy consumption is divided into three categories: (a) resting energy expenditure (REE), which is used for ventilation, circulation, cell syntheses, and other biological activities; (b) activity-related energy expenditure, which is used for physical exercise and non-exercise thermogenesis; and

(c) diet-induced thermogenesis, which is caused by the digestion and processing of macronutrients (Theilade et al., 2021). The principal regulator of metabolic rate is thyroid hormone signalling, which is regulated by a thyroid-stimulating hormone from the pituitary gland and affects energy expenditure through central and peripheral channels (McAninch and Bianco, 2014). The thyroid hormone active form T# exerts its effects on various tissues after attaching to the thyroid hormone receptor, with the hypothalamus coordinating the NPY neurons to stimulate AgRP mediated appetite signalling (Apfelbaum et al., 1971). The REE accounts for 60% to 70% of total energy expenditure, with the remaining 30% to 40% going to activity related energy expenditure and diet-induced thermogenesis (Quatela et al., 2016). Diet-induced thermogenesis increases with caloric content and relies on macronutrient composition, whereas physical exercise increases energy expenditure and overall energy consumption (Theilade et al., 2021).

Energy storage is dependent on the difference between total energy intake and total energy expenditure. Humans have considerable variability in total energy consumption and REE, which may be due to intra-individual differences and changes in the complex neuroendocrine system that regulates food intake, eating behaviour, and metabolism (McAninch and Bianco, 2014). Heritable factors account for a substantial portion of individual adiposity variation, and genome-wide association studies have revealed over 100 loci linked to high BMI and abdominal adiposity (Silventoinen et al., 2016). However, these genetic regions only account for around 20% of the variation in BMI among individuals, highlighting the relevance of environmental factors in influencing eating habits and physical activity levels, significant in developing obesity (Aasbrenn et al., 2019). The relationship has been observed between environmental and genetic influences in humans, but how they interact and modify one another is still poorly understood.

Energy expenditure as a strategy to combat obesity is important since it does not obstruct the absorption of key nutrients such as vitamins and minerals. It can be active alone or in combination with caloric restriction measures (Jimenez-Munoz et al., 2021).

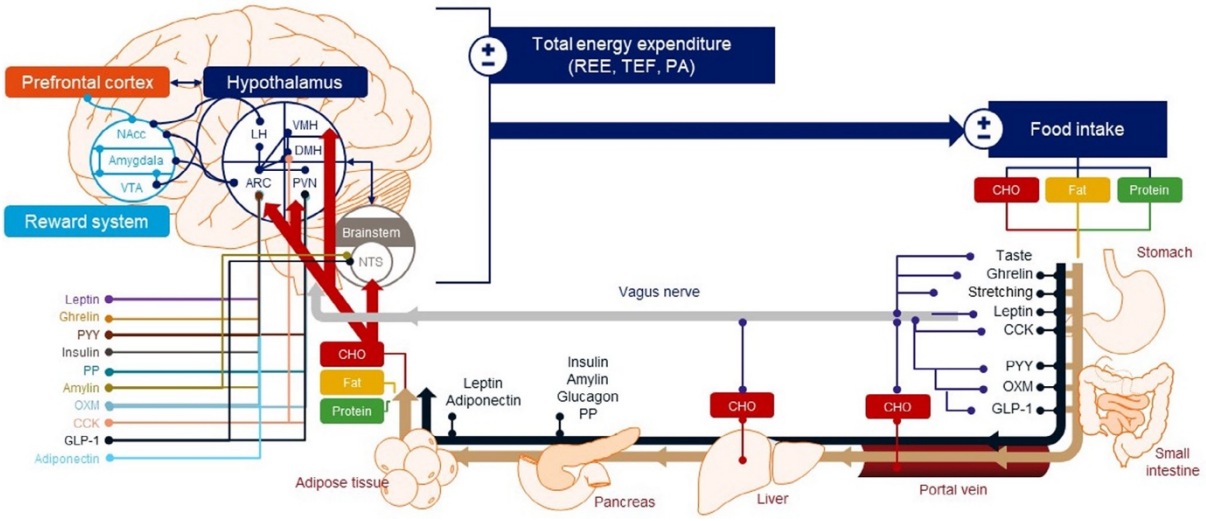

Figure 1.2: Different systemic factors influencing energy homeostasis (Theilade et al., 2021)

Different metabolic processes limit energy preservation in the body as shown in Figure 1.2. the energy is lost as heat and results in weight loss. When there is a significant energy loss, the process is uncoupled (UC) (Tseng et al., 2010). Due to cation leakage along concentration gradients, thermogenesis is possible in most tissues due to uncoupled mitochondrial activities. Increased ATP hydrolysis results from cation leakage, and heat is generated due to this action (Betz and Enerbäck, 2018). For instance, calcium cycling is involved in non-shivering thermogenesis in muscle. During muscle relaxation, the sarcoplasmic reticulum Ca^{2+}-ATPase (SERCA) is a calcium pump found in the sarcoplasmic reticulum and brown adipose tissue (BAT) (Kazak et al., 2015). Sarcolipin therapy decouples ATP hydrolysis from calcium cation transportation, resulting in a heat producing Ca^{2+} cycle (Harper et al., 2008). The creatine cycle has recently been identified as a novel process linked to thermogenesis in beige adipocytes (Nakamura and Nakamura, 2018).

Small compounds called protonophores or chemical uncouplers (like 2,4-dinitrophenol) can uncouple oxidative phosphorylation, compelling the TCA cycle to run faster and produce heat, like uncoupling protein 1 (UCP1). Protonophore therapy causes an increase in energy expenditure that can be prolonged without resistance (Tseng et al., 2010). The central nervous system regulates thermogenesis, and when it is stimulated, it can cause UCP1 overexpression. The melanocortin-4 receptor (MC4R) in the dorsomedial hypothalamus has a role in the regulation of thermogenesis. An increase in BAT- UCP1 mRNA is found after the injection of an MC4R agonist (Jimenez-Munoz et al., 2021). Moreover, thermogenesis is influenced by hormonal control in the hypothalamus. Leptin promotes sympathetic nerve activity, which

increases energy expenditure in interscapular brown adipose tissue and regulates appetite (Chellappa et al., 2019). Leptin resistance can contribute to obesity, although leptin restoration may help to restore leptin sensitivity and help people lose weight.

Gut-derived hormones are linked to eating behaviour, energy consumption, and glucose homeostasis in humans. The interruption of some of these endocrine pathway systems has been considered pathogenetically involved in the development of obesity (Farooqi and O'Rahilly, 2009). The gastrointestinal system consists of many enteroendocrine cells, which emit more than 50 distinct hormones, some of which have been linked to regulation of food intake. They usually circulate through the bloodstream to their target organs/tissues and act on specific G protein-coupled receptors. Many gut-derived hormones linked to appetite regulation interact with specific receptors in the brain's appetite-regulating centres (Jimenez-Munoz et al., 2021). In human trial investigations, antagonists of the receptors that some of these hormones operate on (e.g. glucagon, glucose-dependent insulinotropic polypeptide (GIP), glucagon-like peptide1 (GLP-1) and cholecystokinin (CCK)) have been used to determine the effects of endogenous hormones (Neseliler et al., 2017). However, the interpretation of research using receptor antagonists to delineate appetite regulation is complicated by problems such as the duration of receptor antagonization, insufficient receptors affinity and specificity, and unknown biological compensatory or counter-regulatory processes.

To manage eating behaviour and body weight homeostasis, various signals from nutrients, hormones, neuropeptides, and autonomic afferent nerves converge in the brain. These signals influence several neuronal circuits in the brain that have developed to sense the hedonic, motivational, and metabolic qualities of foods and regulate eating behaviour (Hall et al., 2022). The reward system functions as a key neural stimulus integrator. Typically, the reward system encourages desires, resulting in fitness-related behaviour, such as increased food intake. As a result, the reward system's neuronal circuit identifies and combines motivation, desire, and pleasure (Sarma et al., 2021). The reward system communicates via glutamatergic, dopaminergic, and orexinergic neurotransmitters between the prefrontal cortex, basal ganglia, brainstem, hippocampus, hypothalamus, and amygdala (Vohra et al., 2021). Oxytocin and melanocortin are two important neurotransmitters that regulate metabolism and eating behaviour, and the vagal nerve connects the gut to the reward centre (Klement et al., 2017). Adipokines like leptin and adiponectin regulate long-term body weight homeostasis, whereas short-term satiety signals from several gut hormones drive meal-to-meal appetite regulation

(McCormack et al., 2020). Human fMRI research has discovered an appetite network in which neural activity in response to visual or olfactory food signals represents hunger and energy balance (Zhang et al., 2013). The anterior, tuberal, and mammillary hypothalamic areas are key anatomical regions of the hypothalamus involved in energy homeostasis (Yuan et al., 2020). The hypothalamus-tuberal region includes the ARC, the ventromedial nucleus (VMN), the paraventricular nucleus (PVN), the dorsomedial nucleus (DMN), and the lateral hypothalamus (LH). According to recent research, the hypothalamic ARC nuclei and their neurons are the cornerstones of neural circuits that oversee the body's energy needs (Blevins et al., 2016). The ARC aids in the identification of the melanocortin system, which is known as the first-order centre in energy homeostasis and is involved in the mechanism of energy balance (Lawson et al., 2020).

Oxytocin is a neurohormone produced by the pituitary gland, with receptors found throughout the human body. The oxytocin also stimulates β-cell function, and exogenous oxytocin have been demonstrated to reduce food intake and body weight in obese people (Stock et al., 1989). Exogenous oxytocin enhances thermogenesis and decreases food intake in rodents, resulting in weight loss. Oxytocin levels are higher in fat people than lean people, and oxytocin levels drop after the Roux-en-Y gastric bypass technique (RYGB) (Stock et al., 1989). Synthetic oxytocin is frequently used to induce uterine contractions during labour and postpartum bleeding. The effects of oxytocin are being studied in obese adults and adolescents with hypothalamic obesity (NCT03043053) (McCormack et al., 2020). However, oxytocin-based drugs are not available commercially to treat obesity. In response to insulin and leptin, the pituitary prohormone POMC is converted to MSH, also known as melanocortins. The melanocortins bind to melanocortin receptors (MCRs) in the hypothalamus in the brain (Varela and Horvath, 2012). MSH reduces AgRP synthesis, raises REE, and decreases food intake when it binds to hypothalamic MCRs. AgRP, on the other hand, serves as an antagonist to the MCRs released by NPY neurons, increasing food intake, and decreasing REE (Blevins et al., 2016). Neurotensin is another neuropeptide discovered in the central nervous system. Neurotensin is considered as an anorexigenic neuropeptide based on findings from animal studies; when injected directly into the rodent brain, it accelerates stomach emptying and decreases food intake in rats (Ratner et al., 2016). The peptide neurotensin is released by enteroendocrine N cells in response to food intake, but it may also be secreted by a subset of L cells together with GLP-1 and PYY. Although the precise metabolic role of neurotensin in humans is unknown, neurotensin analogues are being produced to treat obesity (Ratner et al., 2019). In humans,

postprandial levels of neurotensin rise following RYGB, like L cell-derived hormones, but the metabolic significance is unknown (Ratner et al., 2016).

The expression of POMC is abundant in the pituitary, where its products are secreted into the bloodstream, and the hypothalamus, where POMC-derived peptides operate as neuropeptides (Tran et al., 2022b). Endorphins like endorphin, corticotropins like adrenocorticotropin (ACTH), and melanotropins such as, MSH are among the biologically active POMC products (Lama et al., 2022a). Many of these peptides come in different forms, such as the truncated and variably acetylated versions of endorphin (Ehrhart et al., 2018). The ACTH-derived peptides MSH and corticotropin-like intermediate lobe peptide (CLIP) are predominant in the hypothalamus and intermediate pituitary, respectively. POMC-expressing neurons are not uniform and exhibit a wide range of characteristics. While many POMC-processing events are conserved in mammals, there are some processing variations among species (Vohra et al., 2021). β-MSH, for example, is a key human product that is expected to be produced in various other animals, including rodents (e.g., guinea pigs, rabbits, chinchillas). However, not all rodents have β- MSH because the Lys-Lys cleavage site is absent in some species (e.g., mice, rats, and hamsters) (Sarma et al., 2021).

POMC-derived peptides primarily exert their effects through the actions of two types of receptors: MCRs and endorphin/opioid receptors. There are five different melanocortin receptors, each with its own set of functions and tissue distribution (Quarta et al., 2021). Except for MC2R, which is expressed primarily on the adrenal medulla and binds exclusively to ACTH, all other MCRs bind to (α- and β-) MSH peptides and ACTH, with minor affinity differences (Zhang et al., 2004). Only MC3R and MC4R are highly expressed in the brain, with MC4R being particularly abundant in hypothalamic areas linked to food and weight management (Lindberg and Fricker, 2021). In addition to ACTH and α- MSH, the version of MSH that lacks the acetyl group (des-acetyl MSH) has a high affinity for MC4R. POMC knockout mice develop adult-onset obesity due to increased eating and metabolic alterations that lower energy expenditure (Guillemot-Legris and Muccioli, 2017). Mutations in the human POMC is causing defects in formation of α- and β- MSH. Further, this condition leading to alternations in satiety signalling and triggering weight gain (Parande et al., 2022). While α-MSH plays a significant part in body weight management in mice and rats, β- MSH has a more considerable function in humans and other animals.

On the other hand, many animal (mice and rat) models have shown POMC gene and protein expression elevation, resulting in physiological compensation and increased quantities of bioactive melanocortin and/or prolonged precursors (Parande et al., 2022). It is also worth noting that some research focuses on pituitary α-MSH, while other research looks more broadly at hypothalamic α- MSH. A third complication is that commercial radio-immunoassays may not discriminate between extended versions of α- MSH and α- MSH (Kirwan et al., 2018). However, recent developments like peptidomics can detect both forms of MSH (e.g., des-acetyl-MSH, C-terminally-extended MSH). Finally, the energy condition of the body influences the activity of POMC neurons (Fricker et al., 2021). Indeed, as systemic energy levels drop (fasting), POMC messenger RNA (mRNA) expression, and POMC peptide release, were decreased. The use of fibre photometry (by optical canula insertion) and Optetrode electrophysiology (muti channel electrode array insertion) in real-time have shown spiking AgRP neural activity in conscious mice within 1–2 h after the stimulus (Harno et al., 2018). After displaying ordinary chow or palatable food to POMC-ChR2 mice, but before the meal is ingested, rapid activation is identified with food-related sensory cues. Several hours of POMC neural stimulation did not affect food consumption. Persistent neural stimulation (from 24 h to multiple days) is necessary to see the classic appetite-reducing effect (Lindberg and Fricker, 2021).

Insulin, leptin, and serotonin (among others) are extracellular messengers that may impact overall energy balance by acting on various POMC neuronal subpopulations (illustrated in Figure 1.3). POMC cells that express the leptin receptor (LepR) form a molecularly different cluster compared to POMC neurons that express the serotonin receptor 5HT2cR or the insulin receptor, according to single-cell transcriptome data. Systemic glucose control and systemic leptin production are also affected in mice with postnatal LepR ablation. Postnatal deletion of the 5HT2cR protein product in POMC neurons, on the other hand, stimulates hyperphagia, increases glucagon release, and favours diet-induced obesity (DIO) (Quarta et al., 2021).

POMC neuronal activity can alter behavioural and physiological responses related to survival, such as stress, pain, fear, and movement. According to POMC neuronal heterogeneity, different POMC neuronal clusters may have evolved to override potential anxiogenic sensations and painful or even fearful situations that limit locomotion and undermine food acquisition (Lindberg and Fricker, 2021). POMC-ARC neurons are activated by chronic restraint stress or an acute injection of a vehicle solution in mice, which inhibits dopamine neurons in the ventral

tegmental region. In persistently stressed mice, photo-inhibition of the POMC-ARC–ventral tegmental region circuit improves body weight and food intake while lowering depression-like behaviours and anhedonia (a deficit in the ability to experience pleasure) (Quarta et al., 2021).

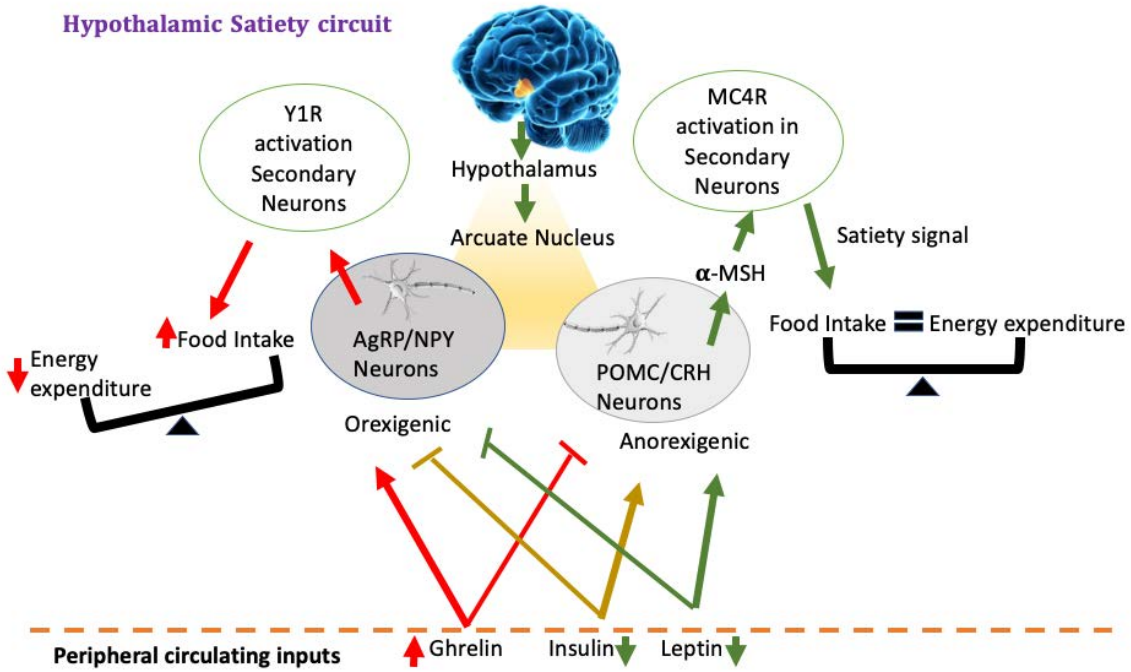

Figure 1.3: Conceptual representation of hypothalamic circuits in energy balance

The LepR-deficient animals do not respond to leptin's hypertensive and sympathomimetic effects. These LepR-positive POMC cells may elevate blood pressure and heart rate via top-down mechanisms (presynaptic neuron stimulus) in response to leptin action (Shi et al., 2020). On the other hand, other subpopulations might have the opposite effect on the heart, as continuous chemo-genetic activation of POMC neurons lowers blood pressure (Hall et al., 2022). As a result, numerous subsets and diverse processes may be able to integrate emotional, cardiovascular, and behavioural outcomes related to food foraging. This evidence shows that POMC neurons may have been programmed to coordinate a more extensive range of biological responses than energy balancing during mammalian evolution (Wu et al., 2021). Genetic attempts to treat POMC neuronal dysfunction in DIO mice have resulted in phenotypic differences. DIO triggers inflammatory biological pathways that may impair neural function (Quarta et al., 2021). IkB kinase-β (IKK-β: a proinflammatory nuclear factor activator) ablation in POMC neuronal cells does not prevent DIO but reduces obesity-induced hypertension (Purkayastha et al., 2011); the specific POMC subsets have been linked to cardiovascular system modulation. Physical activity, energy expenditure, and DIO sensitivity vary between

mice, influenced by subpopulations of POMC neurons that express 5HT2cRs (Jais and Brüning, 2017).

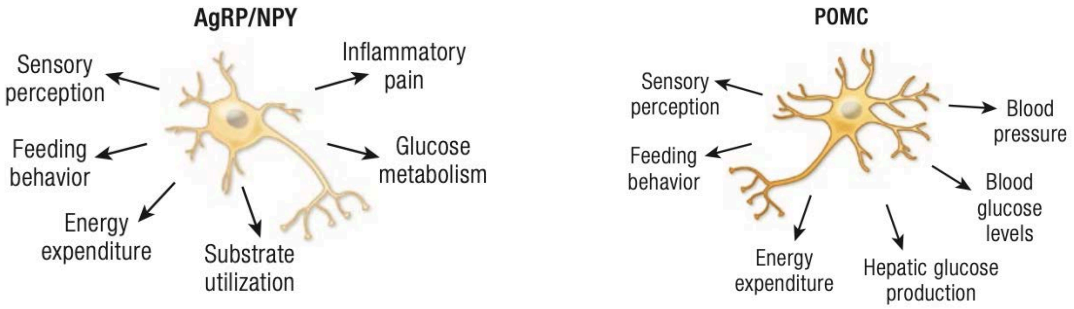

Figure 1.4: Functional aspects of AgRP and POMC neurons involved (Heksch et al., 2017)

Early research focused on the ablation and silencing of AgRP/NPY neurons to determine their involvement in eating behaviour. The ablation of AgRP/NPY neuron in adults caused ablation, whereas in neonates had minimal effect on feeding (Luquet et al., 2005). Ablation or silencing of AgRP/NPY neurons can result in anorexia and rapid weight loss (Vohra et al., 2021). In other investigations, sustained AgRP/NPY neuronal stimulation resulted in a significant rise in AgRP neuronal peptide expression in transgenic obese mice. Food foraging, food hoarding, and food intake were all increased when central AgRP and/or NPY were administered (van Galen et al., 2021). As a result, AgRP/NPY neuropeptides appear to be accountable for and engaged in developing obesity-related symptoms (Vlaardingerbroek et al., 2021). External activation of AgRP/NPY neurons using a photo-stimulus of channelrhodopsin-2 (ChR2) resulted in instantaneous coordination of the neurons and a feeding response within minutes of activation. The essential neuronal populations with the closest and most robust relationship with feeding behaviours are AgRP and NPY-producing neurons (Baptista-de-Souza et al., 2022). AgRP is a 50-amino-acid (AA) neuropeptide generated by cleaving a pro-protein after it has been translated, releasing mature and disulphide-rich AgRP (Mavanji et al., 2021). AgRP-expressing neurons detect signals from the circulating hormones leptin, ghrelin, and insulin and respond via axonal projections to numerous various parts of the brain, including LH and PVN. GABA and NPY activities block POMC neurons, while AgRP neurons send lateral projections to many distinct brain locations that correspond to POMC projections (Jais and Brüning, 2021). Recent research has discovered that Syndecans (heparan sulphate moieties) are essential to modify AgRP signalling in the central melanocortin system to promote orexigenic effects (Vohra et al., 2021).

Nonetheless, by modulating the activity of the AgRP neurons, peripheral hormonal signals generated by the body play a significant part in controlling hypothalamic activities for energy balancing. As a result, AgRP is regarded as critical for the regulation of feeding maintenance (Krishnadas et al., 2018). The peptide NPY is a 36-AA NPY, a neurotransmitter that regulates energy homeostasis and fat accumulation in the brain. Therefore, potential anti-obesity medication targets include NPY (subtype Y5) antagonists. Tamura et al. (2012) discovered that oral treatment of an NPY-Y5 antagonist lowered food intake (Tamura et al., 2012), and Tamura et al. (2013) found that repeated administration of NPY-Y5 antagonists had anti-obesity effects in DIO mice without any abnormal behaviour (Tamura et al., 2013). The Figure 1.4 shows basic pathways that are influenced by POMC and AgRP neurons.

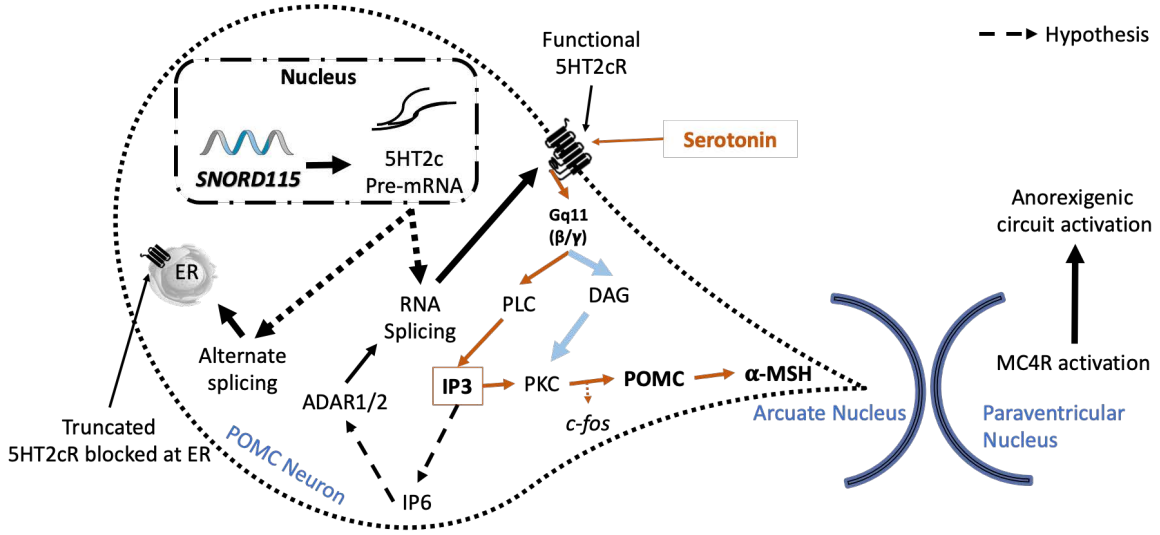

Figure 1.5: Schematic representation of 5HT2cR localisation and pivotal role in POMC neurons, inspired from (Stamm et al., 2017)

In mice, removing POMC from the hypothalamus but restoring its expression in 5HT2cR-positive neurons improved energy expenditure (Crino et al., 2018). Serotonin receptor 2C (5HT2cR) is a G-protein coupled receptor with seven transmembrane domains that regulate essential brain activities such as food intake, anxiety, stress response, and sleep (d'Agostino et al., 2018). In human and rat models of obesity, 5HT2cR are deregulated in depression, schizophrenia, suicidal behaviour, and spinal cord damage (Brandt et al., 2018). Understanding the importance of 5HT2cR in appetite control gave rise to the development of Lorcaserin, an FDA-approved medication for the short-term treatment of obesity that increases 5HT2cR activity (Tran et al., 2022b). Antipsychotic medicines that treat depression, anxiety, and schizophrenia interact with the 5HT2cR, which improves the drug's efficacy but frequently

causes weight gain as a side effect. The 5HT2cR activity in POMC neurons is briefly illustrated in Figure1.5. When serotonin binds to 5HT2cR, the dissociation of the second intracellular loop of 5HT2cR leads to G-protein signal activation. The α- subunit of Gq11 increases the phospholipase-C signal upon dissociation. This signal further leads to activation of IP3 (inositol triphosphate) and diacylglycerol (DAG) expression (Stamm et al., 2017, Pogorelov et al., 2017).

Further, PKC causes c-fos to be phosphorylated by activating the extracellular regulated kinase (ERK) pathway. POMC synthesis is triggered by c-fos activation. POMC is converted to α--melanocyte-stimulating hormone (α-MSH), activating neurons in the PVN through melanocortin 4 receptors. Satiety, or the cessation of eating, is induced by PVN neuron activation. Hyperphagia and obesity are seen in knock-out mice lacking the 5HT2c receptor (Valencia-Torres et al., 2017, Stamm et al., 2017, Ge et al., 2017).

In humans, lean mass (fat-free mass plus muscle mass) is a major predictor of basal metabolism. The ratio of lean mass to total body weight is 60–70% in women and 70–80% in males, according to body size and composition basal metabolic rate and sleeping metabolic rate varies; which could explain the role of skeletal muscle metabolism in overall energy expenditure (Chen et al., 2020). Skeletal muscle metabolism influences baseline metabolism, but it also influences adaptive thermogenesis, such as CIT (Cold induced thermogenesis). Similarly, even in mice fed an HFD, the basal metabolic rate (BMR) is more dependent on lean mass than fat mass. Androgens can augment skeletal muscle, which is controlled by the hypothalamic-pituitary-gonadal axis (Fan et al., 2005). Gonadotropin-releasing hormone (GnRH) boosts the release of anterior pituitary gland luteinizing hormone, which stimulates testosterone synthesis and secretion in the gonads (Clarke et al., 2019). In mice, the androgen receptor in the hypothalamus positively controls fat-free mass, and androgen receptor-null male mice have lower energy expenditure, leading to late-onset obesity (Fan et al., 2005). Erythropoietin is produced in the hypothalamus and kidney diminishes with age and dietary obesity. Central erythropoietin treatment in mice boosts lean mass and muscle function while lowering body weight and fat mass (Tran et al., 2022a, Wang et al., 2020).

In mice, fat mass is another important regulator of metabolic rate: obese mice have a greater baseline metabolism than thin mice (Tran et al., 2022b). A prior study found that leptin-deficient ob/ob mice have no fat mass contribution to energy expenditure, which can be

reversed by physiological leptin replacement. This finding suggests that fat mass contributes to energy expenditure in a leptin-dependent manner (Wang et al., 2020). Despite the relevance of skeletal muscle and fat tissue in basal metabolism, more direct data is needed to determine whether the hypothalamus regulates basal metabolism through lean and fat mass determination. It is difficult to determine the exact relationship between energy expenditure and lean and/or fat mass (Clarke et al., 2019); and how far changes in body mass effect basal energy metabolism in this way (Tran et al., 2022b).

1.5 Importance of 5HT2cR in satiety:

The 5HT2cR belongs to a GPCR family, which includes seven subtypes of serotonin receptors, ranging from 5HT1 to 5HT7 (described in table 1.6). They play a role in various biological processes, including intestinal motility and cognitive functions, as well as mood, appetite, and sleep. Because GPCRs of the same subtype have similar binding sites, a single endogenous ligand can excite multiple GPCR targets simultaneously (Stasi et al., 2014).

Table 1.6: Functional role of individual serotonin receptors(Stasi et al., 2014)

	Signaling Mechanism	**Distribution**	**Effects**
5HT1a	Gi, ↓ cAMP	Raphe nuclei, hippocampus	Regulates sleep, feeding and anxiety
5HT1b	Gi, ↓ cAMP	Substantia nigra, globus pallidus, basal ganglia	Neuronal inhibition, behavioral changes
5HT1d	Gi, ↓ cAMP	Brain	Vasoconstriction
5HT1e	Gi, ↓ cAMP	Cortex, hippocampus	Memory
5HT1e	Gi, ↓ cAMP	Globus pallidus, putamen	Anxiety, vasoconstriction
5HT2a	Gq, ↑ IP_3	Platelets, cerebral cortex	Cellular excitation, muscle contraction
5HT2b	Gq, ↑ IP_3	Stomach	Appetite
5HT2c	Gq, ↑ IP_3	Hippocampus, hypothalamus, substantia nigra	Mood, Anxiety, Satiety
5HT3	Na^+-K^+ ion channel	Area postrema, enteric nerves	Vomiting
5HT4	Gi, ↑ cAMP	Cortex, smooth muscle	Gut motility
5HT5a	Gi, ↓ cAMP	Cortex	Locomotion, smell, sleep
5HT6	Gi, ↑ cAMP	Cortex	Cognition, learning
5HT7	Gi, ↑ cAMP	Hypothalamus, cortex	depression

There are three 5HT2R subtypes among the distinct types of 5HT receptors: 5HT2a, 5HT2b, and 5HT2c. 5HT2aR is widely produced in the brain, particularly in the cerebral cortex and

has been linked to the hallucinogenic effects of substances like lysergic acid diethylamide (LSD) (Fiorino et al., 2017). Schizophrenia and sleeplessness have both been treated with drugs that target 5HT2aR. The 5HT2bR is in the cardiovascular system and linked to deadly valvulopathy, which certain prescription medicines can cause (Fiorino et al., 2017). Drugs or ligand compounds targeting the 5HT2cR have been studied to treat depression, anxiety, anorexia, obsessive-compulsive disorder, chronic conditions, obesity, epilepsy, and erectile dysfunction. The 5HT2cR has different isoforms due to pre-mRNA editing and post transcription modification processes (Pogorelov et al., 2017). The two important forms of 5HT2cR are differentiated based on cellular location: functional 5HT2cR (5HT2cR-fn) appear on the cell membrane, whereas the truncated receptor (5HT2cR-tr) is trapped in the endoplasmic reticulum membrane. As a result of alternative splicing and RNA editing, the 5HT2cR functional activity decreases (Pogorelov et al., 2017). Oligonucleotides can be used to change the ratio of truncated to full-length receptors, allowing for targeted control of 5HT2c receptor activation (Farooqi and O'Rahilly, 2009, Stamm et al., 2017). The 5HT2cR pre-mRNA contains exons I–VI, which are subjected to RNA editing and alternative pre-mRNA splicing. Alternative exon Vb is defined by a proximal and distal splicing site in exon V. Alternative splicing produces two types of RNA: exon Vb free RNA1 and exon Vb containing RNA2. Exon Vb is alternatively spliced in addition to being pre-mRNA edited. RNA1 is the RNA produced when exon Vb is skipped, which causes a frameshift, and an early stop codon in exon VI results in a shortened protein (5HT2c-tr) with three transmembrane domains (Stamm et al., 2017, García-Cárceles et al., 2017). The stop codon lies in the last exon, the mRNA bypasses nonsense-mediated decay, and an antiserum against the 5HT2c-tr specific C-terminus can detect the truncated protein from RNA1 in the brain (Reynolds et al., 2003). Exon Vb and SNORD115, a neuron-specific C/D box snoRNA, have an 18-nucleotide perfect base complementarity (Stamm et al., 2017)

The C/D box snoRNAs (SNORDs) are non-coding RNA that accumulates in the nucleolus and is highly expressed (60–300 bp in length). Half of the known SNORDs are involved in rRNA processing as a guiding molecule for the methyltransferase fibrillarin to rRNA or to pre-rRNAs' cleavage (Stamm et al., 2017). Non-methylating ribonuclear protein complexes containing hnRNPs but without the methylase fibrillarin are formed by SNORD115. As a result, when SNORD115 binds to exon Vb, it promotes exon Vb inclusion (as illustrated in Figure 1.6) in a non-methylating SNORD-complex (Bratkovič et al., 2018). SNORD115 is found in most brain parts but not in the choroid plexus, which lines the ventricles and produces cerebrospinal fluid.

Exon Vb is also mostly contained in all brain areas but not in the choroid plexus, indicating that SNORD115 plays a physiological role in promoting exon Vb inclusion (Ehrhart et al., 2018). Because of pre-mRNA splicing and editing, the 5HT2c gene produces 25 proteins (24 full-length and one truncated isoform), 33 mRNAs, and four miRNAs (Stamm et al., 2017). From Figure 1.6, exon Vb and intron V generate a dsRNA region that is the substrate for ADAR (adenosine deaminase acting on RNA) enzymes, which bind to dsRNA and deaminate adenosine residues, converting them to inosine (García-Cárceles et al., 2017). The A, B, E, C, and D editing sites in exon Vb were discovered by comparing cDNA to genomic DNA (the E site is also known as the C′ site). In comparison to sites C and E, Sites A, B, and D are significantly altered (García-Cárceles et al., 2017).

The examination of ADAR mice knockouts suggests that ADAR1 edits sites A and B, ADAR2 edits sites C and D, and both enzymes edit the E site (Zhang et al., 2016b). In vitro editing tests revealed that the loop opposite the SNORD115 binding site is required for ADAR to be correctly positioned and hence for the editing sites to be recognised. ADAR2 binds Inositol hexa-his-phosphate (IP6) in the enzyme core, essential for ADAR2 activity. Phospholipase C and IP3, which can be transformed to IP6, are produced when 5HT2cR binds to a heterotrimeric G-protein containing Gq/11. Therefore, a feedback loop may influence 5HT2c activity and 5HT2c editing (Stamm et al., 2017). Exon Vb inclusion was not affected by transfection experiments that investigated various splicing factors for their influence on 5HT2c. However, a C/D box snoRNA (SNORD) that binds to the regulated dsRNA structure has been discovered. SNORD115, known initially as HBII-52, is a strong exon Vb activator (Bratkovič et al., 2018, Martin et al., 2013a). SNORD115 was further described to get insight into the underlying process. In humans, there are 47 identical copies of SNORD115. SNORD115, like other C/D box snoRNAs, is found in an intron surrounded by two exons. In the C-terminus of all 5HT2c full-length receptors, a PDZ (postsynaptic density-95 (PSD-95), discs-large, zona occludens 1 (ZO-1): small modular protein entities consisting of 80–110 residues) -ligand motif binds to at least seven different PDZ domain-containing proteins (Jang et al., 2012, Bortolin-Cavaille and Cavaillé, 2012). Unlike the full-length receptor, the shortened receptor lacks a PDZ-ligand sequence, which may explain the discrepancies in membrane attachment and localisation between the full-length and truncated receptors. The 5HT2c-tr cannot bind to a G-protein and does not trigger phospholipase C (PLC) because it lacks the second transmembrane domain. Internal membranes of the endoplasmic reticulum (ER) contain 5HT2c-tr, which is not measurable at the plasma membrane (Morabito et al., 2010, Kishore et al., 2010, Dagher, 2010).

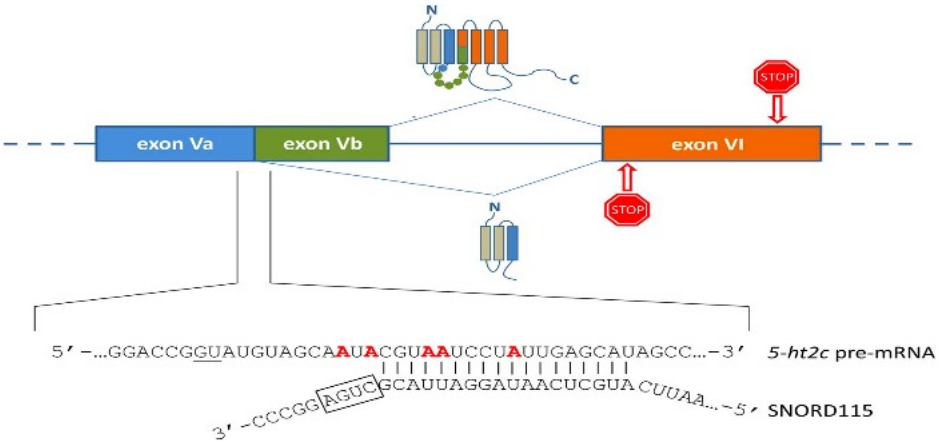

Figure 1.6: The complementary sequence of SNORD115 binding to 5HT2cR pre-mRNA in functional 5HT2cR expression, the absence of SNORD115 binding to pre-mRNA leads to lack of exon VI region and forms the truncated 5HT2cR protein (Stamm et al., 2017)

Furthermore, the editing status of full-length receptors is critical for POMC-neurons signalling, as overexpression of fully edited receptors causes hyperphagia in mice, implying reduced POMC neuron function (Adams et al., 2017, Zhang et al., 2016b). SNORD115 stimulates the production of non-edited full-length receptors, while ADAR1 and ADAR2 causes the formation of edited full-length receptors, as previously stated. Thus, RNA processing of the 5HT2cR regulates food intake in part (Zhang et al., 2016b). A pivotal study focuses on determining how 5HT2c receptor agonists influence food intake regulation and energy metabolism, given that the 5HT2cR is a potential candidate for treating obesity (Garcia-Carceles et al., 2017). Simultaneously, a lot of effort has gone into investigating how 5HT2cR mediated neurotransmission affects forebrain dopamine (DA) systems and networks, which has sparked interest in how modifying 5HT2cR activity affects DA-dependent behaviours (Pogorelov et al., 2017, Huang et al., 2018).

The arcuate nucleus (ARC) of the hypothalamus produces POMC, which is then cleaved into a melanocyte stimulating hormone (α-MSH) when 5HT2cR are activated (McLean et al., 2018). This α-MSH neuropeptide induces satiety by acting on the MC4Rs in the paraventricular nucleus of the hypothalamus. As a result, 5HT2cR agonists are expected to modify metabolic aspects of feeding by acting directly on these hypothalamic circuits (Griggs et al., 2018b, Hassan et al., 2018). However, 5HT2cR agonists are unlikely to affect this element of feeding solely. The impact of 5HT2cR ligands on DA neuronal activity and DA-mediated behaviours

was guided by localisation studies (Ramos-Molina et al., 2018). Serotonin is a primary regulator of DA neuronal activity, both inhibitory and excitatory, and the 5HT2c receptor is a crucial mechanism by which 5HT inhibits DA function (Ramos-Molina et al., 2018, Price et al., 2018). The 5HT2cR agonist lorcaserin is used to treat obesity; however, neither the exact subset of 5HT2cRs that coordinates the therapeutic action nor the neurochemical mediator that these receptors target have been thoroughly characterised (Lindberg and Fricker, 2021, Hebras et al., 2020). Previous genetic manipulation of the receptor indicated that the subset of 5HT2cR co-expressed with brain POMC is both sufficient and essential, given that 5HT2cR agonists boost the activity of POMC-ARC neurons to manage satiety (Jais and Brüning, 2022).

Lorcaserin is the only available specific 5HT2cR agonist that the FDA recognised in June 2012 to treat obesity. The FDA granted approval based on three Phase III trials lasting 1–2 years, each of which contained a dosing arm of 10 mg twice a day and a total patient population of 7789. A meta-analysis of the data found a 3.32 kg weight loss and a 1.16 kg/m^2 reduction in body mass index (BMI) compared to placebo (Aronne, 2019, Tolete et al., 2018). Blood pressure, total cholesterol, low-density lipoprotein (LDL-C), and triglycerides were all found to be improved as secondary outcomes. The most common lorcaserin adverse effects were headache and nausea. According to a systematic review and meta-analysis, lorcaserin is a selective agonist at the 5HT2c receptor with a low binding affinity for 5HT1a and 5HT2b receptors at the prescribed dose (Tchang et al., 2020). Lorcaserin is considered to induce the production of anorexigenic peptides POMC and CART in the hypothalamus by activating 5HT2cR expressed on pro-opiomelanocortin (POMC) and cocaine-and-amphetamine-regulated transcript (CART) neurons (Tolete et al., 2018). POMC neurons have been discovered in the nucleus tractus solitarius (NTS), where 5HT2cR stimulation promotes anorexigenic effects independent of POMC/CART neurons in the hypothalamus arcuate nucleus (Harno et al., 2018). When POMC neurons in the arcuate nucleus were knocked out, this resulted in a muted long-term response to lorcaserin. When POMC neurons in the nucleus tractus solitarius (NTS) were knocked out, this resulted in a blunted acute response to lorcaserin. TrpC5, a cation channel receptor shared with leptin, was involved in the cell signalling process through which 5HT2cR stimulates POMC neurons. TrpC5 subunits are required for POMC-induced hypophagia, weight loss, and better glucose tolerance, and their absence impairs leptin and lorcaserin responses (Phillips et al., 2018).

The 5HT2b receptor has played a significant role in the history of serotonin receptor agonists, despite not being known to regulate hunger directly. The 5HT2bR is located on heart valves, and early investigations on nonselective serotonin receptor agonists like fenfluramine and dexfenfluramine were discovered to cause valvulopathy due to agonistic effects at the 5HT2bR (Ge et al., 2017). Lorcaserin has been found to perform a key role in the meso-cortico-limbic system and its serotonergic actions correlation (Di Giovanni et al., 2020). The lorcaserin reduced risk of cardiac functions in obesity but the rates of valvulopathy, depression, and suicidal risk do not differ between lorcaserin users and those receiving placebo (Vasdeki et al., 2022). When given an HFD, lorcaserin increased 5HT2cR activity in midbrain dopaminergic neurons and attenuated binge-like eating behaviours in a rat model of binge eating disorder (Price et al., 2018). Lorcaserin is one of a few numbers of pharmacotherapies that are effective in treating obesity and associated complications. Polypharmacotherapy is typically necessary to address comorbidities in obese patients due to their high medical complexity (Cheng et al., 2016). Lorcaserin also reduces hepatic gluconeogenesis while increasing glucose disposal rate. Hypoglycaemia has also been mentioned as a possible significant side effect connected with lorcaserin (Tchang et al., 2020, Sutton and Krashes, 2020).

Different lorcaserin clinical efficacy studies include Behavioural Modification and Lorcaserin for Overweight and Obesity Management (BLOOM), Study for Obesity Management (BLOSSOM), Overweight and Obesity Management in Diabetes Mellitus (BLOOM-DM), and Cardiovascular and Metabolic Effects of Lorcaserin in Overweight and Obesity Management in Diabetes Mellitus (CAMELLA-DM). The FDA said earlier in 2020 that its review of the data from the CAMELLIA-TIMI 61 research revealed that 462 patients (7.7%) treated with lorcaserin had cancer, compared to 423 patients (7.1%) in the placebo group (Mathai, 2021). Pancreatic, colorectal, and lung cancer were more common in the lorcaserin group, among the several cancer types described. Therefore, to determine which individuals are likely to be high responders in terms of reaching a significant weight loss benefit, it is necessary to establish parameters that may indicate which individuals are likely to be high responders to achieve a considerable weight loss advantage (Tchang et al., 2020). While the 5HT2cR is a prominent target in obesity, lorcaserin is the only specific agonist molecules that is currently available for use alone or in combination with other anti-obesity drugs. (Patel et al., 2020). One such combination paired the regular dose of lorcaserin (10 mg twice a day) with phentermine (15–30 mg), resulting in more weight loss than lorcaserin alone (Fleming et al., 2013).

1.6 Behavioural changes with high calorie intake and 5HT2cR obligation:

Eating habits are complicated, and both mood and emotions influence them. Mood and emotions, on the other hand, are two different things. In the absence of visible stimuli, psychological arousal is defined by mood, which can endure for several minutes or more (Heisler et al., 2006). On the other hand, emotions are a short-term affective reaction to reinforcing stimuli. A study found that anger and joy have the most significant impact on hunger and food choice of all emotions. Macht's 2008 review, on human behaviour evidence from questionnaires, field investigations, and clinical studies points to an integrative five-way model that predicts five key features of emotional eating (Macht, 2008). The five aspects emotional eating are food choice, food intake, loss of cognitive controls, food-modulating emotions, and binge eating (Macht, 2008). As a result, emotional eating is triggered, where food intake can either grow or decrease within the same individual, depending on the condition of unpleasant emotions or anxiety (Baptista-de-Souza et al., 2022). Food choice, quantity, and meal frequency are influenced by sensory and psychological pathways that may or may not be part of a standard physiological requirement (Macht, 2008). Many psychosomatic theories of obesity claim that obese patients overeat because they cannot sense their physiological state, hunger, and satiety and that overeating relieves emotional distress and anxiety.

Anxiety and depression have an impact on dietary choices and energy metabolism. Obesity and overeating are frequently linked to depression and anxiety in humans, which has also been shown in animal models (Strasser et al., 2016, WHO, 2020). In severe depression, both endocrine and metabolic problems are aggravated. People who are depressed are more, likely to prefer and consume appetising "comfort foods" to help them cope with their unpleasant emotions (Higgins et al., 2017). Although appetising foods can provide some respite from negative emotions and mood states in the short term, persistent consumption of calorie-rich foods leads to obesity, which increases the risk of melancholy and anxiety.

On the other hand, a long-term HFD has been linked to negative affective states, increased stress sensitivity, and changes in basal corticosterone levels (Schachter et al., 2018). As a result, unpleasant emotion influences food selection and intake, affecting mood in a bidirectional manner (Rodriguez and Zigman, 2018). Other interesting changes in mice include decreased pleasure/reward experience, anxiety-like behaviour, and increased stress-induced hypothalamic pituitary adrenal axis (HPA) activity. Furthermore, mice developed a preference

for sucrose and high-fat foods after being exposed to a chronic HFD and then when switched to a regular chow diet, they displayed increased anxiety-like behaviour (Singh, 2014). Finally, when people shifted from a high-fat sugar diet to a low-fat sugar diet, they showed expanded behavioural and physiological indications of despair and anxiety (Martin et al., 2014). These findings indicate that persistent high-fat feeding promotes negative emotional states and potentiates the situation for increased stress sensitivity, leading to a cycle of overeating, weight gain, and depression.

For example, chocolate has a powerful effect on mood, elevating positive sentiments and lowering tension. Chocolate includes psychoactive compounds like amines, which excite the brain and promote contentment. Due to the sensory characteristics involved with chocolate consumption, chocolate's unique taste and feel on the tongue promote chocolate cravings (Osman and Sobal, 2006). Caffeine, which is primarily consumed in coffee and tea, has stimulant effects that increase alertness, attentiveness, and reaction time in susceptible individuals while also increasing anxiety. Omega-3 fatty acids, which can be found in various foods, have been shown to affect mood, behaviour, neuroticism, and impulse control (Crowley et al., 2002).. Diets high in saturated fat and deficient in polyunsaturated and monounsaturated fatty acids have been linked to increased depressive symptoms. Anxiety and mood disorders are more common among obese people (Tidman et al., 2022).

Hypercortisolemic depression, belly fat storage, reduced glucocorticoid-mediated negative feedback, and increased corticotropin-releasing hormone (CRH) release from the paraventricular nucleus are all linked to increased corticotropin-releasing hormone (CRH) release (PVN) (McEwen, 2022). Furthermore, adolescent depression is connected to an increased risk of adult obesity (Handakas et al., 2022). A rudimentary understanding of dopamine-mediated food intake has come from rodent studies. Mice with low dopamine levels die early owing to a lack of motivation for food intake (Nonogaki, 2022). Changes in serotonin 2C receptor (5HT2cR) editing have been linked to dopamine synthesis, reward, mood, eating, and obesity (Xie et al., 2021). Intriguingly, transgenic mice with a dysregulated RNA editing enzyme, ADAR2, show changes in both serotonergic and dopaminergic systems. In ADAR2 transgenic mice, co-morbidities of depression and anxiety behaviours and altered 5HT2cR editing were identified. These findings imply that the changed 5HT2cR in ADAR2 transgenic mice may be connected to co-morbidities of affective illness, overeating, and obesity (Monian et al., 2022). In ADAR2 transgenic mice, post-transcriptional alteration of the 5HT2cR is

linked to changes in mood, food intake, and obesity. Brain-derived neurotrophic factor (BDNF) was demonstrated to have an antidepressant-like effect in another rodent model of depression. The BDNF deficient mice showed with hyperactivity, hyperphagia, and weight gain; BDNF has been a neurotropic modulator on serotonergic neurons (Wan et al., 2020, Pérez-Maceira et al., 2016, Solomon et al., 2013).

The limbic system, which integrates the amygdala with the hypothalamus and septal nuclei, is involved in addiction and spans two main brain regions: (i) the prefrontal area and the amygdala, and (ii) the limbic system, which integrates the amygdala with the hypothalamus and septal nuclei (Koob and Volkow, 2010). Addiction to alcohol and drugs involves neurochemistry and neuroanatomical reward circuitry (Fu et al., 2020), which can be used to develop an addiction model of overeating and obesity. In certain studies, hunger has been shown to alter memory for food-related stimuli, with the orbitofrontal cortex being notably implicated in food-related stimuli in the hungry condition (Hill et al., 2012, Farooqi and O'Rahilly, 2009). Treatments with serotonin potentiating medications reduce depression in seasonal affective disorder, indicating that brain serotonin plays a role in the pathophysiology of depression (Wallace and Fordahl, 2021). Additionally, evolutionary biology in learning and memory may have a role in the development and persistence of anorexia nervosa. Affective disorder, stress, maternal separation, Prader Willi Syndrome (PWS), hyperphagia, and obesity have all been linked to RNA editing of the 5HT2cR (Rebai et al., 2021, Meng et al., 2021, Mavanji et al., 2021, Lindberg and Fricker, 2021, Marin et al., 2020). Through 24 distinct receptor isoforms, RNA editing of the 5HT2cR affects several aspects of serotonin signalling. The fact that these altered 5HT2cR isoforms have varying ratios in different brain regions shows that the 5HT2cR can play a highly variable role in linking mood, food intake, and the development of obesity (Hebras et al., 2020).

One of the most common hereditary causes of morbid obesity and intellectual disability is Prader-Willi syndrome (PWS- a genetic disease) (Dykens et al., 2018). Short stature, severe hypotonia at birth, genital hypoplasia, and distinctive facial traits characterise PWS patients. Loss of paternal allele expression at an imprinted region on chromosome 15q11.2-q13.1 causes PWS, affecting 1 in 10,000 people (Irizarry et al., 2016). Five protein-coding genes (MKRN3, MAGEL2, NECDIN, SNURF-SNRPN, NPAP1/C15orf2) and six orphan C/D box snoRNAs (SNORDs) are expressed only from the paternal allele in the imprinted area that is lacking in PWS: 107, 64, 108, 109, 116 (29 copies falling into five classes) and 115. (47 almost identical

copies). Where, SNORD64 has a role in fear related memory (Leighton et al., 2022) and SNORD116 and 115 (Griggs et al., 2018b) are playing crucial role in appetite regulation in PWS. As previously stated, SNORD115 promotes exon Vb inclusion, which affects the post transcriptional modification of the 5HT2cR-mRNA (Irizarry et al., 2016, Hebras et al., 2020). The targets and functions of the SNORDs that are not found in PWS remain unknown. Mice with the SNORD115 gene overexpressed have autistic characteristics demonstrating that SNORD expression levels must be tightly regulated (Di Giovanni and De Deurwaerdère, 2016). The 5HT2c-tr receptor isoform is increased in POMC neurons in a knockout model for PWS lacking all SNORDs, including SNORD115, as expected by earlier transfection studies revealing that SNORD115 promotes exon Vb inclusion. Because POMC neurons do not efficiently produce c-fos after 5HT2c stimulation, increasing the 5HT2c-tr in these neurons inhibits the anorexic response of these animals (Stamm et al., 2017). The 5HT exhibits downstream connection within hypothalamic pathways - through the 5HT2cR to regulate appetite homeostasis. Serotonin-related pathways are crucial research targets for correcting PWS appetite behaviours (Griggs, 2019, Griggs et al., 2018b).

The modulation of the 5HT2cR via downstream inhibitory pathways such as POMC, α-melanocyte-stimulating hormone (α-MSH) and reward targets such as anticipatory dopamine appetite (Lama et al., 2022a, Wu et al., 2021) are only a few examples. Researchers are targeting 5HT2cR for various psychiatric and obesity treatments due to its function in satiety and eating behavioural factors. Lorcaserin is one such medicine used to treat obesity as a selective agonist for the 5HT2cR receptor (Theilade et al., 2021). Some of the initial insights into the possibility of a 5HT2cR agonist for obesity treatment came from preclinical meta-chlorophenyl-piperazine (mCPP) studies (Jang et al., 2012). However, because it binds to many receptors in addition to the 5HT2cR, this drug is unlikely to find broad application in humans (d'Agostino et al., 2018). The melanocortin system is also implicated in the mechanisms of action of mCPP and other preclinical 5HT2cR agonists (BVT.X and WAY161, 503) on appetite and glycemic control/insulin sensitivity. WAY161, 503 boosts ARC POMC neuronal activity (Wang et al., 2020, Zheng et al., 2020).

According to recent research, in HFD mice, a combination of probiotics and exercise showed synergistic effects on anxiety indicators and obesity (Parande et al., 2022). Animal behaviour investigations in both C57BL/6 mice and ob/ob mice demonstrated increased immobility time in the tail suspension test (TST) (Foroozan et al., 2021), decreased staying time in the middle

square, decreased number of line crossings, and increased faeces in the open field test (OFT) (Patel et al., 2020). Furthermore, it was discovered that *ob/ob* mice demonstrated depression behaviour in the TST and decreased exploratory behaviour and anxiety-like behaviours in the OFT (Foroozan et al., 2021, Braga et al., 2021, McLean et al., 2018). Whereas grape supplementation has beneficial impacts on anxiety-like behaviour and eating behaviour; resulting in improved cognition and memory in HFD fed mice (Parande et al., 2022). Chronic pre-weaning exposure to a high-fat diet (HFD) resulted in increased anxiety-like behaviours in rats, as measured by open-field and elevated plus maze (EPM) testing. In a model of HFD-induced obesity in C57BL/6 mice, adverse effects on mammopoiesis, milk supply, and pup retrieval were also found (Parande et al., 2022). Hence, these studies summarise the importance of behavioural changes related to 5HT2cR expression and HFD exposure.

1.7 Obesity and consequences in cardiac dysfunction:

The impact of a high body mass index (BMI) on chronic diseases is well understood. In studies, hypertension, dyslipidemia, and diabetes have all been linked to excessive BMI (Sarma et al., 2021). However, central obesity was measured by waist circumference, and linked to an increased risk of atherosclerotic cardiovascular disease and may be overlooked if BMI is employed as the sole indicator of obesity (Petrilli et al., 2020). Obesity can have a variety of consequences for chronic illnesses. Exploring the link between obesity and consequent diseases can help guide the rational selection of obesity indicators in the preventive disease process. According to an earlier study, central obesity without general obesity is linked to an increased risk of coronary heart disease (Cercato and Fonseca, 2019). In addition, the development of atherosclerosis is influenced by obesity and increasing adipose tissue. Adipose tissue is classified into two types: white adipose tissue (WAT) and brown adipose tissue (BAT); and is associated with metabolic and inflammatory systems and has protective effects on energy homeostasis (Cercato and Fonseca, 2019). WAT secretes peptides and proteins that affect obesity, insulin resistance, inflammatory and immunological activities, atherosclerosis, and cardiovascular disease via controlling biological and physiological circumstances. Adiponectin is a peptide generated in adipose tissue that is highly expressed in lean, healthy people but gets dysregulated in obese people (Joao et al., 2016).

This adipose tissue infiltration mechanism is linked to a decrease in insulin sensitivity and glucose tolerance, which is particularly significant in controlling insulin resistance in type 2

diabetes (T2D), obesity, hypertension, and atherosclerosis (Yuan et al., 2019). Obesity is usually linked to elevated glucose levels and endoplasmic reticulum stress, which results in increased reactive oxygen and nitrogen species production, affecting insulin secretion and sensitivity. The atherosclerotic inflammatory process, linked to obesity, causes coronary calcification. Even though there is conflicting data, research such as the Framingham Study supports the link between obesity and coronary calcification in persons at minimal risk of CVD (Sun et al., 2020, Yuan et al., 2019). Obesity is linked to elevated levels of leptin and high blood pressure. Leptin causes salt retention, systemic vasoconstriction, and blood pressure increase via influencing nitric oxide synthesis and activating the sympathetic system (Bravo et al., 2006). The manipulation of leptin's effects results in the regulation of energy homeostasis, which allows blood pressure to be balanced by reducing calorie intake and increasing energy expenditure (van Galen et al., 2021). In addition, the renin-angiotensin-aldosterone system is involved in regulating blood pressure and vascular resistance, both of which affect cardiac function and arterial pressure (Cercato and Fonseca, 2019).

Plasma 5HT levels have been linked to obesity, non-alcoholic fatty liver disease (NAFLD), type 2 diabetes, cardiovascular disease (CVD) in mice and humans, and feeding on high fat or high carbohydrate diets (Cole et al., 2021). In mice, genetic, pharmacologic, and dietary inhibition of circulating 5HT levels via Tph1 can protect them from metabolic disorders caused by a high-fat diet (Tack et al., 2012). Furthermore, changes in the microbiota composition caused by antibiotics increase glucose tolerance by decreasing 5HT production in the stomach. Thus, microbiota depletion and suppression of gut-derived 5HT production may have comparable properties on glucose metabolism (Hara et al., 2004). These findings suggest that increased peripheral 5HT synthesis induced by nutrients like overeating, an HFD, or a high-carbohydrate diet, as well as altered microbiota composition (Hara et al., 2004), may contribute to the pathophysiologic mechanisms of obesity-related diseases like metabolic syndrome, NAFLD, type 2 diabetes, and CVD and that suppressing increased peripheral 5HT synthesis could be a novel therapeutic approach for obesity-related diseases (Pérusse and Bouchard, 2000). Feeding effectively involves a well-functioning cardiovascular system that can support high-intensity physical exercise and subsequent oxygen transport to internal organs during food digestion. Because of their ability to influence sympathetic nervous system activity, several POMC neuronal subsets specialise in the modulation of cardiovascular response (Bell et al., 2018). Fasting and a high carbohydrate diet, which includes glucose and fructose, and high fat and low protein diet, raise plasma FGF21 levels in mice. In mice fed an HFD, elevated plasma

FGF21 levels and hepatic FGF21 expression were found to precede hyperinsulinemia, insulin resistance, poor glucose tolerance, and weight gain (Sutton and Krashes, 2020).

In summary, feeding behaviour is regulated by central 5HT network systems via 5HT2cR (Pérez-Maceira et al., 2016). Tph1 can upregulate gut-derived 5HT production when energy intake is increased by a high-fat and/or high-carbohydrate diet. In rats fed an HFD, gut-derived 5HT can upregulate hepatic FGF21 expression and plasma FGF21 levels, leading to hyperinsulinemia, insulin resistance, decreased glucose tolerance, and weight gain (Bell et al., 2018). Increased plasma FGF21 in healthy persons can predict the metabolic syndrome and type 2 diabetes and are linked to insulin resistance, metabolic syndrome, type 2 diabetes, NAFLD, and a higher risk of CVD (Organization, 2020, Cercato and Fonseca, 2019, Aronne, 2019). Therefore, the impacts of central and peripheral 5HT networks on eating signals could play a role in the pathophysiology of obesity-related metabolic illnesses. Therefore, positive modulation of 5HT network could be a promising new preventative or therapeutic strategy.

1.8 *Caralluma fimbriata* extract (CFE) as anti-Obesity treatment

Ayurvedic medicine recognises *Caralluma fimbriata* as a natural appetite suppressor (Kamalakkannan et al., 2010). In India, Pakistan, Afghanistan, the Canary Islands, Sri Lanka, Arabia, and some parts of Europe, *Caralluma* is used as a garden border and grows wild along highways as a shrub (Griggs et al., 2018b). The properties of this cactus succulent have seen it consumed traditionally by tribal communities in India's hot and humid climate. (Kuriyan et al., 2007) This natural therapeutic plant also grows wild in metropolitan areas, and it has been utilised as a vegetable substitute in times of hunger (Kuriyan et al., 2007). Trials on the administration of *Hoodia Gordonii*, which attributed the anorexigenic impact of appetite to the steroidal glycosides, first claimed that a commercially available powdered cactus succulent substance might reduce hunger. After repeated chromatographic extraction of specific pregnane glycosides, researchers discovered similarities between CFE and the traditional African cactus succulent *Hoodia Gordonii* (Vermaak et al., 2011).

Caralluma fimbriata has yielded eleven new pregnane glycosides, four containing a new pregnane type, genin. In Australia, a supplement called "Hunger Control" includes the hydroethanolic extract of *Caralluma fimbriata* (CFE). Gencor Pacific's product is dried and powdered from the plant's aerial portions. The ethanolic extract of *Caralluma adalzielii* has

shown no toxicity (with an LD50 larger than 3000 mg/kg body weight). It resulted in a drop of 7.1 per cent in body weight in the animals given 400 mg/kg, compared to a 38.16 per cent increase in the positive control. The animals in the control group had higher triglyceride and LDL-Cholesterol levels in their serum than the extract treated animals. *Caralluma adalzielii* extract inhibited lipoxygenase by 65.75%per cent (at 1 mg/ml) more than gallic acid, which was employed as a control (54.87%). It also inhibits pancreatic lipase, trypsin, and the DPPH radical effectively (Pare et al., 2019). A single-case study of a girl with Prader-Willi Syndrome (Griggs, 2019), found that an extract from the Indian cactus *Caralluma fimbriata* reduced hyperphagia (over 12 years of treatment). However, excessive hunger returned after the treatment was temporarily halted for six days. As a result, anecdotal evidence suggests that CFE treatment causes alleviation of excessive food appetite sensation within free access, leading to a natural cycle of appetite homeostasis that includes hunger and satiety (Griggs, 2019).

CFE's efficacy in obese people has been established in clinical investigations, with appetite suppression and waist circumference decreases (Kuriyan et al., 2007, Astell et al., 2013). Animal studies show a similar reduction in food consumption, and extensive toxicity assessments ensure the medication CFE is safe (Griggs et al., 2018b). Improvements in the lipid profile and lower leptin levels and/or blood glucose have been observed in animals. CFE also suppressed preadipocyte cell development during adipogenesis in mouse-derived 3T3L1 cell lines dosage and time-dependent (Soundararajan et al., 2011). The experiment promoted pre-adipocyte cell division during adipogenesis in a dose and time-dependent manner. In addition, CFE significantly lowered the amount of leptin in serum and improved the lipid profile level associated with high fat cafeteria food (Kamalakkannan et al., 2010). The pregnane glycosides, both antihyperglycemic and antinociceptive, are thought to be involved in CFE's mechanism of action, and the various steroidal glycosides promote stimulation of the anorexigenic melanocortin pathway (Rao et al., 2021). CFE caused a dose-dependent reduction in food consumption in rats for eight weeks, according to a study (Kamalakkannan et al., 2010). It is also thought that the appetite-suppressing qualities are due to a decrease in ghrelin synthesis, which influences neuropeptide-Y in the hypothalamus (Rao et al., 2021). In a second trial using Wistar rats, lipid profiles were reduced even further. In Wistar rats, CFE treatment (100 mg/kg/d) dramatically reduced body weight gain after consuming a HFD compared to controls and significantly lowered blood glucose levels (Kamalakkannan et al., 2010).

Bioactive pregnane glycosides have been identified as substances with anorexigenic characteristics in research. The safety of pregnane glycoside characteristics has been questioned, notably when they caused vacuolization of the adrenal cortex in rats (Vitalone et al., 2017). The structural features of certain pregnane glycosides studied in swamp milkweed *Asclepias incarnate* and *Hoodia Gordonii* is like cardiac glycosides used to treat cardiac patients with heart failure. However, the pregnane glycosides in Asclepias incarnate and *Hoodia Gordonii* and CFE do not influence on the cardiac system because they lack the lactone ring, which confers the stimulating property of cardiac glycosides (Komarnytsky et al., 2013a). The CFE has undergone extensive toxicity testing, and the treatment's safety has been established. A dose of 5000 mg/kg body weight was safe in mice (Sakore et al., 2012), while issues about the complexity of CFE's action remains a mystery. Pregnane glycosides are found in plants of the *Asclepiadaceae* family, including *C. Fimbriata*, and are known to have appetite-suppressing actions in the hypothalamus (Komarnytsky et al., 2013b).

Further research is required to fully comprehend CFE's mode of action. Hunger is a stimulus since it can originate inside the system (intrinsically) or by an external experience (extrinsically), stimulating feeding. In other words, when it relates to overeating, food taste might be an extraneous confusing factor (Ríos-Hoyo and Gutiérrez-Salmeán, 2016). According to research, when highly appetising food generates feelings of reward, dopaminergic signalling is boosted. As a result, animals will go to great lengths to obtain pleasure (Irizarry et al., 2016). Extrinsic messages (from outside the body) are also experienced intrinsically in shared areas of the brain and areas specific to sensory experience. Intrinsic messages are encountered through increased activation in particular brain regions, such as the hypothalamus, amygdala, and insula cortex. It is unclear if the orbitofrontal cortex's (OFC) conscious impulse to eat is triggered by an internal sense of satiety or perception of hunger, which can also be triggered by reward signalling (Baver et al., 2014). The hormone ghrelin, for example, may convey hunger to the hypothalamus, and the OFC may signal satiety via the hypothalamus afterwards. Alternatively, food visual stimulus can increase ghrelin in blood and can impact by eating behaviour and enhance the signal inside the hypothalamus (Klement et al., 2017, Lynch, 2012). Additional limbic forebrain signals stimulate food "fondness," which can be increased by employing opioid neurotransmission. Therefore, changing reward signalling just through self-control is complicated; thus, pharmacological therapy can mediate reward modulation of the dopamine and serotonin pathways within the CNS (Griggs, 2019).

Previous research suggested that CFE suppresses appetite by downregulating ghrelin synthesis in the stomach and neuropeptide Y (NPY) in the hypothalamus, but the specific mechanism of action is unclear (Griggs et al., 2018b). CFE's appetite-suppressing and weight-loss effects have been studied in preclinical and clinical studies. However, only a few human trials have been undertaken, resulting in a limited understanding of the mechanism. CFE maintained body weight, lowered waist circumference, and reduced daily calorie intake in overweight persons for 16 weeks (Rao et al. 2021) compared to a placebo. On the other hand, the placebo group had higher leptin levels, NPY, and cortisol (Rao et al., 2021).

Key points from the literature:

- In both obesity and overeating disorders, hypothalamic satiety stimulation is a potential method to reduce weight gain and improve energy expenditure.
- The 5HT2cR is one of the receptors involved in activating the melanocortin mediated anorexigenic pathway in the ARC of the hypothalamus to increase satiety.
- The 5HT2cR has different isoforms due to alternate splicing events during expression. The functional and truncated isoforms exist in POMC cells, where the ratio of functional to truncated receptor levels may be crucial for POMC neuron activation of satiety.
- Lorcaserin is the specific agonist available for 5HT2cR and approved for obesity treatment; however, recent results from different studies raise questions about its side effect in long term usage.
- On the other hand, CFE influences weight reduction and waist circumference regulation in overweight/obese people from different clinical studies. However, the exact mechanism of action of CFE in hypothalamic based appetite regulation is still unclear.
- Unpublished studies (Stefen Stamm's group) on 5HT2cR transfected 3T3L-1 cells treated with CFE revealed a change in expression levels of functional 5HT2cR.
- The key points from the literature suggest the feasibility of a combination therapy with CFE and reduced dose of Lorcaserin as a potential treatment to regulate weight gain in obesity and overeating disorders.

1.9 Significance of the Study:

Obesity and overeating disorders are connected through appetite stimulation and lead to an increased food intake. The higher food intake in combination with decreased energy expenditure may lead to metabolic imbalance. Many CNS and peripheral modulators influence fat accumulation and reduced energy expenditure in obesity. However, hypothalamic neurons play a distinctive role in appetite and satiety balance, as well as mood, and emotional status. In weight regulation, satiety regulating pathways are targeted as one of the directions for drug development; for instance, Lorcaserin a selective 5HT2cR agonist drug used for weight loss. The earlier studies (Griggs et al., 2018b) and (Rao et al., 2021)showed that CFE can potentially increase satiety and reduce weight gain. It is proposed that the satiety signalling from POMC neurons was primarily initiated by the serotonin signalling pathway, where 5HTc2R activation leads to melanocortin pathway stimulation via secondary nerve signalling in PVN.

The 5HT2cR function has a vital role in behavioural changes like mood, anxiety, and depression parameters control. The 5HT2cR agonist Lorcaserin showed side effects during prolonged usage in various stages (Tchang et al., 2020). Hence, the alternative ligand development may take time; the studies mentioned Lorcaserin could be reconsidered with a modified dose or combined with other drugs (like GLP-1 agonist). Hence, the weight loss treatments have a potential gap to fill for further research and developments. The study was designed with a novel combination therapy for weight loss in obesity and other overeating disorders with Lorcaserin and CFE. The treatments presumed to stimulate 5HT2cR expression by CFE and further receptor activation by Lorcaserin. The current study may be an initiative to predict the rare combination of a synthetic drug with CFE believed to be safe and available recourse to regulating energy intake and subsequent challenges in obesity and overeating disorders.

1.10 Aims and Objectives:

The study has been comprised of several layers of research on CFE and Lorcaserin treatments targeting obesity related symptoms. The role of CFE in anorexia was discussed in detail, as well as Lorcaserin's specific agonism to 5HT2cR. However, Lorcaserin treatment showed improved depression like behavioural symptoms, prolonged usage casing side effects. CFE, on the other hand, decreased PWS-dependent hyperphagia and weight gain in a variety of clinical and pre-clinical tests, albeit the mechanism of action remains unknown. The study was aimed to regulate obesity related weight gain and energy uptake. To obtain validations for the study, we conducted experiments in three phases. The first phase is to confirm, CFE influence on functional 5HT2cR expression. Then next phase is to find out how CFE and Lorcaserin combination treatments impact mood and emotions in diet-induced obese mice. In the final phase we measured CFE and Lorcaserin combination therapy on body composition in HFD induced mice.

Study I:

To measure the role of CFE on 5HT2cR expression: The SHSY5Y neuroblast cells (both undifferentiated and differentiated neurons) were used to measure 5HT2cR expression in response to different CFE concentrations.

Study II:

To observe mood and emotional behaviour changes induced in mice fed a HFD and any changes in response to CFE and Lorcaserin treatment: Obesity was induced in C57BL/6J background mice and then they were treated with CFE, Lorcaserin and a combination of CFE+LOR. The treatment groups were measured for mood and anxiety-related changes using a range of behavioural tests.

Study III:

To measure body composition and vascular dysfunction in HFD mice treated with CFE and Lorcaserin: The body composition- fat and lean mass deposition and Promethion metabolic cage monitoring used to determine overall energy homeostasis of HFD mice with CFE and Lorcaserin treatments. In addition, the abdominal aortic rings isometric tension analysis was used to measure the effect of the treatments on vascular dysfunction induced by the HFD.

Chapter 2 Materials and Methods

The following Figure 2.1 briefing overall methodology considered to achieve proposed hypothesis.

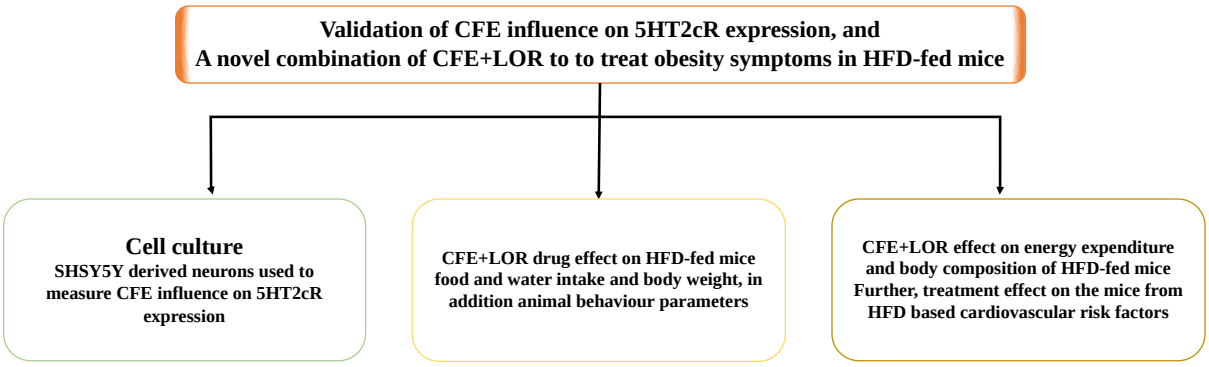

Figure 2.1: The illustration describes methodology according to chapter significance

2.1. Human SHSY5Y cell culture study:

The SHSY5Y neuroblast cells with passage 12 were purchased from the Australian cell bank (CODE: 94030304). The background of SHSY5Y cells in brief: these cells were isolated from human neural tissues (SK-N-SH biopsy), with an adhesive nature and a neuroblast-like morphology. The 5% DMSO stock vials were prepared and stored in liquid nitrogen (-189 to -192 °C) at Victoria University, Werribee facility.

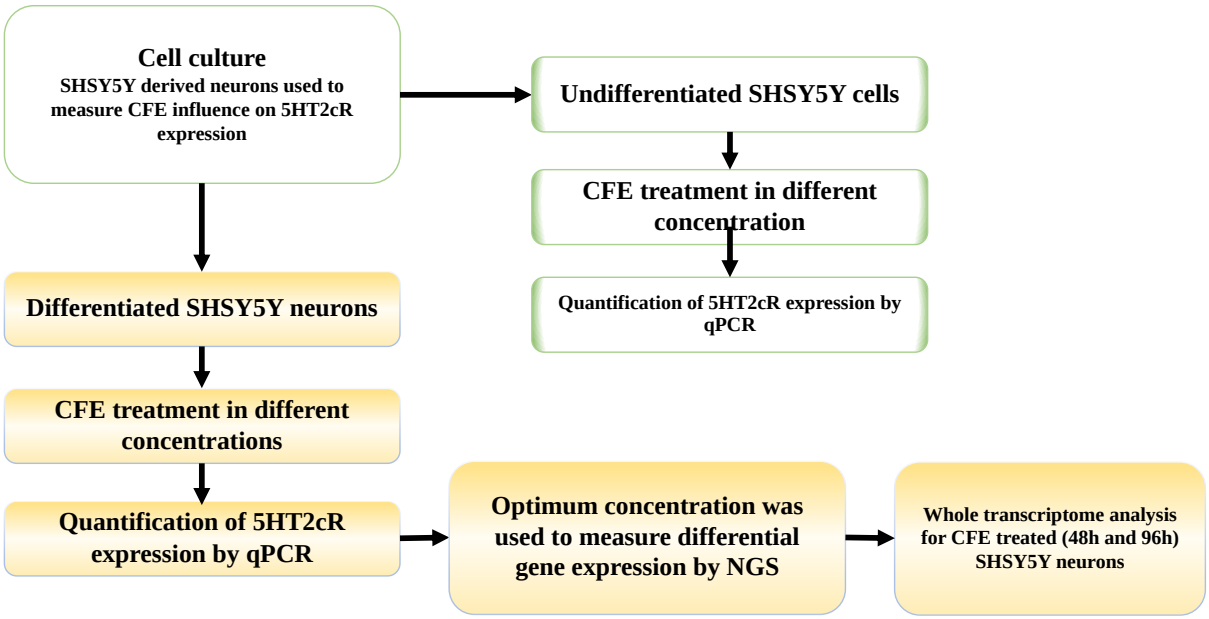

Figure 2.2: Description of SHSY5Y cells for 5HT2cR expression with CFE treatment

2.1.1. SHSY5Y cell culturing:

The growth medium was a modification to Shipley et al., 2017, where 1:1 v/v ratio of DMEM and F12 growth media supplemented with 15% v/v hi-FBS (hi: heat-inactivated), 2mM

Glutamine, and 1x Penicillin/Streptomycin (Gibco, distributed by Invitrogen, Carlsbad, CA) (Shipley et al., 2017). The stock vial was thawed in a water bath at 37°C for 2 to 3 minutes (rapid thawing method). The cells were diluted with 9 mL of growth medium to reduce DMSO effect on cells. Further, cells were pelleted down and removed supernatant; pellet was dissolved in 10mL of fresh growth media. The inoculated culture flask was incubated at 37°C in a CO_2 incubator with 5% continuous CO_2 purging. The cells were checked every 24 hours, and the complete media was replaced every 48h. After five days of incubation, cells were collected from the flask using 0.25% trypsin-EDTA (Gibco) complex, where they attained 80% confluency. The collected cells were centrifuged to remove trypsin and redissolved in fresh growth media. The cells further diluted to achieve $1x10^4$ cells/mL concentration. The cells were inoculated in a six well plates with 40000 cells in each well and supplemented with 2mL of growth media (described in Figure 2.3).

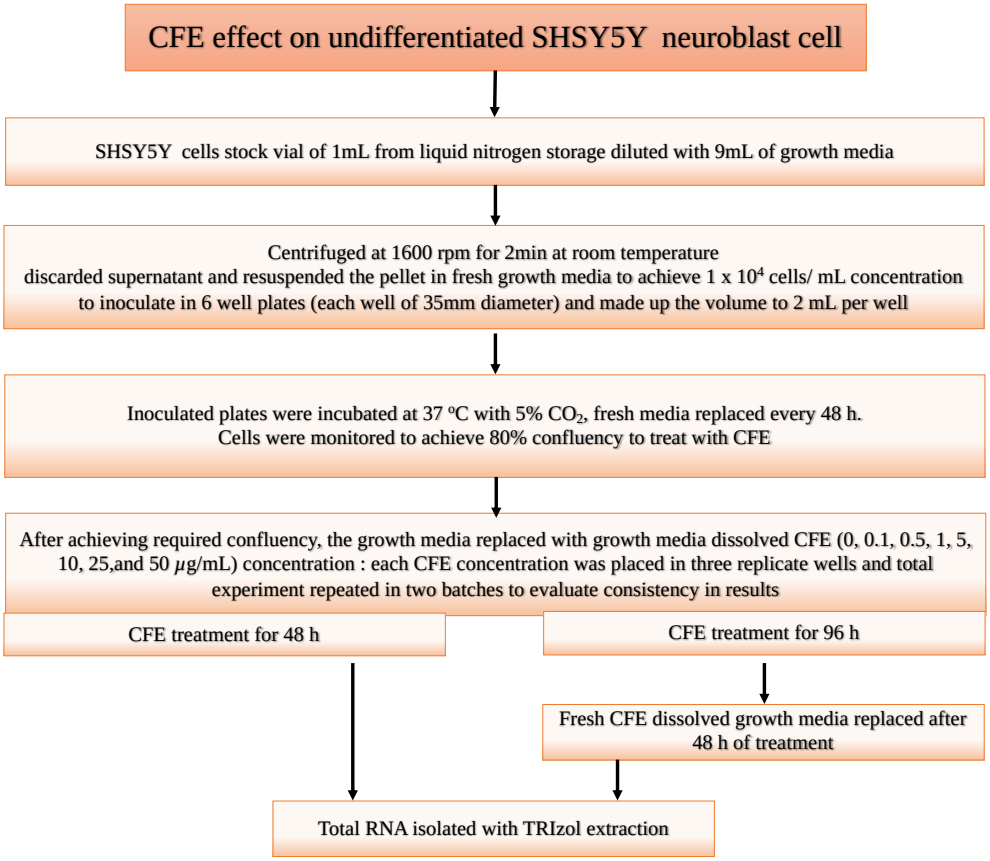

Figure 2.3: Workflow for SHSY5Y cells treatment with CFE

2.1.2. CFE treatment to undifferentiated SHSY5Y cells:

CFE was a hydroethanolic extract supplied in powder form from Gencor Pasific; all the treatments of CFE were made with growth media. The growth media containing desired

concentrations (0, 0.1, 0.5, 1, 5, 10, 25, 50 µg/ml) of CFE was added to the SHSY5Y cells. After being replaced with CFE dissolved growth media, cells were incubated at 37 °C. To meet statistical requirements, each CFE concentration was repeated three replicates (n=3) and the data validated from minimum of two individual sets of runs. The CFE-treated cells were collected after completing 48h and 96h time points to isolate total RNA for further genetic analysis. Individual well samples were used to extract RNA and quantified by Nanodrop (Thermo Scientific Nanodrop 2000 series). The RNA purity was assured by 260nm /280 nm absorbance ratio.

2.2. Human SHSY5Y derived neuronal study:

2.2.1. SHSY5Y cell Differentiation to Neurons:

The differentiation protocol of (Shipley et al., 2016) modified to differentiate SHSY5Y cells to neurons. In three stages, SHSY5Y cells were differentiated into neuron-like cells as shown in Figure 2.5. Initially, the SHSY5Y stock vials were used to grow the cells, as described in section 2.1.1. After achieving 80% confluency in six-well plates, cells were washed and replaced with differentiation media 1 (DF1), supplementing with 2.5% hi-FBS, 1x Pen/Strep, 2mM Glutamine, and 10uM Retinoic acid (RA) in 1:1 DMEM/F12 media and the plates were incubated at 37°C in a 5% CO_2. The cells were replaced with fresh DF1 media every 48h up to the 7th day. On day 8, the cells were rinsed with 0.1M PBS and supplemented with Differentiation Media 2 (DF2). On Day 9, cells were detached, and transferred to ECM-coated plates, and enriched with DF1 medium. Next day cells were replaced with DF2 medium overnight. On day 11, Cells supplemented with the neurobasal media consisting, 1xB-27, 20mM KCl, 1x Pen/Strep, 2mM Glutamax-I, 50ng/mL BDNF, and 10 µM RA and incubated at 37°C with 5% CO_2. The DF3 media was replaced every 48h and dendrite formation observed on day20 (as shown in Figure 2.4). The cells are differentiated to neurons as shown in Figure 2.5; the cells were ready for CFE treatments.

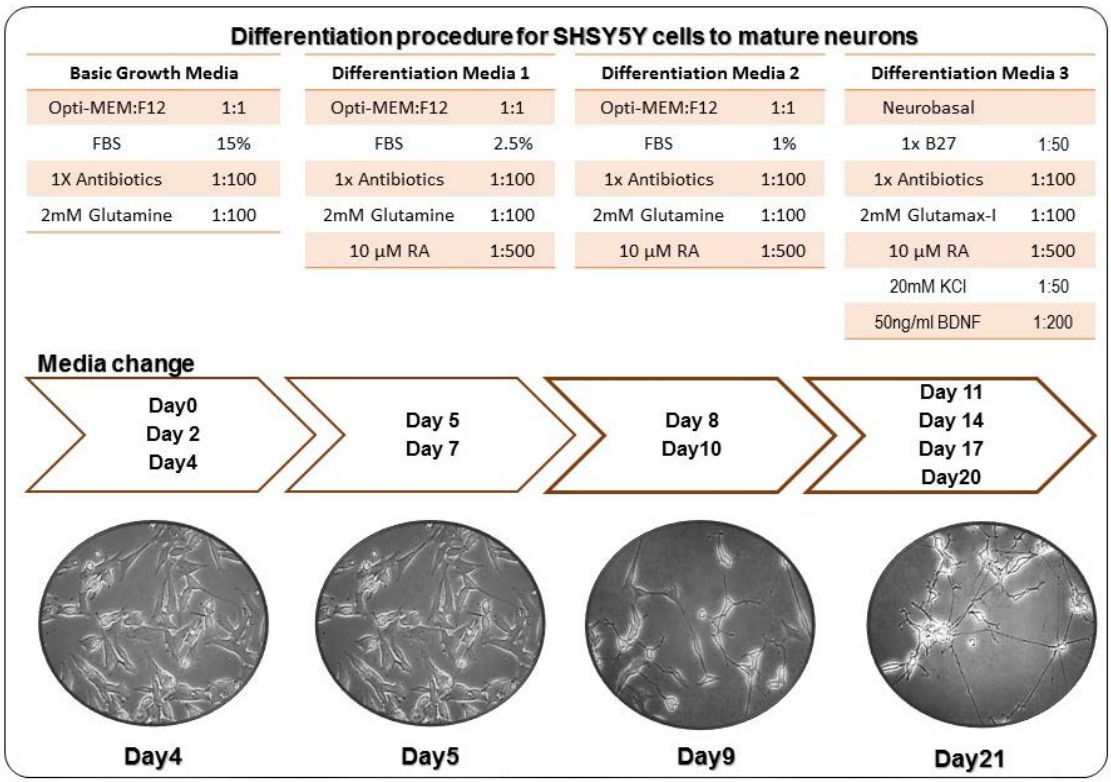

Figure 2.4: Schematic representation of SHSY5Y differentiation media composition. Where, RA: retinoic acid, antibiotics are penicillin and streptomycin, KCl: potassium chloride, BDNF: brain-derived neurotrophic factor.

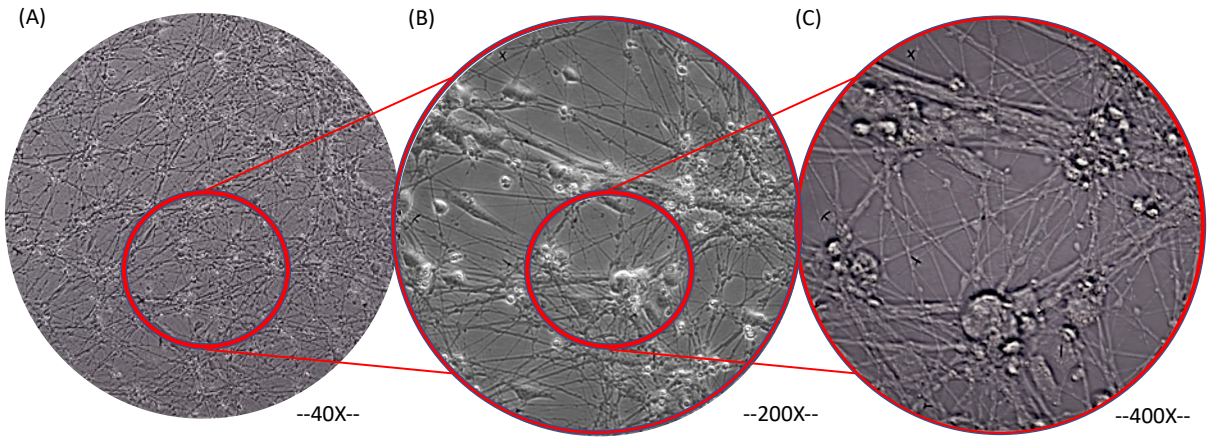

Figure 2.5: Microscopic visualisation (Labomed-TCM400) of SHSY5Y-derived neurons from SHSY5Y neuroblasts and at (A) 4X, (B) 20X, and (C) 40X lenses.

2.2.2. CFE treatment:

The SHSY5Y derived neurons were treated with CFE in six-well culture plates. The CFE stock concentrations of 0, 0.1, 0.5, 1, 5, 10, 25, and 50 µg/mL were made in DF3 medium. The cells were replaced with CFE dissolved DF3 and incubated at 37°C with 5% CO_2. Each concentration of CFE was replicated in three wells (n=3) in two completely different sets of experiments. The CFE-treated cells were extracted at 48h and 96h time intervals for RNA isolation and to perform further gene expression analysis. The workflow has been illustrated in Figure 2.6.

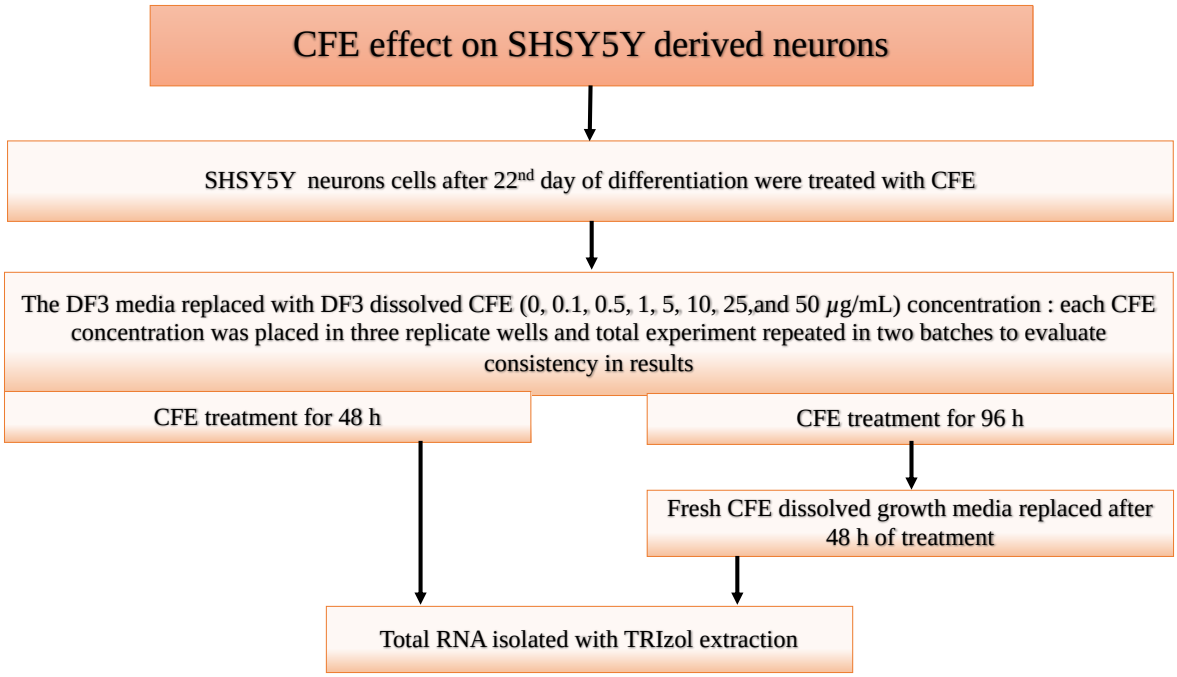

Figure 2.6: CFE treatment workflow for SHSY5Y-derived neurons

2.3. RNA Analysis

The CFE-treated cells were harvested into 1.5 mL Eppendorf tubes using 1ml ice-cold TRIzol (Sigma-Aldrich) reagent, and the cells were promptly frozen at -80 °C for further RNA extraction.

2.3.1. RNA Extraction

RNA was extracted from the TRIzol-preserved cells. The cells were added with 250 µl/1mL of TrIzol of Chloroform and inverted to mix both reagents. The vials were incubated for 5 min, according to the modified Sultan et al., 2014 RNA extraction procedure (as shown in Figure 2.7). These cells were centrifuged for 15 min at 13000 rpm and 4 °C temperature to separate the liquid phases. The clear upper layer of centrifuged samples was collected into a fresh

collection tube containing 400 µl Isopropanol and 10 µl of 5M NaCl, samples inverted to mix well. The tubes were incubated at -20°C overnight and observed for RNA pellet. After overnight incubation, samples were centrifuged at 13000rpm for 20 min at 4°C to separate RNA pellets. The clear supernatant was carefully discarded without damaging the particle. This supernatant was centrifuged at 9000 rpm for 8 min at 4°C after being rinsed with 400 µl of 75% ethanol. The ethanol was gently aspirated, and the pellet was air-dried at room temperature for 3 to 5 min. The DEPC water of 30 µl was used (pre-warmed at 65°C for 2min) to dissolve the RNA pellet. Further, 1 µl of dissolved RNA was diluted with 19 µl DEPC water for quantification. (Sultan et al., 2014, Simões et al., 2013, Hummon et al., 2007).

2.3.2. RNA Quantification

The concentration of the DEPC water-diluted RNA samples were measured for quantification. The total RNA quantity was determined using a Thermo Fisher Nanodrop^{TM} 2000 spectrophotometer with a 260nm absorbance. The ration of 260/280nm measurement was used to determine RNA quality. Each sample was tested for absorbance until it reached two consistent data points to avoid pipetting mistakes, and average concentration value used for cDNA synthesis.

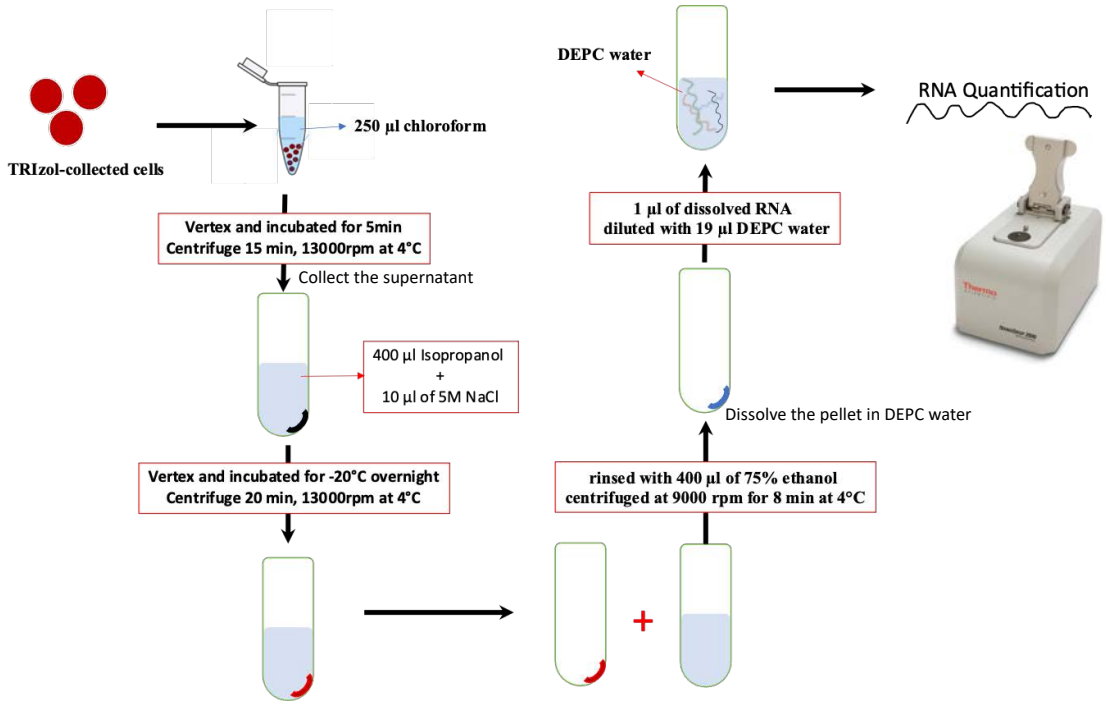

Figure 2.7: Schematic representation of Total RNA isolation by TRIzol extraction protocol

2.3.3. Reverse transcription of RNA samples

The RNA concentrations were normalised using DEPC water before cDNA conversion. The Biorad iScript cDNA synthesis kit was utilised for the reverse transcription process, and 0.5 µg RNA was added to DEPC treated water in a volume of up to 7.5 µl. The 0.5 µl volume of iScript reverse transcriptase and 2 µl of 5x iScript reaction mix were added to cDNA, and a final reaction volume of 10 µl was made. The following PCR conditions were used for reverse transcription: 5 minutes at 25 °C, 30 minutes at 42 °C, 5 minutes at 85 °C, and hold at 4°C. The cDNA samples were diluted in DEPC-treated water at a 1:20 ratio to measure the absorbance.

2.3.4. Primer sequences

The selected gene sequences FASTA files were downloaded from the NCBI database, and the NSBI Primer blast was performed to design the primers. The designed forward and reverse primers were verified for cross-matching of the other gene sequences of the same species (https://blast.ncbi.nlm.nih.gov/Blast.cgi). The GC content, length of the primer sequence, and melting temperature parameters are considered for effective design. These primers were used for further qPCR analysis in a gene expression study. All the gene expression studies were carried out after primer concentration optimisation.

Table 2.1: Selected human genes and primers, Syp38: Synaptic vesicle protein 38, GAP43: growth-associated protein 43, Akt1: Protein kinase, 5Ht2cR: serotonin receptor 2c, ExonVb: exon Vb sequence of 5Ht2cR.

Gene	Forward primer (5' to 3')	Reverse primer (5' to 3')
Syp38	GGTTCCTCCAGCAATGATGC	CTTAAAGCCTCGCCCCTTCT
GAP43	CAACCATGCTGTGCTGTATGA	GCGGGGTGGCATAATTCAGA
Akt-1	ATCCTGGTCCTGTCTTCCTCA	TGATGTACTCCCCTCGTTTGTG
5HT2cR	TGTCTCTCCTGGCAATCCTT	CGCAGAACGTAGATGGTCAG
ExonVb	GTGCCCCGTCTGGATTTCTT	GATGGCCTTAGTCCGCGAAT

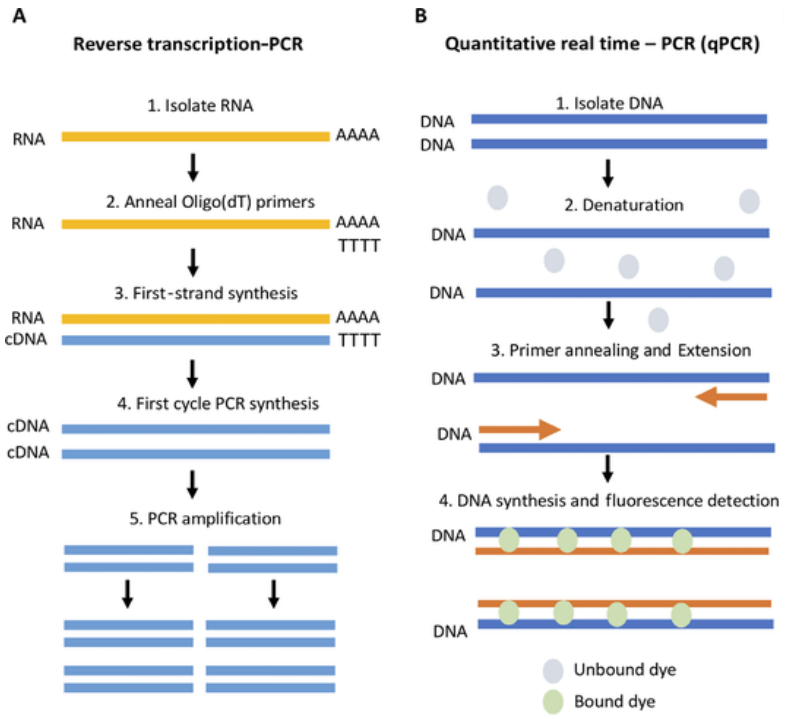

Figure 2.8: Schematic representation of Polymerase chain reaction (PCR), where (A) Reverse transcription PCR: RNA translated into cDNA copies and (B) Quantitative analysis of the desired gene of expression by qPCR assay (Adams, 2020).

2.3.5. Quantitative real-time PCR (qPCR)

The quantitative PCR was performed with Master cycler epRealplex^{2}R (Eppendorf) and principle behind PCR amplification illustrated in Figure 2.8. The Biorad master mix, primers, and cDNA were prepared using the epMotion robot system (epMotion 5070 series, Eppendorf). The total 10 µL of each reaction contains 2 µL cDNA sample, 0.5 µL forward primer, 0.5 µL reverse primer, 2 µL DEPC treated water, and 5 µL of SsoAdvanced Universal SYBR Green Supermix (Bio-Rad). In the modified method of Stam S. et al. 2017, qPCR cycling starts with an initial denaturation at 95°C for 3 minutes, followed by 40 cycles with denaturation at 95 °C for 15 seconds, annealing at 60ºC for 40sec and extension at 72°C for 30 seconds (Stam et al., 1994, Stamm et al., 2017). The housekeeping genes GAP43, Syp38, and Akt-1, were used to compensate for variations of targeted RNA, and the efficiency of reverse transcription with fluorescence was analysed with the cycle threshold (Ct) value. In addition, the relative fold change quantification of gene expression was analysed by double-delta Ct ($2^{-\Delta\Delta CT}$) value calculation (Kummerfeld et al., 2022).

2.3.6. Gel electrophoresis

The qPCR amplified gene products were assayed by 1% agarose gels for gel electrophoresis. The 1% agarose gels were prepared with selected nine well comb gel casters (Ruiz-Villalba et al., 2017, Barbau-Piednoir et al., 2010) with SYBR safe DNA stain (S33102 from Thermo Fisher Scientific). The electrophoresis tank was filled with 1x-TAE buffer (Biorad) and each sample was carefully loaded with 6x-gel loading dye from Biorad. The power supply was maintained at 100v to the electrodes to run the gels and bands observed under the Gel imaging system (Biorad Chemidoc^{TM} MP-XRS+).

2.4. Next Generation Sequencing

2.4.1. RNA preparation and quality check

The total RNA was extracted from SHSY5Y neurons (CFE 25 µg/mL treated) by QIAGEN RNeasy plus mini kit (100ug RNA extraction); and further sample were purified by gDNA eliminating columns. The quantity was initially checked with Nanodrop, and quality analysis was performed by RNA integrity number (RIN) estimation. The Agilent 6000 RNA Nano kit (Sun, 2020) was used to estimate individual sample RIN values; samples with RIN >8 was preferred for further analysis.

2.4.2. Brief description of NGS conditions

The RIN value greater than 8 samples were sent for NGS analysis in the MICROMON Genomics facility at Monash University. The facility initially prepared cDNA libraries with a minimum of 1µg of total RNA after polyA removal. Then, the libraries were QC checked and prepared for loading flow-cell containing NGS probes. Finally, the NGS process was carried out for paired-end sequencing with a minimum of 60M reads coverage for each sample. The data obtained from NGS stored in "bam" files are further converted to "*Fastq*" file format for easy access.

2.5. High fat-induced mouse model

The male c57BL/6 (4 weeks old) mice(n=80) were procured from the animal supply recourse centre (ARC), Australia. After one week of acclimatisation, the mice were randomly divided into five groups. Each animal was housed individually in divided cages. In the Werribee animal house facility, the animal cages were environmentally controlled under temperature (22-24^{o}C)

and humidity (35-55%) conditions. The light and dark cycles of 12h were maintained by auto controlled BMS system (Lee et al., 2020, Zheng et al., 2020, Zou et al., 2020). The high fat (SF04-001) and control diet (SF13-081) (composition in Figure 2.9) were procured from Specialty Feeds, Australia (150 Great Eastern Highway Glen Forrest, WA 6071). The high-fat diet (HFD) induction was carried out for the first eight weeks as shown in Figure 2.10. Further, the CFE of 100mg/kg body weight (Griggs et al., 2018a) and Lorcaserin 5mg/kg body weight (modified low dose (He et al., 2021)); during week 8 to 16. The overall animal study flow was illustrated in Figure 2.11 and 2.12.

Rodent diet from: SPECIALTY FEEDS, 150 Great Eastern Hwy Glen Forrest Western Australia 6071	**SF13-081** 	**SF04-001** 
Protein	23.0%	22.60%
Total fat	5.3%	23.50%
Crude fibre	5.4%	5.40%
Ad fibre	5.4%	5.40%
Digestible Energy	15.6 MJ / Kg	19 MJ / Kg
% Total calculated digestible energy from lipids	12.3%	43.00%
% Total calculated digestible energy from protein	25.5%	21.00%

Figure 2.9: The brief description of rodent high fat diet and control diet composition details

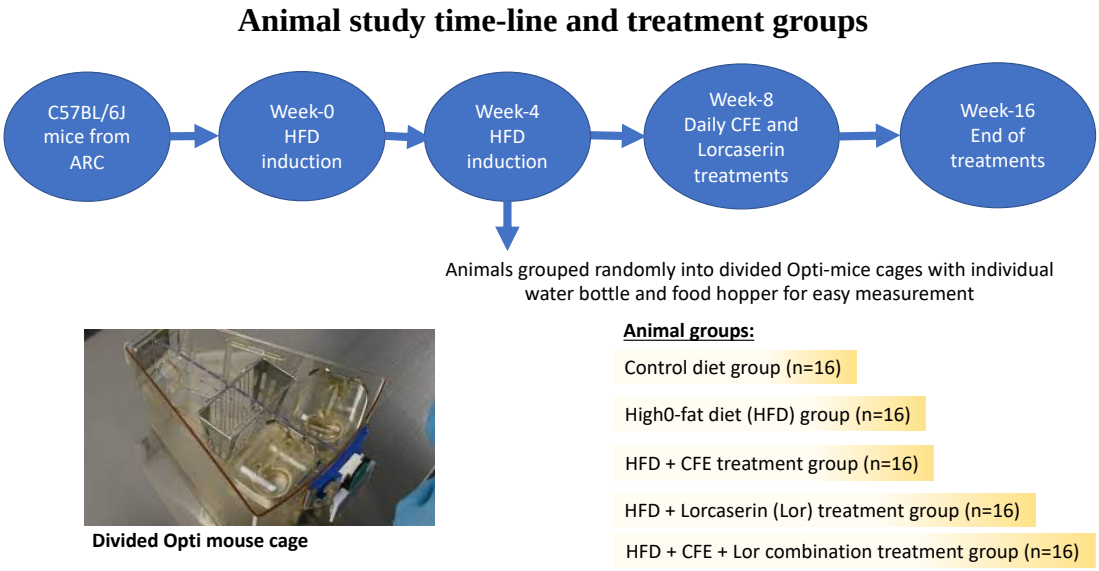

Figure 2.10: Schematic representation of animal groups with special diet induction and treatment time points

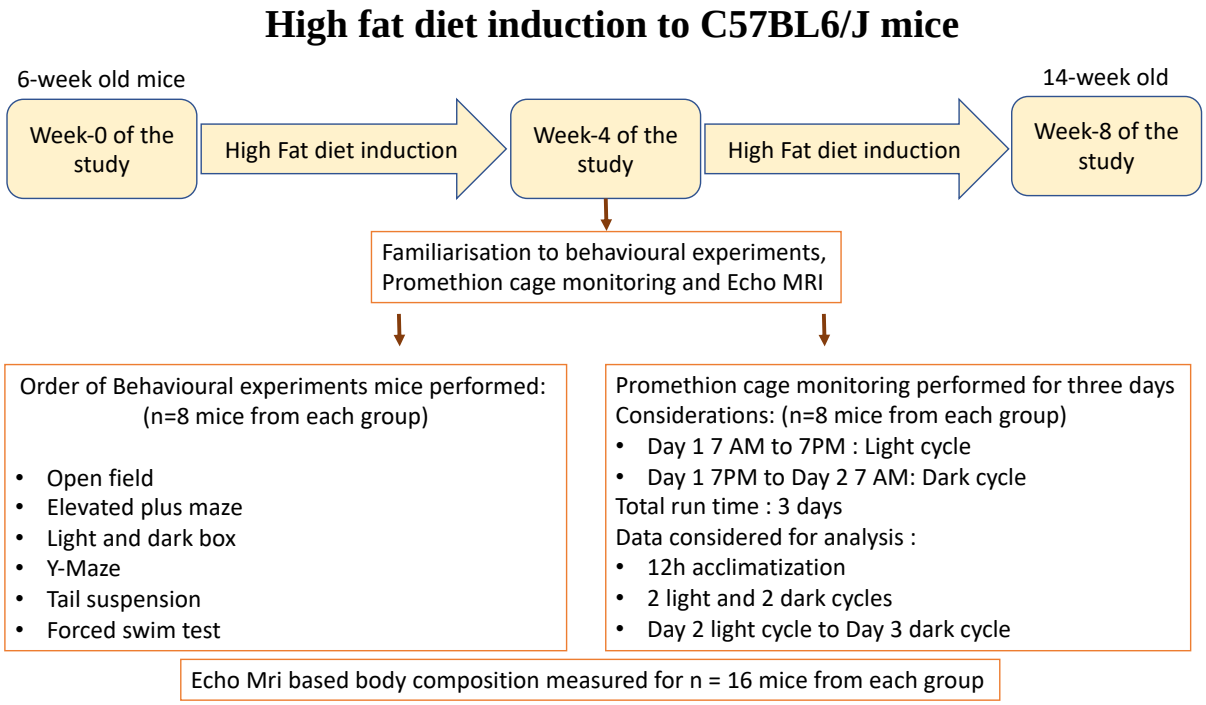

Figure 2.11: Schematic representation of animal study flow

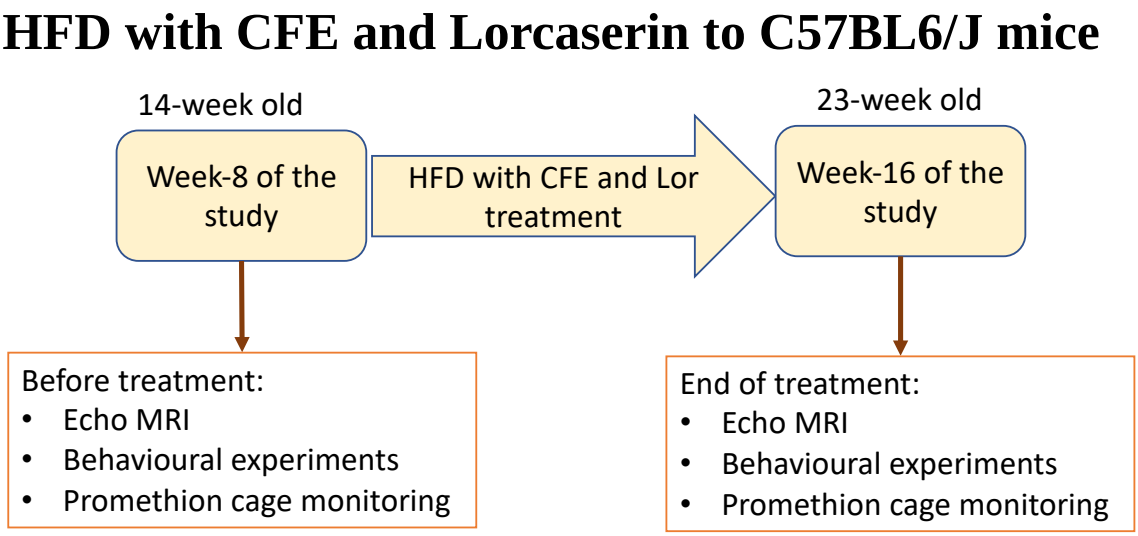

Figure 2.12: Schematic representation of animal study flow

2.5.1. Parameters monitored during treatment

2.5.1.1. Body weight, Food, and water consumption

A standard facility weighing machine was used to measure animal body weight. In addition, the animal food and water consumption were recorded weekly (Lee et al., 2020). The difference in food weight from the previous week given to the present week's leftovers will be assumed as Food consumed. In similar, the consumption of water was also measured by weighing the water bottle. Both Food and water consumption were mentioned in grams.

2.5.1.2. Jelly dosage

All the treatments were made into jelly form with saccharine as low-calorie taste enhancer by 7.5% gelatine concentration. The Figure 2.13 was describing preparation flow chart of vehicle, CFE and LOR treatment jelly. The concentration of 100mg/kg bwt/d of CFE was chosen based on previous studies from our lab (Griggs et al., 2018a) The relatively low dose of Lorcaserin (5 mg/kg bwt/d) was chosen to observe any synergistic effect with CFE for weight management studies in mice (Wagner et al., 2022).

The week 8 of HFD induction period, animals were trained to habituate with jelly cube for a week without any dose of treatments. The trained animals were impressively picking up the jelly in short time after giving to the animals in the home cages. All the jelly treatments were given in 3 cm diameter sterile bottle caps, at 3 to 4 PM before the dark cycle every day. Animals

were checked everyday morning for any leftover jelly on cage/bedding. During study period, LOR and CFE+LOR treatment animals were noticed with leftover jelly in the cage for minimum 3 to 5 days on an average.

Description	Animal Groups				
	Control	HFD	CFE	LOR	CFE+LOR
Gelatin	7.5%	7.5%	7.5%	7.5%	7.5%
Saccharine	1mg/ml	1mg/ml	1mg/ml	1mg/ml	1mg/ml
CFE (mg/kg bwt)	-	-	100		100
LOR (mg/kg bwt)	-	-	-	5	5

Silicon tray for jelly cube preparation
(each well volume 1cm^3)

Jelly cube preparation steps

Gelatin added to room temperature water and dissolved with continuous stirring on hot plate at 45 - 50 ˚C.

↓

Saccharine mixed with gelatin dissolved solution and cool down the solution to 35 ˚C

↓

Add required quantity of CFE and LOR to the solution and mix quickly and pour into the jelly cube making mold to set

Note: The volume required for each mouse were pre calculated and accordingly poured that volumes with respect to animal weight and dose required into each jelly mold to set

Figure 2.13: Jelly dose treatment to individual mice

2.5.1.3. Echo Magnetic Resonance Imaging (Echo-MRI)

The fat, and lean mass, in addition to free water (not bound in various tissues, usually urine), and total water (also known as total body water (TBW), contained total fluids and a bound state in tissues) content in the whole body of a live animal were measured using a nuclear magnetic resonance. Quantitative magnetic resonance (QMR) is another name for it. QMR differentiates from MRI in that the signal is collected from the entire body at once, T2-MRR in that both T1 and T2 are engaged, and MRS in that the time domain signal (rather than the spectrum) is directly processed. A scan provides a record of nuclear magnetic resonance responses (NMR echoes) to a succession of radio pulses, which is the essence of the QMR approach. The sequence comprises multiple Carr-Purcell-Meiboom-Gill segments (CPMG segments) that are separated by pauses of varying lengths. The lengths of the periodic sections and the durations of the pauses are chosen to capture all the relevant characteristic (relaxation) time scales of NMR responses (transverse, "T2," and longitudinal, "T1," relaxation) found in fat, lean, and free water. The signal from a body is a linear mixture of fat, lean, and free water contributions. The differences in the relaxation rates of the three fundamental components allow linear regressions to compute fat, lean, and free water levels. These regressions are based on

measurements of phantoms made of canola oil for fat, chicken breast (small animals) or lean pork (bigger animals) for lean and tap water for free water. For high-dimensional regressions, the algorithm for optimising these regressions is a form of multivariate calibration (popular in chemometric research) that uses partial least squares optimisation mixed with principal component analysis.

2.5.2. Energy expenditure by Promethion cage monitoring

Each mouse was assessed for 72h in promethion cage during each run; where, the initial 24h considered acclimatisation time, and the last 48h data considered for different parameters. The parameters estimated were including food and water intake, body mass, general cage activity, and energy expenditure.

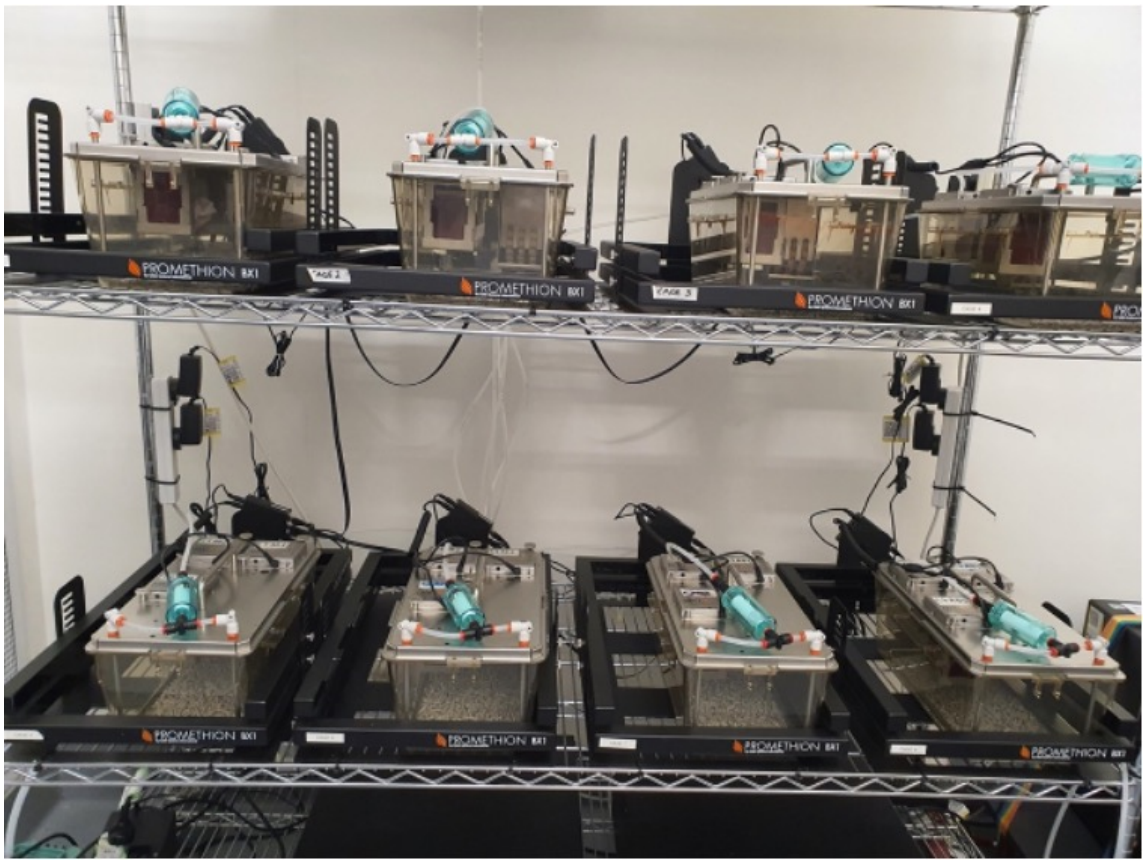

Figure 2.14: Overview of Promethion cage monitoring system

2.5.3. Animal behavioural studies

Behavioural studies for Exploration (Open field, Y-maze), depression (Force swim test and Tail suspension), and anxiety (Elevated plus maze and Light and dark box) were conducted during week 8 (pre-treatment), and week 16 (post-treatment).

2.5.3.1. Measuring Anxiety with Elevated Plus Maze and Light and Dark box analysis

- **Elevated Plus Maze (EPM):** The EPM was a commonly used test for mouse anxiety-like behaviour estimation in novel environments. The rodents were tend to explore novel areas and inclined to avoid open/brighter environments. In addition, the healthy mice were interested to explore both open and closed arms initially in the EPM. In contrast, rodents with depression and anxiety will spend more time in closed arms with less (Moy et al., 2007, Alsiö et al., 2009, de Smith et al., 2009).

- **Light and dark exploration:** The mice will undergo two coloured boxes separated by a small window opening. The bright light chamber has a larger area than the darker side chamber. The mice were placed in a dark arena and allowed to explore for 1min, and the window opened to explore towards a brighter arm. The overall exploration time was 10 min for each animal 10min. The time spent in and number of bouts into brighter chamber were considered to estimate anxiety like behaviour (Moy et al., 2007).

2.5.3.2. Measuring Exploration behaviour by Open field and Y-maze experiments

- **Open field:** To measure the exploration behaviour and motor activity as a measure of anxiety. The instrument is made of a square with 60 x 60 x 60 cm (l x w x h) Plexiglas chamber. The animal movements were recorded through video recording software, and this recording used for analysis. The parameters were included like, time of immobility, average speed, and time spent in the central and peripheral arena of the chamber. The animal with anxiety was not spent much time to explore center area and try to stick to corner area (Moy et al., 2007).

- **Y-Maze:** The Y-maze consists of three identical arms of 30 X 10 x 15 cm (l x w x h), two arms were considered as known arms for the first 1min after the study. The unknown third arm entry was allowed after 1min and noticed number of entries into unknown arm as

exploration intension. The number of entries and time spent in each arm (known arm vs. novel arm) gives spatial exploration a measurement of anxiety levels (Conrad et al., 2003).

2.5.3.3. Measuring Depression with Tail Suspension and Force Swim test

- **A forced swim test (FST):** uses immobility to measure "behavioural depression." In this test, the animal was placed in a cylindrical vessel filled with lukewarm water. The initial period of normal test animals exhibits escape (climbing), and swimming behaviour gradually increases the immobility (floating) time. The antidepressants show different swimming behaviours depending on the class of antidepressants. For instance, increased swimming behaviour with selective-serotonin reuptake inhibitors (SSRIs) increased climbing behaviour with tricyclic antidepressants. The run time of the test for mice is 6min in which the first 2min is considered as the escape time phase and the last 4min considered as the immobility phase (Nordsborg et al., 2014).

- **Tail Suspension Test (TST):** The test involves suspending an animal by its tail. The test is suitable for mice and less stressful than FST. The test is performed for 6min duration and time spent immobile will be considered parameters to measure stress. The treated animal spends less time immobile during the test period (Di Giovanni and De Deurwaerdere, 2016).

2.5.3.4. Quantification of behavioural parameters with Cleversys software tool

The animal behaviour experiments were video recorded with analogue cameras provided by CleverSys. The Cleversys Topscan suite was used for recording; and these videos futher assessed for differenrt behavioural parameters. The parameters were normalised and calibrated as per the service provider protocols.

2.5.4. Anaesthesia, tissue collection, and storage

Mice were deeply anesthetised with 4% isoflurane and 1% O_2 to cull at the end of the treatment. The brain will be dissected to collect the hypothalamus and hippocampus and weighed for gene expression (stored at -80^{o}C). Half of the animals from each group were 4% formalin perfused for immunohistochemistry.

2.6. Statistical analysis:

All the data obtained during the current study was assessed for statistical significance by Prism 9.1a MacOS version. The result plots represented in further chapters with mean ± standard mean error (SEM). When interaction and/or the main effects were significant; means were compared using Sidak multiple-comparison post hoc test. A p-value of <0.05 was considered as statistically significant. The animal numbers were considered for parameters, body weight, food intake and fat deposition and according to G*Power 3.1 version, with effect size of 0.4, error probability 0.05, Power 0.8 (Miyamoto et al., 2018) results n= 80 total number of animals needed to justify the statistical significance.

Chapter 3 CFE induced 5HT2cR expression in SHSY5Y derived neurons

3.1 Abstract

Serotonin signalling in the central nervous system influences feeding behaviour. Reduced serotonin receptor 2c (5HT2cR) expression leads to hyperphagia and further weight gain. Conversely, the improved agonism of 5HT2cR causes hypophagia and weight loss. The appetite signalling in overeating disorders like PWS is linked to a decreased expression of functional 5HT2cR expression relative to the truncated 5HT2cR form. The 5HT2cR specific agonist like Lorcaserin showed significant improvement in weight loss in obesity. However, reduced expression of functional 5HT2cR may not improve satiety signalling even after agonist treatment. On the other hand, the *Caralluma fimbriata* extract (CFE) showed improved satiety and waist circumference reduction in people. The study was designed to know the influence of CFE's role in functional 5HT2cR expression in SHSY5Y cells, when treated with CFE for 48h and 96h. The CFE treated cells were measured for functional 5HT2cR expression by quantitative PCR reaction. Further, CFE treated SHSY5Y derived neurons were assessed for whole transcriptome NGS analysis as a pilot-scale study. The results were describing that CFE treatment with 25 and 50 mg/ mL concentrations showed significant increase in functional receptor expression in both 48h and 96h treated cells. In addition, the whole transcriptome data analysis showed anorexigenic genes like 5HT2cR, BDNF and PCSK1 increased expression levels, whereas appetite promoting genes NPY and NPY2R reduced their expression. However, the NGS transcriptome data need further larger scale analysis with more replicates. In conclusion, the study reveals CFE induced 5HT2cR expression may increase anorexigenic pathway activation which may further influence appetite regulation.

3.2 Introduction

The monoamine serotonin (5-hydroxytryptamine, 5HT) is produced from tryptophan. The enzyme Tph1, which is primarily expressed in the enterochromaffin (EC) cells of the gut, converts tryptophan to 5HT in the periphery. In contrast Tph2, is predominantly expressed in the raphe nuclei of the brainstem, and produces central 5HT (Garfield et al., 2016). The discovery of at least 14 functionally different 5HT receptor subtypes has aided in understanding the processes behind the effects of 5HT on hunger and energy homeostasis (Garfield and Heisler, 2009). Gene knockout research has focused on 5HT2cR, one of the five (5HT1aR, 5HT1bR, 5HT2aR, 5HT6R, and 5HT7R) 5HTR subtypes expressed in the hypothalamic areas and implicated in controlling satiety and energy metabolism (Di Giovanni and De Deurwaerdère, 2016, Nonogaki, 2022). In mice fed a chow diet, genetic excision/mutation of 5HT1aR, 5HT2aR, 5HT6R, and 5HT7R does not affect food intake or body weight (Donovan and Tecott, 2013). 5HT2cR transcripts are found throughout the central nervous system (CNS) and neuraxis, which are expected to play a vital role in appetite and energy homeostasis regulation (Strasser et al., 2016). Leptin-independent hyperphagia is shown in mice with a genetic mutation in 5HT2cRs, which leads to late-onset obesity, insulin resistance, and decreased glucose tolerance. In the 5HT2cR mutants, hyperphagia occurs before hyperinsulinemia and weight gain (Nonogaki, 2022). In addition, they also had reduced levels of activity-related energy expenditure without affecting their baseline metabolic rate (Higgs et al., 2011). Hence, functional 5HT2cR expression and activity was a potential target in weight loss and energy expenditure parameters in obesity and other overeating disorders.

The anti-obesity effects of pharmacologic drugs like fenfluramine and sibutramine appear to be mediated by 5HT2cR (Xu et al., 2010). However, these medications were withdrawn from the international market due to non-specificity and cardiac side effects caused by 5HT2bR activation (Xu et al., 2010). Furthermore, 5-HT2cR mutants are more sensitive to high-fat and high-sucrose diets than wild-type mice, resulting in obesity and type 2 diabetes at an earlier age (Higgs et al., 2011). The non-selective serotonergic agonist mCPP (meta-Chlorophenyl piperazine) by systemic injection results in feeding suppression in wild-type mice, and the anorexic effect of mCPP is attenuated in fasting 5-HT2cR-deficient mice (Tecott et al., 1995). 5-HT2cRs are found in the arcuate nucleus (ARC) of the hypothalamus on pro-opiomelanocortin (POMC) neurons, suggesting that 5-HT2cR and the melanocortin pathway may interact in the control of eating behaviour (Morley, 1987, Sargent et al., 1997). The d-

fenfluramine and mCPP both promote the activation of POMC neurons in the ARC. Furthermore, d-fenfluramine and mCPP activate melanocyte-stimulating hormone (MSH) containing neurons, supporting this concept (Monian et al., 2022). The activation of a subset of POMC neurons by mCPP is assumed to be mediated via the hypothesised transient receptor potential C (TRPC) channels (Harno et al., 2018). Another drug, lorcaserin, which is a selective 5HT2cR agonist, caused clinically significant weight loss and was licenced as a novel anti-obesity agent by the Food and Drug Administration (FDA) in 2012 (Nonogaki, 2022)

Hence with the specificity of lorcaserin to 5HT2cR, it is unlikely to enhance the risk of cardiac valvulopathy by 5-HT2bR activation (Nonogaki, 2012). The CAMELLIA-TIMI 61 study found no significant differences in major cardiovascular events between the lorcaserin-treated and placebo groups (Bohula et al., 2018). Furthermore, compared to placebo, lorcaserin lowered the risk of incidence of diabetes and microvascular complications in overweight and obese patients and the incidence of new-onset or progressive renal impairment (Nonogaki, 2022). Furthermore, neither the occurrence of cancer nor the occurrence of cancer in obese participants administered with lorcaserin or placebo differed substantially. Despite this, the FDA recommended that lorcaserin be voluntarily removed from the US market in 2020 after clinical safety research revealed a possible elevated risk of cancer in obese people treated with the drug (Mathai, 2021). As a result, anti-obesity medicines that target central 5-HT systems are still being developed.

Alternative pre-mRNA splicing controls the expression of the functional 5HT2cR, which modulates food intake. From chapter-I literature, the 5HT2cR gene consist of six exon regions, in which exon V differentiated into two parts Va and Vb. The exon Vb alternative splicing and adenosine to inosine editing at five locations (as shown Figure 3.1) leads to different variants of 5HT2cR (Shimogori et al., 2010). There were two polyadenylation sites in the 5HT2cR gene with single promoter sequence. Exon Vb is affected by pre-mRNA editing and splicing in the longest transcript, with six exons (Stamm et al., 2017). The Exon V provides an extended secondary structure, which allows RNA editing by adenosine deaminases operating on RNA (ADAR1 and ADAR2) with RNA duplex as a substrate (Shimogori et al., 2010). The utilisation of the distal alternative splice site is controlled by conformational changes in the RNA secondary structure following binding to synthetic ligands. By changing three amino acids in the receptor's second intracellular loop that links to the effector Gq protein, RNA editing generates at least 24 full-length proteins (Morley, 1987, Shimogori et al., 2010). The amino

acids I, N, and I (isoleucine, asparagine, and isoleucine) are found at positions 156, 158, and 160 of the receptor protein in the non-edited version. The INI isoform is constitutively active and has the highest coupling effectiveness to the G- protein in response to serotonin (Stamm et al., 2017).

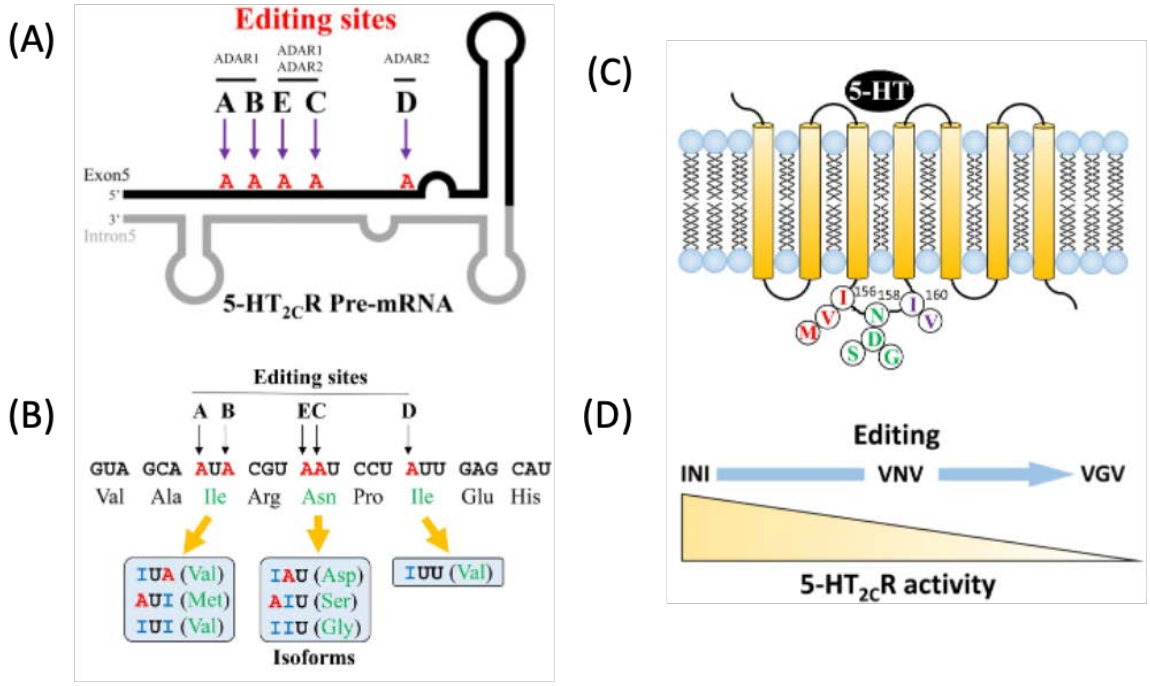

Figure 3.1: The editing variants of 5HT2cR: (A) Five sites (A to E) in exon 5 of 5-HT2CR mRNA. Adenosine to Inosine (A to I) RNA editing occurs in the region where exon 5 makes a double strand with intron 5. Editing enzyme ADAR1 acts on A and B sites, whereas ADAR2 acts on D sites. E and C sites are edited by both ADAR1 and ADAR2 (B) The structure of 5-HT2CR has seven transmembrane regions. Three amino acids (156, 158, 160) in the second intracellular loop may be edited by RNA editing. (C) The variation of edited isoforms. From A and B editing sites, non-edited isoleucine (Ile) can be edited to valine (Val) or methionine (Met). Asparagine (An) in E and C sites may be edited to aspartic acid (Asp), serine (Ser), or glycine (Gly). Amino acid isoleucine at the D site may be edited to valine (Val). (D) 5-HT2CR activity is reduced in relation to an increase in RNA editing.

On the other hand, the highly edited isoforms have a decreased sensitivity to serotonin binding and resulting in minimal or negligible constitutive activation. In mice, sole expression of the fully edited version of the receptor produces hyperphagia, suggesting that altered 5HT2cR signalling is required to maintain proper energy balance (d'Agostino et al., 2018). The skipping of exon Vb region was resulting a shorter protein isoform with only three transmembrane

domains (Price et al., 2018). The endoplasmic reticulum (ER) is home for tagged proteins coded by cDNAs for the shortened protein. Because these proteins can dimerise with the full-length serotonin receptor, ER retention likely inhibits serotonin signalling (Palacios et al., 2017, Ge et al., 2017). Moreover, overeating disorders like Prader–Willi syndrome (PWS), which is a common syndromic form of obesity characterised by hyperphagia, demonstrates the need of appropriate hypothalamic food regulation (Griggs et al., 2018b). The lack of 5HT2cR gene expression from a prenatally imprinting region on chromosome 15q11.2 causes the syndrome. Numerous proteins and two clusters of C/D box small nucleolar RNAs are found in this region (snoRNA). Recent genetic investigations have found that the deletion of these snoRNAs plays a significant role in PWS (Griggs et al., 2018b, Shimogori et al., 2010). The processing of the 5HT2c pre-mRNA is regulated by one of these snoRNAs. One of the snoRNAs called SNORD115 is involved in functional 5HT2cR (5Ht2cR-fn) formation by being involved in pre-mRNA splicing. The SNORD115 knockdown mice showed decreased functional 5HT2cR expression, contributing to hyperphagia (Bratkovič et al., 2018). Earlier studies showed that alternate oligo sequences that mimic the SNORD115 sequence enhanced the functional receptor expression. Therefore, functional 5HT2cR is a potential target for appetite regulation in obesity and overeating diseases (Stamm et al., 2017). The reduced expression of truncated 5HT2cR (5HT2cR-tr) plays a crucial role in increasing functional receptor expression in POMC neurons (Bratkovič et al., 2018).

The current study aims to understand the effect of CFE treatment in functional 5HT2cR expression in SHSY5Y derived neurons. In addition, to understand the differential expression of functional and truncated receptor expression with CFE concentration optimisation. Further, the whole transcriptome analysis of CFE treated cells may reveal other patterns of anorexigenic gene expression influenced by CFE treatment.

3.3 Methods

RNA isolation for sequencing:

The RNeasy Plus Mini kit from Qiagen (cat. no. 74134) was used to extract the total RNA from SHSY5Y derived neurons for whole transcriptome analysis. The cells were pelleted down after 48hr and 96h of CFE treatment from individual wells separately. The protocol provided in the kit was followed stepwise, as mentioned below.

- The cells were harvested a maximum of 1 x 10^4 cells as a cell pellet.
- The appropriate 350 µl volume of lysis Buffer RLT Plus was added and vortexed for the 30s.
- The lysate was transferred to a genomic DNA eliminator spin column and placed in a 2 ml collection tube.
- The columns were centrifuged for 30 s at ≥8000 x g (≥10,000 rpm), and elution was collected.
- The volume (350 µl) of 70% ethanol was added to the flow-through and mixed well by pipetting.
- The sample was transferred up to 700 µl, including any sediment, to a RNeasy spin column placed in a 2 ml collection tube.
- The lid was closed, centrifuged for 15 s at ≥8000 x g, and then discarded the flow-through.
- Added 700 µl wash Buffer RW1 to the RNeasy Mini spin column placed in a 2 ml collection tube and centrifuged at ≥8000 x g for 15 s.
- Then discard the flow-through, and 500 µl wash Buffer RPE was added to the RNeasy spin column and centrifuged for 15 s at ≥8000 x g.
- After discarding the flow-through, 500 µl Buffer RPE was added to the RNeasy spin column and centrifuged for 2 min at ≥8000 x g (≥10,000 rpm).
- The RNeasy spin column was placed in a new 1.5 ml collection tube and added 40 µl RNase-free water directly to the spin column membrane and centrifuge for 1 min at ≥8000 x g to elute the RNA.

Next-generation sequencing

The RNA integrity was checked before processing for transcriptome sequencing by Agilent 2100 Bioanalyzer. The Agilent RNA 6000 nano kit was used to measure the RNA integrity number (RIN) based on the intactness of 18s and 28s rRNA sequences. The bioanalyzer was

able to detect the dye-RNA complex through laser induced fluorescence and resulting a gel like bands in the image (as represented in Figure 3.10A). All the samples of CFE treated for 48h, and 96h and respective controls were analysed for quality using RIN measurement. The RIN values of samples were noted between 8.9 to 10, which is ideal for sequencing (Sigurgeirsson et al., 2014). The MGI Tech MGISEQ2000RS hardware was used to perform the sequencing with 60 million read pairs per sample, which is a preferred read depth (number of usable reads from the instrument sequencing) for global view of gene expression (illumina, 2017). The Figure 3.2 was describing brief workflow of transcriptome sequencing. The raw data from sequencing was normalised to a *fastq* file format. The sequencing and normalisation of data were conducted by Micromon Genomics at Monash University.

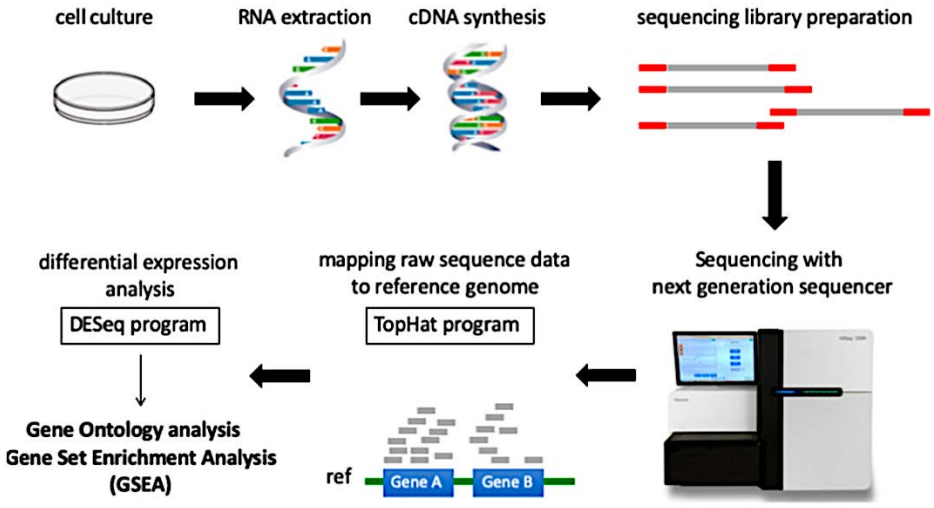

Figure 3.2: Schematic representation of the workflow for whole transcriptome analysis steps (Adilijiang et al., 2019)

NGS analysis

The RNAseq pipeline (Tsyganov et al., 2018) was used to align raw data (*fastq* files) with the GRCh38/hg38 (reference genome version used) reference by using the STAR aligner (Dobin et al., 2013). After the alignment SAM files were converted into BAM files to do downstream analysis. The alignment quality has been checked with Qualimap. The gene counts obtained from aligned files, using Feature Counts (Liao et al., 2014), reads were quantified. Degust (Wanhainen et al., 2019) is a web tool that performs differential expression analysis using limma-voom normalisation (Law et al., 2014), producing counts per million (CPM). The library volume normalisation and trimmed mean of M values (TMM) normalisation (for gene

coverage and depth) (Oshlack et al., 2010) were used for RNA composition normalisation to analyse raw counts. Degust (Wanhainen et al., 2019) also includes several high-quality graphs, such as conventional multidimensional scaling (MDS) and MA plots. Finally, Gene Ontology (GO) was performed to determine pathway enrichment analysis to compare the treated and control samples.

We identified the top 5233 DEGs (differentially expressed genes) based on the dataset. These DEGs were imported into the STRING V11.5 database to obtain a ". TSV" (tab separated values) file of protein interactions. The hub genes were identified by topological analysis by using methods MCC: Multiple consensus Clustering Framework, DMNC: Multiple consensus Clustering Framework, MNC: Multiple consensus Clustering Framework and Degree values.

The CytoHubba tool was used to identify closely interacting hub genes for both upregulated and down regulation gene sets. Necessary clustering modules related to the hub genes were abstracted by CytoHubba, which had 133 nodes and 1077 edges. The node represents each gene and edge represents the interaction with other genes. The more edges found from one node to other genes represents much interaction and its importance of the note. The current study 5HT2cR node was considered to represent its interaction with other genes in different pathways. We obtained two clustering modules with the highest score from the PPI (protein-protein interaction) network of all DEGs by the MCODE algorithm (Chin et al., 2014).

3.4 Results and Discussion

3.4.1 CFE influence on undifferentiated SHSY5Y cells

The undifferentiated SHSY5Y neuroblastoma cells were used to estimate the toxicity of the proposed CFE concentrations. The undifferentiated cells were treated with 0, 0.1, 0.5, 1, 5, 10, 25, 50µg/mL of CFE for 48h and 96h duration. The microscopic observation of the CFE treated cells showed no toxicity, and cell proliferation was observed to align with control well plates. The quantified RNA converted to cDNA and normalised to optimise qPCR run for 5HT2cR, Exon Vb and housekeeping genes like GAP43, SYP38 and Akt1 expression. However, there is no variation found in 5HT2cR expression levels from $2^{-\Delta\Delta Ct}$ analysis from the qPCR data. The gel picture showed in Figure 3.3 representing not much variation of functional and truncated 5HT2cR expression with varying concentrations of CFE.

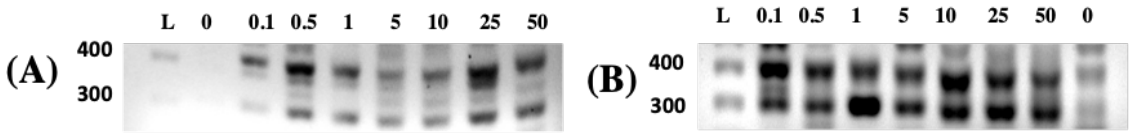

Figure 3.3: CFE induced 5HT2cR expression visualisation from qPCR products of undifferentiated SHSY5Y cells on agarose gel: The 5HT2cR expression in both functional (at 400bp) and truncated (at 300bp) isoforms, (A) 48h and (B) 96h of the treatment period. Where L represents 100bp DNA ladder and concentrations of CFE represented over each lane representing from 0 to 50 in μg/mL.

3.4.2 Differentiated SHSY5Y neuronal cells

Following the three-week differentiation protocol, the SHSY5Y derived neurons were treated with CFE at 0, 0.1, 0.5, 1, 5, 10, 25, 50μg/mL concentrations for 48h and 96h duration. The cells were healthy in the wells, and no toxicity was observed with treatment. Microscopic observations were captured to visualise neuron like cells interaction as showed in Figure 3.4. The CFE treated cells were harvested for total RNA and used for cDNA conversion. The qPCR data revealed further validations of 5HT2cR expression with functional and truncated receptor differentiation.

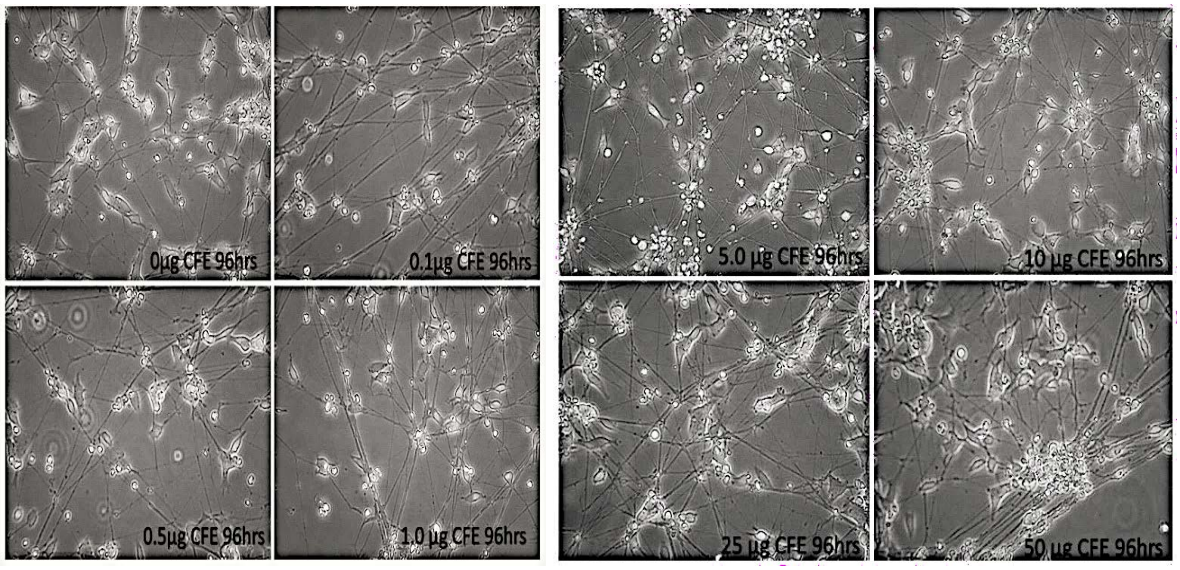

Figure 3.4: The SHSY5Y derived neurons during CFE treatment: all the pictures were captured with a regular inverted microscope (Labomed-TCM400) available in the lab. The images represented are at 400x zoom.

The Figure 3.5 shows the qPCR assessment data, which represents 5HT2cR expression in CFE treated SHSY5Y neurons. Figure 3.5A reveals that after 48h of CFE exposure, there was a significant increase in 5HT2cR mRNA expression with 25 and 50 µg/mL concentrations with p-values of 0.01 and <0.001, respectively. The exon Vb region expression levels measured to validate the CFE treatments enhance only functional 5HT2cR expression rather than truncated. Exon Vb expression levels from qPCR data demonstrated in Figure 3.5C define that exon Vb expression levels align with full-length 5HT2cR measured. The CFE concentrations of 25 and 50 µg/mL for 48h of duration showed a significant increase in exon Vb region expression in SHSY5Y derived neurons with p= 0.004 and <0.001, respectively.

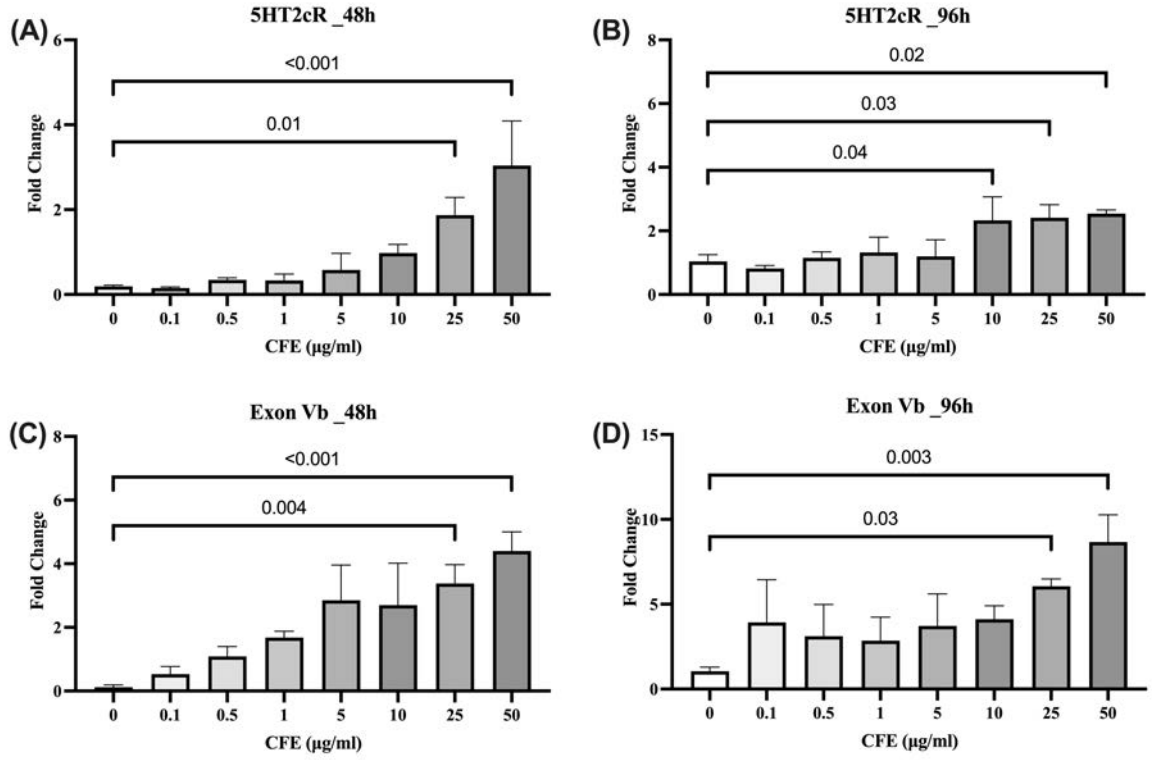

Figure 3.5: CFE induced serotonin receptor expression: 5HT2cR expression in SHSY5Y neurons after (A) 48h and (B) 96h of CFE treatment; The exon Vb region (present in functional and lacks for truncated 5HT2cR) quantified after (A) 48h and (B) 96h of CFE treatment. The data represented the Mean ± SEM with n = 3 replicates from individual wells.

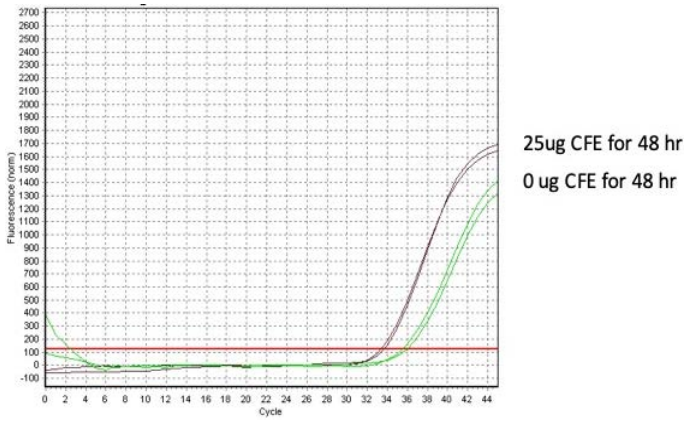

Figure 3.6: The qPCR run for Exon Vb region between control and CFE treatment

Following 96h duration of treatment with CFE, the SHSY5Y neurons showed significant increase of 5HT2cR expression at 10 (p= 0.04), 25 (p= 0.03) and 50 (p= 0.02) µg/mL concentrations (as shown in Figure 3.5B). Further, Figure 3.5D reveals the expression of the exon Vb region also significantly higher in SHSY5Y neurons treated with 25 (p = 0.03) and 50 (p = 0.003) µg/mL concentrations of CFE. Therefore, it is evident that during CFE treatment, there is an increase in the expression of the functional 5HT2cR sequence compared to the inactive or truncated isoform. The Figure 3.6 was representing exon Vb differential expression with CFE treatment.

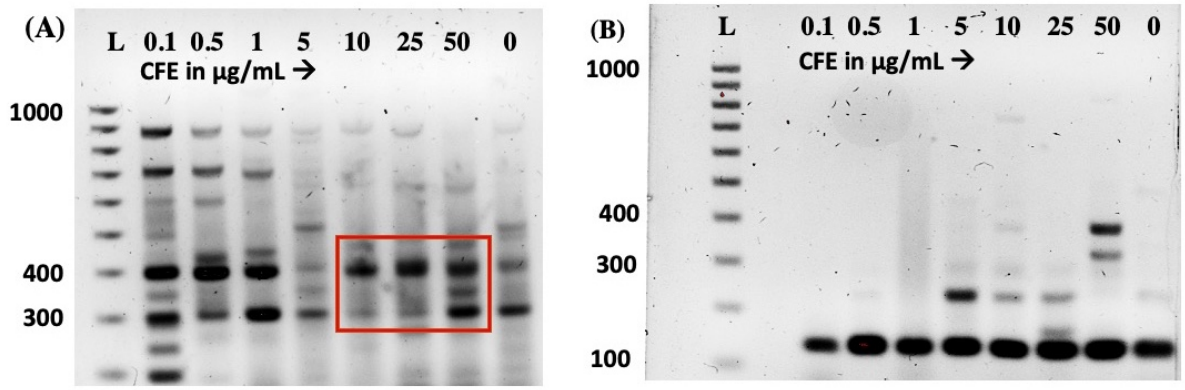

Figure 3.7: CFE induced 5HT2cR expression in SHSY5Y derived neurons after 48 h of treatment: The qPCR derived products were used to visualise (A) The 5HT2cR expression in both functional (at 400bp) and truncated (at 300bp) isoforms, (B) Exon Vb (at 140bp) region-specific to functional 5HT2cR visualisation at 140bp by agarose gel electrophoresis with SYBER green staining.

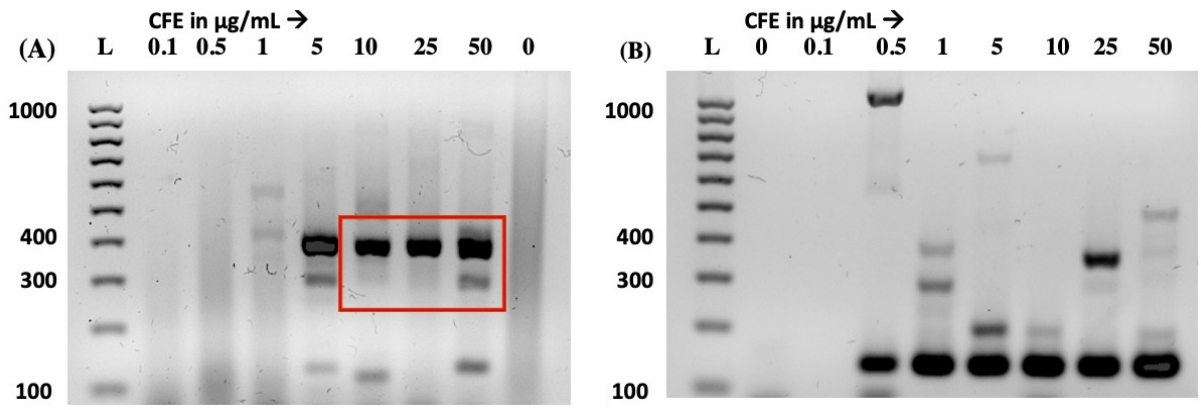

Figure 3.8: CFE induced 5HT2cR expression in SHSY5Y derived neurons after 96 h of treatment: (A) The visualisation of 5HT2cR expression levels in both functional (at 400bp) and truncated isoform (at 300bp), (B) Exon Vb (at 140bp) region-specific to functional 5HT2cR visualisation at 140bp band length on the gel.

Table 3.1: Lane and Band Volume/intensity analysis from Chemidoc™ MP of gel images of PCR products from CFE treated SHSY5Y neurons. Where, fn: functional and tr: truncated 5HT2cR.

		48h		
CFE treatment	**5HT2cR-fn**	**5HT2cR-tr**	**Ratio of fn to tr**	**Exon Vb**
10 µg/mL	13,648,705	16,205,623	0.84	19,157,220
25 µg/mL	7,804,328	4,106,739	1.9	27,300,960
50 µg/mL	6,069,091	5,726,083	1.05	28,276,245

		96h		
CFE treatment	**5HT2cR-fn**	**5HT2cR-tr**	**Ratio of fn to tr**	**Exon Vb**
10 µg/mL	27,185,356	7,737,614	3.51	26,920,224
25 µg/mL	42,048,876	3,347,512	12.56	29,759,824
50 µg/mL	26,951,354	7,014,448	3.84	31,451,392

In addition, qPCR products were further assessed by gel electrophoresis to visualise the functional vs truncated receptor expression (as shown in Figures 3.7 and 3.8). The gel images were demonstrating RNA expression reduced for truncated 5HT2cR receptors (at 300bp length) in 10, 25 and 50 µg/mL concentrations. Furthermore, the Table 3.1 shows that the exon Vb gels band intensity was increased at 25 and 50 µg/mL concentrations of CFE.

The 5HT2cR editing and alternative splicing appear to be important in biological activities. The adenosine deaminases working on pre-mRNA second intracellular loop to convert adenosine to inosine is unique to the 5HT2cR type among other 5HT receptors. Editing reduces both the receptor's interaction with its downstream signalling system and its constitutive activity, according to in vitro experiments (Martin et al., 2013b). Recently, several mutant mice lines expressing solely the fully edited VGV (residual positions: 156-Val, 158-Gly and 160-Val as shown in Figure 3.9) 5HT2cR were created. The increased motor responses to 5HT2cR ligands were leading to added behavioural and metabolic alterations, further changes in functional 5HT2cR expression (Stamm et al., 2017). BALB/c VGV mice showed more significant energy expenditure and fat mass loss, as well as lower cholesterol, as compared to wild-type (WT) mice (Englander et al., 2005).

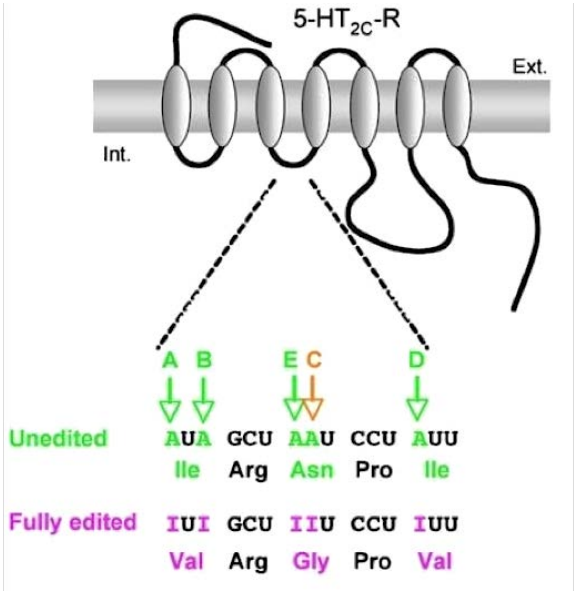

Figure 3.9: Representation of Unedited and fully edited amino acid residues at 16, 158 and 160 positions of exon V region in 5HT2cR.

Studies confirm that change in 5Ht2cR editing are linked to behaviour and emotion in people and animals (Phillips et al., 2018). C57BL/6J /VGV animals had less RNA encoding the truncated form (5HT2cR-tr), a naturally occurring receptor that will not bind 5HT (serotonin) and other 5HT2cR ligands, in the C57BL/6J brain regions investigated (Shimogori et al., 2010). In VGV mice, the functional to shortened receptor ratio approximately doubled compared to WT mice, which coincided with increased receptor density (Wanhainen et al., 2019). A decrease in the 5-HT2cR-tr isoform would eventually increase 5HT2cR-mediated suppression of stress-induced 5-HT release. According to the literature, shortened receptors are not simply a by-product of unusual splicing; they play a role in interacting with fully synthesised 5HT2cR-

fi (functionally inactive) and forming protein dimers (Stamm et al., 2017, Shimogori et al., 2010). The trafficking pattern of 5HT2cR-tr was significantly different from that of 5HT2cR-fi. 5HT2cR-tr accumulated in the ER instead of being transferred to the Golgi apparatus and the plasma membrane (Shimogori et al., 2010, Oshlack et al., 2010). 5HT2cR-tr forms heterodimers with 5HT2cR-fi, trapping 5HT2cR-fi in the ER, suggesting that 5HT2cR-tr may have a regulatory function. The 5HT2cR-fn produces dimers in the plasma membrane, like the seven-transmembrane receptors. These dimers occur in the endoplasmic reticulum during the production of 5HT2cR (Nonogaki, 2022). 5HT2cR creates two types of dimers, according to disulphide trapping tests based on the rhodopsin structure: one dimer class is created by interactions between transmembrane region 1 (TM1), and connections between TM4 and TM5 form the other dimer class. Ligand interaction does not modify the structure of TM1 domain dimers (Filizola, 2010). However, it does change the structure of one of the protomers in the TM4–TM5 dimer, implying that TM4–TM5 is a conformational heterodimer when activated (Filizola, 2010). The TM1 domains found in both proteins are probably involved in heterodimerisation (Stamm et al., 2017).

The heterodimer of 5HT2cR-tr and 5HT2cR-fn is found in the endoplasmic reticulum, reflecting the tight intracellular localisation of 5HT2cR-tr (Martin et al., 2013b). 5HT2cR-tr inhibits 5HT2cR-fn signalling, evidenced by a dose-dependent decrease in diacylglycerol production in transfection experiments (Zhang et al., 2016a). Therefore, the 5HT2cR-tr isoform inhibits the full-length receptor's constitutive activity, either by blocking inside the cell or modifying the 5HT2C homodimer formation required for coupling the Gq/11 (Herrick-Davis et al., 2004). The full-length receptor heterodimerises with the ghrelin receptor GHSR1a and interacts with the 5HT2cR-tr, reducing ghrelin's orexigenic impact (Schellekens et al., 2015). The truncated to full-length receptors ratio regulates 5HT2C activity since an increased truncated receptor accumulates the full-length cytosolic receptor, resulting in reduced 5HT2C signalling. Further, studies revealed improved energy expenditure and behavioural parameters in mice with reduced expression of 5HT2cR-tr RNA (Morabito et al., 2010). In addition, the 5HT2cR-fn receptors are essential for the signalling of POMC neurons. Therefore, overexpression of truncated receptors results in hyperphagia in mice and reduced activity of POMC neurons (Morabito et al., 2010). The 5Ht2cR knockout mice has developed hyperphagia and obese symptoms (Morabito et al., 2010). Moreover, activation of the 5HT2cR via selective agonist such as the FDA approved drug lorcaserin inhibits food intake (Patel et al., 2020).

The SNORD115 microRNA sequence promotes full-length receptor expression in neurons to regulate food intake and its role in alternative splicing in 5HT2cR-fn receptor synthesis (Morabito et al., 2010). One of the most common hereditary causes of morbid obesity and cognitive incapacity in humans was seen in disorders like PWS (Hebras et al., 2020). The imprinted region, which is absent in PWS, includes five protein-coding genes (MKRN3, MAGEL2, NECDIN, SNURF-SNRPN, and NPAP1/C15 or f2) as well as six orphan C/D box snoRNAs (SNORDs): 107, 64, 108, 109, 116 (29 copies divided into five classes), and 115 (47 almost identical copies) (Kishore and Stamm, 2006). The SNORD 115 modulates splicing of 5HT2cR by increasing exon Vb inclusion to form full-length receptors, as stated in the literature chapter I of this study. In POMC neurons, a knockout model for PWS that lacks all SNORDs, including SNORD115, reveals an increase in the 5HT2cR-tr isoform (Zhang et al., 2016a). Because POMC neurons do not efficiently produce c-fos after 5HT2C stimulation, increasing 5HT2cR-tr in these neurons inhibits the anorexic response of these animals. The lack of this signal is likely to promote hyperphagia, a symptom of PWS (Garfield et al., 2016). Thus, an increase in the shortened 5HT2c isoform in Prader–Willi syndrome likely lowers the serotonin response by heterodimerising with the 5HT2cR-fn forms (Smith et al., 1997), thereby inhibiting the satiety response.

The current study results of CFE treated SHSY5Y neurons showed an increase in full-length 5HT2cR expression. Furthermore, the agarose gel supports the reduced expression of the truncated receptor in 25 and 50 mg/mL concentrations (Table 3.2). Therefore, CFE may have a potential role in 5HT2cR mediated signalling in satiety regulation. In addition to support the CFE treated 5HT2cR expression and further activation of anorexigenic genes were estimated with whole transcriptome analysis. Next-generation sequencing was used to measure whole transcriptome analysis.

Micromon services at Monash University performed the NGS studies sample preparation and sequencing for data normalisation. The Figure 3.10A confirms the RNA stability of each sample performed for sequence. The overall number of differentially expressed genes were plotted under the volcano plot as shown in Figure 3.10B, C, and D. The RIN number for all the samples was 8 to 10, which is in line with the required level of purity for this type of analysis.

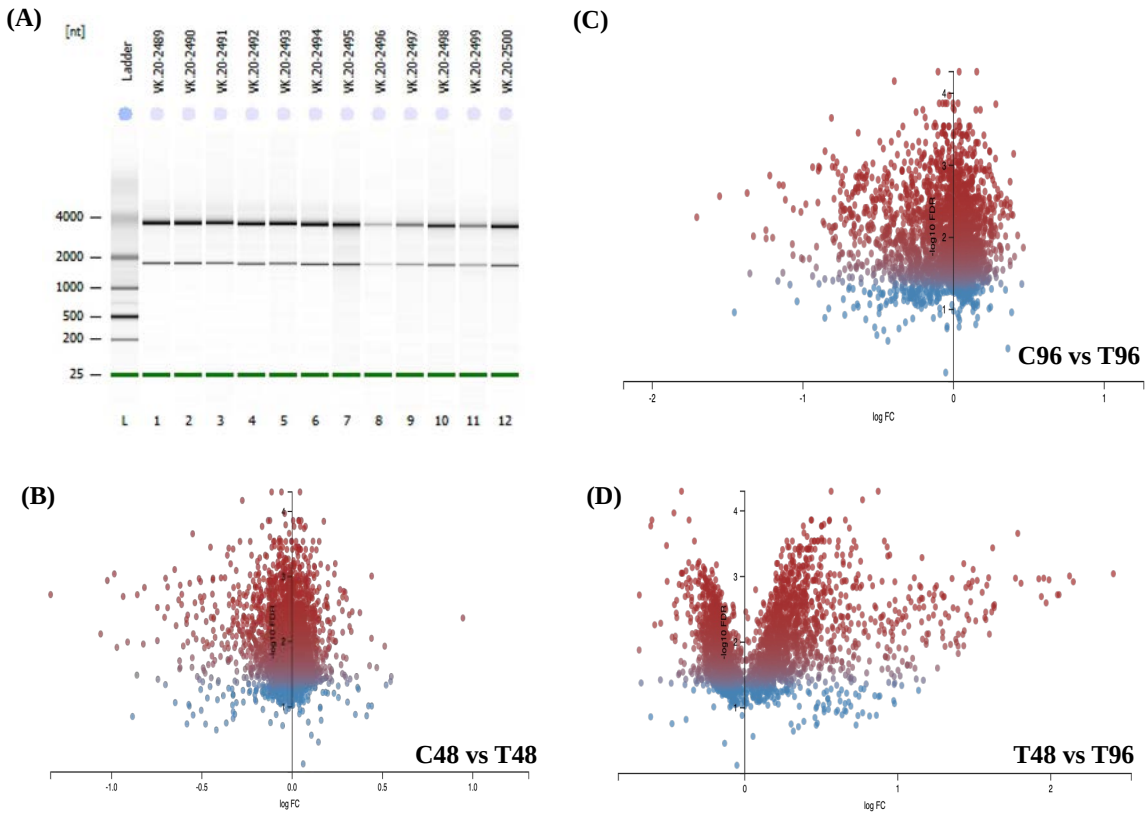

Figure 3.10: Next-generation sequencing of SHSY5Y neurons: (A) RNA intactness for NGS analysis (gel image shows 18s and 28s rRNA consistency), (B) Volcano plot of differentially expressed genes identified between control and CFE-treated SHSY5Y neurons after 48h of treatment, (C) Volcano plot between control and CFE treated neurons after 96 h of treatment and (D) comparison of both CFE treated neurons for 48 h and 96 h. FC represents fold change in expression and FDR represents false discovery rate.

RNA sequencing (RNA-seq) analysis was performed to find differences in expression of genes between control and CFE treatments at 48 h and 96 h of duration. The differentially expressed genes with CFE (25 µg/mL) treatments were analysed in both at 48 h and 96 h time points. The normalised data resulted in 17396 genes being differentially expressed; after adjusting for p-value, the upregulated genes were 5298, and downregulated genes were 1974. The upregulated and downregulated genes were further screened for different metabolic pathway analyses. The gene ontology (GO) studies enrichment analysis of pathways showed Figures 3.11, 3.12, 3.13 and 3.14 based on the clustering of genes expression. The gene ontology study was demonstrating that CFE treated neurons significant increase in gene expression in protein transport, cellular protein localisation, nervous system development, regulation of biosynthetic pathways, pre-mRNA processing, and macromolecule modification procedures.

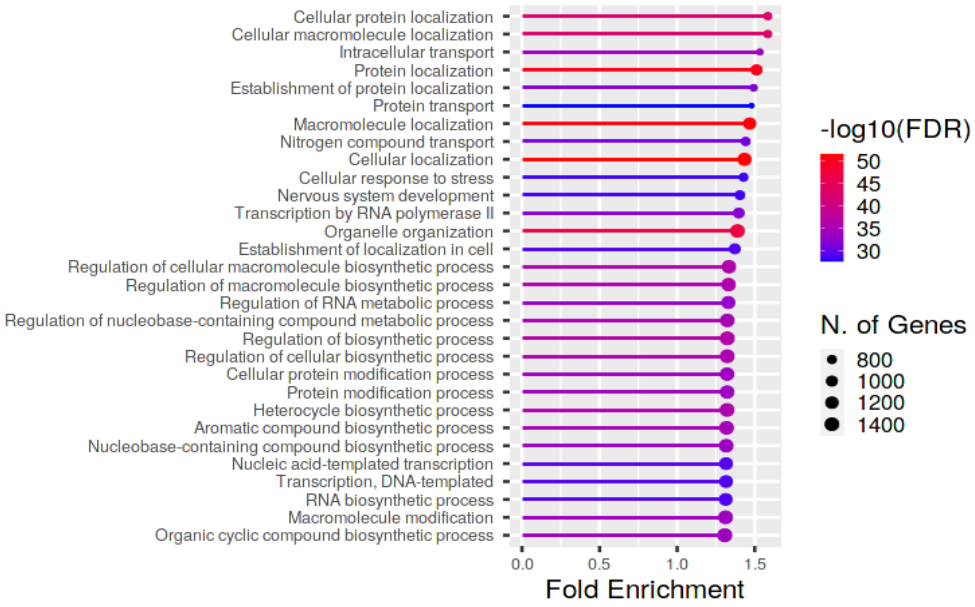

Figure 3.11: Enriched gene ontology (GO) representation in dot plot: The 30 GO processes with the highest gene ratios (initial group of selection) are plotted in the direction of gene ratio. The number of genes with differentially expressed gene list (which are significant) by the size of the dots in respective process, and the colour of the dots denotes the FDR cut off values.

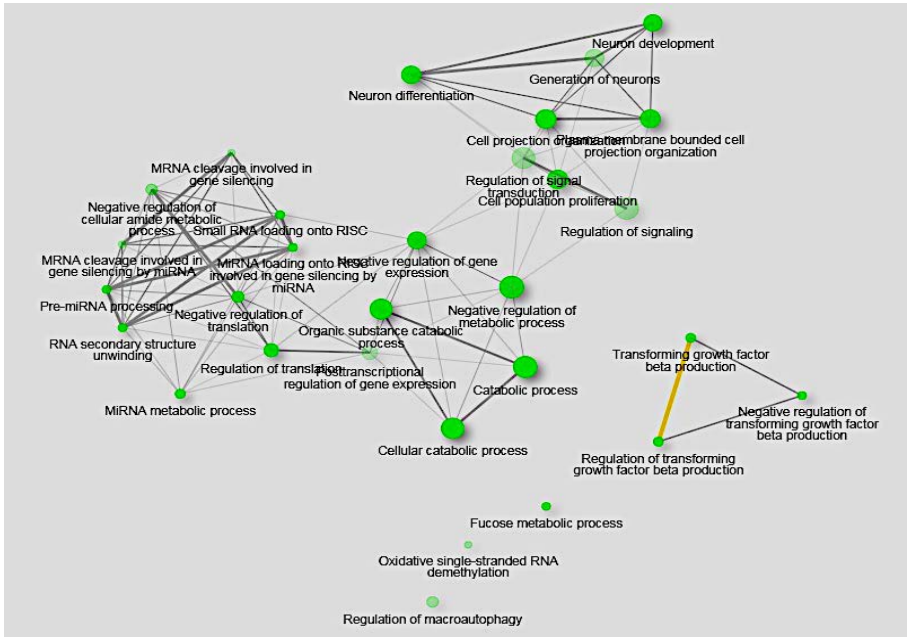

Figure 3.12: Enrichment GO plot: The top 30 highly enriched GO terms (as determined by P-adjusted values) are displayed, with related terms clustered together. The size of the terms denotes the number of significant genes from the list of the significant genes, and the colour shows the p- values compared to the other established terms.

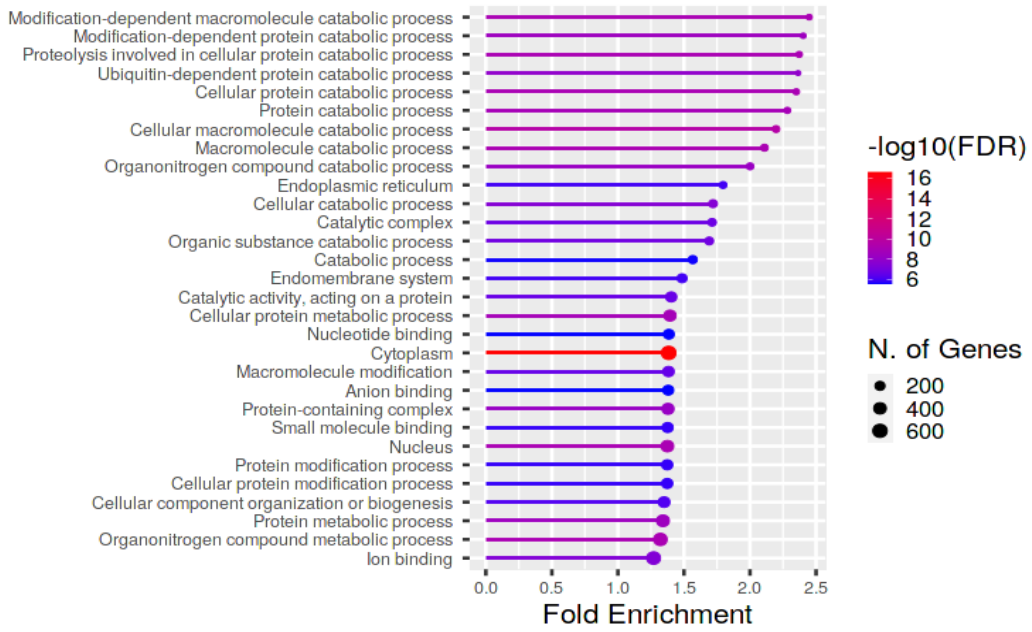

Figure 3.13: Enriched gene ontology (GO) representation in dot plot: The 30 (second group of interest) GO processes with the most significant gene ratios are plotted in the direction of gene ratio. The size of the dots represents the number of genes in the differentially expressed gene list associated with the GO process, and the colour of the dots represents the FDR cut off values.

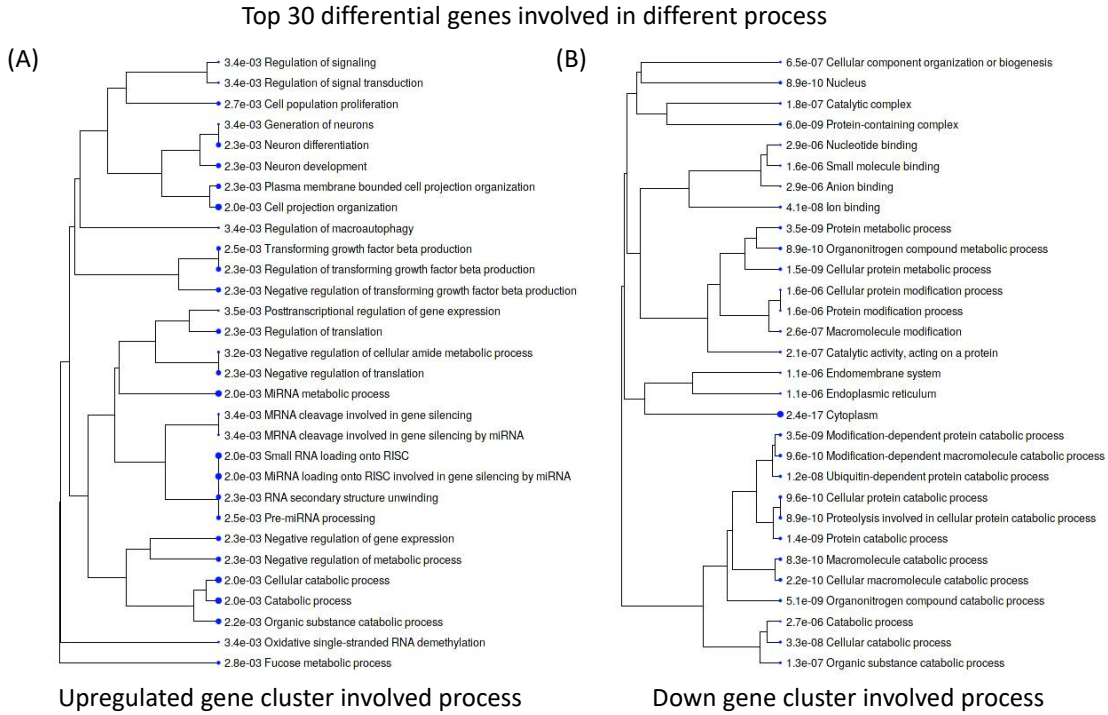

Figure 3.14: The phylogenetic connection plot of GO stands for the interlink between the top 30 pathways selected, and their inter-connection was represented with corrected p values.

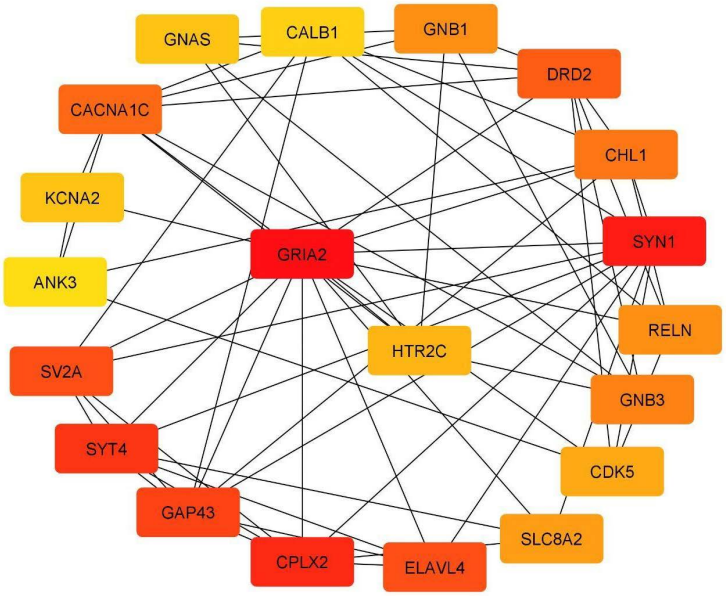

Figure 3.15: 5HT2cR interaction with top differentially expressed genes involved in the dendrite communication process, the plot derived from CytoScape tool; Where brighter colour represents more significant increased and lighter colour means significantly reduced levels.

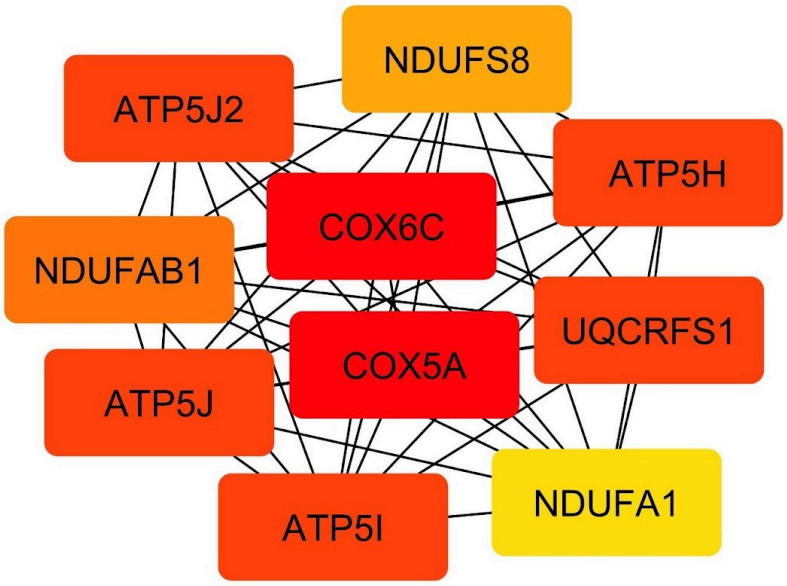

Figure 3.16: Differentially expressed gene cluster involved in thermogenesis process, the plot derived from CytoScape tool; brighter colour represents more significant increased and lighter colour means significantly reduced levels.

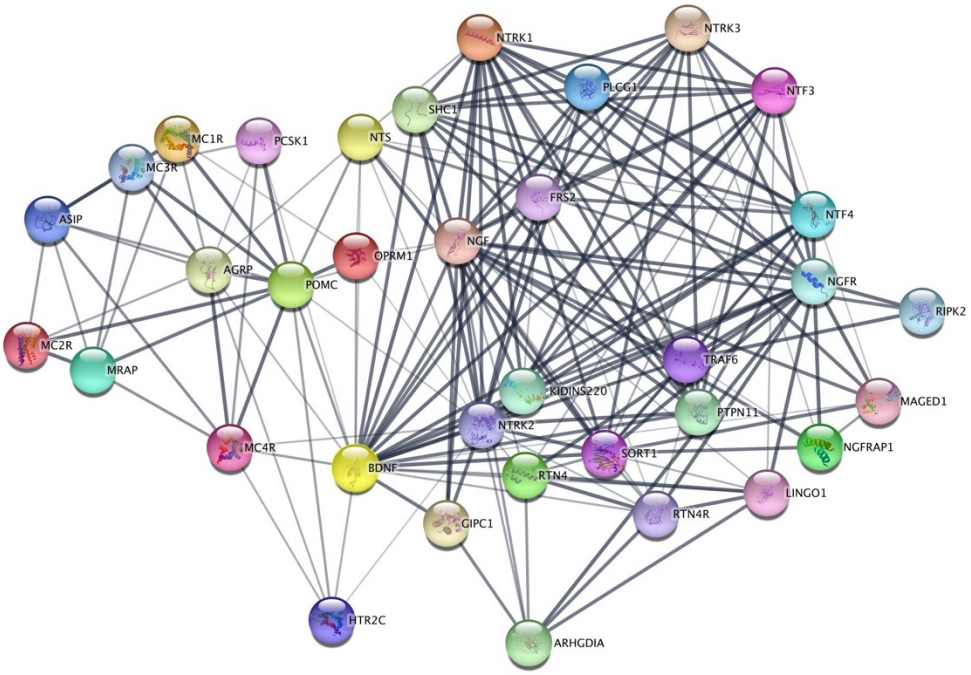

Figure 3.17: String network has drawn of proteins identified from upregulated anorexigenic genes after adjusted p-value by using string database. The brightness of the connecting line represents the strength of association.

The CytoHubba clustering showed in Figure 3.15, a brief network displaying of 5HT2cR role in dendrite guidance related to differentially expressed genes and Figure 3.16 shows the genes cluster of thermogenesis. Whereas Figure 3.17 represents a combination of DEG's from transcriptome analysis which have been identified as key molecules in anorexigenic signalling. The genes PHIP, KSR2, NPY, MRAP2, SH2B1, NTRK2, PCSK1, GIPR, BDNF, ADCY3, HDAC5, DGKI and PRLH were considered for further discussion (as shown in Figure 3.18). Interestingly, all these genes are associated with 5HT2cR and having a role in regulation of food intake and energy expenditure in obesity and other overeating disorders.

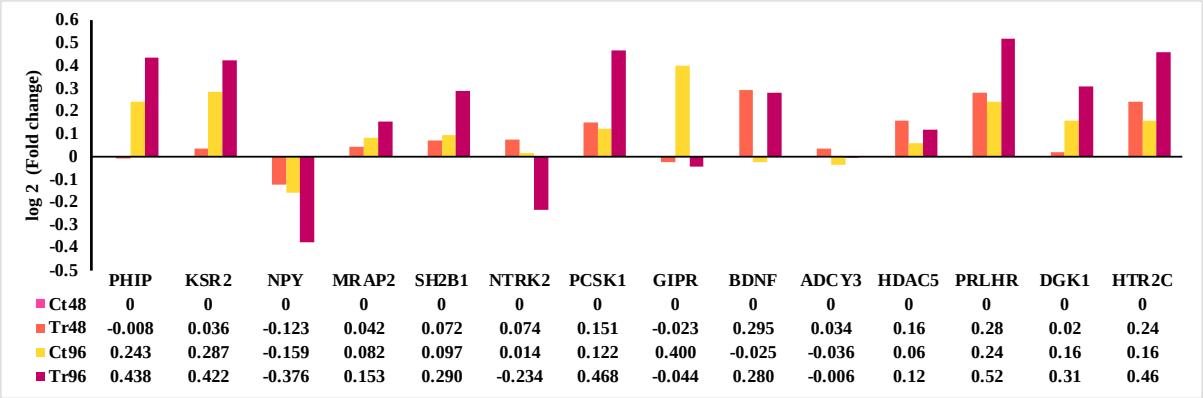

	PHIP	KSR2	NPY	MRAP2	SH2B1	NTRK2	PCSK1	GIPR	BDNF	ADCY3	HDAC5	PRLHR	DGK1	HTR2C
Ct48	0	0	0	0	0	0	0	0	0	0	0	0	0	0
Tr48	-0.008	0.036	-0.123	0.042	0.072	0.074	0.151	-0.023	0.295	0.034	0.16	0.28	0.02	0.24
Ct96	0.243	0.287	-0.159	0.082	0.097	0.014	0.122	0.400	-0.025	-0.036	0.06	0.24	0.16	0.16
Tr96	0.438	0.422	-0.376	0.153	0.290	-0.234	0.468	-0.044	0.280	-0.006	0.12	0.52	0.31	0.46

Figure 3.18: DEGs associated with obesity and energy expenditure: The gene expression in SHSY5Y derived neurons after 25 µg/mL of CFE treatment for 48 h and 96 h. All the expression values are represented with adjusted p values.

PHIP (Pleckstrin homology domain interacting protein): Individuals with developmental delay, intellectual disability, and dysmorphic characteristics have been documented with deletions and frameshift mutations in this gene, and in some instances, patients have been observed to be overweight (Marenne et al., 2020). The functional consequences of the seventeen coding variations (as shown in Figure 3.19) observed in obese individuals.

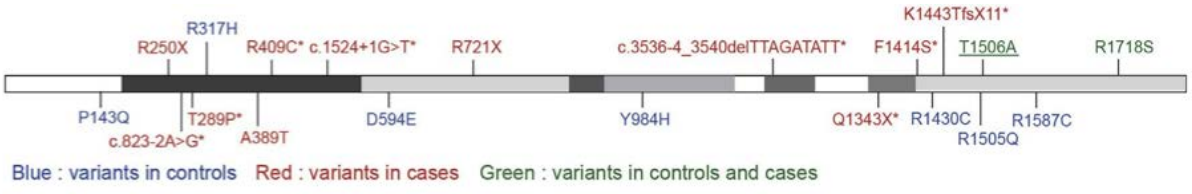

Figure 3.19: The variants of PHIP found in obese cases and control samples of a clinical study, the diagram adopted from (Marenne et al., 2020).

Human PHIP is divided into two isoforms, each of which has a different cellular location. Insulin and insulin-like growth factor (IGF-1) signalling need a small cytoplasmic PHIP (104 kDa) isoform that interacts with insulin receptor substrate (IRS)-1 and -2 (Webster et al., 2016). On the other hand, the nucleus is exclusively home to a long (230-kDa) PHIP isoform. Nuclear PHIP (known as DDB1- and CUL4-associated factor 14 (DCAF14) or replication initiation determinant protein (REPID)) is a chromatin-binding protein that promotes DNA replication and gene transcription by binding directly to chromatin (Farhang-Fallah et al., 2000). Using a POMC luciferase reporter experiment, it was discovered that in the absence of leptin, wild-type (WT) PHIP potentiated POMC transcription, while PHIP mutations reduced POMC transcription. Furthermore, four mutants (T289P, D594E, Q1343X, and R1505Q) display a

dominant-negative effect in co-transfection assays with various WT and mutant PHIP doses (Farhang-Fallah et al., 2000). These findings potentially help with the mechanism-based therapy of PHIP variant carriers with a melanocortin receptor agonist, which is now being tested in clinical trials and leads to significant weight loss in people with severe obesity (Marenne et al., 2020). The current results showed an increase in PHIP expression in SHSY5Y neurons of 96 h CFE treatment. Earlier studies suggest an average level of PHIP is required to promote POMC transcription, and POMC is directly involved in satiety regulation and energy expenditure, as discussed in the literature chapter.

KSR2 (Kinase suppressor of Ras 2): Multiple signalling pathways are aided by this intracellular scaffolding protein. KSR2 deletion causes obesity in mice, implying that it plays a function in energy regulation (Pearce et al., 2013). The Ras kinase suppressors (KSR1 and KSR2) were discovered by genetic screening in Drosophila and C. elegans. Both KSR1 and KSR2 bind to Raf/MEK/ ERK, as kinase cascade and activation of these proteins (Kim, 2010). Some of the energy balance and metabolism problems reported in $Ksr2^{-/-}$ mice, such as obesity, elevated insulin levels, and reduced glucose tolerance, have been linked to the interaction between KSR2 and AMPK (Kim, 2010).

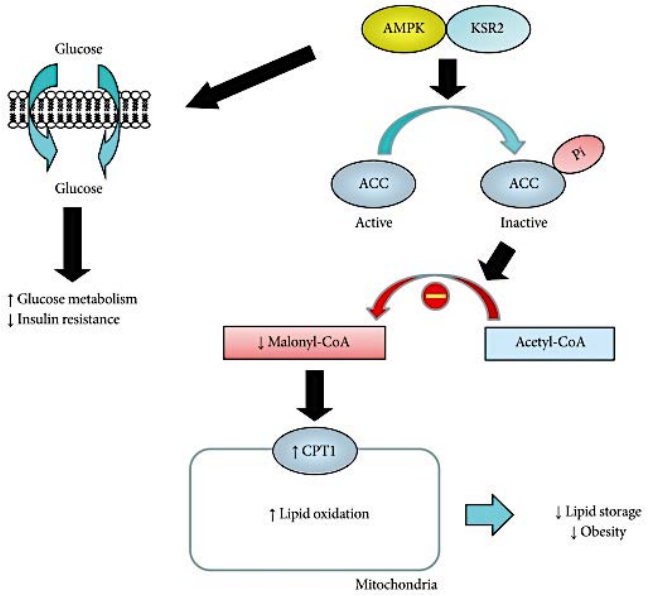

Figure 3.20: KSR2 - AMPK mediated lipid oxidation in energy expenditure (Kim, 2010)

Although one significantly obese person was homozygous for two KSR2 mutations (R253W and D323E), twenty-three of the discovered variations were only detected in obese people (Pearce et al., 2013). Several of these variations were predicted to be functionally unfavourable

as they altered highly conserved residues, implying that they could have functional effects. KSR2 controls food intake, basal metabolic rate, FAO, and glucose oxidation in humans. As shown in Figure 3.20, the KSR2 interaction with AMPK may play a crucial role in glucose intolerance and high insulin circulation. Modulation of the amplitude and duration of ERK signalling could be one mechanism linking KSR2 mutations to metabolic illness (Kim, 2010). Diet-induced obesity in mice and humans is linked to increased ERK1 activity in adipose tissue, whereas $ERK1^{-/-}$ mice appear to be resistant to obesity and remain insulin sensitive even when fed an HFD (Pearce et al., 2013). The SHSY5Y derived neurons after CFE treatment for 96 h showed enhanced KSR2 mRNA expression compared to control cells.

NPY (Neuropeptide-Y): The first group of orexigenic peptides that produce appetite-stimulating effects during a metabolic shortage are AgRP and NPY (Tran et al., 2021). NPY antagonists have been identified as possible anti-obesity therapeutic targets in several investigations. (Tamura et al., 2012) and (Kurebayashi et al., 2013) found that repeated injection of NPY antagonists had anti-obesity effects in diet-induced obesity (DIO) mice without any aberrant behaviour. Furthermore, (Fukasaka et al., 2018) investigated the impact of two new NPY receptor antagonists, S-2367 and S-234462, on body weight growth and food consumption. NPY subtype Y5 KO mice, on the other hand, had higher adiposity, food intake, and body weight (Shi et al., 2010). NPY acts as an orexin by inhibiting the binding of melanocortin system family members, supporting positive energy balance, and activating the hunger state (Shi et al., 2013). Overall, the downregulation of NPY expression observed in the current study after 48 and 96h of treatment with CFE may be an additional inhibitory signal for food appetite.

MRAP2 (Melanocortin-2 receptor accessory protein): MRAP and MRAP2 are small transmembrane proteins that promotes melanocortin receptors assembly in the endoplasmic reticulum. The role of MRAP2 on food intake and energy expenditure was briefly illustrated in Figure 3.21. The MRAP involves in G-coupled receptor subunit Gs binding to ACTH and further activation of MC2R. The MC2R activation leads to functioning of adenylate cyclase, further producing cyclic adenosine monophosphate (cAMP) (Berruien and Smith, 2020). Because effective ACTH signalling is required to produce glucocorticoids, genetic variations of MRAP have been related to familial glucocorticoid insufficiency (Novoselova et al., 2018). The brain and the adrenal gland have significant levels of MRAP expression, and MRAP has been shown to alter the differentiation of progenitor cells inside the adrenal gland. MRAP2 has

about 40% sequence homology with MRAP and forms a heterodimer (Berruien and Smith, 2020). However, unlike MRAP, which supports MC2R localisation and signalling, MRAP2 does not. The signalling of melanocortin receptors (MC1-5), orexin receptor, ghrelin receptor, and growth hormone secretagogue receptor 1a (GHSR-1a) is influenced by MRAP2, which has lower receptor fidelity (Berruien and Smith, 2020). Both MC3 and MC4 play significant roles in appetite regulation, and their deficits have been associated with obesity. Data from in vitro studies, MRAP2 transgenic mice, and MRAP2 variants in metabolic syndrome populations show that MRAP2 regulates appetite control, with MRAP2 genetic variants causing obesity (Berruien and Smith, 2020). In line with previous statements, MRAP2 is upregulated in CFE-induced neurons suggesting that CFE may play a role in MRAP2-based anorexigenic gene cluster activation to increase satiety.

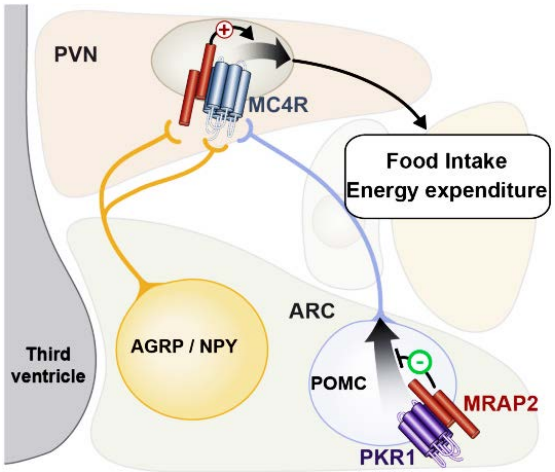

Figure 3.21: The MRAP2 signalling hypothalamic pathway illustration (Rouault et al., 2017)

SH2B1 (Src-homology 2 B adapter protein 1): Leptin is a 16-kDa systemic hormone that regulates energy balance via leptin receptor-expressing hypothalamus neurons (LEPR) (Doche et al., 2012). Resistance to endogenous and exogenous leptin characterises diet-induced obesity in rodents and typical forms of obesity in humans (Doche et al., 2012). A congenital lack of leptin and its receptor causes severe obesity in mice and humans, suggesting that leptin-mediated signalling regulates food intake, energy expenditure, carbohydrate metabolism, and neuroendocrine function (Doche et al., 2012). SH2B1 is an endogenous positive regulator of leptin sensitivity. Mutation or deletion of SH2B1 resulted in severe leptin resistance, insulin resistance, morbid obesity, and glucose intolerance in SH2B1 knock out mice (Ren et al., 2007). The signal transducer and activator of transcription 3 (STAT3) are activated through the action of SH2B1 (Figure 3.22). With the use of Tubby bipartite transcription factor (TUB),

STAT3 will move to the nucleus and activate its target genes involved in energy balance and mediate the anorexigenic actions of leptin (Doche et al., 2012). Moreover, insulin resistance and insulin signalling are also compromised in SH2B1-null mice (Doche et al., 2012). SH2B1 is expressed in many isoforms in the brain, but neuron-specific restoration of recombinant SH2B1β alone is enough to retrieve from obesity symptoms in SH2B1 knockout mice (Doche et al., 2012). SH2B1 mutations, on the other hand, were discovered to have a crucial role in obesity-related behaviours such as aggression and anxiety, according to the study.

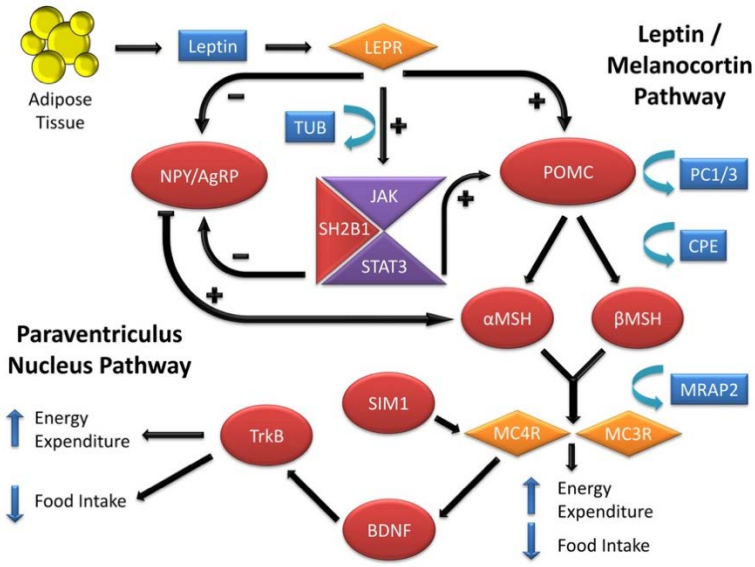

Figure 3.22: Leptin - melanocortin pathway regulates food intake in PVN of the hypothalamus showing the influence of SH2B1 (Yazdi et al., 2015)

NTRK2 (Neurotrophic tyrosine kinase receptor type 2): During 48 and 96 hours of treatment, the CFE-induced SHSY5Y neurons had higher NTRK2 expression than the control samples. When NTRK2 is injected into the ventromedial hypothalamus (VMH) and paraventricular nucleus (PVN) of the hypothalamus, it inhibits feeding and increases energy expenditure (Rask-Andersen et al., 2011). FTO (fat mass and obesity gene) may influence BDNF-NTRK2, PRKACB, STAT3, and PFN2 to control ligand-induced neural plasticity (Gray et al., 2007). BDNF plays a role in neuronal survival, differentiation, and memory formation and reduced expression of BDNF has been linked to obesity in GWA (genome wide association) investigations (Rask-Andersen et al., 2011). The current study results showed both 48, and 96h of CFE-induced neurons enhance BDNF expression.

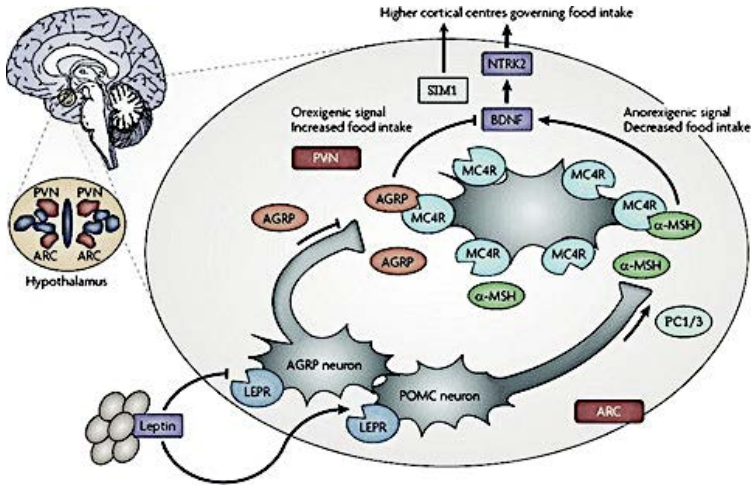

Figure 3.23: NTRK2 mediated food intake regulation signalling in the arcuate nucleus of the hypothalamus (Choquet and Meyre, 2010)

PCSK1 (proprotein convertase kexin type 1): Prohormone convertase 1/3 (PC1/3) is a serine endoprotease involved in converting a range of pro-neuropeptides and prohormones. The PCSK1 gene encodes PC1/3 (Stijnen et al., 2016). An obese mouse strain was found to have the N222D mutation in the PCSK1 gene. When mice were fed an HFD, their body weight increased significantly, and their body fat content increased (Stijnen et al., 2016). As a result, the PC1/3-N222D mice are glucose intolerant (but insulin sensitive), hyperphagic, have increased fat gain efficiency and average resting energy expenditure, as shown by others (Ramos-Molina et al., 2016). PCSK1 is a crucial molecule for processing the POMC-mediated signalling cascade in the arcuate nucleus. As a result of this mutation, the processing of substrates such as proinsulin and hypothalamic and pituitary POMC was reduced. The discovery of severely obese patients who are heterozygous for PCSK1 mutations and the link between PCSK1 SNPs and obesity has been studied (Ramos-Molina et al., 2016). These SNPs do not affect PCSK1 expression, RNA stability, or PC1/3 function. More research is required on the effects of PCSK1 SNPs and mutations on PC1/3 function and expression (Stijnen et al., 2016). Interestingly, after 96 h of CFE treatment, the PCSK1 expression was increased, suggesting that CFE might be used to treat POMC-mediated satiety signalling.

GIPR (Glucose-dependent insulinotropic polypeptide receptor): The GIP was one the two incretin hormones, which involves in food intake with systemic metabolism. GIPR agonism and antagonism both are positively impacting obesity symptoms (Campbell, 2021). Human genome-wide association studies (GWAS) have identified GIPR as a gene that contributes to body mass index, further GIP is having possible involvement in obesity (BMI) (Campbell,

2021). The functional loss of GIPR was promoted by polymorphisms in the GIPR locus linked to increased glycemia, decreased insulin production, and reduced incretin response. In addition, it was linked to a low body weight gain in GIPR knockout mice, confirming pre-clinical findings (Killion et al., 2018, Boer et al., 2021). Further, compared to diet-matched controls, $GIPR^{-/-}$ mice BAT (brown adipose tissue) had higher UCP1 levels and much-reduced lipid accumulation (Campbell, 2021). Further, $GIPR^{-/-}$ animals did not maintain their body temperature during a cold challenge, suggesting that the absence of the GIPR increases thermogenesis. BAT-specific GIPR knockout mice ($GIPR^{Myf5-/-}$) were created utilising Myf5-Cre mice to test this directly (Campbell, 2021). On the other hand, in rodents, a HFD increases GIP expression in the intestine, which drives K cell (cells found in duodenum) hyperplasia and boosts GIP levels in the blood. Depending on the extent of agonism produced, chronic GIPR agonism in mice is either weight-neutral or weight-reducing (Campbell, 2021). The literature supports the idea that a GIPR chronic agonism and antagonist activities could be a potential anti-obesity strategy. However, it was poorly studied to understand both agonist and antagonist activity of GIPR effecting weight loss. The current transcriptome data revealed, that the CFE treated SHSY5Y neurons showed decrease in GIPR expression levels during 96h of treatment compared to control cells.

PrRPR (prolactin-releasing hormone receptor): The gene PRLH in humans encodes the anorexigenic prolactin-releasing peptide. PrRPR is named for its capacity to stimulate prolactin secretion from cell lines in culture (Cheng et al., 2021). However, it does not affect prolactin release in humans. PRLH, which is found mainly in the nucleus tractus solitarius (NTS), lateral reticular nucleus (LRt), and dorsomedial hypothalamic nucleus (DMH), regulates food intake and expenditure (Cheng et al., 2021). Overexpression of PRLH decreased food intake and body weight in a PRLH mouse model, according to a recent study by (Cheng et al., 2021) (Shown in the Figure 3.24).

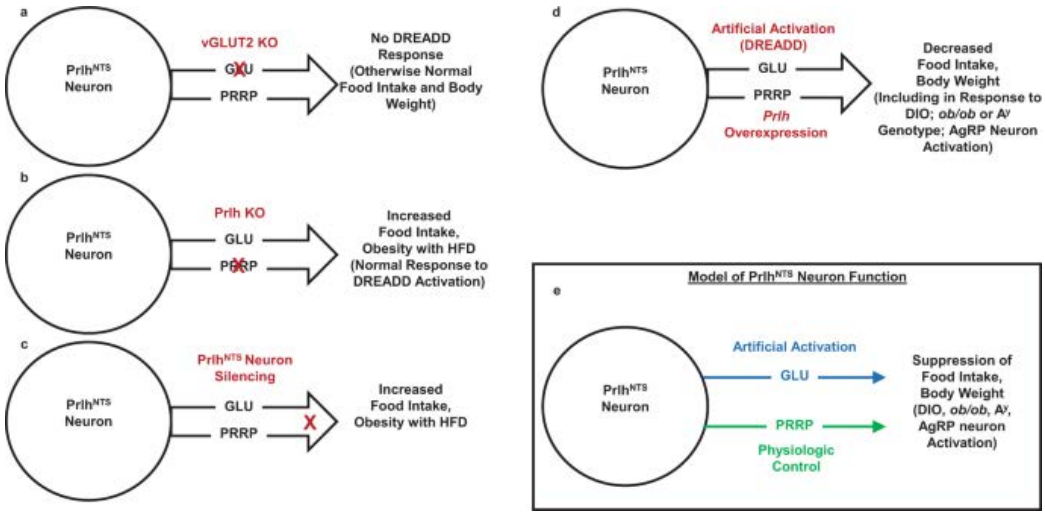

Figure 3.24: PRLH mouse model study illustrating the importance of food intake and body weight (Cheng et al., 2021)

Food intake and weight gain are inhibited by PRLH-NTS neuron transmission, especially during HFD eating. The weight loss occurred during optical stimulation (20Hz, 1 Second with 430nm) of AgRP neuron in hypothalamus, where AgRP neurons showed overexpression of PRLH.(Cheng et al., 2021). Increased PRLHR expression may improve NTS-mediated satiety signals to overcome orexigenic hypothalamic signals and restrict food and obesity. The CFE treated SHSY5Y neurons were expressed two-fold quantity of PRLH gene compared to control cells.

DGKI (diacylglycerol kinase iota): DGKI is a potential DGK isoform involved in energy balance and metabolism because it is expressed in multiple brain regions (hippocampus, hypothalamus, caudate nucleus, and cortex) as well as the thyroid (Marenne et al., 2020). DAG kinases inhibit DAG signalling and are critical regulators of synaptic plasticity mechanisms like induction and long-term depression (Marenne et al., 2020). According to phenotyping, homozygous DGKI$^{em1(IMPC)Wtsi}$ mice exhibit larger fat mass and fat percentage, poorer bone mineral density, and elevated plasma glycerol. In addition, DGKI knockout mice have delayed habituation to unfamiliar surroundings (Yoon et al., 2019). The biological function of DGKI is unknown, as is the mechanism by which they maintain energy homeostasis. The current data reveals increased expression of DGKI in 96h CFE treated SHSY5Y neurons.

5HT2cR: The serotonin 2c receptor expression was increased in CFE induced neurons at 48 and 96h. The CFE effect on 5HT2cR expression was consistent with qPCR quantification and whole transcriptome data. As described in the literature, 5HT2cR promotes POMC mediated

satiety signal, and the Figure 3.25 shows 5HT2cR association with other obesity influencing genes discussed in this chapter.

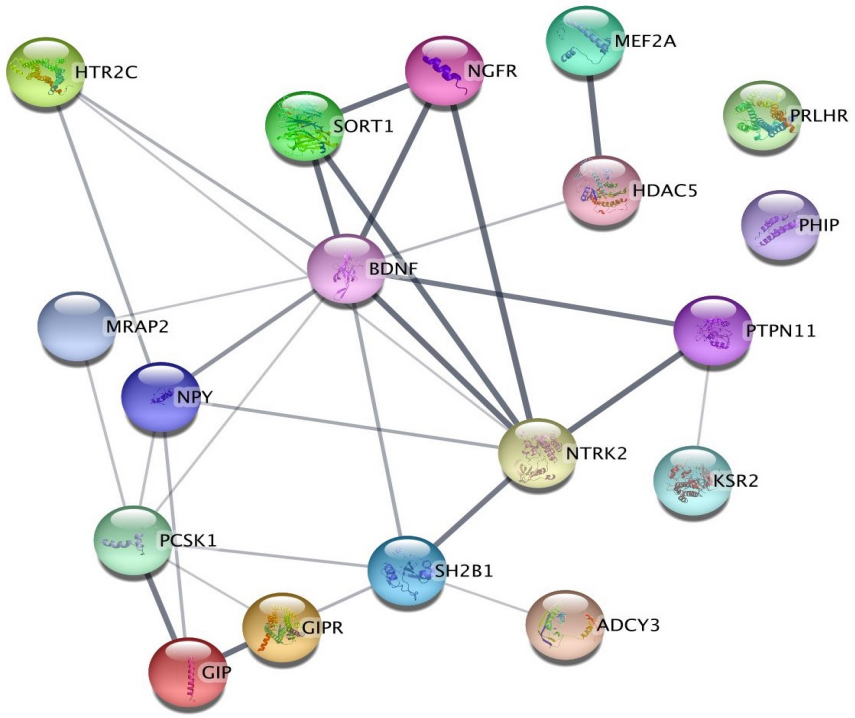

Figure 3.25: The string database derived protein network: Overall genes associated with food intake and weight loss were clustered to understand the 5HT2cR interaction with them.

Outcomes of the study

- In CFE-treated SHSY5Y neurons, functional 5HT2cR expression was increased, while the expression of truncated 5HT2cR was reduced.
- Whole transcriptome analysis of CFE-treated neurons reveals effects on anorexigenic genes that may promote satiety.
- The pilot scale transcriptome data shows interesting results towards CFE influence on different anorexigenic genes either directly or indirectly in pathways. The data pointing to assess a greater number of replicates for further confirmation of CFE impact on energy homeostasis.

3.5 Conclusion

The experiments and analyses in this chapter show that CFE treatment of neuronal cells induces the expression of several genes that influence appetite and energy homeostasis. The genes like BDNF, PCSK1 and 5HT2cR have a key role in POMC neuron activation in the hypothalamus. On the other hand, it is interesting to explore how 5HT2cR expression could be altered in case of PWS, where PWS loci mutations (SNORD115) play a key part in 5HT2cR-fn expression. Transcriptome data showed increased expression of genes like SNURF, MAGEL2 (MAGE family member L2) and NDN (Necdin) genes, which are present on PWS loci in chromosome 15q11-q13. The mechanism of CFE in 5HT2cR expression is a big challenge to understand at the level of messenger RNA processing and transcript assembly. However, at this stage, increased expression of the functional receptor is evident in SHSY5Y neurons, implying CFE influence in satiety signalling. It is significant to recognise the CFE effect on SHSY5Y neurons, however it is correspondingly valuable to understand how CFE involved in different physiological and behavioural aspects. Further elucidation of the effect of CFE on behaviour, weight reduction and body composition of mice maintained on an obesogenic diet is discussed in the next chapters.

Chapter 4 Food and water intake rate and behaviour response in CFE and Lorcaserin treated high-fat diet mice model

4.1 Abstract

The critical prevalence of obesity and overeating metabolic disorders are emerging in populations worldwide. Obesity is prevalent due to high caloric intake and reduced activity. The food intake rate is regulated by appetite and satiety pathways centrally in the hypothalamus of the brain region. A hypercaloric diet influences several neuropeptides like MSH, POMC, NPY, and AgRP in the brain. In addition, it can impact mood and behavioural parameters like anxiety and depression levels. Studies confirm that 5HT2cR-linked activation of POMC neurons is responsible for activating satiety signals via anorexigenic pathways. The 5HT2cR is not limited to the satiety signal; it also plays a crucial role in regulating anxiety and depression behaviours. Therefore, it is essential to realise how anti-obesity drugs or overeating disease therapies alter individuals' mood and behavioural changes parallel to body weight regulation. The current chapter of the thesis used a speciality diet to induce obesity in C57BL/6j mice within eight weeks of feeding. The HFD-induced mice were randomised to CFE, LOR and CFE+LOR treatment groups. The HFD-induced mice went through 8weeks of treatment; and were continuously monitored for food, water intake and body weight changes. In addition, animals were assessed for exploration, anxiety, and depression behavioural changes with respect to given treatments. The observations revealed food and body weights of CFE+LOR and CFE treated groups showed significant differences and resistance to HFD. Interestingly, behavioural experiments indicated CFE+LOR treatment group data resembling the control diet-fed group anxiety and depression parameters. The study concludes that body weight and behaviour parameters due to induced HFD were effectively sustained in CFE+LOR treatment rather than in CFE and LOR-alone treatment groups.

4.2 Introduction

Obesity may increase the risk of developing pathological health conditions, including diabetes mellitus, anxiety, depression, and gastrointestinal disorders. High-calorie foods (high in sugar and fat) and low energy expenditure contribute to obesity development (Mavanji et al., 2022, van Galen et al., 2021, Loos and Yeo, 2021). The role of hypothalamic peptides in modulating feeding behaviour and energy homeostasis has been demonstrated in mouse studies. Neuropeptide Y (NPY) is well-known for its orexigenic effects, mediated by NPY neurons in the hypothalamus. However, many peripheral factors also affect these neurons, which provide energy status signals to the brain (Pondugula et al., 2021, Aghili et al., 2021, Fu et al., 2020, Petridou et al., 2019). Leptin, for example, is a hormone released by adipocytes that reduces NPY expression, induces satiety, and promotes energy expenditure (Sarma et al., 2021, Fernández-Galaz et al., 2010). Surprisingly, leptin resistance, which is common in obesity, is related to increased NPY transcription levels and a higher incentive for feeding behaviour, which frequently activates the obsessive-compulsive phenotype seen in obese patients (Manocha and Khan, 2012, Fernández-Galaz et al., 2010, Crowley et al., 2002).

In addition, Orexins are highly produced in the hypothalamus lateral and dorsomedial areas, projected throughout the brain and spinal cord; orexins increase appetite (Mavanji et al., 2022, Pondugula et al., 2021). The OX1R and OX2R, like orexin-A (OXA) and B (OXB) peptides, in the central neuraxis and isolated peripheral areas. Orexin therapy increases the expression of peroxisome proliferator-activated receptor-gamma (PPAR- γ and improves adipose tissue browning (Mavanji et al., 2022, Borgers and Heemels, 2014). Furthermore, orexin treatment of adipose tissue causes an increase in glycerol release, indicating enhanced lipolysis. The role of OX1R in eating behaviour has been demonstrated in previous research. For example, the OX1R antagonist SB334867 reduces OXA-induced feeding, self-administration of high-fat pellets in food-restricted rats and ad-libitum-fed mice, binge-like intake of palatable food in mice and rats, and cue-driven food consumption in mice and rats (Sharf et al., 2010, Cason and Aston-Jones, 2013b).

Similarly, knocking down OX1R in the paraventricular nucleus of the thalamus (PVT) with OX1R shRNA (short/small hairpin RNA) lowers food intake in rats. At the same time, SB334867 treatment to the fourth ventricle inhibits high-fat meal-conditioned location preference (Mavanji et al., 2022, van Galen et al., 2021). Moreover, according to a recent study,

mice lacking OX1R develop obesity resistance when fed an HFD (Teske et al., 2006), whereas mice were lacking OX2R develop decreased thermogenesis when fed an HFD (Needham et al., 2022, Mavanji et al., 2022, Lama et al., 2022b, Yoshizaki et al., 2020).

Other neurotransmitter, serotonin regulates leptin internalisation and subsequent action in the brain leads to satiety signalling. As a result, serotonin can alter appetite and energy homeostasis via regulating leptin and activation of the anorexigenic pathways in the brain (Cason and Aston-Jones, 2013a, Crowley et al., 2002). According to previous research, serotonin activates spinal cord motor neurons and increases the frequency of locomotor activity. Following DRN (dorsal raphe nucleus) GABA treatment, mice exhibited depression-like behaviour (Mavanji et al., 2022, van Galen et al., 2021, Loos and Yeo, 2021, Yoshizaki et al., 2020). Furthermore, serotonergic neurons in the DRN have been found to influence several behavioural characteristics in mice, including sensory input, motor action, and reward, implying serotonin importance. A human study found that the specific binding ratio of the serotonin transporter (SERT) in the pons was favourably connected with BMI in obese subjects' midbrain and negatively correlated with BMI (la Fleur and Serlie, 2014). In addition, hypermethylation of the SERT promoter gene (*SLC6A4*) increases BMI and waist circumference in obese people (Mavanji et al., 2022, Petridou et al., 2019). Moreover, hypothalamic SERT gene expression increased in rats fed with a high-carbohydrate diet, indicating that serotonin turnover role in developing visceral adiposity (la Fleur and Serlie, 2014).

The key mechanism for serotonin's involvement in the energy balance is activating the 5HT2c receptor. The literature indicates that 5HT2cR mutant mice have abnormalities in mRNA expression for proteins involved in energy balance, hyperphagia, and late-onset obesity. In addition, overeating disorders like PWS are interlinked with 5HT2cR mutation or under-expression conditions (Griggs et al., 2018b). The activation of 5HT2cR showed a significant reduction in body weight and waist circumference in overweight individuals (Chaiyasut et al., 2021). Therefore, a specific agonist like Lorcaserin was developed to treat obesity. In obese people, lorcaserin substantially reduces calorie consumption, weight gain, and cardiometabolic problems. Unlike fenfluramine and dexfenfluramine, which has non-specific serotonergic agonistic activity on all 5HT receptors (5HT2a, 2b, 2c), lorcaserin (LOR) has an 8 to 15-fold greater potency for 5HT2cR compared to 5HT2aR and a 45- to 90-fold more potency for 5HT2cR compared to 5HT2bR (Hebras et al., 2020, Fu et al., 2020).

As a result, activation of 5HT2aR and 5HT2bR is unlikely, although theoretically possible, depending on the plasma drug level. However, after a re-evaluation by the FDA in 2012, lorcaserin was approved with a cardiovascular outcome trial (Nonogaki, 2022). There is no substantial increase in valvulopathy or neuropsychiatric symptoms (depression or suicidal risk) with lorcaserin. Nausea, dizziness, and a temporary headache are the most common side effects reported with lorcaserin. The FDA subsequently reported in 2020 that an examination of the data from the CAMELLIA-TIMI 61 trial revealed that 462 patients (7.7% of the cohort) treated with lorcaserin developed cancer, compared to 423 patients (7.1%) in the placebo group. Pancreatic, colorectal, and lung cancers were more common in the lorcaserin group, among the several cancer types reported. As a result, the FDA requested that the drug manufacturer, Eisai, voluntarily withdraw the medicine from distribution in the United States (Mathai, 2021).

However, it was recommending, lorcaserin to increase safety while maintaining a therapeutic effect on weight loss. These conditions were including a short-term adjunct therapy to diet and exercise, in a lower dose, in combination with other weight-loss medicines, are considered as possible alternate options to continue Lorcaserin treatment (Mathai, 2021, Patel et al., 2020). The literature (chapter I) mentioned that altering 5HT2cR expression consequences lead to changes in animal behaviours like mood, depression, and anxiety.

The current study aims to reduce the risk factors by dropping Lorcaserin dose to 5mg compared to normal dosage in mice 9mg/kg bwt/day (He et al., 2021) and CFE of 100mg/kg body weight per day. The HFD-induced mice are the recommended animal model to determine the effect of anti-obesity drug response (He et al., 2021). The current chapter is to study the influence of CFE and Lorcaserin treatment response in HFD-fed mice. The food and water intake and body weight parameters were considered as primary factors to know the obesity influence. From chapter III, the CFE enhancing 5HT2cR expression SHSY5Y derived neurons. In addition, the 5HT2cR was identified as crucial molecule in representing mood, depression and anxiety like behaviour as discussed in chapter I.

4.3 Materials and methods:

4.3.1 Animal food, water, and body weight measurement:

The C57BL6/J mouse obtained from ARC were acclimatised for one week after arrival at Victoria University, Werribee facility. The animals were assessed for behavioural parameters

during weeks 4, 8 and 16; week 4 data considered familiarisation of animals with different behavioural experiments. Bodyweight is the crucial parameter to elucidate overweight or obesity conditions in animal models. The intake of food and water quantity was measured in grams (g) using the standard weighing machine available in the facility. The animal body weights were measured every week and monitored for the HF-diet induction effect. Promethion experimental period data were excluded in all the food and water intake data groups shown in this chapter.

4.3.2 Behavioural Experiments:

Animal behaviour research has profited from recent technical breakthroughs in machine vision and machine learning, which have enabled the capture and automatic quantification of massive volumes of data (Moulin et al., 2021). Behavioural patterns that a human observer previously overlooked can now be studied at multiple scales and eliminating human error, by allowing uniformity among studies. The Cleversys TopScan tool has been used to validate the behaviour video data from Open field, elevated plus maze, light and dark box, and Y-maze experiments. The depression-scan suite was used to measure the depression-like behaviour data from Tail suspension and forced swim test recordings. All the behavioural testing was performed during light phase of the animals dark/light cycle. The behavioural room temperature was always 22 ± 3 °C. C. The animals with home cages were transferred to behavioural testing room 30min before to each test to acclimatise.

4.3.4 Exploration behaviour:

Animal exploration behaviour can be measured by placing the animal in an unfamiliar field to explore (Crawley, 1985). The animal explorative behaviour was estimated based on time spent in the unknown areas and distance travelled. The current study chose open field and Y-maze experiments (Foroozan et al., 2021, Nemes et al., 2019) to measure the explorative behaviour of the animal groups.

4.3.5 Open field analysis:

The area of 72 x 72 x 60 cm (l x b x h) was placed under an analogue camera unit with 50lux light intensity. The animals were placed for 10min duration at the centre of the open field area (Yoshizaki et al., 2020). The instrument was cleaned and dried between each animal placement to avoid potential behavioural influences of the previous animal. The recordings were analysed

using Cleversys top-scan software. The following parameters, such as total distance covered, average speed, time spent in the outer area, and centre area (approximately 36 x 36 cm area), were measured and quantified.

4.3.6 Y-maze analysis:

The primary aim of the test is to determine the locomotion and transitional relativity or spontaneous activity of the animal. In mice, the Y-maze can be used to test short-term memory. Spontaneous alternation, a test of spatial working memory, is measured by letting mice explore all three arms of the maze. It is motivated by rodents' natural desire to explore locations they have never seen before (Schachter et al., 2018, Jin et al., 2018). A mouse with healthy working memory, and thus healthy prefrontal cortex functioning, will remember the arms it has visited previously and will be more likely to enter a less recently seen arm. The hippocampus's spatial reference memory can also be assessed by placing the test mice in the Y-maze with one arm closed off during training. The animal was initially exposed to two arms of the Y-maze. After exploring for 3min, the animal was allowed to explore the unknown arm/ third arm for the rest of the experiment time (Yoshizaki et al., 2020, Kraeuter et al., 2019b). In a total experiment period of 10min, parameters of unknown arm entries and time spent in the novel arm are considered for evaluating spontaneous exploration behaviour. All the experiments were recorded with a standard camera setup, and the video recordings were used for desired parameter analysis.

4.3.7 Anxiety and depression assessment:

In the lateral habenula (LHb), anxiety-like behaviours were accompanied by neuronal hyperexcitability and downregulation of M-type potassium channels (M-channels); and serotonin (5-HT) activated LHb neurons via type 2C receptors (5HT2cR). In mouse hypothalamic neurons, 5HT2cR activation is also known to decrease M- channels function (Di Giovanni and De Deurwaerdere, 2016, Fu et al., 2020).

4.3.8 Elevated plus maze (EPM):

The elevated plus maze comprises four elevated arms that radiate from a central platform in the shape of a plus symbol. Aside from the ceiling, entrance and exit points, the remaining two opposed arms should be open. In the experiment, the animal was placed in the centre of the maze and then left to explore it for 10min duration. As a measure of worry or fear, the amount

of time spent in the walled arms contrasts with the amount spent in the open arms. In theory, a less anxious mouse will explore open arms frequently (Kraeuter et al., 2019a). Conversely, more anxious animals spend more time in walled arms. The experiments were recorded, and the videos were used to measure the time spent in open and closed arms, the number of bouts/entries into open arms and centre area exploration time.

4.3.9 Light and dark box analysis (LDB):

Like EPM, LDB is also used to measure anxiety levels in mice. The instrument is made of white and black chambers separated by a wall and consists of a narrow opening via a sliding door to cross between the sections. The animal was initially exposed to the dark compartment for 1min and allowed to explore the brighter compartment (Jin et al., 2018) with 150lux light intensity for the rest of the experimental period. An anxious animal will spend more time in the dark chamber, whereas a less anxious one can visit the lightroom more times.

4.3.10 Tail suspension test (TST):

The tail suspension test was used to determine the depression-like behaviour in all the animal groups. The animal tail was tied with surgical tape to the hook attached to the roof of the testing chamber (Foroozan et al., 2021, Wu et al., 2021). The animal was allowed to sustain the stress due to hanging for 6 min, and recorded videos were used to do the depression scan analysis.

4.3.11 Forced swim test (FST):

The animal was placed in a 3L beaker filled with a 2L depth of (temperature between 23 to 26 ^{o}C) water level. The animal was left in the water for 6 min and video recorded from side view to analyse depression parameters (Hassan et al., 2019). The water was replaced after each run; each animal activity after the test was monitored in a dry towel containing cage placed at 27 ^{o}C incubator for 15min.

4.3.12 CleverSys tool conditions:

All the behavioural experiments were recorded with a camera module, and videos were used to do the offline analysis by CleverSys software. The TopScan module was used to measure the behavioural parameters from Open field, Y-maze, EPM and LDB (overview shown in figure 4.1). A Depression suite scan from CleverSys was used to assess the video recordings from TST and FST (Grech et al., 2019, Ong-Pålsson et al., 2022, Fang et al., 2022).

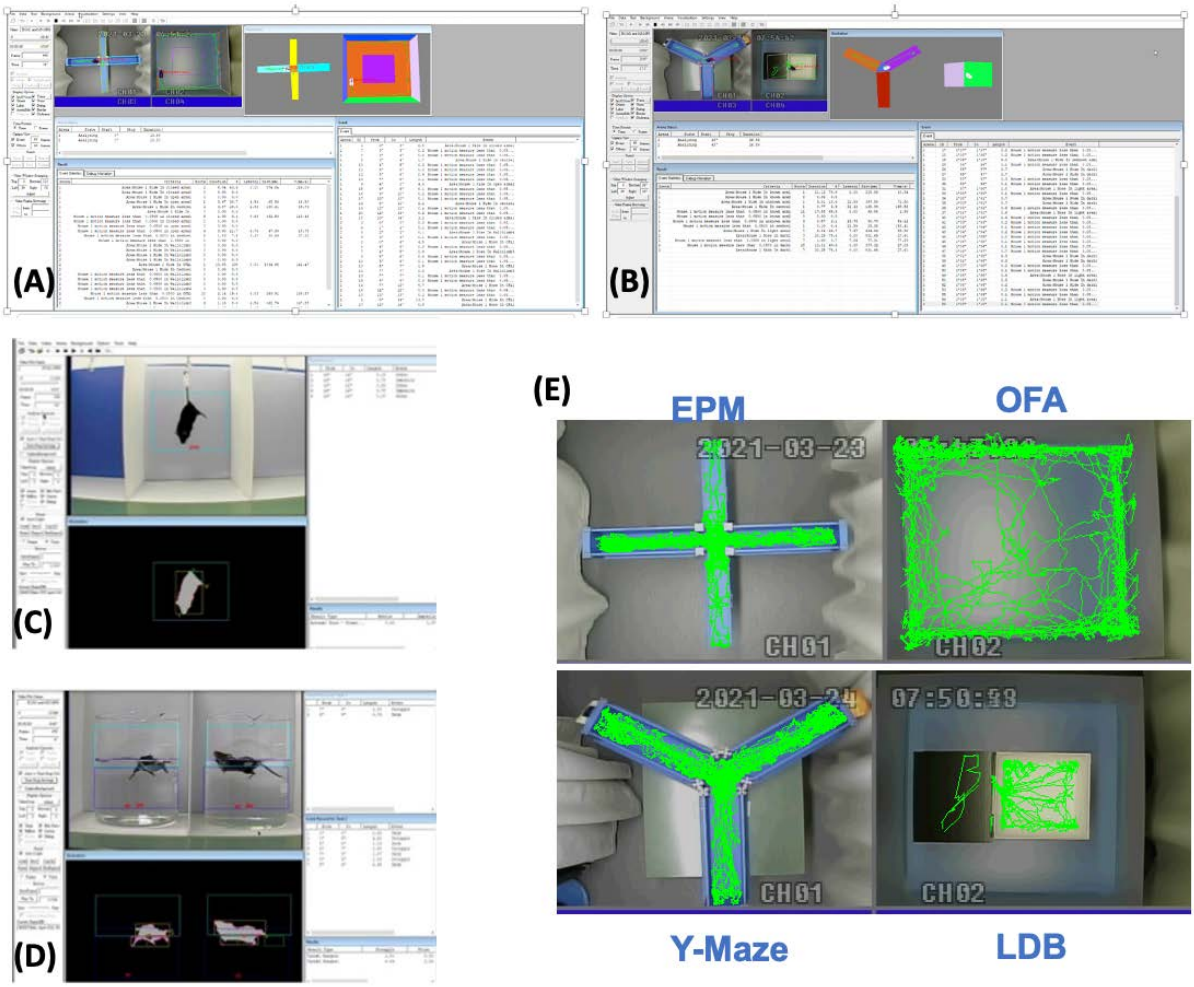

Figure 4.1: Cleversys TopScan and depression analysis: (A) TopScan suite analysis for EPM and OFA (B) Y-maze and LDB analysis using TopScan suite; Depression scan suite for (C) TST, (D) FST analysis, and (E) After analysis tracking patterns from TopScan data.

4.3.13 Statistical analysis:

All the data were statistically validated at 95% confidence by Two-way ANOVA with correction factor by Sidak's post-hoc multiple comparison test. The data analysis was performed using Graph Pad Prism version 9.3.1.

4.4 Results and Discussion:

4.4.1 Effect of CFE and Lorcaserin on body weight, food, and water intake:

One of the essential factors in proving obesity in animal models is body weight. Compared to the control diet-fed animals, the current findings revealed a significant increase in body weight of the high fat diet-fed groups. The treatments were aimed to restrict the body weight gain

during high fat diet feeding as shown in Figure 4.2. Over 12 weeks, diet-induced obesity 1.5-fold increases body weight gain and body composition (fat mass) in the C57BL/6 strain (Parande et al., 2022, Yoshizaki et al., 2020).. The equilibration of energy intake and expenditure are regulating factors of energy homeostasis. Therefore, the balance between energy intake and energy expenditure is crucial for maintaining body weight (Yan and Li, 2022). During the first week of treatment, there is no significant difference between the HFD, CFE, LOR and CFE+LOR groups.

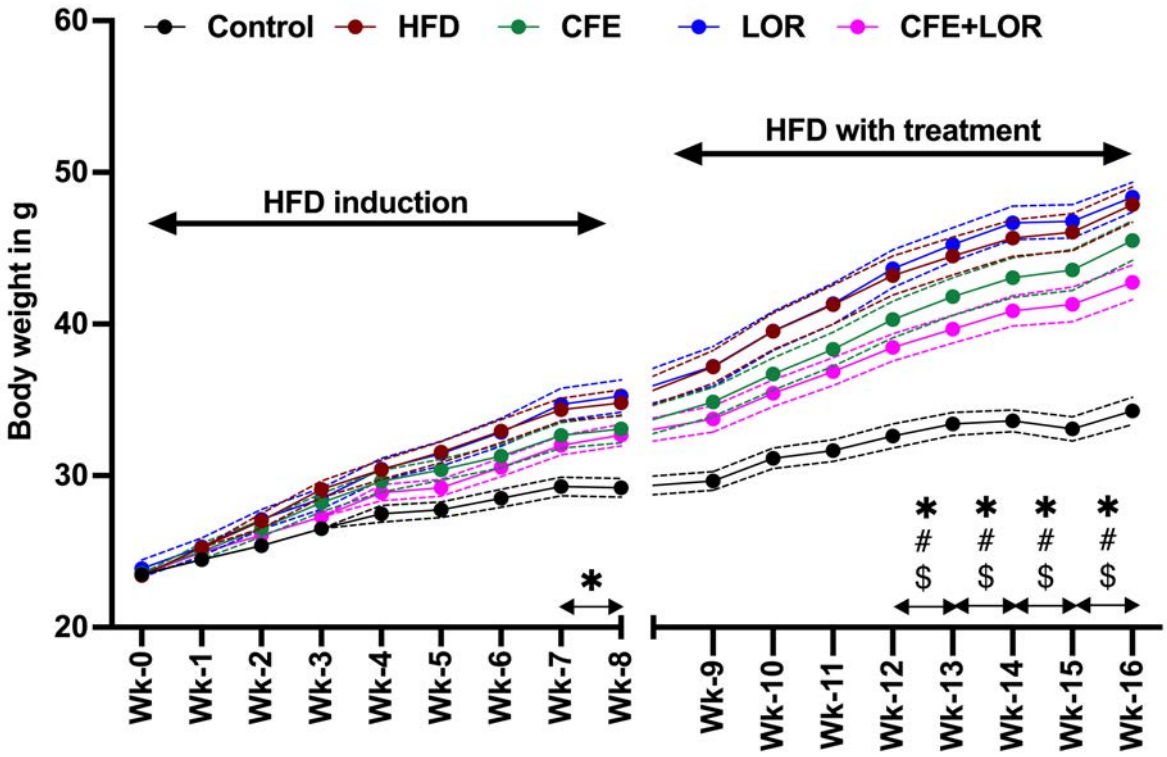

Figure 4.2: Bodyweights during 16 weeks of the study: The animal body weight is shown each week during high-fat diet induction from week 0 to week 8. The body weights represented from week 9 to week 16 are during treatment with CFE and Lorcaserin. All the data are derived with n=16 mice in each group and values plotted are Mean ± SEM. The statistical significance p-value < 0.5 as '* 'represents the comparison between control and HF groups,' #' represents HFD with CFE+LOR, and '$' represents LOR with CFE+LOR (where Control: control diet group, HF: high-fat diet group, CFE: high-fat diet with CFE, LOR: high-fat diet with Lorcaserin treatment, CFE+LOR: high-fat diet with CFE and lorcaserin treatments.

Figure 4.2 shows that during the treatment period (week 9 to week 16), there was a significant increase in body weight gain in the treated groups compared to the control group. However,

from week 12, the CFE+LOR group showed significantly restricted weight gain than the HFD group. From week 12 to week 16, the CFE+LOR group showed considerably reduced body weight than the conventional drug Lorcaserin treated animals. Compared to individual drug treatments with CFE and LOR, the CFE+LOR treated group weight gain weight gain was significantly decreased from Figure 4.3. The weight gain comparisons revealed more details about weight gain phenomena with respect to CFE and LOR treatments in HFD-fed mice.

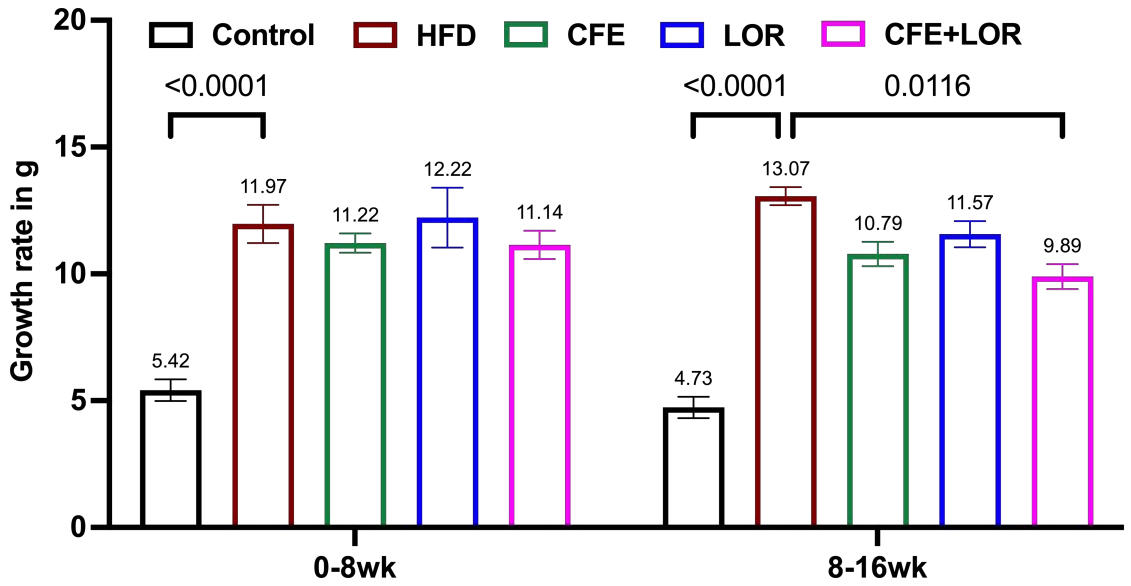

Figure 4.3: Change in weight gain during 16 weeks of the study: The weight gain of all the groups during HFD induction and treatment periods are represented individually. Each group had n=8 mice and values plotted are Mean ± SEM. (where Control: control diet group, HF: high-fat diet group, CFE: high-fat diet with CFE, LOR: high-fat diet with Lorcaserin treatment, CFE+LOR: high-fat diet with CFE and lorcaserin treatments). Statistically significant differences between the groups (p-values <0.05) are shown.

The weight gain body weight of the HFD group was significantly higher than the control diet group with significance of $p<0.0001$ during pre- (0 to 8 weeks) and post- treatment (8th to 16th week) periods. However, the CFE+LOR group showed a significantly ($p = 0.011$) decreased weight gain than the HFD group. Moreover, overall weight gain plotted in figure 4.4, demonstrates CFE+LOR group was also significantly reduced weight gain compared to the HFD and LOR groups. Despite considerable changes in daily food consumption and energy expenditure, most adults maintain nearly consistent body weight. As a result, it requires consideration of a complex physiological system to understand energy expenditure and food intake (Hill et al., 2012). Energy balance is modulated by peripheral signals (hormones)

integrated with brain regions such as the hypothalamus, brainstem, and reward centres (Wallace and Fordahl, 2021). Some hormones, such as leptin, insulin, and possibly adiponectin, reflect the body's long-term nutritional status. In contrast, ghrelin, peptide YY, pancreatic polypeptide, oxyntomodulin, glucagon-like peptides 1 and 2, and cholecystokinin, act more acutely to initiate or terminate a meal and cause appetite stimulation or satiety (Wallace and Fordahl, 2021, Heisler et al., 2006).

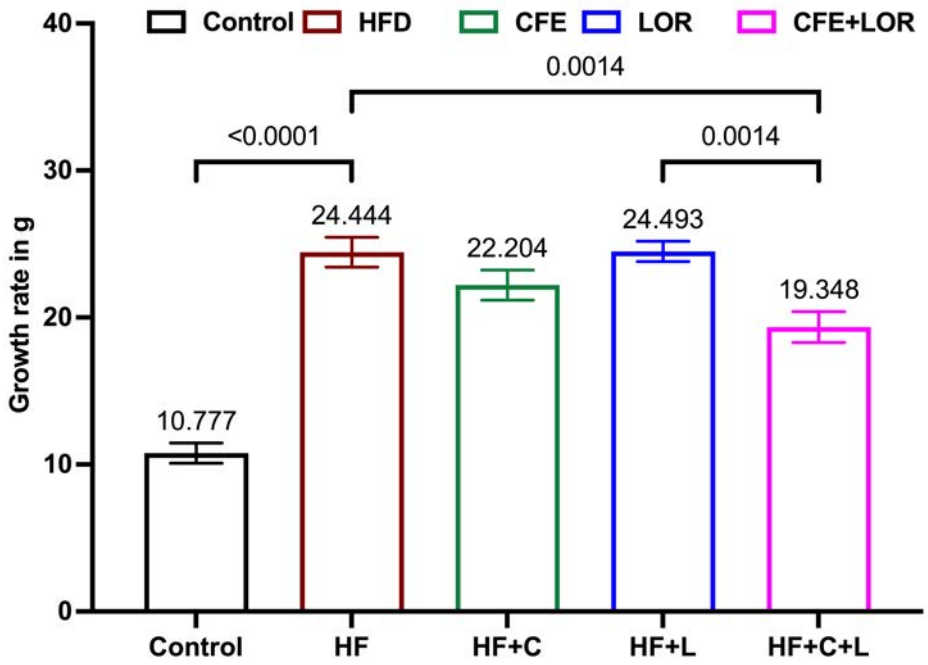

Figure 4.4: Overall weight gain during 16 weeks of the study: The body weight change between week 0 to week-16. Each group had n=16 mice and values plotted are Mean ± SEM. (where Control: control diet group, HF: high-fat diet group, CFE: high-fat diet with CFE, LOR: high-fat diet with Lorcaserin treatment, CFE+LOR: high-fat diet with CFE and lorcaserin treatments). Statistically significant differences between the groups (p-values <0.05) are shown.

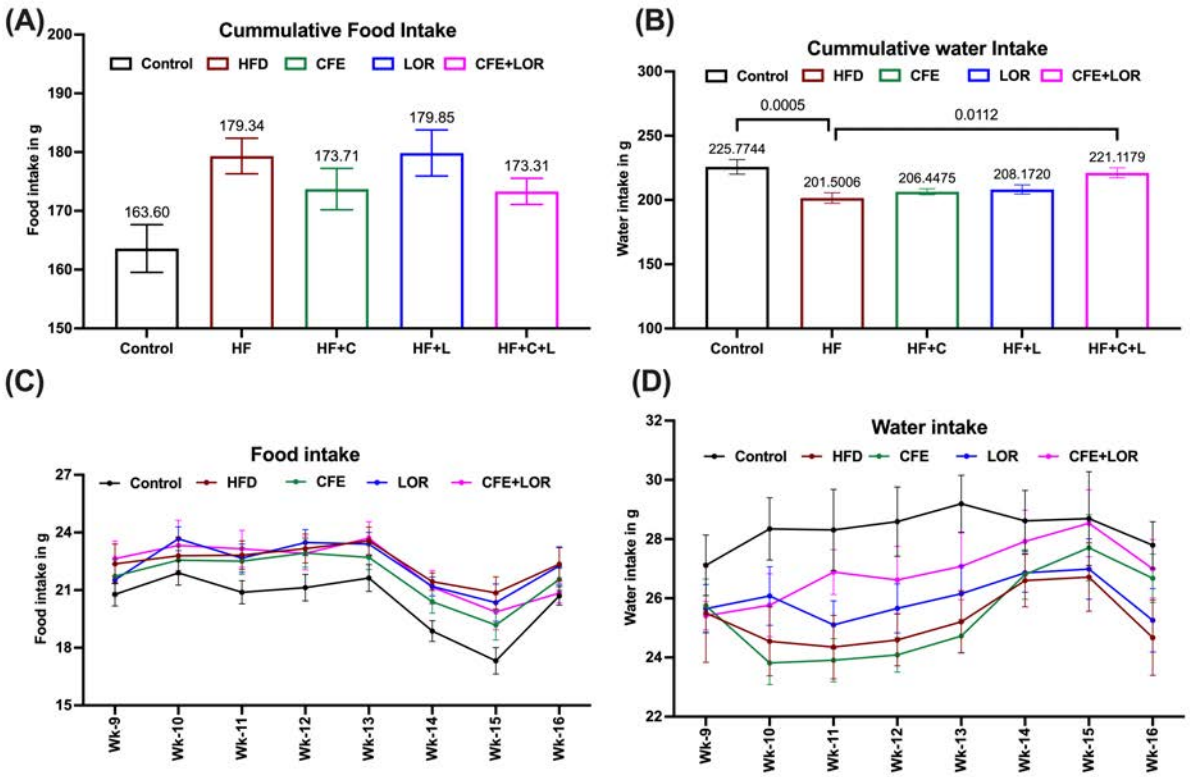

Figure 4.5: Water and food intake: The cumulative (A) Food and (B) Water intake represent the change in intake with respect to treatments from week 9 to week 16. The weekly (C) Food and (D) Water intake data are drawn on a line plot. Each group had n=8 mice and values plotted are Mean ± SEM. (where Control: control diet group, HF: high-fat diet group, CFE: high-fat diet with CFE, LOR: high-fat diet with Lorcaserin treatment, CFE+LOR: high-fat diet with CFE and lorcaserin treatments). Statistically significant differences between the groups (p-values <0.05) are shown.

The energy consumption via cumulative food intake (Figure 4.5 A) was measured from weekly data, and the results revealed that CFE and CFE+LOR groups have less overall food intake than HFD and LOR groups. However, the reduction is not significant due to higher variations in individual animals in the group. In contrast, the water intake significantly increased in the CFE+LOR group compared to the HFD group. There was a decrease in water intake with an increase in food intake of *db/db* mice (Chen et al., 2018). From Xiao et al 2021, HFD mice consumed less sucrose water than control mice; this reveals overall fluid intake was less when the mice increased their intake of high-calorie food (Xiao and Guo, 2021). The current study showed the cumulative water consumption (Figure 4.5 B) in the CFE+LOR group increased when compared to the HFD group. Overall, food and water consumption during treatment time

are shown in Figures 4.5C and 4.5D. Different animal and human studies proposed that CFE influences the control of food intake. However, the exact mechanism of action of CFE is unclear. The food intake alteration was observed in *snord116del* mouse with CFE treatment (Griggs et al., 2018a).

Similarly, other *Caralluma* species like *Caralluma dalziel* with a low level of toxicity (with an LD50 larger than 2000 mg/kg body weight) decreased body weight by 7.1% in the rats given 400 mg/kg, compared to a 38.16% increase in the positive control (Ugwah-Oguejiofor et al., 2019). Food intake and body weight are reduced synergistically when lorcaserin and a glucagon-like-peptide-1 (GLP-1) co-agonist are combined. Compared to individual treatments, repeated treatment with lorcaserin and the co-agonist resulted in increased body weight loss over time, owing to a reduction in fat mass (subcutaneous, retroperitoneal, mesenteric, and epididymal fat) (Patel et al., 2020). The current study is designed to validate Lorcaserin in combination with CFE effect on HFD-fed mice. The results discussed in this chapter supporting positive impact on weight gain and fat deposition with CFE+LOR treatment.

Table 4.1: Bodyweight measurements during 16weeks of the study: The table represents the weekly body weights of each group with n=16 animals, the data represented with Mean ± SEM. The significant changes represented p<0.0001 (****/####/$$$$), p<0.001(***/###/$$$), p<0.01 (**/ ##/$$), and p<0.05 (*/#/$) where '* 'represents the comparison between control with all HFD groups,' #' represents HFD with CFE+LOR, and '$' represents LOR with CFE+LOR. (Where Control: control diet group, HF: high-fat diet group, CFE: high-fat diet with CFE, LOR: high-fat diet with Lorcaserin treatment, CFE+LOR: high-fat diet with CFE and lorcaserin treatments.

Week	Control	HFD	CFE	LOR	CFE+LOR
Wk-0	23.49 ± 1.28	23.43 ± 1.33	23.55 ± 1.67	23.88 ± 2.01	23.49 ± 1.40
Wk-1	24.47 ± 1.33	25.26 ± 1.58	25.01 ± 1.86	25.30 ± 2.04	24.94 ± 1.39
Wk-2	25.38 ± 1.65	27.01 ± 1.72	26.52 ± 1.92	27.11 ± 2.32	26.07 ± 1.55
Wk-3	26.50 ± 1.74	29.11 ± 1.93	28.22 ± 2.03	28.48 ± 2.42	27.28 ± 1.67
Wk-4	27.49 ± 2.15	30.40 ± 2.24	29.63 ± 2.48	30.44 ± 2.48	28.87 ± 1.90
Wk-5	27.75 ± 1.99	31.55 ± 2.45	30.39 ± 2.44	31.44 ± 2.84	29.19 ± 1.93
Wk-6	28.52 ± 2.34	32.94 ± 2.63	31.28 ± 2.64	32.86 ± 3.23	30.54 ± 2.17
Wk-7	29.28 ± 2.39	34.36 ± 2.61***	32.65 ± 2.92**	34.70 ± 3.69**	31.99 ± 2.21**
Wk-8	29.21 ± 2.42	34.81 ± 3.01***	33.09 ± 3.24***	35.25 ± 3.69***	32.69 ± 2.48***
Wk-9	29.64 ± 2.42	37.16 ± 3.75***	34.85 ± 3.38	37.22 ± 4.55	33.74 ± 2.99
Wk-10	31.14 ± 2.63	39.53 ± 4.23****	36.70 ± 3.73	39.54 ± 4.49	35.44 ± 3.08
Wk-11	31.66 ± 2.75	41.28 ± 4.43****	38.34 ± 3.94	41.35 ± 4.67	36.87 ± 3.19
Wk-12	32.62 ± 3.09	43.19 ± 4.47****	40.30 ± 4.16	43.65 ± 4.33	38.46 ± 3.09$^{\#\$}$
Wk-13	33.42 ± 2.93	44.48 ± 4.33****	41.81 ± 4.29	45.24 ± 3.84	39.67 ± 3.18$^{\#\$}$
Wk-14	33.61 ± 2.83	45.68 ± 4.17****	43.06 ± 4.55	46.68 ± 3.82	40.87 ± 3.48$^{\#\$\$}$
Wk-15	33.09 ± 3.12	46.05 ± 4.24****	43.58 ± 4.68	46.77 ± 3.87	41.30 ± 3.94$^{\#\$}$
Wk-16	34.26 ± 3.51	47.88 ± 4.05****	45.50 ± 4.56	48.37 ± 3.41	42.74 ± 3.98$^{\#\$\$}$

4.4.2 The effect of CFE and Lorcaserin on behavioural changes:

The behavioural changes due to variations in 5HT2cR expression were discussed in chapter-I. In previous investigations, HFD-fed animal models demonstrated alterations in mood, anxiety, and depression symptoms (Fu et al., 2020, Sarma et al., 2021, Baptista-de-Souza et al., 2022, Needham et al., 2022, Parande et al., 2022). The animals were tested for changes in anxiety and depression-like behaviours in response to CFE and Lorcaserin treatment. According to the results plotted in figure 4.6 open-field analysis, both the control and CFE, LOR, and CFE+LOR treated groups of mice significantly increased the number of bouts/entries into the centre arena (As shown in figure 4.6 A). During the 16th week, the time spent in the central region was more ($p = 0.0305$) in the CFE+LOR group than in the HFD group (Figure 4.6 C).

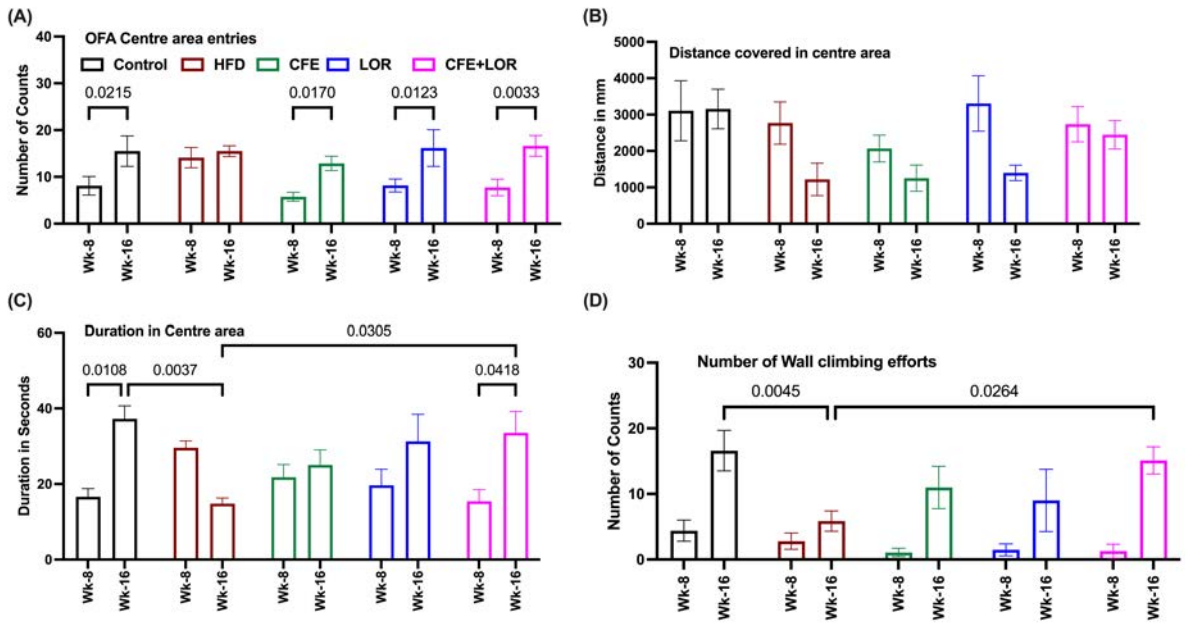

Figure 4.6: Open field analysis (OFA) - During exploring Centre area: The behavioural testing for exploration parameters before and after treatment with CFE and Lorcaserin. The OFA parameters included are (A) Number of entries into the centre area, (B) Distance covered in mm during centre area exploration, (C) Time spent in the centre area and (D) Number of random wall-climbing efforts attempted during exploration. Each group had n=8 mice and values plotted are Mean ± SEM. (where Control: control diet group, HF: high-fat diet group, CFE: high-fat diet with CFE, LOR: high-fat diet with Lorcaserin treatment, CFE+LOR: high-fat diet with CFE and lorcaserin treatments). Statistically significant differences between the groups (p-values <0.05) are shown.

Furthermore, there was a considerable increase in time spent in the centre area in the CFE+LOR group from week 8 to week 16. Spending more time in the centre of the open field was considered as superior exploratory behaviour than time spent in the corner zones (Parande et al., 2022). In the present study, the open field results showed an increase in the number of entries significantly into the centre area within the group between pre and post treatment assessments. Moreover, CFE+LOR group spent more time in centre area of the open field compared to the HFD group as well as within the group from week 8 to week 16 (Figure 4.6 C). In the (Rebai et al., 2021) study, the HFD groups showed a reduced time in climbing activity. Interestingly, figure 4.6 D also showed reduced wall climbing efforts in the HFD group compared to the control diet group. On the other hand, in the HFD with CFE+LOR group, climbing activity was significantly greater than in the HFD group. Figure 4.7 C demonstrates that time spent in the outer area by LOR and CFE+LOR treated groups significantly decreased with p = 0.035 and 0.008 during week 16 than HFD group. In contrast, the HFD group significantly increased in outer area duration compared to the control diet-fed group with a p-value of 0.0009.

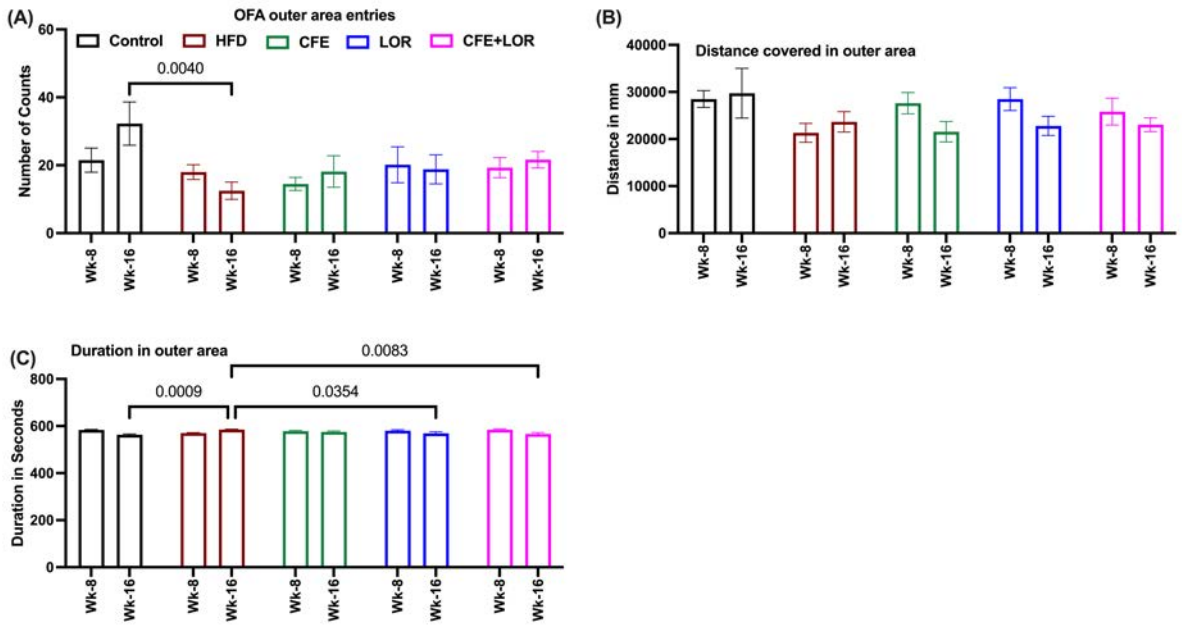

Figure 4.7: Open field analysis - During the exploration of the Outer area: The behavioural testing for exploration parameters before and after treatment with CFE and Lorcaserin. The OFA parameters included are (A) The number of entries into the outer area, (B) the distance covered in mm during outer area exploration, and (C) the time spent in the outer area. Each group had n=8 mice and values plotted are Mean ± SEM. (where Control: control diet group,

HF: high-fat diet group, CFE: high-fat diet with CFE, LOR: high-fat diet with Lorcaserin treatment, CFE+LOR: high-fat diet with CFE and lorcaserin treatments). Statistically significant differences between the groups (p-values <0.05) are shown.

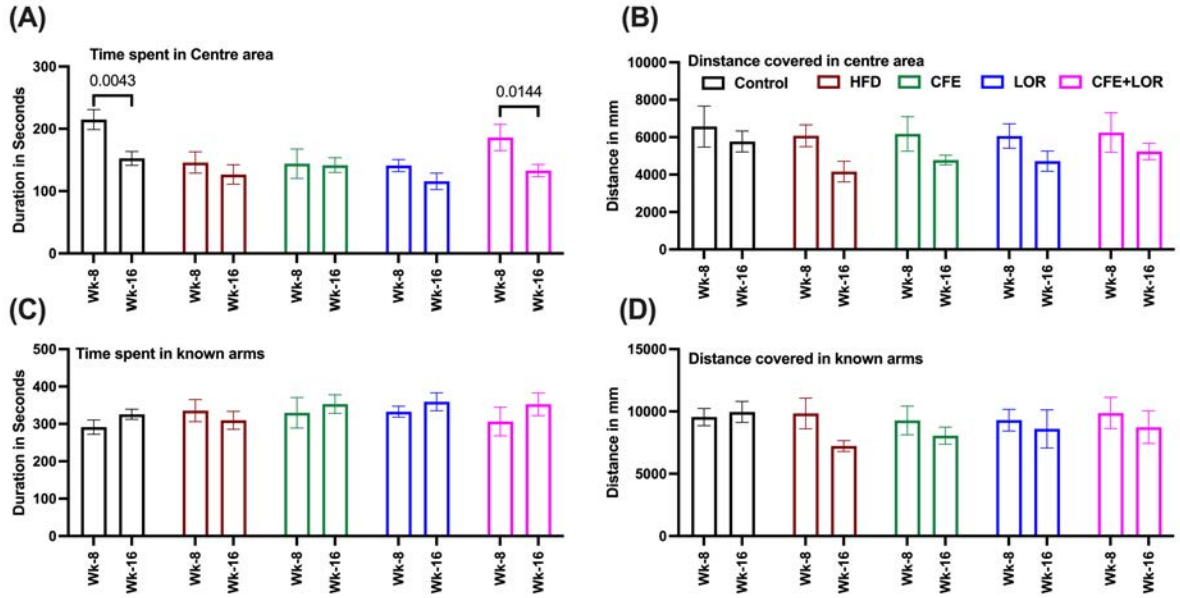

Figure 4.8: Y-maze analysis - Centre area and known arms exploration: The behavioural testing for exploration parameters before and after treatment with CFE and Lorcaserin. The Y-maze parameters included are (A) Time spent in the outer area, (B) Distance covered in mm during centre area exploration, (C) Time spent in the known arms, and (D) Distance covered in known arms. Each group had n=8 mice and values plotted are Mean ± SEM. (where Control: control diet group, HF: high-fat diet group, CFE: high-fat diet with CFE, LOR: high-fat diet with Lorcaserin treatment, CFE+LOR: high-fat diet with CFE and lorcaserin treatments). Statistically significant differences between the groups (p-values <0.05) are shown.

On the other hand, the Y-maze study reveals spontaneous memory and the exploratory nature of the animals based on unknown arm entries and the frequency with which the same arm is revisited. From figure 4.9 A, the HFD group's number of entries into the unknown arm decreased from week 8 to 16. In contrast, the treated groups' number of entries remained almost unchanged before and after the treatment study. The time spent in the unknown arm also increased in the CFE+LOR group in post-treatment experiments than in pre-treatment conditions. However, the Y-maze data shown in Figures 4.8 and 4.9 was not statistically significant. However, the current study found HFD was not showing hyperlocomotion

behaviour, which can be concluded from a greater number of altered entries to the arms. Interestingly, time spent in centre area of the Y-maze was significantly decreased in CFE+LOR treatment group compared to HFD. The decreased time spent in central area of the Y-maze was indicating an improved spontaneous memory of the rodents (Wei et al., 2022). The reduced time spent in central area was revealing a new dimension of the study, there could be a chance of CFE's role in memory signal cascade. However, this was too early to state CFE role in memory improvement, needs further memory functioning tests to measure.

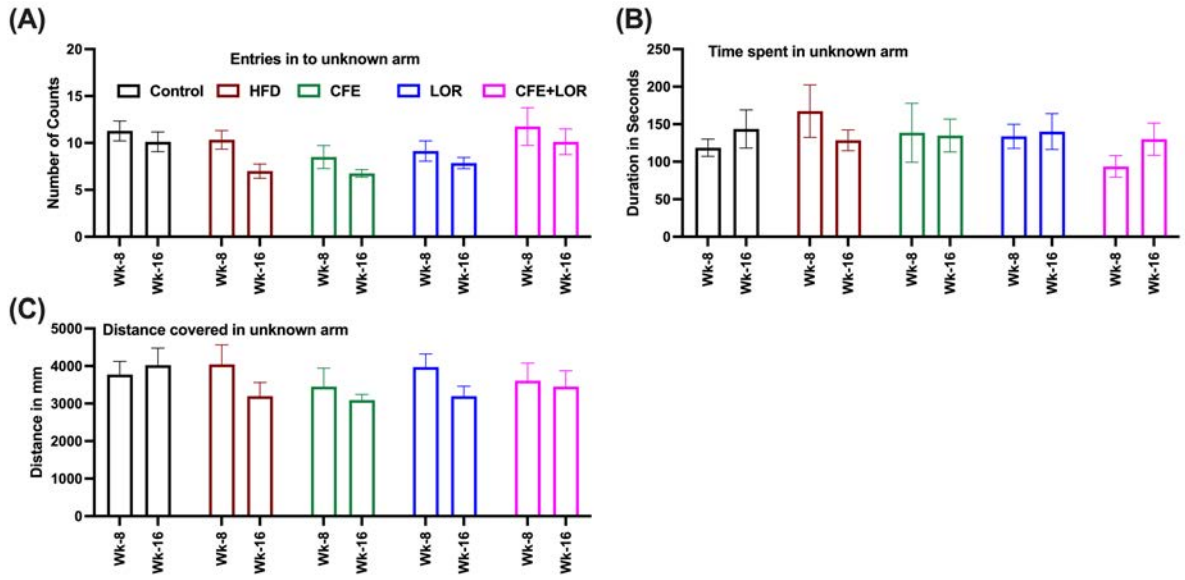

Figure 4.9: Y-maze analysis - Unknown arm exploration: The behavioural testing for exploration parameters before and after treatment with CFE and Lorcaserin. The Y-maze parameters included are (A) Number of entries into the unknown arm, (B) Time spent in the unknown arm, and (C) Distance covered in the unknown arm. Each group had n=8 mice and values plotted are Mean ± SEM. (where Control: control diet group, HF: high-fat diet group, CFE: high-fat diet with CFE, LOR: high-fat diet with Lorcaserin treatment, CFE+LOR: high-fat diet with CFE and lorcaserin treatments). Statistically significant differences between the groups (p-values <0.05) are shown.

4.4.3 Anxiety-like behaviour alteration assessment:

HFD may cause dysfunction in the hypothalamic-pituitary-adrenal axis (HPA) and leading to higher circulating corticosterone levels (Mello et al., 2003). Increased systemic inflammation and behavioural problems have been linked to excessive corticosterone production. Even in the absence of dyslipidemia, which may be linked to anxiety, the HFD has detrimental effects on

neurovascular coupling and cerebrovascular function (Takao et al., 2013, Jin et al., 2018, Adingupu et al., 2019, Braga et al., 2021). The EPM analysis describes (Figure 4.10 A) the CFE+LOR group number of entries into open arms significantly (p=0.036) more compared to HFD during post treatment assessment. In continuation, time spent in open arms plotted in Figure 4.10 B, describes LOR and CFE+LOR treated animals spent substantially more time in open arms with p = 0.023 and 0.036 than the HFD group during post-treatment experiments. Previous mice study unfolding an increase in open arm entries and time spent in open arms proportional to a decrease in anxiousness of the animals (Parande et al., 2022) ; current EPM results were correlating with it. In addition, all the treated groups showed significantly increase in distance covered in open arms within groups during EPM assessment of post treatment compared to pre-treatment stage. The results revealed that CFE+LOR significantly reduced anxiety-like behaviour in HFD-induced animals. In addition to this, the time spent in closed arms and the number of entries to closed arms were reduced in treated groups. Moreover, Figure 4.12 shows time spent in the centre area reduced in CFE and CFE+LOR groups compared to HFD fed group during week 16. The time spent in central area of EPM significantly reduced in CFE and CFE+LOR groups compared to HFD. The anxiety like behaviour was determined from previous studies stating that, animals explore open field central area were explore open arms in EPM. In addition, rodents were measured for anxiety like behaviour through spending more time in EPM central area (Knight et al., 2021). The current data was supporting anxiety like behaviour from HFD reverted by CFE+LOR treatment. The time spent in central area of EPM was significantly reduced with CFE, CFE+LOR treatment compared to HFD.

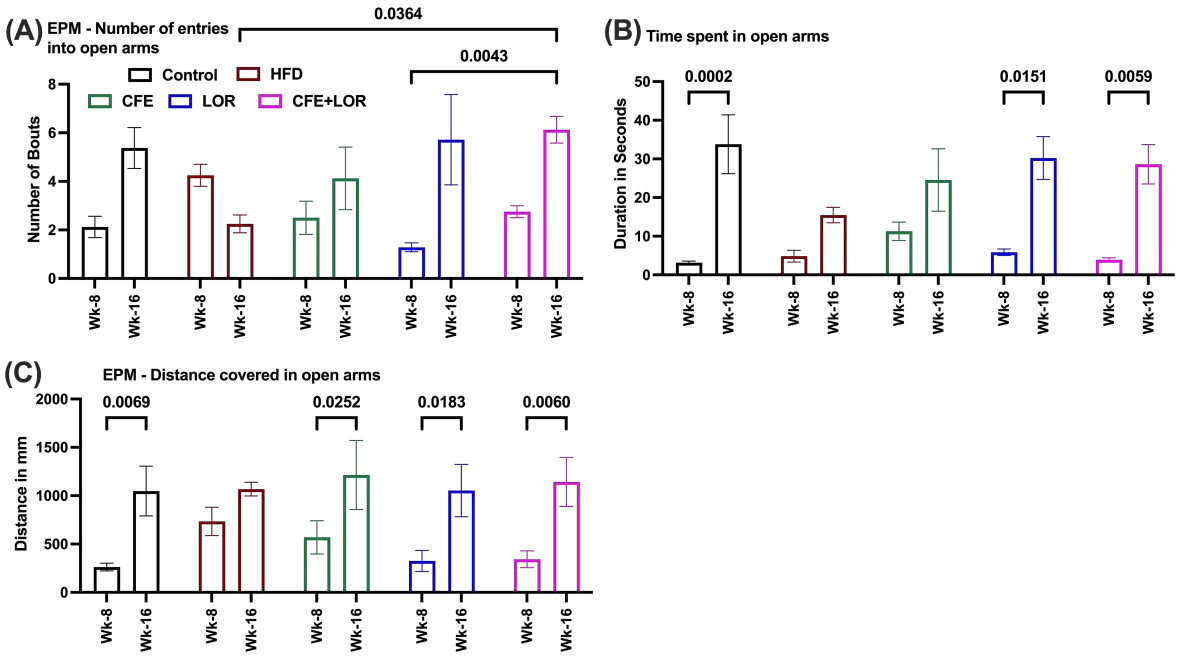

Figure 4.10: Elevated plus maze analysis - to validate anxiety-like behaviour: The behavioural testing for anxiety level before and after treatment with CFE and Lorcaserin. The EPM parameters included are (A) Number of entries into the open arms, (B) Time spent in open arms, and (C) Distance covered in open arms. Each group had n=8 mice and values plotted are Mean ± SEM. (where Control: control diet group, HF: high-fat diet group, CFE: high-fat diet with CFE, LOR: high-fat diet with Lorcaserin treatment, CFE+LOR: high-fat diet with CFE and lorcaserin treatments). Statistically significant differences between the groups (p-values <0.05) are shown.

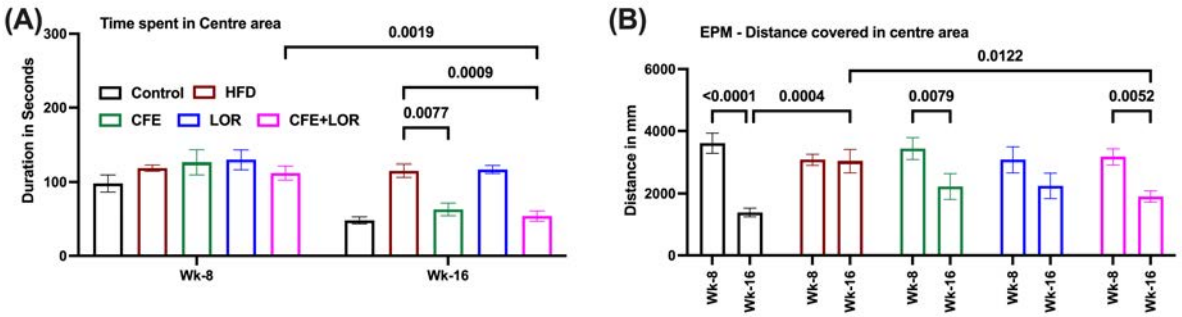

Figure 4.11: Elevated plus maze analysis - to validate anxiety-like behaviour: The behavioural testing for anxiety level before and after treatment with CFE and Lorcaserin. The EPM parameters included are (A) Time spent in the centre area of EPM and (B) Distance covered in the EPM centre area. Each group had n=8 mice and values plotted are Mean ± SEM. (where Control: control diet group, HF: high-fat diet group, CFE: high-fat diet with CFE, LOR: high-

fat diet with Lorcaserin treatment, CFE+LOR: high-fat diet with CFE and lorcaserin treatments). Statistically significant differences between the groups (p-values <0.05) are shown.

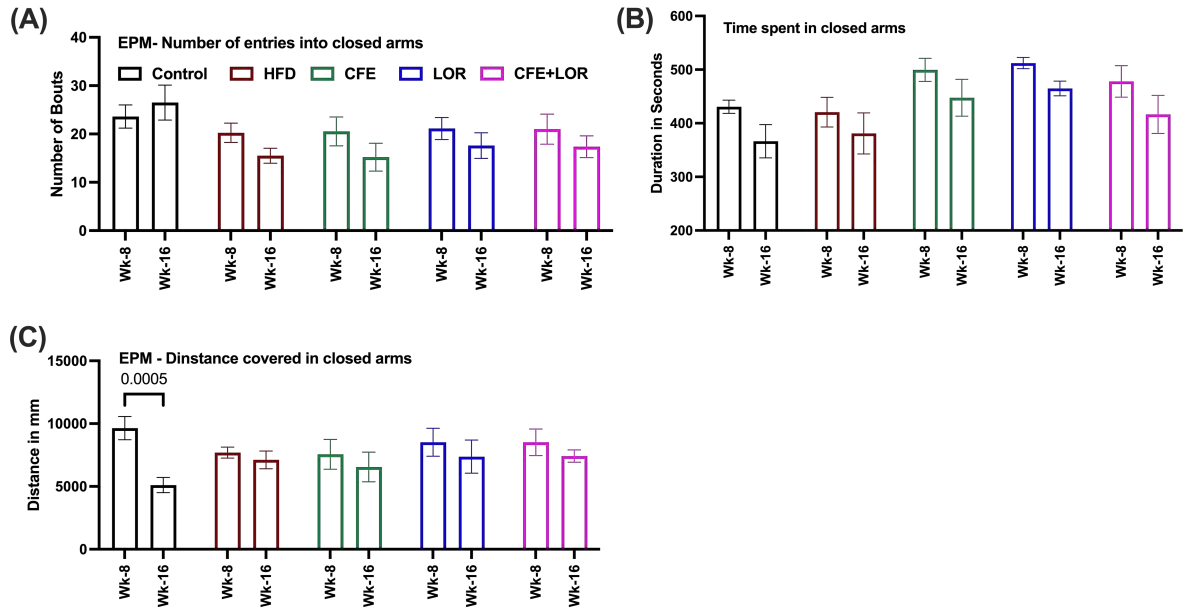

Figure 4.12: Elevated plus maze analysis - to determine anxiety: The behavioural testing for anxiety level before and after treatment with CFE and Lorcaserin. The EPM parameters included are (A) Number of entries into the closed arms, (B) Time spent in closed arms, and (C) Distance covered in closed arms. Each group had n=8 mice and values plotted are Mean ± SEM. (where Control: control diet group, HF: high-fat diet group, CFE: high-fat diet with CFE, LOR: high-fat diet with Lorcaserin treatment, CFE+LOR: high-fat diet with CFE and lorcaserin treatments). Statistically significant differences between the groups (p-values <0.05) are shown.

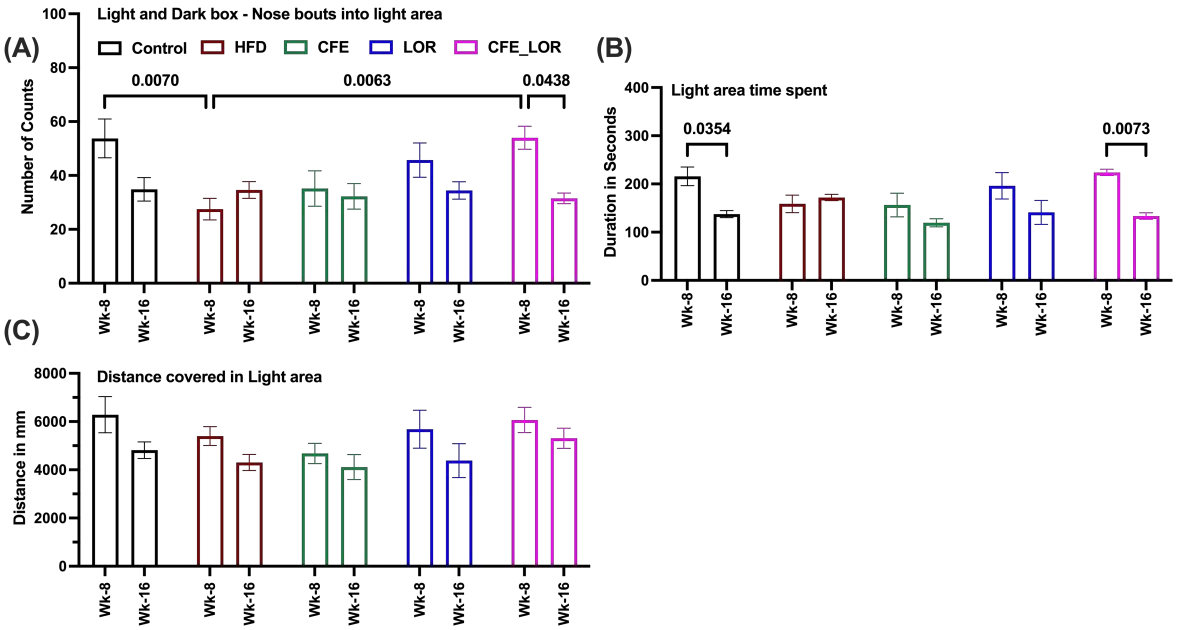

Figure 4.13: Light and dark box analysis - to determine anxiety-like behaviour: The light and dark box parameters included are (A) The Number of nose bouts in the light area, (B) the Time spent in the brighter chamber area, and (C) the Distance covered in the light area. Each group had n=8 mice and values plotted are Mean ± SEM. (where Control: control diet group, HF: high-fat diet group, CFE: high-fat diet with CFE, LOR: high-fat diet with Lorcaserin treatment, CFE+LOR: high-fat diet with CFE and lorcaserin treatments). Statistically significant differences between the groups (p-values <0.05) are shown.

4.4.4 Depression-like behaviour analysis:

Depression is a mental illness caused by genetic, environmental, and psychological factors. According to recent research, chronic neuroinflammation has been linked to changes in mood and behaviour (Cui et al., 2012, Halford and Harrold, 2012, Relkovic and Isles, 2013, Parande et al., 2022). Both HFD and chronic mild stress (CMS)-treated rats (Wang et al., 2018) displayed more abnormal behaviour than HFD-fed mice (Wu et al., 2019), showing that both HFD and CMS may cause animals to acquire depression-like behaviour. An investigation with 34 healthy volunteers who received an intravenous LPS injection revealed higher levels of cortisol and proinflammatory cytokines in the blood and increased anxiety, which negatively impacted on mood and behaviour (Schachter et al., 2018). However, it is complex to differentiate depression and anxiety from animal behaviour. The current results from the tail suspension test (TST) and forced swim test (FST) were used to infer the behavioural effects of CFE and Lorcaserin treatment in the HFD model.

Antidepressant research has used TST-based immobility time as an effective index of depression in mice. The animal immobility time is proportional to depression level, and several antidepressant drugs reduce the immobility time in TST and promote escape behaviour (Cryan et al., 2005). The TST based depression assessment revealed that the HFD caused depression-like symptoms in mice (Figure 4.14). There was a significant decrease in the immobility of the mice within the control diet and treated groups, whereas the HFD group did not show any variation. The CFE (p=0.015), LOR (p=0.005), and CFE+LOR (p=0.001) groups all showed a significant reduction in immobilisation in TST between pre-and post-treatment runs. In addition, the CFE+LOR post-treatment significantly decreased the immobility time compared to HFD with p value 0.02.

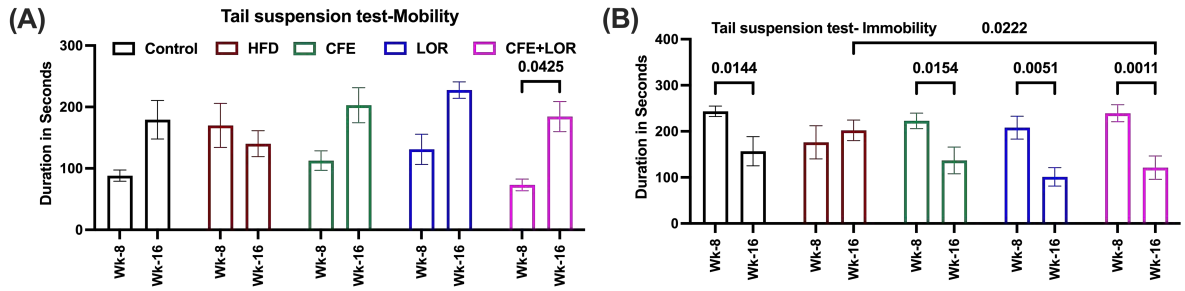

Figure 4.14: Tail suspension analysis - to determine depression behaviour: The behavioural testing for depression level before and after treatment with CFE and Lorcaserin. The tail suspension parameters included are (A) Mobility and (B) immobility duration during test time; Each group had n=8 mice and values plotted are Mean ± SEM. (where Control: control diet group, HF: high-fat diet group, CFE: high-fat diet with CFE, LOR: high-fat diet with Lorcaserin treatment, CFE+LOR: high-fat diet with CFE and lorcaserin treatments). Statistically significant differences between the groups (p-values <0.05) are shown.

.

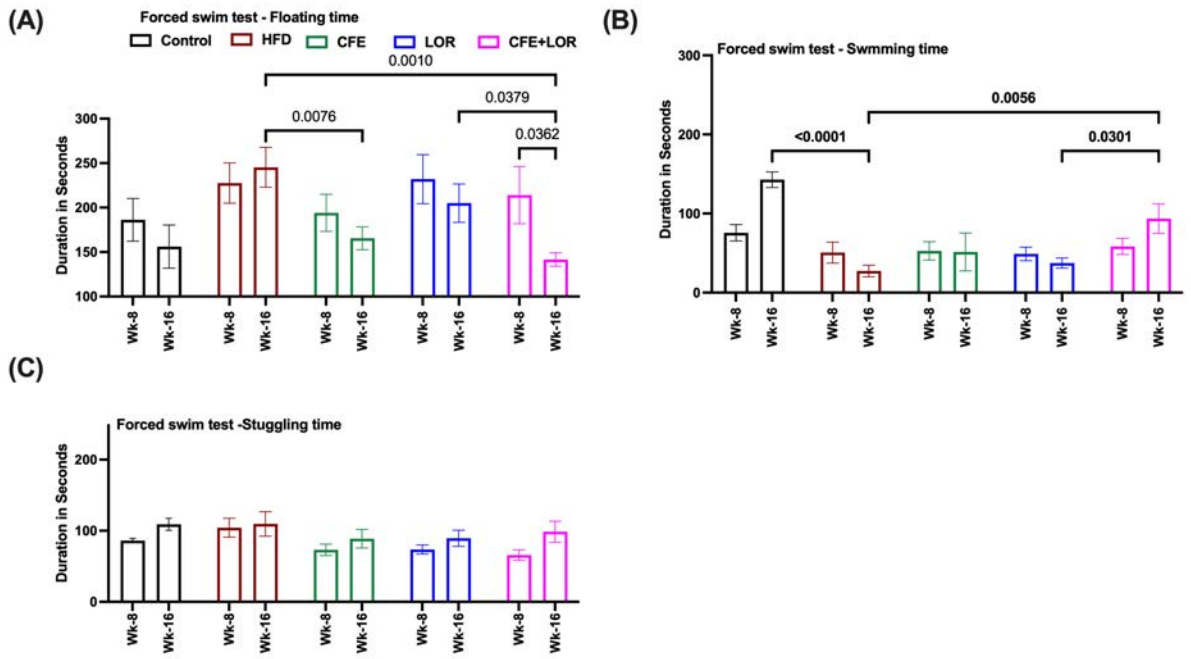

Figure 4.15: Forced swim test (FST) analysis - to determine depression level: The behavioural testing for depression behaviour before and after treatment with CFE and Lorcaserin. The FST parameters included are (A) Floating time, (B) Swimming time, and (C) Struggling time. Each group had n=8 mice and the values plotted are Mean ± SEM. (where Control: control diet group, HF: high-fat diet group, CFE: high-fat diet with CFE, LOR: high-fat diet with Lorcaserin treatment, CFE+LOR: high-fat diet with CFE and lorcaserin treatments). Statistically significant differences between the groups (p-values <0.05) are shown.

Similarly, the forced swim test parameters like floating represents immobility of the mice during swim test. Antidepressants like serotonin reuptake inhibitors showed reduced immobility duration in FST and promoted escape behaviour. The molecules with antidepressant activity showed decrease in immobility and improved swimming duration in mice (Monchaux De Oliveira et al., 2021). In correlation to this, current study results showed reduced floating/immobile time in CFE (p=0.007) and CFE+LOR (p=0.001) groups compared to HFD in post treatment experiments as shown in Figure 4.15. In addition, CFE+LOR group significantly (p-value = 0.036) improved escape behaviour as shown in Figure 4.15A, where floating time reduced within the groups when comparing pre- and post-treatment analysis. On the other hand, the CFE+LOR treatment group was indicated significant improvement in swimming duration with p values 0.005 and 0.03 compared to HFD and LOR, respectively.

Outcomes of the study:

- HFD-induced mice bodyweight/weight gain is restricted by CFE+LOR treatment
- Food intake and water uptake were controlled by CFE as well as CFE+LOR treatments
- The Anxiety and Depression behaviours induced by the HFD were alleviated in the CFE+LOR group, indicating that activation of 5HT2cR signalling may be mediating the improvement in mood as assessed by the behavioural parameters.

4.5 Conclusion:

In summary of the current chapter, the HFD-fed mice showed a significant increase in anxiety and depression-like behaviours compared to control diet mice. The CFE, LOR and CFE+LOR treatments showed significant effects of restoring the typical behaviour of the mice. Together, from the TST and FST experiments, one can conclude that depression-like behaviour was reversed with CFE+LOR treatment. while LOR alone did not significantly recover HFD-fed mice from depression-like behaviour; there was a significant effect of CFE to improve escape behaviour in the mice. In addition to behavioural effects, the treatments reduced weight gain and food intake during HFD feeding. However, the metabolic rate and energy homeostasis are further key elements in obesity regulation. The next chapter describes the energy expenditure and body composition (fat and lean mass) data to elucidate the effects of CFE+LOR treatment in HFD-fed mice.

Chapter 5 Effect of CFE and Lorcaserin on energy expenditure and vascular dysfunction in a high-fat diet-induced mice model of obesity

5.1 Abstract:

Energy homeostasis is one of the critical factors in regulating body weight in obesity and related metabolic diseases. In general, energy homeostasis is associated with caloric intake and expenditure coordinated by compensatory modulation within the system. Obesity occurs when one's energy intake exceeds energy expenditure for an extended period. The alteration to energy homeostasis with excess calorie intake led to fat deposition. Fat storage will result in an increase in body weight, which will cause disease conditions like obesity and related comorbidities. In humans' obesity may raise the risk of cardiac diseases; however, in HFD-induced mice, limited data is available. The present study aims to validate the energy expenditure of CFE and LOR treatments. Further, we measured vascular dysfunction by isometric tension analysis of abdominal aortic rings. The energy expenditure was estimated using the Promethion metabolic cage system. The study looked at body fat composition and the effects of HFD induction on vascular dysfunction in addition to energy expenditure. The results unveiled CFE and LOR treatment influencing body fat and energy expenditure in HFD-fed mice. The fat deposition was decreased in CFE and CFE+LOR groups compared to HFD and LOR-treated groups. Interestingly, the energy expenditure was significantly higher in CFE and CFE+LOR groups compared to the HFD-fed group. Furthermore, according to the isometric tension study, all the treated groups of mice were protective against vascular dysfunction compared to HFD mice. In conclusion, CFE and LOR treatments were potentially working against fat accumulation and low energy expenditure. In addition, CFE and LOR treatment may reduce cardiac risk factors in obesity.

5.2 Introduction:

Obesity is associated with a broad disruption of metabolic homeostasis, which results in insulin resistance, dyslipidemia, irregular blood pressure management, and an increased risk of diabetes and cardiovascular diseases (Lang et al., 2019). A new expression, "cardiometabolic-based chronic disease" (CMBCD) (Mechanick et al., 2020), was recently coined to encourage prompt and ongoing preventative therapy for cardiometabolic disorders caused by genetics, environment, and behavioural signals. CMBCD has been linked to coronary heart disease, heart failure, and atrial fibrillation (AF), common in obese people (Ren et al., 2021). According to population-based data, increased BMI is also linked to early CVD morbidity or cardiometabolic multimorbidity (Khan et al., 2018).

In the recent times, Coronavirus disease 2019 (COVID-19) is a pandemic respiratory sickness caused by a novel coronavirus. It can cause severe acute respiratory syndrome (SARS-CoV-2) and was discovered in late 2019 in Wuhan, China, before quickly spreading worldwide (Aghili et al., 2021). Obesity and the severity of COVID-19 have been linked in recent research. Obesity was associated with a higher risk of critical illness in COVID-19 patients in a meta-analysis encompassing 7,196 individuals from 13 different trials (Goldenshluger et al., 2021, Aghili et al., 2021). Obesity is becoming apparent as an independent risk factor for heart failure, as evidence of abnormalities in cardiac structure and function in moderately obese person growth. This scenario could be enlarged to include cardiac irregularities in obese people, which are not caused by coronary artery disease, hypertension, diabetes mellitus, or any other complicating cause (Nieto-Martínez et al., 2021). With the emergence of the "obesity paradox," the relationship between BMI and cardiac function becomes increasingly sensitive (Ross and Bradshaw, 2009). Arterial stiffness, a chronic pathological process characterised by a progressive loss of major artery distensibility, emerges as an independent risk factor that worsens cardiovascular disease progression (CVD) in obese people (Sarma et al., 2021, Ren et al., 2021). Endothelial dysfunction, extracellular matrix remodelling, calcification, and inflammation all contribute to the initiation and progression of vascular stiffness, which compromises vascular function(Ren et al., 2021). The fundamental driving forces for Left ventricular (LV) wall stress in normotensive obesity are higher central blood volume, stroke volume, and CO, which tend to lead to LV dilatation and eccentric hypertrophy (Aghili et al., 2021, Buettner et al., 2007). If LV wall thickening does not keep up with chamber dilatation, systolic dysfunction can develop later because of excessive wall stress. Previous research on the association between BMI and aortic valve stenosis (AVS) has yielded mixed results

(Aggarwal et al., 2013). Obesity increases blood pressure, which can cause geometric alterations in the LV and aortic valves (Martínez-Martínez et al., 2021, Mechanick et al., 2020). Elevated plasma lipids cause lipid deposits on the aortic valve leaflets and valvular interstitial injury (Martínez-Martínez et al., 2021).

On the other hand, Pancreatic polypeptide (PP) levels in fasting plasma are much lower, but leptin levels are significantly higher (Dimitriadis et al., 2013). Ghrelin secretion from the stomach was known to influence hunger and glucose homeostasis by interacting with plasma peptide YY (PYY), leptin, glucagon-like peptide-1 (GLP1), cholecystokinin (CCK), and the hypothalamic anorexigenic and orexigenic pathways (Wren and Bloom, 2007). Depleting central serotonin with selective neurotoxins causes hyperphagia and obesity (Lam et al., 2008). Unlike the absence of other serotonin receptors in mice, animals lacking 5HT2cRs were observed to be hyperphagic and fat (Clifton et al., 2000). As a result, the 5HT2cR was identified as a potential target for in obesity and other overeating disorders. According to an earlier study, functional 5HT2cR needed to maintain energy homeostasis and to avoid excess weight gain (Nonogaki et al., 2008, Lam et al., 2008). Pharmaceutical agents that increase 5HT2cR function, such as d-fenfluramine, inhibit hunger and help to reduce weight (Higgs et al., 2011). The therapeutic success of a broadly acting serotonergic medication d-fenfluramine, sparked interest in discovering selective 5HT2cR agonists. Unfortunately, d-fenfluramine was linked to cardiac valvulopathy and pulmonary hypertension, leading to its discontinuation from clinical usage. (Nonogaki, 2022, Jais and Brüning, 2022). The overall role of different serotonin receptors in the system are important to regulate different functions. Hence, it is necessary to identify specific agonist for 5HT2cR which has a role in mood, behaviour, and satiety regulation.

Research continued to find specific agonist compounds after considering the risk factors in the absence of 5HT2cR activation. Lorcaserin, a selective 5HT2cR agonist, marketed in the United States under the brand name Belviq since 2013, received FDA approval in 2012 (He et al., 2021, Hayden and Banks, 2021). Lorcaserin is the first selective 5HT2c receptor agonist approved for human use, and its full clinical potential is unclear because of problems since its recent approval (Mathai, 2021). Precision medicine is the practice of tailoring therapies to a patient's unique traits, including genetics, environment, and lifestyle factors (Hayden and Banks, 2021). Therefore, Lorcaserin’s full clinical potential for other diseases was unknown. Combining Lorcaserin with other pharmaceutical or nutraceutical molecules could be a better

approach in treating body weight gain in obesity (Singh and Singh, 2020). The *Caralluma fimbriata (C. Fimbriata)*, a succulent plant native to India, Pakistan, and Afghanistan, belongs to the *Asclepiadaeceae* family. Pregnane glycosides are found in plants of the *Asclepiadaceae* family, including C. *Fimbriata*, and have appetite-suppressing actions in the hypothalamus (Rao et al., 2021). Previous research has suggested that *C. Fimbriata* extract (CFE) suppresses appetite by downregulating ghrelin synthesis in the stomach and neuropeptide Y (NPY) in the hypothalamus (Vitalone et al., 2017). However, the specific mechanism of action was unknown. The CFE's appetite-suppressing and weight-loss effects have been studied in humans (Rao et al., 2021) and animals (Vitalone et al., 2017, Gujjala et al., 2019) models. The clinical data of the CFE group maintained their baseline body mass during the 16-week supplementation period, but the placebo group significantly increased body mass. In addition, the placebo group experienced an increase in android fat that was not observed in the CFE group. The CFE group's body mass maintenance was accompanied by a considerable reduction in calorie consumption and was not found in the placebo group. Despite reducing calorie intake in the CFE group, the postprandial satiety score remained the same (Rao et al., 2021). In addition, CFE also showed appetite suppression in snord116del mouse (Griggs et al., 2018a). These findings suggest that CFE supplementation helped maintain body weight by lowering calorie intake and limiting fat development.

Literature states, CFE can regulate appetite and fat deposition in overweight condition. On the other hand, Lorcaserin a selective agonist for 5HT2cR improved satiety signal and decreased weight gain (Hall et al., 2022, Vlaardingerbroek et al., 2021, van Galen et al., 2021, Georgescu et al., 2021). The current study aims to understand the energy homeostasis balance in HFGD-fed mice with CFE and LOR treatments. The impact of given treatments on body composition and energy expenditure was estimated. The study's outcome revealed that a CFE+LOR therapy by lowering the Lorcaserin dose might regulate obesity and other overeating disorders simultaneously, and additionally reducing the Lorcaserin side effects with long-term usage. A limited study on HFD induced mice model and vascular dysfunction estimation is available. Abdominal aortic rings were used to estimate the involvement of high cholesterol diet influence in vascular endothelial dysfunction by vascular dilation with isometric tension analysis (Zulli et al., 2003). The HFD induced obese mice showed significantly reduced vasodilatory activity compared to the mice maintained on the control diet. The percentage of vascular dilation in HFD induced mice was increased by CFE, LOR and CFE+LOR treatments in this study. The

treatments showed potential reduction of vascular pathology dysfunction compared to HFD group.

5.3 Materials and Methods:

5.3.1 Body composition analysis:

The body composition of the mice was determined using EchoMRI equipment (Echo-MRI^{TM} 900, Houston, TX, United States of America) and works on the principle of nuclear magnetic resonance (NMR). In mice, EchoMRI is a reliable approach for determining body composition (Taicher et al., 2003). EchoMRI is a non-invasive technique for determining body composition in live mice that does not require anaesthesia. The instrument entailed using canola oil, the fat content in the oil was given as standard to calibrate the instrument. To assess body composition, animals were placed in a cylindrical holder with breathing vents and scanned three times in an EchoMRI as shown in Figure 5.1. Mice were acclimatised to the process at week four, after which measurements were obtained at week 8 (baseline) and 16 (post-treatment). The time points of Echo MRI analysis for all the groups during the study period was mentioned in the Figure 5.1. The data obtained from Echo MRI consists of Fat mass (all fat molecules in the body), Lean mass (tissues containing water, excluding fat, bone minerals, and substances that do not contribute to the NMR signal, such as hair and claws), and total water content (water contained urine, tissue, and blood); all these parameters were expressed in grams with respect to bodyweight.

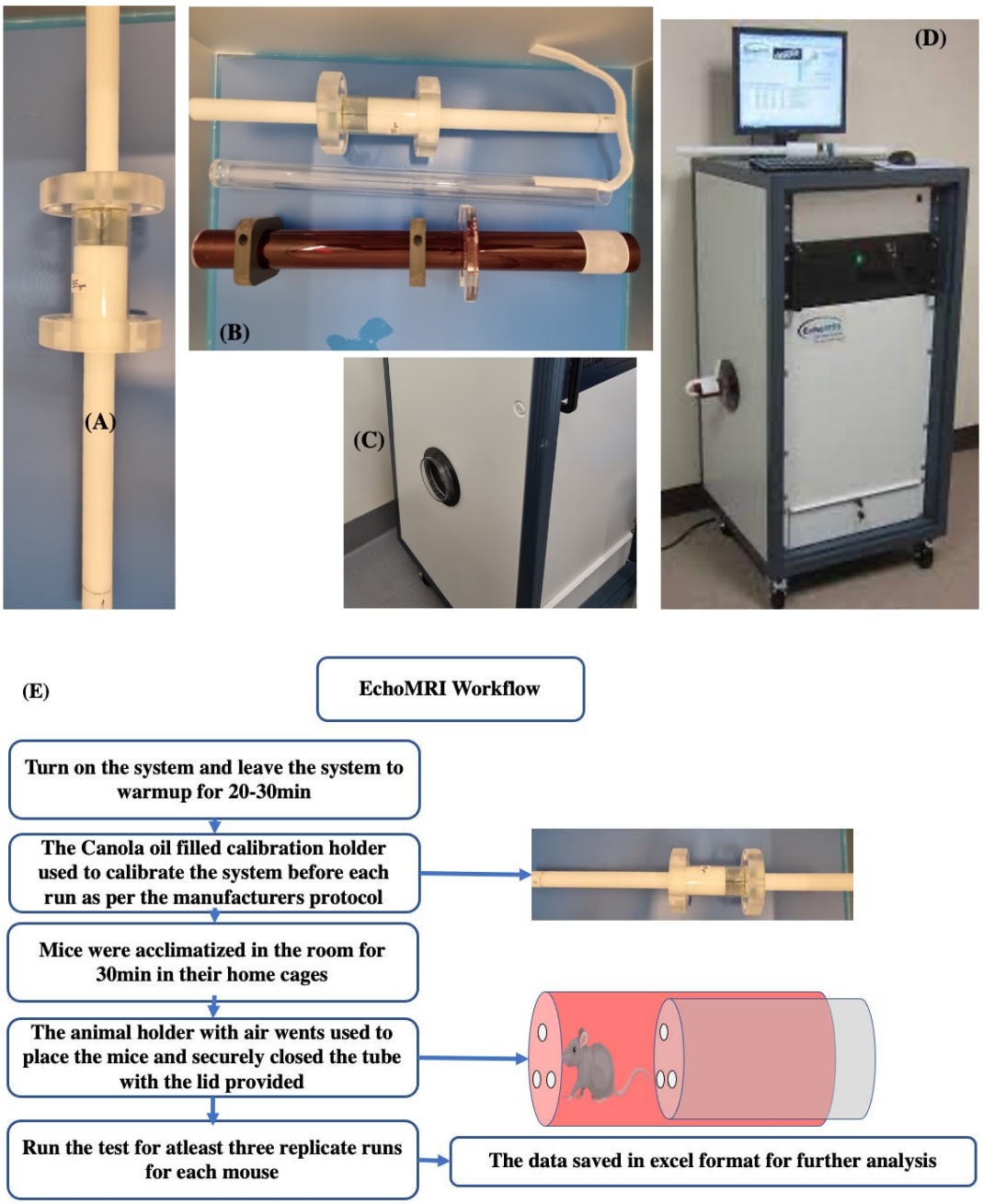

Figure 5.1: EchoMRI-900 and workflow of the body composition measurement: (A) Canola oil holder for EchoMRI calibration with fat content of 35.68g, (B) The red holder is used to place the animal to measure the body composition, (C) The slot to place the animal holder into the instrument, (D) After placing the animal holder into the system, and (E) workflow of EchoMRI to measure the mice body composition.

5.3.2 Promethion cage monitoring:

The Promethion cage monitoring system was used to measure the metabolic data with behavioural synchronisation (Kanshana et al., 2021). The Promethion system used in this study

was supplied by Sable systems international, North Las Vegas, USA. The system consists of individual animal cages with food, water, and body weigh measuring/ housing hoppers connected with mass modules as shown in the Figure 5.2. In addition, each cage is individually supplied with a controlled gas inlet (2000ml/min) and outlet channels connected to a standard gas analyser to measure O_2 and CO_2 utilisation during mouse monitoring. The study was conducted excluding running wheel and gated food access; we used mass modules to measure food, water, and body mass (housing); gas analysis to estimate energy expenditure, lipid oxidation, and glucose oxidation parameters. The animals were familiarised with the Promethion cage environment during week-4 of the study time. The animals were under Promethion cage monitoring for 72 hr during week-8 and 16, as pre-and post-treatment time points. A live software platform controlled the Promethion system, and the raw data obtained was converted by Expdata conversion tool and Universal Macros tool as shown in the workflow Figure 5.2G.

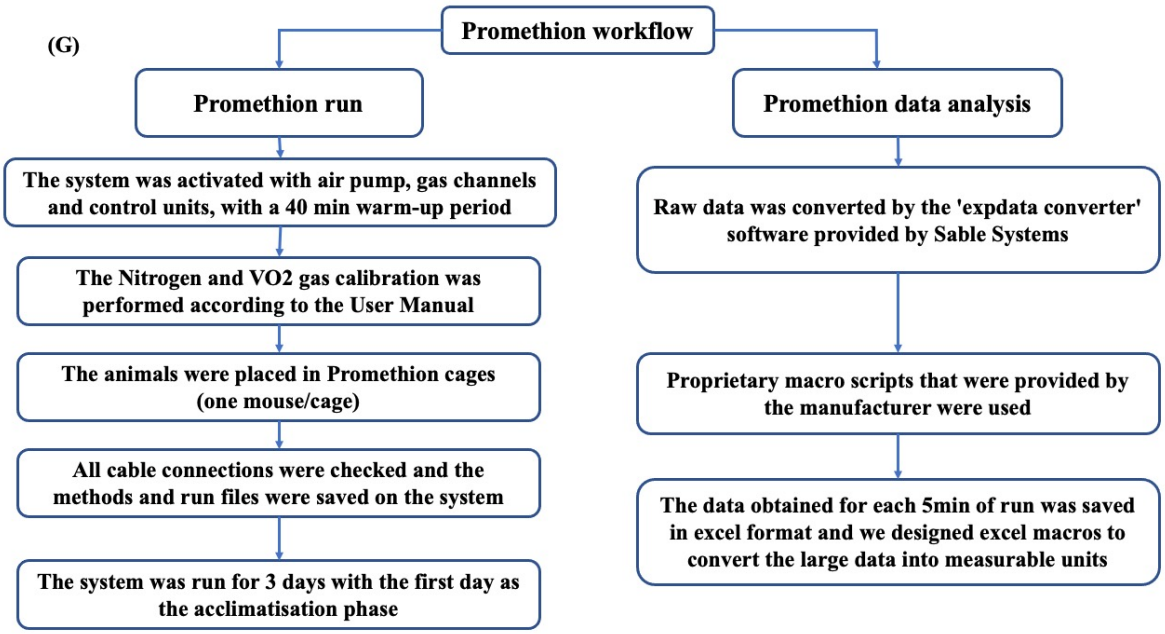

Figure 5.2: Components of Promethion cage and workflow of Promethion metabolic cage monitoring: (A) Promethion cage base with gas channel, (B) and (C) cage lid with mass module inserts, (D) Different hoppers that can go with each mass module in the cage, (E) Hoppers hanging to the respective mass module, (F) Gas tubes connected to the gas channel in the cage and (G) Overall brief workflow of Promethion system handling

The gas analyser data was utilised to calculate individual mice's energy expenditure, glucose, and lipid oxidation during overall, light, and dark cycles. The data initially obtained from software consist of 5min interval points and are manually segregated to each hour for all the data. The rodent nature, active cycle timings, and treatment timing were considered, during dark cycle metabolic rate. The hourly based data was used to separate the first day one night as acclimatisation time the second day 7 am to 7 pm, considered as first light cycle and the second day 7 pm to the third day 7 am as a first light cycle shown in the figure. The two dark cycles (2nd and 3rd day night 12hrs) average were considered as overall dark cycle average data points to compare between the groups. All the data from different mouse groups of treatments comparisons obtained from Promethion was used for statistical analysis.

5.3.3 Isometric tension analysis:

Isometric tension study on abdominal aortic rings was used to examine the CFE and Lorcaserin influence on blood vessel function of HFD induced mice. Isometric tension analysis was a functional study used to identify pharmacodynamic effects on blood vessel function (Zulli et al., 2009, Zulli and Hare, 2009). In Hyperhomocysteinemia (HHcy) (Yun et al., 2013) and atherosclerosis (Wang et al., 2017, Zhou and Austin, 2009), severe endothelial and vascular dysfunction leads to decreased vasodilation in response to Ach (Acetylcholine). Therefore, abdominal aortic rings were constricted with phenylephrine (a post-synaptic alpha-1 adrenergic receptor agonist) and relaxed by cumulative doses of the neurotransmitter Ach to assess the capacity of the different treatments to improve vasodilation. For statistical analysis, the responses to vasodilation were converted to a percentage (Qaradakhi et al., 2019). The isometric tension analysis brief description has been mentioned in Figure 5.3.

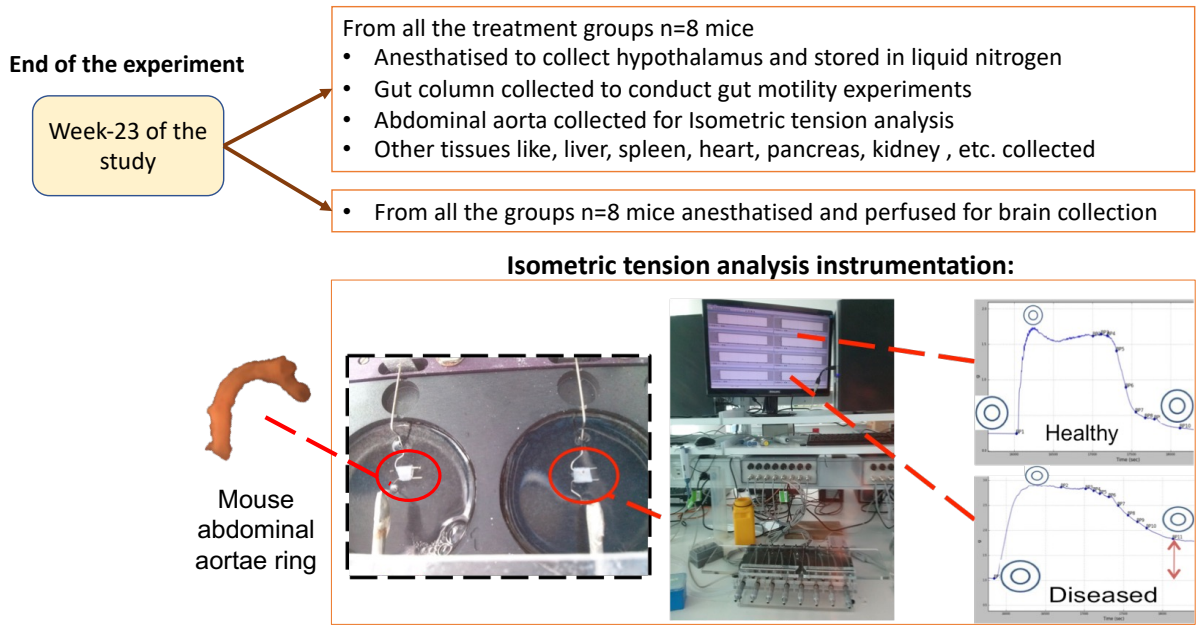

Figure 5.3: Isometric tension analysis workflow description

- The abdominal aorta of a mouse was removed, cleaned of connective and adipose tissue, and dissected into 2-3 mm rings.
- Rings were acclimatised in Krebs solution-filled organ baths for 30 minutes at 37 degrees Celsius, with 95% carbogen continually bubbling.
- The rings were stretched to 0.2 to 0.3 g of tension between two metal organ hooks connected to force-displacement transducers.
- Rings were re-stretched and refreshed after 30 minutes with buffer.

- A 5uL injection of U46619 (bath concentration of $2´10^{-5}$M) was used to constrict the rings (a thromboxane analogue)
- An acetylcholine dosage response (bath concentration of $1´10^{-8}$ M to $1´10^{-5}$ M serial dilutions) was used to dilate arteries once a plateau is reached.
- Dilation responses were translated to percentages, and significance effects determined by statistical analysis.

5.3.4 Statistical analysis:

All the data were statistically validated at 95% confidence by Two-way ANOVA with Sidak's post-hoc multiple comparison test. The data analysis was performed using Graph Pad Prism version 9.3.1.

5.4 Results and Discussion:

The 5HT2cR is highly expressed in brain compared to peripheral tissues and they influence feeding behaviour in mice (Levine et al., 1987). Leptin-independent hyperphagia is resulting in mice with a genetic mutation in 5-HT2cRs, which leads to late-onset obesity, insulin resistance, and decreased glucose tolerance (Sarma et al., 2021, Singh and Singh, 2020, Levine et al., 1987). The 5HT2cR mutants may cause hyperphagia condition before hyperinsulinemia and weight gain (Hayden and Banks, 2021). The findings are stating that 5HT2cR do not directly govern the central outflow of the vagal nerve to the pancreatic cells (Aghili et al., 2021, Nonogaki, 2012). Furthermore, 5HT2cR mutants are more sensitive to high-fat and high-sucrose diets than wild-type mice, resulting in obesity and type 2 diabetes at an earlier age. Hyperphagia is associated with decreased hypothalamic POMC expression and increased hypothalamus orexin activity in 5HT2cR mutants. Increased wakefulness in 5HT2cR mutants could be due to a compensatory increase in functional orexin activity (Nonogaki et al., 2008, Bovetto and Richard, 1995, Kitchener and Dourish, 1994, He et al., 2021).

Thus, the 5HT2cR-mediated regulation of feeding and energy balance, is acts through anorexic pathways plays a critical role in obesity regulation (He et al., 2021). Energy expenditure (EE) is mainly depending on thermogenesis, basal metabolic rate, and physical activity. In the body, protein and carbohydrate synthesis and breakdown are linked to variations in water and extracellular fluid levels (Hall et al., 2012). Protein is made up of amino acids and not "stored" in higher-order structures like carbohydrates or triglycerides (Martínez-Martínez et al., 2021,

Goldenshluger et al., 2021, Gepner et al., 2019, Patel et al., 2018). Protein synthesis was requiring more energy than glycogen or triglyceride synthesis. As a result, low-carbohydrate diets can increase total energy expenditure. Diet-induced EE alterations depend on how the nutrients are processed, partitioned into tissues, and mobilised (Blüher, 2019). A regulatory feedback loop may control energy expenditure and intake, connecting central and peripheral nervous systems and neuroendocrine signalling. By adjusting energy homeostasis and, integrating these signals helps the body to maintain its weight and fat composition (Nieto-Martínez et al., 2021, Kanshana et al., 2021, Singh and Singh, 2020, Löffler et al., 2021). Even when there is no change in body weight, fat mass rises, and lean mass declines, commonly associated with ageing (Lang et al., 2019). Variations in body composition could be caused by changes in resting metabolic rate and macronutrient oxidation. Obesity can cause a positive energy balance, with low resting metabolic rate and low non-exercise activity thermogenesis (NEAT) being two risk factors in a high energy intake scenario (Löffler et al., 2021). Even though majority of experimental methods used in neuroscience have been effective in probing brain mechanisms and circuits, it is still unclear to what extent artificial activation or inhibition of neurons can recreate their physiological function. Homeostatic circuits must constantly integrate sensory inputs with the caloric content of food; how these pathways are affected by obesity-predisposing factors, such as the ingestion of HFD, is still a debatable challenge (Moura-Assis et al., 2021). Additionally, a complex CNS network regulates autonomic outflow to regulate interescapular brown adipose tissue (iBAT) thermogenesis and white adipose tissue (WAT) metabolism. Like peripheral insulin sensitivity, peripheral glucose metabolism is but not entirely controlled by the central nervous system (Moura-Assis et al., 2021).

The body composition results from Echo MRI were showing increased lean mass and a decline in fat content of HFD mice during CFE and CFE + LOR treatments. In detail, the fat content of the HFD group showed in the Figure 5.4 increased 8.99g during week 8 to week 16 with a significance of $p<0.0001$ compared to control diet mice (increased 3.33g only). On the other hand, the LOR treated group fat content increased similarly to the HFD group and determining LOR treatment alone was not effective with the selected dose. Interestingly CFE alone significantly ($p=0.0306$) reduced the fat mass deposition in HFD induced animals after week-16 when compared to HFD group. Similarly, CFE+LOR (7.51 g) treated mice reduced significantly (p-value 0.0179 and 0.0108 respectively) in fat mass gain compared to both HFD (8.99g) and Lorcaserin (9.14g) groups. The increase in fat mass of the Lorcaserin group may be due to the low dose 5 mg compared to regular 9mg/kg bwt/day (He et al., 2021).

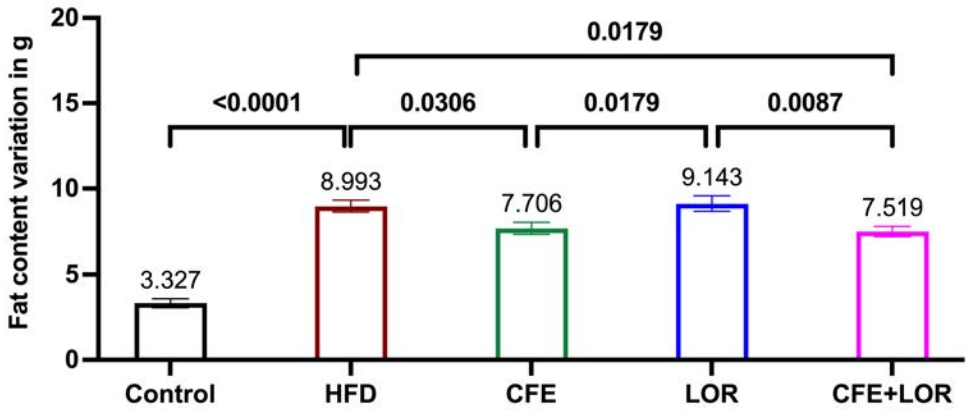

Figure 5.4: Fat content - change in fat during the treatment period (8weeks): Echo MRI based fat mass measurement difference between week 8 to week 16. Each group had n=8 mice and values plotted are Mean ± SEM. (where Control: control diet group, HF: high-fat diet group, CFE: high-fat diet with CFE, LOR: high-fat diet with Lorcaserin treatment, CFE+LOR: high-fat diet with CFE and lorcaserin treatments). Statistically significant differences between the groups (p-values <0.05) are shown.

The study from Rao et al (2021), describes the potential influence of CFE in fat content regulation and waist circumference reduction in humans during 16 weeks of CFE treatment (Rao et al., 2021). In the current study body composition data also showed a significant decrease in fat mass during CFE and CFE+LOR treatments. In line with it, percentage of fat mass showed in the Figure 5.5A also demonstrating significant decrease with CFE+LOR treatment compared to HFD and LOR groups. The fat percentage was significantly more during week 8 in all the groups than control diet-fed fed mice with p=0.001. Interestingly, after treatment assessment in week 16 results revealed fat content of animals treated with CFE and CFE+LOR were significantly reduced compared to the HFD group as shown in Figure 5.4. However, fat percentage from Figure 5.5A describing, the CFE treatment group was not significant. Whereas CFE+LOR treated mice showed a significant decrease when compared to both HFD (p=0.03) and the LOR treated (p=0.09) mice. In addition, there was a significant increase in lean mass percentage CFE+LOR treated group compared to HFD mice. The macronutrients like glucose and lipid oxidation were measure using indirect calorimetric analysis from Promethion cage monitoring to further support the CFE and LOR effect on fat deposition.

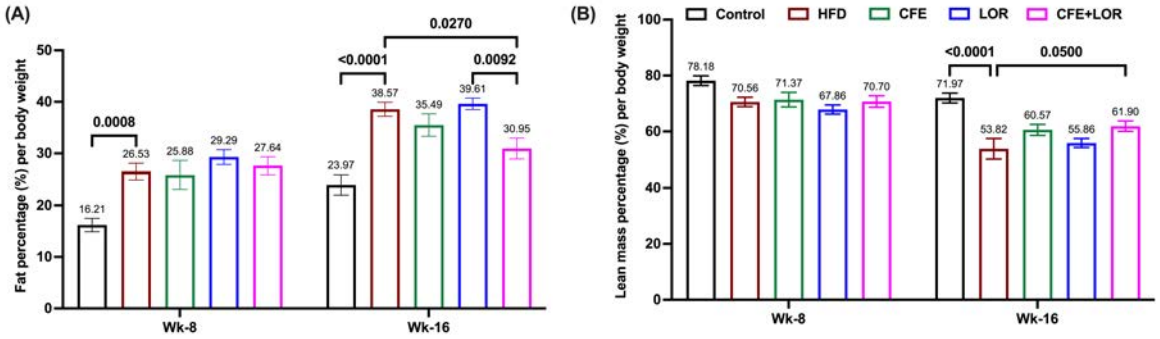

Figure 5.5: Fat and lean mass percentage with respect to bodyweight: (A) Fat mass percentage (B) Lean mass percentage during the 8th and 16th week of all the groups with respect to bodyweights by Echo MRI; Each group had n=8 mice and values plotted are Mean ± SEM. (where Control: control diet group, HF: high-fat diet group, CFE: high-fat diet with CFE, LOR: high-fat diet with Lorcaserin treatment, CFE+LOR: high-fat diet with CFE and lorcaserin treatments). Statistically significant differences between the groups (p-values <0.05) are shown.

As described earlier in this chapter, low resting metabolic rate is one of the factors of energy expenditure in obesity condition. To understand the HFD effect on resting metabolic rate as well as CFE and LOR treatment influence in restoring resting metabolic rate animals were assessed in promethion cages. The energy expenditure measured by indirect calorimetry was calculated based on the method described in a previous study (Kaiyala et al., 2019) description. The VO_2 (Volume of oxygen consumed) and VCO_2 (Volume of carbon dioxide produced) gas analyser data from Promethion cages was assessed for energy expenditure, glucose, and lipid oxidation parameters. The data in Figure 5.6A, representing no significant changes of EE during pre-treatment analysis irrespective of the diet. Surprisingly, HFD mice EE was relatively low (p=0.0008) during post-treatment assessment of the study compared to control fed animals. In the CFE-treated group during week 16, EE was maintained at a 1.4-fold greater than the HFD group (with p<0.0001 significance). Similarly, CFE+LOR treated group EE was significantly (p=0.0002) higher than HFD in week 16.

As described previously, macronutrients (lipid and carbohydrates) can be stored in their higher-order structures, unlike proteins; the degradation/ oxidation of these higher-order structures for energy production is essential for balancing energy equilibrium. The glucose oxidation (GOX) and lipid oxidation (LOX) data were plotted in the Figure 5.6B and 5.6C for all the study

groups. The GOX was significantly decreased from week 8 to 16 in HFD animals as shown in Figure 5.6B. Whereas, the lipid oxidation (LOX) was significantly decreased in week 16 compared to week 8 of HFD mice. Interestingly, the after-treatment LOX was describing in Figure 5.6C that, all the treatments significantly increased in lipid oxidation compared to HFD mice with p-values 0.017 (CFE), 0.0196 (LOR) and 0.0021(CFE+LOR). Therefore, from fat content data and lipid oxidation were concluding influence of CFE+LOR may retrieve the mice from HFD stress by improving LOX (macronutrient oxidation) and EE to reduce obesity symptoms.

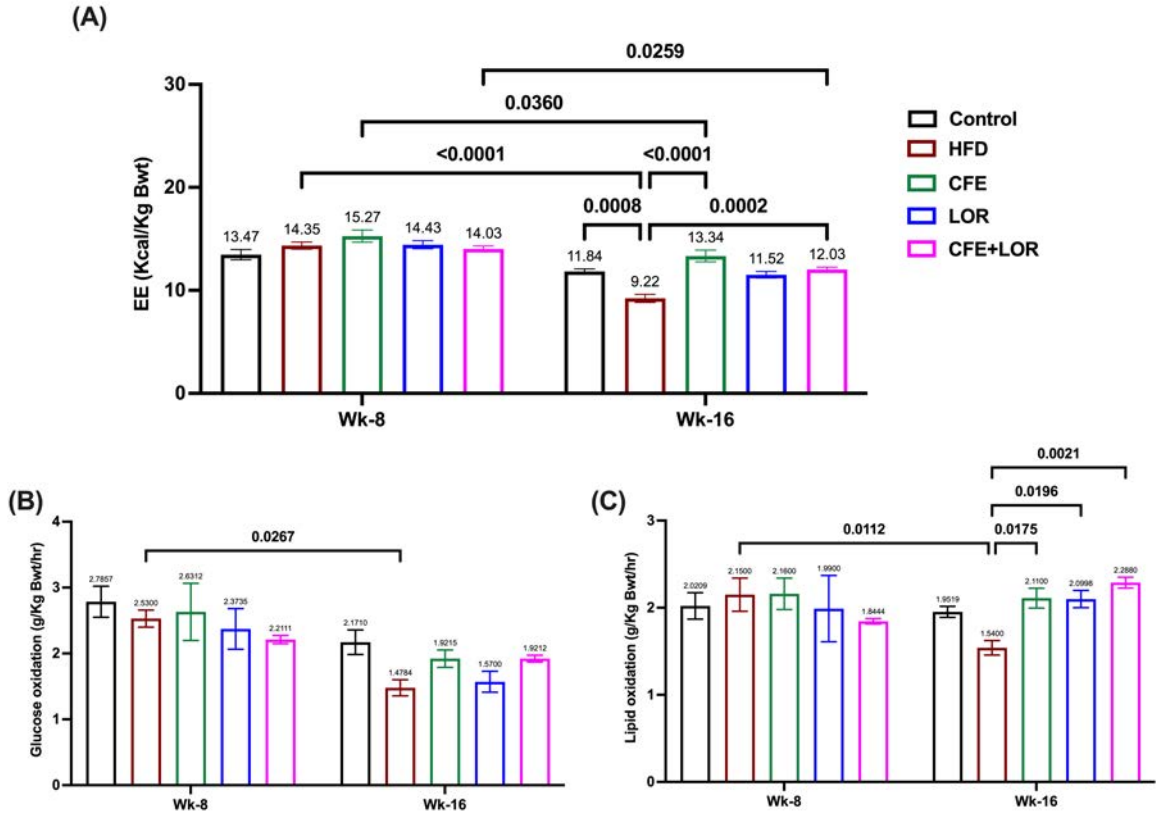

Figure 5.6: Energy expenditure, glucose, and lipid oxidation analysis: (A) Energy expenditure (B) Glucose oxidation and (C) Lipid oxidation during the 8th and 16th week of all the groups with respect to bodyweights. The glucose and lipid oxidation were calculated by estimating VO2 and VCO2 gas emission values from each cage using the Promethion system. Each group had n=8 mice and values plotted are Mean ± SEM. (where Control: control diet group, HF: high-fat diet group, CFE: high-fat diet with CFE, LOR: high-fat diet with Lorcaserin treatment, CFE+LOR: high-fat diet with CFE and lorcaserin treatments). Statistically significant differences between the groups (p-values <0.05) are shown.

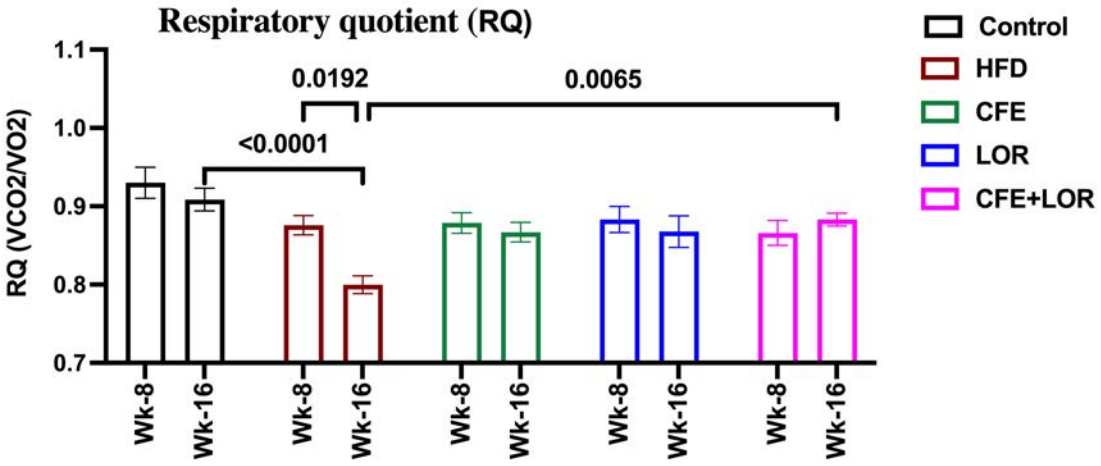

Figure 5.7: Respiratory quotient over 48hr (RQ): The VCO_2/VO_2 ratio was represented as RQ for all the groups during week 8 and week 16. Each group had n=8 mice and values plotted are Mean ± SEM. (where Control: control diet group, HF: high-fat diet group, CFE: high-fat diet with CFE, LOR: high-fat diet with Lorcaserin treatment, CFE+LOR: high-fat diet with CFE and lorcaserin treatments). Statistically significant differences between the groups (p-values <0.05) are shown.

Besides EE, LOX and GOX estimation, the current study was measured respiratory quotient (RQ) as plotted in the Figure 5.7. The respiratory quotient (RQ) is a ratio of VCO_2 to VO_2 that generally ranges between 0.7 and 1.0, depending on the proportions of carbohydrate, fat, and protein combusted. Perfusion occurs through the alveoli's capillary network when inspired oxygen is collected in the alveolar sac. The red blood cell transports the perfused oxygen to the surrounding tissues. When blood passes through the capillary bed, oxygen is liberated from the RBC and delivered to the tissue site. During this time, the tissue releases CO_2 into the red blood cell transports it to the lungs. The breakdown of carbs, fats, and proteins requires oxygen in the presence of macronutrients. Carbohydrates ($C_6H_{12}O_6 + 6O_2$) have a six-carbon chain and metabolise to two pyruvate substrates via glycolysis, generating CO_2 as a by-product when converted to acetyl CoA. When two-carbon acetyl CoA combines with 4-carbon citrate in the Krebs cycle, 3-CO_2 is produced in each metabolising cascade. If the starting molecule is a fatty acid with 12, 18, 20, or 22 carbon molecules, it undergoes beta-oxidation to produce acetyl Co-A, not carbon dioxide. As a result, when fat is used as a fuel instead of carbs, less CO_2 is produced per unit of oxygen consumed. The results showed a significant decrease in RQ value in HFD during week-16 than week-8 run. However, Luger et al. 2021, mentioned that RQ was controversial phenomenon during weight gain or reduction. Modifications in macronutrient

intake per unit mass (fats versus carbohydrates) during the day have been accompanied by changes in oxidation rates, implying a link between RQ and plasma substrate concentrations (e.g., glucose and fatty acids) (Goldenshluger et al., 2021).

Furthermore, increased postprandial RQ was associated with a higher glycemic index of meals (Galgani et al., 2008). There was limited evidence that variations in RQ are linked to diet type rather than individual macronutrients (Goldenshluger et al., 2021). Tea has been observed to alter RQ in varied ways throughout the day, lowering RQ found after resting and fasting but not right after drinking tea (Zhang et al., 2020). A greater RQ in a fasted state has been linked to increased weight gain and fat accumulation (Weinsier et al., 1995). However, sticking to our current results, reduced LOX values and reduced RQ of HFD mice indicate less CO_2 release, increased fat deposition and prone to obesity risk. This scenario was regulated, and RQ values of treated groups unchanged from week 8 to 16 means CFE and Lorcaserin promote lipid oxidation against positive energy balance in HFD induced mice.

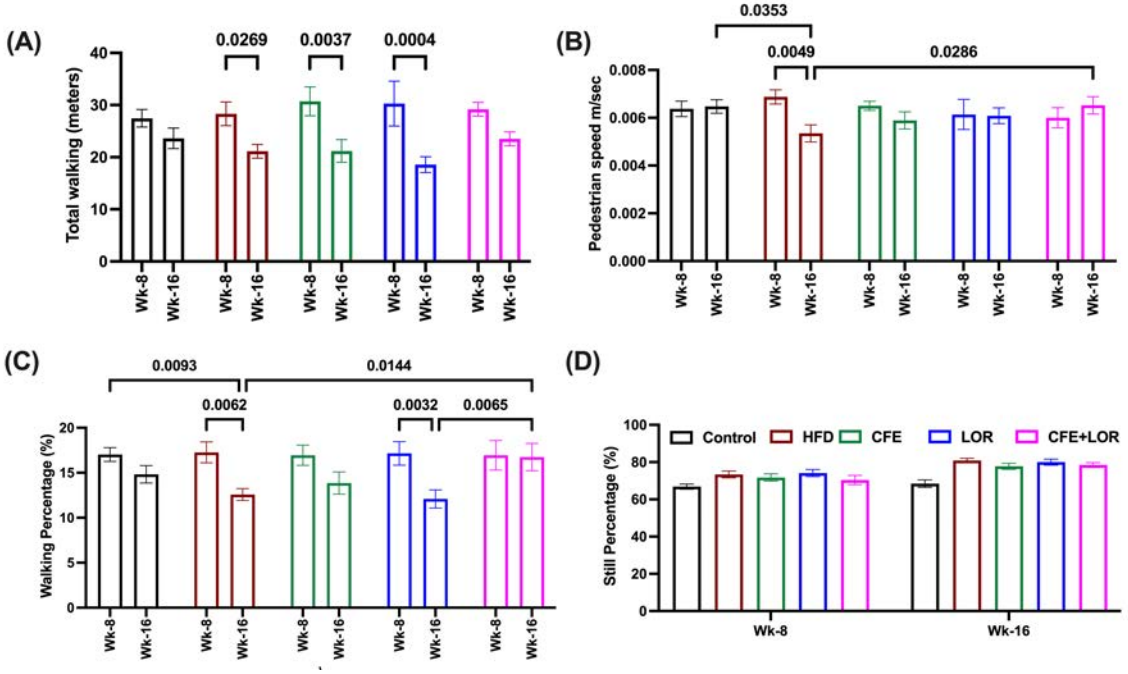

Figure 5.8: Promethion analysis - Dark cycle: (A) Total walking distance (B) Average speed of walking, (C) total percentage of walking, and (D) Still percentage (immobility) during 8th and 16th week of all the groups. Each group had n=8 mice and values plotted are Mean ± SEM. (where Control: control diet group, HF: high-fat diet group, CFE: high-fat diet with CFE, LOR: high-fat diet with Lorcaserin treatment, CFE+LOR: high-fat diet with CFE and lorcaserin treatments). Statistically significant differences between the groups (p-values <0.05) are shown.

Thus, the intake of macronutrients will be affecting the energy expenditure, GOX, LOX and RQ during metabolic cage analysis in the dark cycle. Further investigated the regular activities like walking, sleeping, food and water intake were changing with treatments in dark cycle. The total walking distance was significantly reduced from pre-treatment to post-treatment study in HFD, CFE and LOR groups as shown in the Figure 5.8A. Surprisingly, as shown in Figure 5.8C, walking percentage and average speed of walking increased with the CFE+LOR treatment in week-16 compared to week-8. In addition, walking percentage was significantly increased in CFE+LOR compared to both HFD and LOR groups in week 16 with p-values 0.014 and 0.0065, respectively.

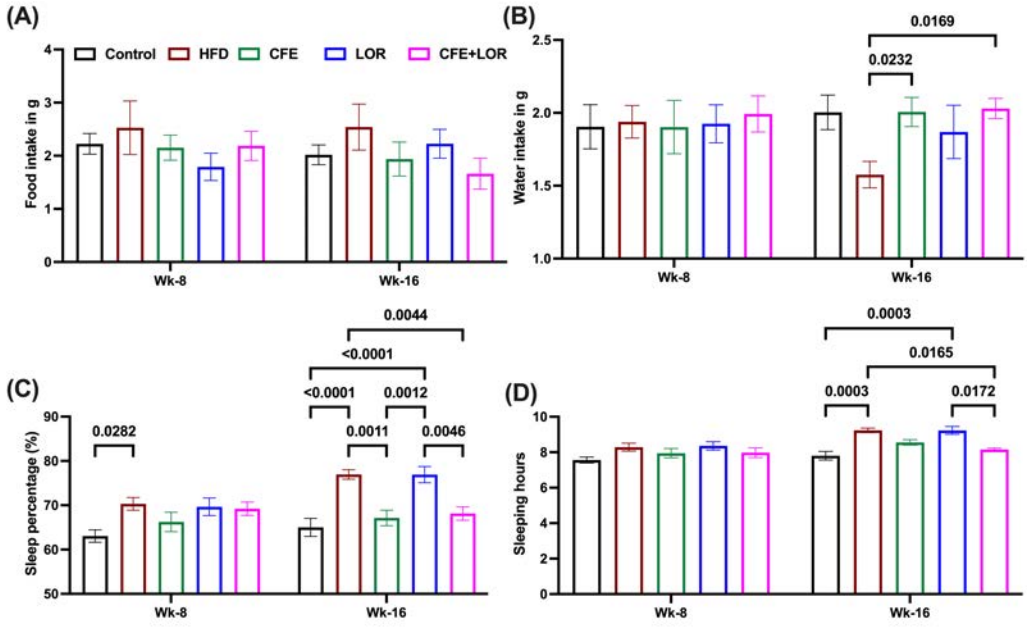

Figure 5.9: Promethion analysis- Dark cycle: (A) Food intake, (B) Water intake, (C) Sleep percentage, and (D) Sleep hours during the 8th and 16th week of all the groups. Each group had n=8 mice and values plotted are Mean ± SEM. (where Control: control diet group, HF: high-fat diet group, CFE: high-fat diet with CFE, LOR: high-fat diet with Lorcaserin treatment, CFE+LOR: high-fat diet with CFE and lorcaserin treatments). Statistically significant differences between the groups (p-values <0.05) are shown.

The dark cycle sleep percentage and sleep hours were significantly reduced with CFE and CFE+LOR compared to HFD and Lorcaserin groups from the Figure 5.9C and 5.9D. This implies CFE and CFE+LOR treatment animals were active during the dark cycle compared to other HFD groups. Interestingly, the sleep percentage of CFE and CFE+LOR groups is approximately equal to control diet-fed mice. The water intake of CFE and CFE+LOR groups

during the dark cycle was significantly higher than HFD with p-values 0.023 and 0.0169, respectively as showed in Figure 5.9B. The Food intake from Figure 5.9A was showing variation between groups; however, it is not significant. We are suspecting the food intake measurement was not giving much information because all the HFD fed mice were just making the food crumbled powdered in 24hr of Promethion acclimatisation as showed in Figure 5.10. Multiple studies were assessed to understand the interaction between sleep and overweight in obesity. However, majority of these studies were conducted in knockout animals like narcoleptic mice, leptin deficient (ob/ob) mice, and polygenic rats like OP/OR models (Panagiotou et al., 2018). Only limited number of studies available on diet induced rats or mice; probably diet induced models are more closure to human obesity. There were different characteristic changes found in sleep of humans with obesity or excess body weight. In rodents circadian sleep distribution is polyphasic, whereas in humans, it is monophasic. Apart from this variation overall homeostatic, circadian, and neurochemical signalling of sleep are similar in all species (Panagiotou et al., 2018).

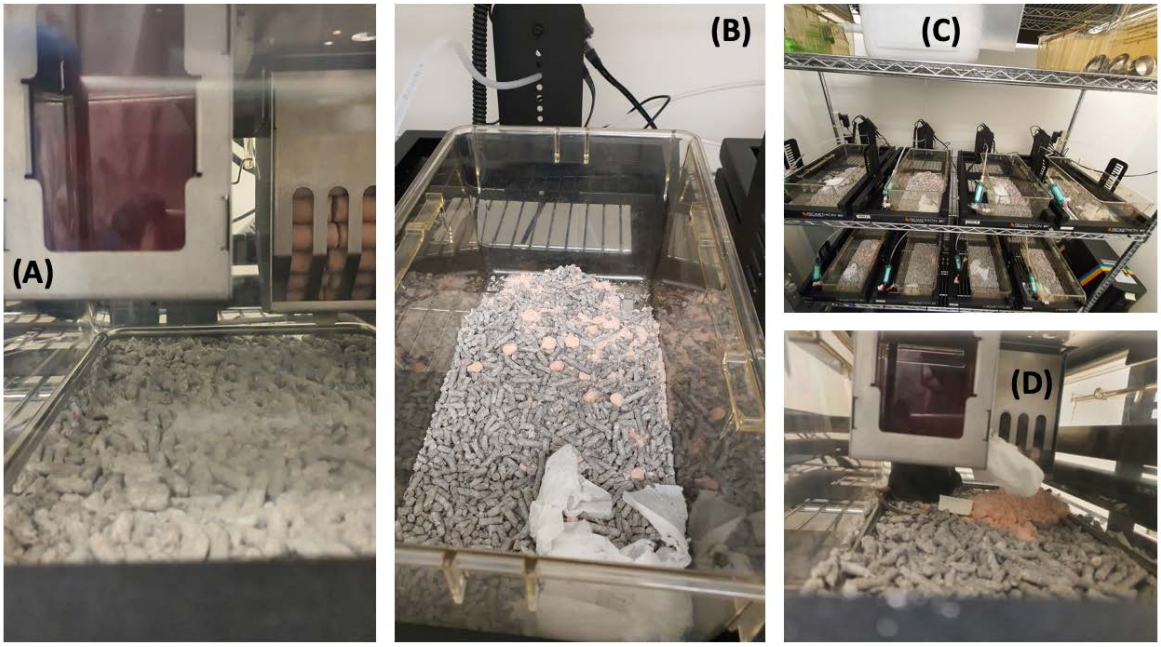

Figure 5.10: During Promethion run HFD fed mice making food pellets into smaller particles and the Promethion system couldn't measure exact food intake. The figure shows (A) Organised food before the run, (B) end of the run most of the food is in powder form and unable to differentiate from bedding, (C) Except control diet animals all HFD groups are doing same in all three runs (week 4, 8 and 16), and (D) After 24h of Promethion run one that just pulled all the food out of the hopper.

Overall sleep cycle from Promethion cage monitoring reveals that, HFD mice were significantly sleepier in active/dark cycle compared to treated groups. The sleep percentage during dark cycle of CFE alone and CFE+LOR groups were relatively low compared to HFD in week 16 with p-values 0.001 and 0.004. In similar CFE and CFE+LOR treated animals showed reduced sleep percentage in week 16 than LOR treated mice.

The Promethion cage XYZ-beam break analysis correlating with waking percentage and average speed of walking during the dark cycle. The z-beam break assessment describing climbing efforts of mice, where CFE treated, mice were significantly increased compared to both HFD and LOR (from Figure 5.11C). The regular activity in dark cycle may influence the positive metabolic homeostasis in treated mice and benefiting the animals to increase energy expenditure.

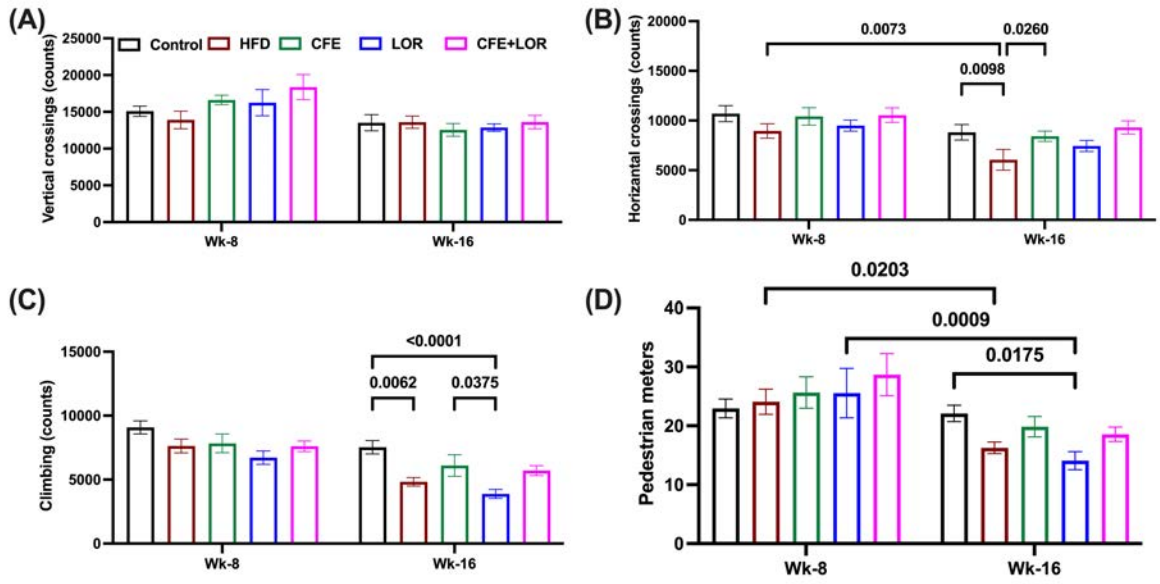

Figure 5.11: Promethion analysis- Dark cycle: (A) Y-axis Lane crossing counts (B) X-axis Lane crossing counts, (C) Z-axis Lane crossing counts (climbing), and (D) XY- plane walking distance, during 8th and 16th week of all the groups. Each group had n=8 mice and values plotted are Mean ± SEM. (where Control: control diet group, HF: high-fat diet group, CFE: high-fat diet with CFE, LOR: high-fat diet with Lorcaserin treatment, CFE+LOR: high-fat diet with CFE and lorcaserin treatments). Statistically significant differences between the groups (p-values <0.05) are shown.

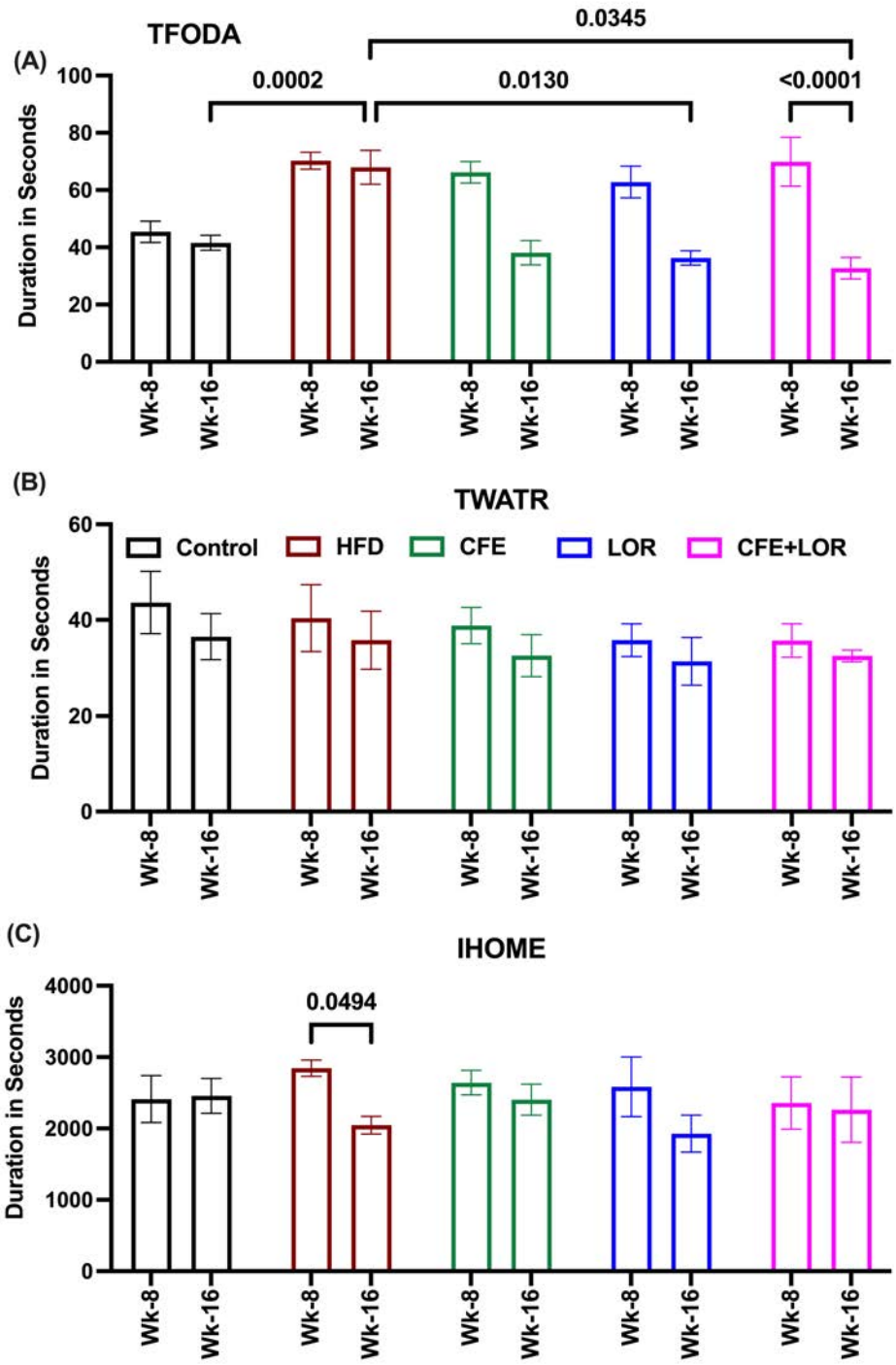

Figure 5.12: Promethion analysis- Interaction with hoppers: (A) Interaction with food hopper (TFODA), (B) Interaction with water hopper (TWATR), (C) Time spent in housing hopper (IHOME), during 8th and 16th week of all the groups. Each group had n=8 mice and values plotted are Mean ± SEM. (where Control: control diet group, HF: high-fat diet group, CFE: high-fat diet with CFE, LOR: high-fat diet with Lorcaserin treatment, CFE+LOR: high-fat diet with CFE and lorcaserin treatments). Statistically significant differences between the groups (p-values <0.05) are shown.

The food, water, and housing hoppers interaction data in the Figure 5.12 reveal that HFD mice spent more time interacting with the food hopper than the animals that received the treatments. There is no significant difference in interaction with the water hopper during the dark cycle.

Isometric tension analysis:

Through excess weight and adiposity, obesity is linked to metabolic and cardiovascular problems. Diet-induced obesity has been an excellent experimental model for studying the pathophysiology of obesity-related comorbidities like metabolic syndrome and cardiovascular abnormalities (Powell-Wiley et al., 2021). For eight weeks, mice fed the HFD exhibited a significant rise in body and epididymal fat weight and increased total cholesterol, triglycerides, and glucose, confirming the model's appropriateness. Individuals with central adiposity are more likely to develop neurogenic hypertension (Pavlovska et al., 2021, Nieto-Martínez et al., 2021, Löffler et al., 2021). Recent human research suggests that beta-adrenergic receptors play a crucial role in preventing sympathetically mediated vasoconstriction and consequently sympathetic blood pressure support. Blood vessels adjust their structure in response to mechanical and hemodynamic stimuli associated with several disorders, including hypertension, diabetes, and obesity, resulting in changes in vessel lumen calibre (Martínez-Martínez et al., 2021).

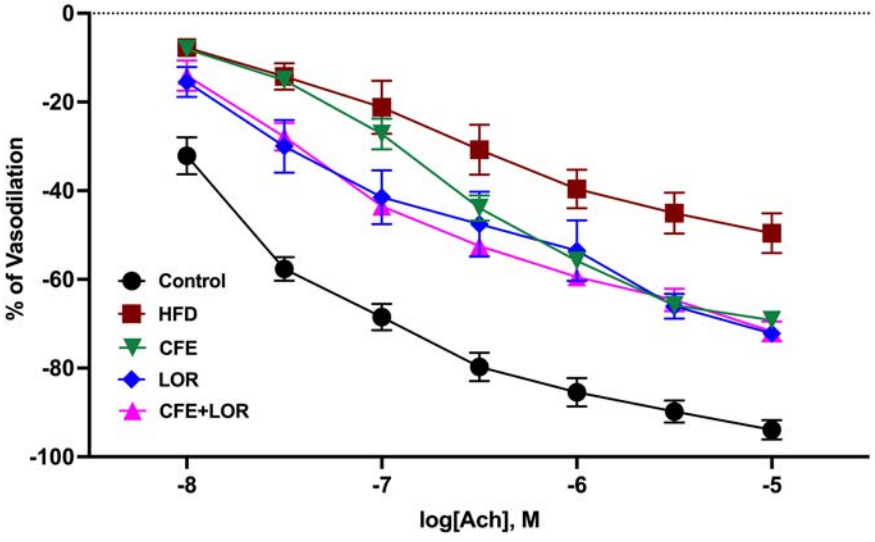

Figure 5.13: Isometric tension analysis of abdominal aortic rings: The abdominal aortic rigs were used to measure the vasodilation pattern of HF-diet induced mice with CFE and Lorcaserin treatments. Each group had n=6 (only HF group had n=5) mice and values plotted are Mean ± SEM. (where Control: control diet group, HF: high-fat diet group, CFE: high-fat

diet with CFE, LOR: high-fat diet with Lorcaserin treatment, CFE+LOR: high-fat diet with CFE and lorcaserin treatments). Statistically significant differences between the groups (p-values <0.05) are shown.

Vascular remodelling occurs due to normalising wall stress and restoring wall tension to maintain the proper lumen size for normal blood flow. Obesity is linked to vascular remodelling, characterised by media thickening and arterial stiffness in large arteries like the aorta and smaller ones like the mesenteric, renal, and coronary arteries (Gil-Ortega et al., 2016). This remodelling was also seen in overweight or obese hypertension patients' subcutaneous small arteries, accompanied by an increase in fibrosis or a decrease in flexibility. Vascular homeostasis necessitates a finely tuned equilibrium between a vasodilator state, often linked to antioxidant, anti-inflammatory, and antithrombotic qualities, and a vasoconstrictor state, which is linked to prooxidant, pro-inflammatory, and prothrombotic properties (Zeeni et al., 2015, Wang and Liao, 2012, Sampey et al., 2011). The endothelium maintains vascular homeostasis by counteracting the effects of vasodilators such as nitric oxide (NO), prostacyclin, and hyperpolarising factor, which are produced by the endothelium vasoconstrictors like endothelin-1, angiotensin II (Ang II), and thromboxane A2 (Zulli et al., 2009, Nonogaki, 1999, Nonogaki et al., 1998, Tecott et al., 1995). Obesity is a risk factor for heart disease and metabolic disorders. Endothelial dysfunction, a condition in which endothelial cells convert to a pro-atherosclerotic phenotype, is one of the early vascular changes seen in obesity. The risk of obesity in cardiovascular dysfunction and limited results on mice model with HFD induced cardiac dysfunction analysis motivated us to understand how the desired treatments influence cardiac vessels. The isometric tension analysis of abdominal aortic rings with response to Ach showed significant variations among the study groups.

The output of percentage vasodilation plotted in the Figure 5.13 and Figure 5.14A demonstrates HFD group vascular dilation was significantly reduced compared to the control diet-fed mice group during different doses of Ach. As a result, the aortic rings were not reaching baseline after constricting with U46619 in the HFD group. Whereas CFE (Figure 5.14B), Lorcaserin (Figure 5.14C), and CFE+LOR (Figure 5.14D) treated mice were significantly improved vasodilation and deviated significantly from HFD mice during Ach based dilation. The current data considered as pilot scale plot, the vascular dysfunction and HFD induced cardiovascular risk factors need to be assessed in future with larger group numbers at various time points of the study.

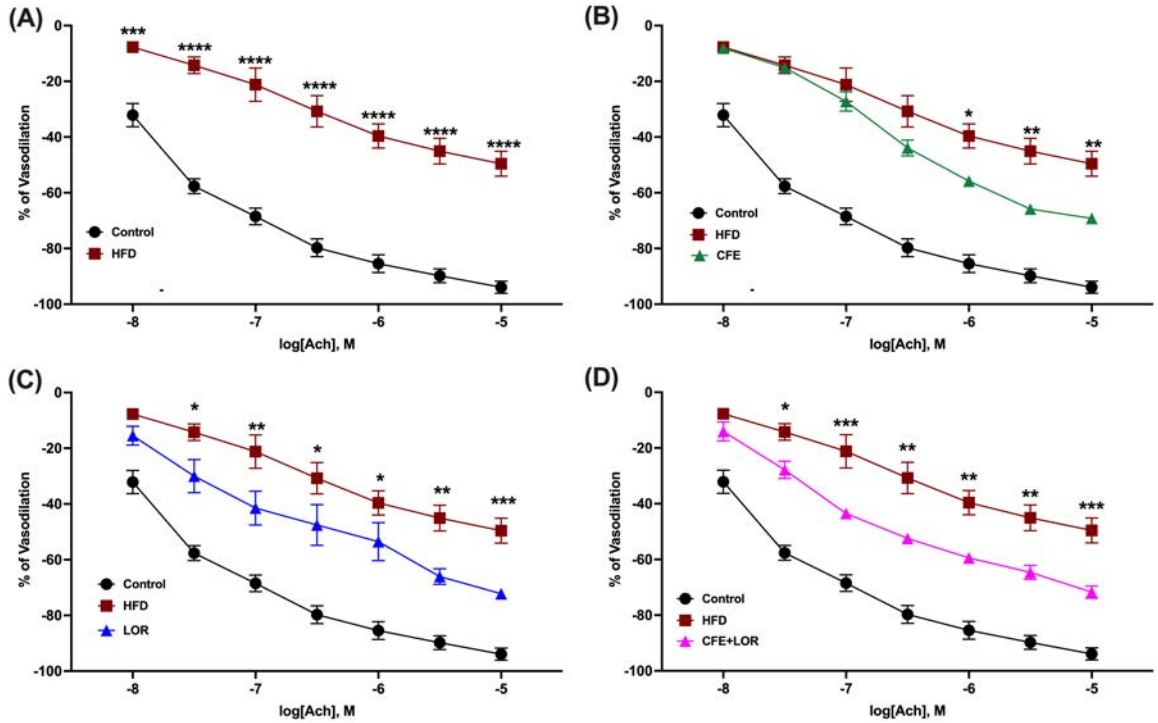

Figure 5.14: Isometric tension analysis of abdominal aortic rings: Statistical difference comparison of the percentage of vasodilation between (A) Control vs HFD, (B) HFD vs CFE treated, (C) HFD vs LOR treated, and (D) HFD vs CFE+LOR groups. Each group had n=6 (only HF group had n=5) mice and values plotted are Mean ± SEM. (where Control: control diet group, HF: high-fat diet group, CFE: high-fat diet with CFE, LOR: high-fat diet with Lorcaserin treatment, CFE+LOR: high-fat diet with CFE and lorcaserin treatments). Statistically significant differences between the groups (p-values <0.05) are shown. The significant changes were represented with p<0.0001 (****), p<0.001(***), p<0.01 (**), and p<0.05 (*).

Therefore, isometric tension analysis of aortic rings was demonstrating, there is a considerable influence of CFE and LOR treatment on HFD induction. The treatments were rescuing mice from HFD stress and might be leading to reduced cardiovascular risk factors.

Outcomes of the study:

- The study shows that HFD induced mice can be rescued from fat deposition and reduced energy expenditure by the CFE + LOR combination treatment.
- Promethion metabolic cage analysis showed that macronutrient oxidation and increased physical activity (walking and climbing) contributes to the overall increase in energy expenditure of the HFD-fed mice treated with CFE + LOR.
- The HFD-fed obese mice model can be recovered from vascular endothelial dysfunction parameters by CFE and CFE+LOR treatments may help in reducing the risk of hypertension and cardiovascular risk factors with obesity.

5.5 Conclusion:

CFE and LOR treatments in HFD induced obese mice for 8-weeks reduced fat deposition and improved energy expenditure. However, CFE+LOR treatments showed significant variation compared to the HFD group in fat percentage and metabolic parameters as shown by Promethion cage analysis. The outcomes of the *ex-vivo* studies of abdominal aortic rings by isometric tension analysis revealed CFE, Lorcaserin and CFE+LOR treatments significantly improved vasodilation dysfunction induced by the HFD. The role of CFE+LOR in obesity and cardiovascular diseases. In summary, the combination of CFE+LOR showed a stronger effect on HFD mice in most of the parameters compared to the effect of CFE and LOR alone. The combination treatment could be a better alternative in terms reducing of obesity risk factors and improvement of energy homeostasis.

Chapter 6 Overall Summary

Obesity and related comorbidities are increasing in prevalence due to changes in dietary habits and low energy expenditure in sedentary lifestyles. As mentioned in Chapter I, the current treatments available for weight management have limitations in terms of their efficacy and long-term usage. The hydroethanolic extract of *Caralluma fimbriata* has been shown to reduce body weight and food intake in different studies. However, the exact mechanism of action of CFE is unclear and preliminary studies had suggested that central signalling of satiety via the serotonin 5HT2c receptor was involved. Similarly, Lorcaserin is a specific 5HT2cR agonist that induces body weight reduction, and it was approved as a treatment for obesity. However, recent studies have reported on potential side effects such as increased incidence of cancer, and it has been withdrawn from use in some countries (Mathai, 2021). Thus, there is an ongoing need to develop new compounds and strategies to treat obesity. The current study investigates an alternative treatment where a lower concentration of Lorcaserin is used in combination with CFE to reduce obesity. As discussed in Chapter I, the 5HT2cR may alter mood and behaviour in addition to mediating anorexigenic pathways that increase satiety signalling. The role of CFE in 5HT2cR expression in modified 3T3L1 cells (unpublished results from Stefan Stamm's lab) prompted replication of this effect in SHSY5Y neuroblast cells. The 5HT2cR expression studies are complex due to expression in two major isoforms from alternate mRNA splicing. The two major isoforms of the 5HT2cR proteins differ in their cellular location within neurons. Functionally active receptor (5HT2cR-fn) is located as a transmembrane surface protein expressed from six exon mRNA sections. In comparison, the non-functional or truncated form (5HT2cR-tr) of the receptor remains on the endoplasmic reticulum surface due to a lack of the exon Vb region in its expressed mRNA. The ratio of 5HT2cR-fn to the truncated form was identified as a key factor in weight gain in overeating diseases like PWS (Stamm et al., 2017).

In the initial experiments described in chapter III, the SHSY5Y-derived neurons showed a significant increase in functional 5HT2cR compared to truncated receptor mRNA expression after CFE treatment. This study was also designed to investigate the expression of other genes involved in anorexigenic pathways by transcriptome analysis. The overall study revealed that CFE concentrations of 25 and 50 μg/mL treatment for 48 and 96h of duration significantly increased functional receptor mRNA expression more than two-fold. The whole transcriptome analysis further revealed that the expression of genes associated with anorexigenic pathways and satiety signalling was upregulated. The increase in PCSK1 and BDNF gives some insight of how CFE may influence anorexigenic pathways. Figure 3.25 from chapter III briefing

proteins involved in satiety regulation by anorexigenic pathway and their relationship with 5HT2cR. Transcriptome analysis confirmed the results from the qPCR study that CFE treatment increases 5HT2cR expression in SHSY5Y neurons. However, the transcriptome analysis needs to be extended in the future with more replicates, to further clarify CFE's role in satiety regulating pathways.

Chapter IV investigated the in vivo effect of combined CFE and Lorcaserin treatments in HFD mice. The animal groups were fed with 23.5% HFD, as mentioned in Chapter II, for eight weeks to induce obesity. The HFD successfully increased body fat composition and weight gain compared to control diet-fed mice. The animals treated with CFE and CFE+LOR showed significant improvement in depression-like behaviour compared to the HFD group (during tail suspension and forced swim tests). In addition, the increased time spent in open arms of the EPM and light chamber of the LDB analysis reveals reduced anxiety-like behaviour in CFE+LOR treated mice compared to HFD group. The mice showed a reduction in anxiety-like behaviour by spending less time in open arms of EPM and exploring for more time in the bright chamber of LDB (Lama et al., 2022b). Body weight gain was significantly decreased by the CFE+LOR combination treatment compared to the control HFD treatment. These results are consistent with the effects of CFE to increase functional 5HT2cR mRNA expression and the increased activation of these receptors by Lorcaserin. Importantly, the observations of reduced obesity and fat mass were accompanied by an improvement in mood-based parameters. For instance, CB-1 receptor antagonist, rimonabant is increasing depression like mood disorders and anxiety (Juhasz et al., 2009). The data supports the potential use of a CFE+LOR combined treatment to improve body weight management and reduce obesity. In future studies, the measurement of 5HT2cR mRNA or protein in the hypothalamus (by in situ hybridisation or immunohistochemistry) may confirm the action of CFE on neuronal pathways involved in food intake and energy metabolism.

In chapter V, the body composition and energy expenditure data were showed that CFE+LOR had a positive effect inn HFD mice. The fat percentage was significantly reduced in CFE+LOR treated group of mice compared to LOR treatment alone as well as high fat fed mice. In addition to animal behaviour and energy expenditures, the current treatments also showed beneficial towards cardiovascular function. The isometric tension analysis of abdominal aortic rings of CFE and LOR treatments showed and improved vasodilatory responses in comparison to the HFD mice. Although blood pressure was not measured in this study, this result indicates an

unexpected cardiovascular benefit of the CFE and LOR treatments. Since hypertension and other cardiovascular co-morbidities are often associated with obesity, this treatment may have an added therapeutic effect of improving vascular health.

In summary, CFE can be considered as a potential treatment to assist with healthy weight management. Lorcaserin showed long-term side effects like cancer showed in studies like CAMELLIA-TIMI 61, making a question on lorcaserin usage in future obesity treatment with current dosage (Mathai, 2021). However, other studies have also addressed improved lorcaserin effect with the combination of other drugs. The Lorcaserin (7.5mg/kg bwt) in combination with GLP-1 agonist liraglutide (0.1mg/kg bwt) was proposed as alternate weight loss treatment. The results from LOR+ liraglutide in combination reduced short-term feeding in GLP1-R^{NTS} knockdown and MC4R null mice (Wagner et al., 2022). Similarly, another GLP-1R agonist exendin-4 was used in combination with LOR (10mg/kg bwt); resulting short-term feeding reduction in MC4R null mice (Wagner et al., 2022). The current combination of CFE and 5mg/kg bwt of lorcaserin could be one of the alternative treatments in obesity and other overeating disorders. The role of CFE in appetite generation PWS like diseases was mentioned in recent studies. In this study, CFE+LOR treatment in high fat fed mice showed a significant reduction of fat composition and body weight reduction. In addition, to physiological parameters, the current treatments showed positive effects on depression and anxiety-like behavioral parameters. Further, beneficial effects on vasodilation may suggests that reduced cardiovascular risk factors with obesity. However, the mechanism through which CFE increases functional 5HT2cR expression is still unclear, needing more genetic analysis to understand the active pathways behind in this effect. The systemic effects of CFE shown in this study can be extended further by studying hypothalamic pathways involved with POMC neurons to regulate satiety signalling.

Future directions and limitations of the current study:

Overall, this thesis has measured that CFE treatment reduces body weight and fat composition in obese mice. While the evidence suggests that the effects are mediated through the increase in 5HT2c receptor expression, the exact mechanism of action of CFE stays unclear. The limitations of each chapter are noted below and considered for future extension of the study. From chapter III, the SHSY5Y neurons are showing increased functional mRNA expression from CFE treatment. However, it would be important to confirm the functionality of these receptors by further investigation. This could be done by a confocal imaging study, where the control and CFE-treated cells are measured for 5HT2cR activity by increased intracellular calcium release in response to treatment of the cells with LOR. The 5HT2cR antagonist SB242084 could be used to show the specificity of the activation of this receptor by LOR. In addition, more replicates (minimum of n=6) of CFE-treated SHSY5Y neurons will be assessed for transcriptome analysis in future to further define the patterns of gene expression underpinning the amplifying effect of CFE on functional 5HT2cR expression.

From the animal studies mentioned in Chapter IV and V, physiological and behavioural parameters showed the effects of CFE and LOR treatments against HFD-induced changes. The genetic analysis of functional vs truncated receptors of 5HT2cR, BDNF, MC4R and PCSK1 like anorexigenic molecules could be an added advantage in CFE role explanation. Future studies with brown fat quantification and thermogenesis estimation can give us CFE and LOR treatment influence on batokines (Myostatin and FGF21, etc.) secretion and metabolic diseases. Apart from behavioral and physiological effects, the study revealed cardiovascular benefits with CFE+LOR treatments. Nitric oxide (NO) is a key mediator of vasodilation in peripheral vessels. The Nitricoxide synthase (eNOS) is a crucial enzyme in NO mediated vasodilation (Mees et al., 2007) the increased activity of eNOS can be measured with immunohistochemical analysis of a range of markers including TypeIII eNOS, serine 1177 (phosphorylation of eNOS), and nitrotyrosine. NADPH oxidase-2 (NOX2), NOX3 and NOX4 enzymes are involved in superoxide mediated inactivation of nitric oxide; by measuring these markers it is possible to determine the mechanisms underpinning the improvement of vascular function that was induced by CFE+LOR treatments.

The confocal imaging study and immunohistochemistry experiments were initially part of the thesis. However, due to COVID19 lockdowns delayed the overall study and further affected funds and scholarship deadlines that prevented the execution of planned experiments. The

animals culled at the end of the study from all the groups collected gut columns to understand rhythmic contraction of the gut (Swaminathan et al., 2016) and enteric nervous system (ENS) functioning with HFD and CFE+LOR treatments. However, the experiments were performed, and motility videos were recorded for future analysis. In addition, the significant increase in energy expenditure that was observed during CFE+LOR treatment can be further investigated by quantifying further markers from liver steatosis (AMPK and SREBP1c), skeletal muscles - lipid quantification (Delgadillo-Puga et al., 2020), and brown adipose tissues (UCP-1) (Andrade et al., 2014). The gut motility study with faecal energy quantification and microbiome analysis together may determine the overall treatment effect, on gut health and enteric nervous system functioning.

Chapter 7 References

AASBRENN, M., SCHNURR, T. M., HAVE, C. T., SVENDSTRUP, M., HANSEN, D. L., WORM, D., BALSLEV-HARDER, M., HOLLENSTED, M., GRARUP, N. & BURGDORF, K. S. 2019. Genetic determinants of weight loss after bariatric surgery. *Obesity surgery,* 29**,** 2554-2561.

ADAMS, G. 2020. A beginner's guide to RT-PCR, qPCR and RT-qPCR. *The Biochemist,* 42**,** 48-53.

ADAMS, W. K., BARKUS, C., FERLAND, J.-M. N., SHARP, T. & WINSTANLEY, C. A. 2017. Pharmacological evidence that 5-HT 2C receptor blockade selectively improves decision making when rewards are paired with audiovisual cues in a rat gambling task. *Psychopharmacology,* 234**,** 3091-3104.

ADILIJIANG, A., HIRANO, M., OKUNO, Y., AOKI, K., OHKA, F., MAEDA, S., TANAHASHI, K., MOTOMURA, K., SHIMIZU, H. & YAMAGUCHI, J. 2019. Next generation sequencing-based transcriptome predicts bevacizumab efficacy in combination with temozolomide in glioblastoma. *Molecules,* 24**,** 3046.

ADINGUPU, D. D., GÖPEL, S. O., GRÖNROS, J., BEHRENDT, M., SOTAK, M., MILIOTIS, T., DAHLQVIST, U., GAN, L.-M. & JÖNSSON-RYLANDER, A.-C. 2019. SGLT2 inhibition with empagliflozin improves coronary microvascular function and cardiac contractility in prediabetic ob/ob−/− mice. *Cardiovascular Diabetology,* 18**,** 1-15.

AGGARWAL, S. R., CLAVEL, M.-A., MESSIKA-ZEITOUN, D., CUEFF, C., MALOUF, J., ARAOZ, P. A., MANKAD, R., MICHELENA, H., VAHANIAN, A. & ENRIQUEZ-SARANO, M. 2013. Sex differences in aortic valve calcification measured by multidetector computed tomography in aortic stenosis. *Circulation: Cardiovascular Imaging,* 6**,** 40-47.

AGHILI, S. M. M., EBRAHIMPUR, M., ARJMAND, B., SHADMAN, Z., PEJMAN SANI, M., QORBANI, M., LARIJANI, B. & PAYAB, M. 2021. Obesity in COVID-19 era, implications for mechanisms, comorbidities, and prognosis: a review and meta-analysis. *International Journal of Obesity,* 45**,** 998-1016.

ALSIÖ, J., ROMAN, E., OLSZEWSKI, P. K., JONSSON, P., FREDRIKSSON, R., LEVINE, A. S., MEYERSON, B. J., HULTING, A. L., LINDBLOM, J. & SCHIÖTH, H. B. 2009. Inverse association of high‐fat diet preference and anxiety‐like behavior: a putative role for urocortin 2. *Genes, Brain and Behavior,* 8**,** 193-202.

ANDRADE, J. M. O., FRADE, A. C. M., GUIMARAES, J. B., FREITAS, K. M., LOPES, M. T. P., GUIMARÃES, A. L. S., DE PAULA, A. M. B., COIMBRA, C. C. & SANTOS, S. H. S. 2014. Resveratrol increases brown adipose tissue thermogenesis markers by increasing SIRT1 and energy expenditure and decreasing fat accumulation in adipose tissue of mice fed a standard diet. *European journal of nutrition,* 53**,** 1503-1510.

ANDRÉ, A. & GONTHIER, M.-P. 2010. The endocannabinoid system: its roles in energy balance and potential as a target for obesity treatment. *The international journal of biochemistry & cell biology,* 42**,** 1788-1801.

APFELBAUM, M., BOSTSARRON, J. & LACATIS, D. 1971. Effect of caloric restriction and excessive caloric intake on energy expenditure. *American Journal of Clinical Nutrition,* 24**,** 1405-1409.

ARONNE, L. J. 2019. *Obesity Management: A Clinical Casebook*, Springer.

ASTELL, K. J., MATHAI, M. L., MCAINCH, A. J., STATHIS, C. G. & SU, X. Q. 2013. A pilot study investigating the effect of Caralluma fimbriata extract on the risk factors of metabolic syndrome in overweight and obese subjects: a randomised controlled clinical trial. *Complementary Therapies in Medicine,* 21**,** 180-189.

ASTRUP, A., MADSBAD, S., BREUM, L., JENSEN, T. J., KROUSTRUP, J. P. & LARSEN, T. M. 2008. Effect of tesofensine on bodyweight loss, body composition, and quality of life in obese patients: a randomised, double-blind, placebo-controlled trial. *The Lancet,* 372**,** 1906-1913.

BÄCKBERG, M., MADJID, N., ÖGREN, S. & MEISTER, B. 2004. Down-regulated expression of agouti-related protein (AGRP) mRNA in the hypothalamic arcuate nucleus of hyperphagic and obese tub/tub mice. *Molecular brain research,* 125**,** 129-139.

BAGGIO, L. L. & DRUCKER, D. J. 2007. Biology of incretins: GLP-1 and GIP. *Gastroenterology,* 132**,** 2131-2157.

BAPTISTA-DE-SOUZA, D., TAVARES, L. R. R., CANTO-DE-SOUZA, L., NUNES-DE-SOUZA, R. L. & CANTO-DE-SOUZA, A. 2022. Behavioral, hormonal, and neural alterations induced by social contagion for pain in mice. *Neuropharmacology,* 203**,** 108878.

BARBAU-PIEDNOIR, E., LIEVENS, A., MBONGOLO-MBELLA, G., ROOSENS, N., SNEYERS, M., LEUNDA-CASI, A. & VAN DEN BULCKE, M. 2010. SYBR® Green qPCR screening methods for the presence of “35S promoter” and “NOS terminator” elements in food and feed products. *European Food Research and Technology,* 230**,** 383.

BARISH, G. D., NARKAR, V. A. & EVANS, R. M. 2006. PPARδ: a dagger in the heart of the metabolic syndrome. *The Journal of clinical investigation,* 116**,** 590-597.

BAVER, S. B., HOPE, K., GUYOT, S., BJØRBAEK, C., KACZOROWSKI, C. & O'CONNELL, K. M. 2014. Leptin modulates the intrinsic excitability of AgRP/NPY neurons in the arcuate nucleus of the hypothalamus. *Journal of Neuroscience,* 34**,** 5486-5496.

BELL, B. B., HARLAN, S. M., MORGAN, D. A., GUO, D.-F. & RAHMOUNI, K. 2018. Differential contribution of POMC and AgRP neurons to the regulation of regional autonomic nerve activity by leptin. *Molecular metabolism,* 8**,** 1-12.

BERGER, J. P., AKIYAMA, T. E. & MEINKE, P. T. 2005. PPARs: therapeutic targets for metabolic disease. *Trends in pharmacological sciences,* 26**,** 244-251.

BERRUIEN, N. N. & SMITH, C. L. 2020. Emerging roles of melanocortin receptor accessory proteins (MRAP and MRAP2) in physiology and pathophysiology. *Gene,* 757**,** 144949.

BESSELL, E., MARKOVIC, T. P. & FULLER, N. R. 2021. How to provide a structured clinical assessment of a patient with overweight or obesity. *Diabetes, Obesity and Metabolism,* 23**,** 36-49.

BETZ, M. J. & ENERBÄCK, S. 2018. Targeting thermogenesis in brown fat and muscle to treat obesity and metabolic disease. *Nature Reviews Endocrinology,* 14**,** 77-87.

BILLES, S. K. & GREENWAY, F. L. 2011. Combination therapy with naltrexone and bupropion for obesity. *Expert opinion on pharmacotherapy,* 12**,** 1813-1826.

BLEVINS, J. E., THOMPSON, B. W., ANEKONDA, V. T., HO, J. M., GRAHAM, J. L., ROBERTS, Z. S., HWANG, B. H., OGIMOTO, K., WOLDEN-HANSON, T. & NELSON, J. 2016. Chronic CNS oxytocin signaling preferentially induces fat loss in high-fat diet-fed rats by enhancing satiety responses and increasing lipid utilization. *American Journal of Physiology-Regulatory, Integrative and Comparative Physiology,* 310**,** R640-R658.

BLÜHER, M. 2019. Obesity: global epidemiology and pathogenesis. *Nature Reviews Endocrinology,* 15**,** 288-298.

BOER, G. A., KEENAN, S. N., MIOTTO, P. M., HOLST, J. J. & WATT, M. J. 2021. GIP receptor deletion in mice confers resistance to high-fat diet-induced obesity via alterations in energy expenditure and adipose tissue lipid metabolism. *American Journal of Physiology-Endocrinology and Metabolism,* 320**,** E835-E845.

BOHULA, E. A., WIVIOTT, S. D., MCGUIRE, D. K., INZUCCHI, S. E., KUDER, J., IM, K., FANOLA, C. L., QAMAR, A., BROWN, C. & BUDAJ, A. 2018. Cardiovascular safety of lorcaserin in overweight or obese patients. *New England journal of medicine,* 379**,** 1107-1117.

BORGERS, D. P. & HEEMELS, W. M. H. 2014. Event-separation properties of event-triggered control systems. *IEEE Transactions on Automatic Control,* 59**,** 2644-2656.

BORTOLIN-CAVAILLE, M.-L. & CAVAILLÉ, J. 2012. The SNORD115 (H/MBII-52) and SNORD116 (H/MBII-85) gene clusters at the imprinted Prader–Willi locus generate canonical box C/D snoRNAs. *Nucleic acids research,* 40**,** 6800-6807.

BOVETTO, S. & RICHARD, D. 1995. Functional assessment of the 5-HT 1A-, 1B-, 2A/2C-, and 3-receptor subtypes on food intake and metabolic rate in rats. *American Journal of Physiology-Regulatory, Integrative and Comparative Physiology,* 268**,** R14-R20.

BRADLEY, R. L. & CHEATHAM, B. 1999. Regulation of ob gene expression and leptin secretion by insulin and dexamethasone in rat adipocytes. *Diabetes,* 48**,** 272-278.

BRAGA, S. P., DELANOGARE, E., MACHADO, A. E., PREDIGER, R. D. & MOREIRA, E. L. G. 2021. Switching from high-fat feeding (HFD) to regular diet improves metabolic and behavioral impairments in middle-aged female mice. *Behavioural Brain Research,* 398**,** 112969.

BRANDT, C., NOLTE, H., HENSCHKE, S., RUUD, L. E., AWAZAWA, M., MORGAN, D. A., GABEL, P., SPRENGER, H.-G., HESS, M. E. & GÜNTHER, S. 2018. Food perception primes hepatic ER homeostasis via melanocortin-dependent control of mTOR activation. *Cell,* 175**,** 1321-1335. e20.

BRATKOVIČ, T., MODIC, M., CAMARGO ORTEGA, G., DRUKKER, M. & ROGELJ, B. 2018. Neuronal differentiation induces SNORD115 expression and is accompanied by post-transcriptional changes of serotonin receptor 2c mRNA. *Scientific reports,* 8**,** 1-11.

BRAVO, P. E., MORSE, S., BORNE, D. M., AGUILAR, E. A. & REISIN, E. 2006. Leptin and hypertension in obesity. *Vascular health and risk management,* 2**,** 163.

BRENNAN, A. M. & MANTZOROS, C. S. 2006. Drug Insight: the role of leptin in human physiology and pathophysiology—emerging clinical applications. *Nature clinical practice Endocrinology & metabolism,* 2**,** 318-327.

BUETTNER, R., SCHÖLMERICH, J. & BOLLHEIMER, L. C. 2007. High‐fat diets: modeling the metabolic disorders of human obesity in rodents. *Obesity,* 15**,** 798-808.

CACCIARI, E., ZUCCHINI, S., CARLA, G., PIRAZZOLI, P., CICOGNANI, A., MANDINI, M., BUSACCA, M. & TREVISAN, C. 1990. Endocrine function and morphological findings in patients with disorders of the hypothalamo-pituitary area: a study with magnetic resonance. *Archives of disease in childhood,* 65**,** 1199-1202.

CAMPBELL, J. E. 2021. Targeting the GIPR for obesity: to agonize or antagonize? Potential mechanisms. *Molecular metabolism,* 46**,** 101139.

CASON, A. M. & ASTON-JONES, G. 2013a. Attenuation of saccharin-seeking in rats by orexin/hypocretin receptor 1 antagonist. *Psychopharmacology,* 228**,** 499-507.

CASON, A. M. & ASTON-JONES, G. 2013b. Role of orexin/hypocretin in conditioned sucrose-seeking in rats. *Psychopharmacology,* 226**,** 155-165.

CERCATO, C. & FONSECA, F. 2019. Cardiovascular risk and obesity. *Diabetology & metabolic syndrome,* 11**,** 1-15.

CHAIYASUT, C., SIVAMARUTHI, B. S., KESIKA, P., KHONGTAN, S., KHAMPITHUM, N., THANGALEELA, S., PEERAJAN, S., BUMRUNGPERT, A., CHAIYASUT, K. & SIRILUN, S. 2021. Synbiotic supplementation improves obesity index and metabolic biomarkers in Thai obese adults: A randomized clinical trial. *Foods,* 10**,** 1580.

CHEE, B. W., BERLIN, R. & SCHATZ, B. Predicting adverse drug events from personal health messages. AMIA Annual Symposium Proceedings, 2011. American Medical Informatics Association, 217.

CHELLAPPA, K., PERRON, I. J., NAIDOO, N. & BAUR, J. A. 2019. The leptin sensitizer celastrol reduces age‐associated obesity and modulates behavioral rhythms. *Aging Cell,* 18**,** e12874.

CHEN, C., YOU, L.-J., HUANG, Q., FU, X., ZHANG, B., LIU, R.-H. & LI, C. 2018. Modulation of gut microbiota by mulberry fruit polysaccharide treatment of obese diabetic db/db mice. *Food & function,* 9**,** 3732-3742.

CHEN, K. Y., BRYCHTA, R. J., SATER, Z. A., CASSIMATIS, T. M., CERO, C., FLETCHER, L. A., ISRANI, N. S., JOHNSON, J. W., LEA, H. J. & LINDERMAN, J. D. 2020. Opportunities and challenges in the therapeutic activation of human energy expenditure and thermogenesis to manage obesity. *Journal of biological chemistry,* 295**,** 1926-1942.

CHEN, X., MATTHEWS, J., ZHOU, L., PELTON, P., LIANG, Y., XU, J., YANG, M., CRYAN, E., RYBCZYNSKI, P. & DEMAREST, K. 2008. Improvement of dyslipidemia, insulin sensitivity, and energy balance by a peroxisome proliferator–activated receptor α agonist. *Metabolism,* 57**,** 1516-1525.

CHENG, J., MCCORVY, J. D., GIGUERE, P. M., ZHU, H., KENAKIN, T., ROTH, B. L. & KOZIKOWSKI, A. P. 2016. Design and discovery of functionally selective serotonin 2C (5-HT2C) receptor agonists. *Journal of medicinal chemistry,* 59**,** 9866-9880.

CHENG, W., NDOKA, E., MAUNG, J. N., PAN, W., RUPP, A. C., RHODES, C. J., OLSON, D. P. & MYERS, M. G. 2021. NTS Prlh overcomes orexigenic stimuli and ameliorates dietary and genetic forms of obesity. *Nature communications,* 12**,** 1-12.

CHIN, C.-H., CHEN, S.-H., WU, H.-H., HO, C.-W., KO, M.-T. & LIN, C.-Y. 2014. cytoHubba: identifying hub objects and sub-networks from complex interactome. *BMC systems biology,* 8**,** 1-7.

CHOQUET, H. & MEYRE, D. 2010. Genomic insights into early-onset obesity. *Genome Medicine,* 2**,** 1-12.

CLARKE, M. V., RUSSELL, P. K., ZAJAC, J. D. & DAVEY, R. A. 2019. The androgen receptor in the hypothalamus positively regulates hind-limb muscle mass and voluntary physical activity in adult male mice. *The Journal of steroid biochemistry and molecular biology,* 189**,** 187-194.

CLIFTON, P. G., LEE, M. D. & DOURISH, C. T. 2000. Similarities in the action of Ro 60-0175, a 5-HT2C receptor agonist, and d-fenfluramine on feeding patterns in the rat. *Psychopharmacology,* 152**,** 256-267.

COLE, L. K., ZHANG, M., CHEN, L., SPARAGNA, G. C., VANDEL, M., XIANG, B., DOLINSKY, V. W. & HATCH, G. M. 2021. Supplemental berberine in a high-fat diet reduces adiposity and cardiac dysfunction in offspring of mouse dams with gestational diabetes mellitus. *The Journal of Nutrition,* 151**,** 892-901.

COLEMAN, P. J. & RENGER, J. J. 2010. Orexin receptor antagonists: a review of promising compounds patented since 2006. *Expert opinion on therapeutic patents,* 20**,** 307-324.

COMINATO, L., FRANCO, R. & DAMIANI, D. 2021. Adolescent obesity treatments: news, views, and evidence. *Archives of Endocrinology and Metabolism*.

CONRAD, C. D., GROTE, K. A., HOBBS, R. J. & FERAYORNI, A. 2003. Sex differences in spatial and non-spatial Y-maze performance after chronic stress. *Neurobiology of learning and memory,* 79**,** 32-40.

COSTET, P., LEGENDRE, C., MORÉ, J., EDGAR, A., GALTIER, P. & PINEAU, T. 1998. Peroxisome proliferator-activated receptor α-isoform deficiency leads to progressive dyslipidemia with sexually dimorphic obesity and steatosis. *Journal of Biological Chemistry,* 273**,** 29577-29585.

COTA, D., SANDOVAL, D. A., OLIVIERI, M., PRODI, E., D'ALESSIO, D. A., WOODS, S. C., SEELEY, R. J. & OBICI, S. 2009. Food intake‐independent effects of CB1 antagonism on glucose and lipid metabolism. *Obesity,* 17**,** 1641-1645.

COX, C. D., BRESLIN, M. J., WHITMAN, D. B., SCHREIER, J. D., MCGAUGHEY, G. B., BOGUSKY, M. J., ROECKER, A. J., MERCER, S. P., BEDNAR, R. A. & LEMAIRE, W. 2010. Discovery of the dual orexin receptor antagonist [(7 R)-4-(5-chloro-1, 3-benzoxazol-2-yl)-7-methyl-1, 4-diazepan-1-yl][5-methyl-2-(2 H-1, 2, 3-triazol-2-yl) phenyl] methanone (MK-4305) for the treatment of insomnia. *Journal of medicinal chemistry,* 53**,** 5320-5332.

CRAWLEY, J. N. 1985. Exploratory behavior models of anxiety in mice. *Neuroscience & Biobehavioral Reviews,* 9**,** 37-44.

CRINO, A., FINTINI, D., BOCCHINI, S. & GRUGNI, G. 2018. Obesity management in Prader-Willi syndrome: current perspectives. *Diabetes Metab Syndr Obes,* 11**,** 579-593.

CROWLEY, V. E., YEO, G. S. & O'RAHILLY, S. 2002. Obesity therapy: altering the energy intake-and-expenditure balance sheet. *Nature reviews Drug discovery,* 1**,** 276-286.

CRYAN, J. F., MOMBEREAU, C. & VASSOUT, A. 2005. The tail suspension test as a model for assessing antidepressant activity: review of pharmacological and genetic studies in mice. *Neuroscience & Biobehavioral Reviews,* 29**,** 571-625.

CUI, H., SOHN, J. W., GAUTRON, L., FUNAHASHI, H., WILLIAMS, K. W., ELMQUIST, J. K. & LUTTER, M. 2012. Neuroanatomy of melanocortin‐4 receptor pathway in the lateral hypothalamic area. *Journal of Comparative Neurology,* 520**,** 4168-4183.

D'AGOSTINO, G., LYONS, D., CRISTIANO, C., LETTIERI, M., OLARTE-SANCHEZ, C., BURKE, L. K., GREENWALD-YARNELL, M., CANSELL, C., DOSLIKOVA, B. & GEORGESCU, T. 2018. Nucleus of the solitary tract serotonin 5-HT2C receptors modulate food intake. *Cell metabolism,* 28**,** 619-630. e5.

DAGHER, A. 2010. The neurobiology of appetite: hunger as addiction. *Obesity Prevention***,** 15-22.

DANESCHVAR, H. L., ARONSON, M. D. & SMETANA, G. W. 2016. FDA-approved anti-obesity drugs in the United States. *The American journal of medicine,* 129**,** 879. e1-879. e6.

DE SMITH, A. J., PURMANN, C., WALTERS, R. G., ELLIS, R. J., HOLDER, S. E., VAN HAELST, M. M., BRADY, A. F., FAIRBROTHER, U. L., DATTANI, M. & KEOGH, J. M. 2009. A deletion of the HBII-85 class of small nucleolar RNAs (snoRNAs) is associated with hyperphagia, obesity and hypogonadism. *Human molecular genetics,* 18**,** 3257-3265.

DELGADILLO-PUGA, C., NORIEGA, L. G., MORALES-ROMERO, A. M., NIETO-CAMACHO, A., GRANADOS-PORTILLO, O., RODRÍGUEZ-LÓPEZ, L. A., ALEMÁN, G., FURUZAWA-CARBALLEDA, J., TOVAR, A. R. & CISNEROS-ZEVALLOS, L. 2020. Goat's milk intake prevents obesity, hepatic steatosis and insulin resistance in mice fed a high-fat diet by reducing inflammatory markers and increasing energy expenditure and mitochondrial content in skeletal muscle. *International Journal of Molecular Sciences,* 21**,** 5530.

DI GIOVANNI, G., BHARATIYA, R., PUGINIER, E., RAMOS, M., DE DEURWAERDÈRE, S., CHAGRAOUI, A. & DE DEURWAERDÈRE, P. 2020. Lorcaserin alters serotonin and noradrenaline tissue content and their interaction with dopamine in the rat brain. *Frontiers in Pharmacology,* 11**,** 962.

DI GIOVANNI, G. & DE DEURWAERDERE, P. 2016. New therapeutic opportunities for 5-HT2C receptor ligands in neuropsychiatric disorders. *Pharmacol Ther,* 157**,** 125-62.

DI GIOVANNI, G. & DE DEURWAERDÈRE, P. 2016. New therapeutic opportunities for 5-HT2C receptor ligands in neuropsychiatric disorders. *Pharmacology & Therapeutics,* 157**,** 125-162.

DIMITRIADIS, E., DASKALAKIS, M., KAMPA, M., PEPPE, A., PAPADAKIS, J. A. & MELISSAS, J. 2013. Alterations in gut hormones after laparoscopic sleeve gastrectomy: a prospective clinical and laboratory investigational study. *Annals of surgery,* 257**,** 647-654.

DOBIN, A., DAVIS, C. A., SCHLESINGER, F., DRENKOW, J., ZALESKI, C., JHA, S., BATUT, P., CHAISSON, M. & GINGERAS, T. R. 2013. STAR: ultrafast universal RNA-seq aligner. *Bioinformatics,* 29**,** 15-21.

DOCHE, M. E., BOCHUKOVA, E. G., SU, H.-W., PEARCE, L. R., KEOGH, J. M., HENNING, E., CLINE, J. M., DALE, A., CHEETHAM, T. & BARROSO, I. 2012. Human SH2B1 mutations are associated with maladaptive behaviors and obesity. *The Journal of clinical investigation,* 122**,** 4732-4736.

DONOVAN, M. H. & TECOTT, L. H. 2013. Serotonin and the regulation of mammalian energy balance. *Frontiers in neuroscience,* 7**,** 36.

DYKENS, E. M., MILLER, J., ANGULO, M., ROOF, E., REIDY, M., HATOUM, H. T., WILLEY, R., BOLTON, G. & KORNER, P. 2018. Intranasal carbetocin reduces hyperphagia in individuals with Prader-Willi syndrome. *JCI insight,* 3.

EHRHART, F., JANSSEN, K. J., COORT, S. L., EVELO, C. T. & CURFS, L. M. 2018. Prader-Willi syndrome and Angelman syndrome: Visualisation of the molecular pathways for two chromosomal disorders. *The World Journal of Biological Psychiatry***,** 1-13.

ENGLANDER, M. T., DULAWA, S. C., BHANSALI, P. & SCHMAUSS, C. 2005. How stress and fluoxetine modulate serotonin 2C receptor pre-mRNA editing. *Journal of Neuroscience,* 25**,** 648-651.

ERONDU, N., WADDEN, T., GANTZ, I., MUSSER, B., NGUYEN, A. M., BAYS, H., BRAY, G., O'NEIL, P. M., BASDEVANT, A. & KAUFMAN, K. D. 2007. Effect of NPY5R antagonist MK‐0557 on weight regain after very‐low‐calorie diet‐induced weight loss. *Obesity,* 15**,** 895-905.

EVANS, R. M., BARISH, G. D. & WANG, Y.-X. 2004. PPARs and the complex journey to obesity. *Nature medicine,* 10**,** 355-361.

FAN, W., YANASE, T., NOMURA, M., OKABE, T., GOTO, K., SATO, T., KAWANO, H., KATO, S. & NAWATA, H. 2005. Androgen receptor null male mice develop late-onset obesity caused by decreased energy expenditure and lipolytic activity but show normal insulin sensitivity with high adiponectin secretion. *Diabetes,* 54**,** 1000-1008.

FANG, Y., DING, X., ZHANG, Y., CAI, L., GE, Y., MA, K., XU, R., LI, S., SONG, M. & ZHU, H. 2022. Fluoxetine inhibited the activation of A1 reactive astrocyte in a mouse model of major depressive disorder through astrocytic 5-HT2BR/β-arrestin2 pathway. *Journal of neuroinflammation,* 19**,** 1-20.

FARHANG-FALLAH, J., YIN, X., TRENTIN, G., CHENG, A. M. & ROZAKIS-ADCOCK, M. 2000. Cloning and Characterization of PHIP, a Novel Insulin Receptor Substrate-1 Pleckstrin Homology DomainInteracting Protein. *Journal of Biological Chemistry,* 275**,** 40492-40497.

FAROOQI, I. S. & O'RAHILLY, S. 2009. Leptin: a pivotal regulator of human energy homeostasis. *The American journal of clinical nutrition,* 89**,** 980S-984S.

FERNÁNDEZ VÁZQUEZ, G., REITER, R. J. & AGIL, A. 2018. Melatonin increases brown adipose tissue mass and function in Zücker diabetic fatty rats: implications for obesity control. *Journal of pineal research,* 64**,** e12472.

FERNÁNDEZ-GALAZ, M. C., FERNÁNDEZ-AGULLÓ, T., CARRASCOSA, J. M., ROS, M. & GARCIA-SEGURA, L. M. 2010. Leptin accumulation in hypothalamic and dorsal raphe neurons is inversely correlated with brain serotonin content. *Brain research,* 1329**,** 194-202.

FILIZOLA, M. 2010. Increasingly accurate dynamic molecular models of G-protein coupled receptor oligomers: Panacea or Pandora's box for novel drug discovery? *Life sciences,* 86**,** 590-597.

FIORINO, F., MAGLI, E., KĘDZIERSKA, E., CIANO, A., CORVINO, A., SEVERINO, B., PERISSUTTI, E., FRECENTESE, F., DI VAIO, P. & SACCONE, I. 2017. New 5-HT1A, 5HT2A and 5HT2C receptor ligands containing a picolinic nucleus: synthesis, in vitro and in vivo pharmacological evaluation. *Bioorganic & medicinal chemistry,* 25**,** 5820-5837.

FLEMING, J. W., MCCLENDON, K. S. & RICHE, D. M. 2013. New obesity agents: lorcaserin and phentermine/topiramate. *Annals of Pharmacotherapy,* 47**,** 1007-1016.

FONTAINE, K. & BAROFSKY, I. 2001. Obesity and health‐related quality of life. *Obesity reviews,* 2**,** 173-182.

FOROOZAN, P., KOUSHKIE JAHROMI, M., NEMATI, J., SEPEHRI, H., SAFARI, M. A. & BRAND, S. 2021. Probiotic Supplementation and High-Intensity Interval Training Modify Anxiety-Like Behaviors and Corticosterone in High-Fat Diet-Induced Obesity Mice. *Nutrients,* 13**,** 1762.

FRAYLING, T. M., TIMPSON, N. J., WEEDON, M. N., ZEGGINI, E., FREATHY, R. M., LINDGREN, C. M., PERRY, J. R., ELLIOTT, K. S., LANGO, H. & RAYNER, N. W. 2007. A common variant in the FTO gene is associated with body mass index and predisposes to childhood and adult obesity. *Science,* 316**,** 889-894.

FRICKER, L. D., TASHIMA, A. K., FAKIRA, A. K., HOCHGESCHWENDER, U., WETSEL, W. C. & DEVI, L. A. 2021. Neuropeptidomic analysis of a genetically defined cell type in mouse brain and pituitary. *Cell chemical biology,* 28**,** 105-112. e4.

FRIEDMAN, J. M. & HALAAS, J. L. 1998. Leptin and the regulation of body weight in mammals. *Nature,* 395**,** 763-770.

FU, R., MEI, Q., SHIWALKAR, N., ZUO, W., ZHANG, H., GREGOR, D., PATEL, S. & YE, J.-H. 2020. Anxiety during alcohol withdrawal involves 5-HT2C receptors and M-channels in the lateral habenula. *Neuropharmacology,* 163**,** 107863.

FUKASAKA, Y., NAMBU, H., TANIOKA, H., OBATA, A., TONOMURA, M., OKUNO, T. & YUKIOKA, H. 2018. An insurmountable NPY Y5 receptor antagonist exhibits superior anti-obesity effects in high-fat diet-induced obese mice. *Neuropeptides,* 70**,** 55-63.

GALGANI, J. E., MORO, C. & RAVUSSIN, E. 2008. Metabolic flexibility and insulin resistance. *American journal of physiology-endocrinology and metabolism,* 295**,** E1009-E1017.

GARCIA-CARCELES, J., DECARA, J. M., VÁZQUEZ-VILLA, H., RODRIGUEZ, R., CODESIDO, E., CRUCES, J., BREA, J., LOZA, M. I., ALEN, F. & BOTTA, J. 2017. A positive allosteric modulator of the serotonin 5-HT2C receptor for obesity. *Journal of medicinal chemistry,* 60**,** 9575-9584.

GARCÍA-CÁRCELES, J., DECARA, J. M., VÁZQUEZ-VILLA, H., RODRÍGUEZ, R. N., CODESIDO, E., CRUCES, J., BREA, J., LOZA, M. I., ALÉN, F. & BOTTA, J. 2017. A positive allosteric modulator of the serotonin 5-HT2C receptor for obesity. *Journal of medicinal chemistry,* 60**,** 9575-9584.

GARFIELD, A. S., DAVIES, J. R., BURKE, L. K., FURBY, H. V., WILKINSON, L. S., HEISLER, L. K. & ISLES, A. R. 2016. Increased alternate splicing of Htr2c in a mouse model for Prader-Willi syndrome leads disruption of 5HT2C receptor mediated appetite. *Molecular brain,* 9**,** 1-9.

GARFIELD, A. S. & HEISLER, L. K. 2009. Pharmacological targeting of the serotonergic system for the treatment of obesity. *The Journal of Physiology,* 587**,** 49-60.

GARFIELD, A. S., LAM, D. D., MARSTON, O. J., PRZYDZIAL, M. J. & HEISLER, L. K. 2009. Role of central melanocortin pathways in energy homeostasis. *Trends in Endocrinology & Metabolism,* 20**,** 203-215.

GE, T., ZHANG, Z., LV, J., SONG, Y., FAN, J., LIU, W., WANG, X., HALL, F. S., LI, B. & CUI, R. 2017. The role of 5‐HT2c receptor on corticosterone‐mediated food intake. *Journal of biochemical and molecular toxicology,* 31**,** e21890.

GEIGER, S. D., YAO, P., VAUGHN, M. G. & QIAN, Z. 2021. PFAS exposure and overweight/obesity among children in a nationally representative sample. *Chemosphere,* 268**,** 128852.

GEORGESCU, T., LYONS, D. & HEISLER, L. K. 2021. Role of serotonin in body weight, insulin secretion and glycaemic control. *Journal of neuroendocrinology,* 33**,** e12960.

GEPNER, Y., SHELEF, I., KOMY, O., COHEN, N., SCHWARZFUCHS, D., BRIL, N., REIN, M., SERFATY, D., KENIGSBUCH, S. & ZELICHA, H. 2019. The beneficial effects of Mediterranean diet over low-fat diet may be mediated by decreasing hepatic fat content. *Journal of hepatology,* 71**,** 379-388.

GERKEN, T., GIRARD, C. A., TUNG, Y.-C. L., WEBBY, C. J., SAUDEK, V., HEWITSON, K. S., YEO, G. S., MCDONOUGH, M. A., CUNLIFFE, S. & MCNEILL, L. A. 2007. The obesity-associated FTO gene encodes a 2-oxoglutarate-dependent nucleic acid demethylase. *Science,* 318**,** 1469-1472.

GIL-ORTEGA, M., MARTÍN-RAMOS, M., ARRIBAS, S. M., GONZÁLEZ, M. C., ARÁNGUEZ, I., RUIZ-GAYO, M., SOMOZA, B. & FERNÁNDEZ-ALFONSO, M. S. 2016. Arterial stiffness is associated with adipokine dysregulation in non-hypertensive obese mice. *Vascular pharmacology,* 77**,** 38-47.

GOLDENSHLUGER, A., CONSTANTINI, K., GOLDSTEIN, N., SHELEF, I., SCHWARZFUCHS, D., ZELICHA, H., YASKOLKA MEIR, A., TSABAN, G., CHASSIDIM, Y. & GEPNER, Y. 2021. Effect of Dietary Strategies on Respiratory Quotient and Its Association with Clinical Parameters and Organ Fat Loss: A Randomized Controlled Trial. *Nutrients,* 13**,** 2230.

GONZÁLEZ-AMOR, M., VILA-BEDMAR, R., RODRIGUES-DÍEZ, R., MORENO-CARRILES, R., ARCONES, A. C., CRUCES-SANDE, M., SALAICES, M., MAYOR, F., BRIONES, A. M. & MURGA, C. 2020. Myeloid GRK2 regulates obesity-Induced endothelial dysfunction by modulating inflammatory responses in perivascular adipose tissue. *Antioxidants,* 9**,** 953.

GRANT, S., SOLTANI PANAH, A. & MCCOSKER, A. 2022. Weight-Biased Language across 30 Years of Australian News Reporting on Obesity: Associations with Public Health Policy. *Obesities,* 2**,** 103-114.

GRAY, J., YEO, G., HUNG, C., KEOGH, J., CLAYTON, P., BANERJEE, K., MCAULAY, A., O'RAHILLY, S. & FAROOQI, I. 2007. Functional characterization of human NTRK2 mutations identified in patients with severe early-onset obesity. *International journal of obesity,* 31**,** 359-364.

GRECH, A. M., DU, X., MURRAY, S. S., XIAO, J. & HILL, R. A. 2019. Sex-specific spatial memory deficits in mice with a conditional TrkB deletion on parvalbumin interneurons. *Behavioural Brain Research,* 372**,** 111984.

GREENWAY, F. L., WHITEHOUSE, M., GUTTADAURIA, M., ANDERSON, J. W., ATKINSON, R. L., FUJIOKA, K., GADDE, K. M., GUPTA, A. K., O'NEIL, P. & SCHUMACHER, D. 2009. Rational design of a combination medication for the treatment of obesity. *Obesity,* 17**,** 30-39.

GRIGGS, J. 2019. Single-Case Study of Appetite Control in Prader-Willi Syndrome, Over 12-Years by the Indian Extract Caralluma fimbriata. *Genes,* 10**,** 447.

GRIGGS, J. L., MATHAI, M. L. & SINNAYAH, P. 2018a. Caralluma fimbriata extract activity involves the 5-HT2c receptor in PWS Snord116 deletion mouse model. *Brain Behav,* 8**,** e01102.

GRIGGS, J. L., MATHAI, M. L. & SINNAYAH, P. 2018b. Caralluma fimbriata extract activity involves the 5‐HT2c receptor in PWS Snord116 deletion mouse model. *Brain and Behavior,* 8**,** e01102.

GUILLEMOT-LEGRIS, O. & MUCCIOLI, G. G. 2017. Obesity-induced neuroinflammation: beyond the hypothalamus. *Trends in Neurosciences,* 40**,** 237-253.

GUJJALA, S., PUTAKALA, M., BONGU, S. B. R., RAMASWAMY, R. & DESIREDDY, S. 2019. Preventive effect of Caralluma fimbriata against high-fat diet induced injury to heart by modulation of tissue lipids, oxidative stress and histological changes in Wistar rats. *Archives of Physiology and Biochemistry***,** 1-9.

GUO, Y., YUE, X.-J., LI, H.-H., SONG, Z.-X., YAN, H.-Q., ZHANG, P., GUI, Y.-K., CHANG, L. & LI, T. 2016. Overweight and obesity in young adulthood and the risk of stroke: a meta-analysis. *Journal of Stroke and Cerebrovascular Diseases,* 25**,** 2995-3004.

HALFORD, J. C. & HARROLD, J. A. 2012. 5-HT 2C receptor agonists and the control of appetite. *Appetite Control.* Springer.

HALL, K., HEYMSFIELD, S., KEMNITZ, J., KLEIN, S., SCHOELLER, D. & SPEAKMAN, J. 2012. Energy balance and its components: Implications for body weight regulation (American Journal of Clinical Nutrition (2012) 95,(989-994). *American Journal of Clinical Nutrition,* 96**,** 448.

HALL, K. D., FAROOQI, I. S., FRIEDMAN, J. M., KLEIN, S., LOOS, R. J., MANGELSDORF, D. J., O'RAHILLY, S., RAVUSSIN, E., REDMAN, L. M. & RYAN, D. H. 2022. The energy balance model of obesity: beyond calories in, calories out. *The American Journal of Clinical Nutrition*.

HANDAKAS, E., LAU, C. H., ALFANO, R., CHATZI, V. L., PLUSQUIN, M., VINEIS, P. & ROBINSON, O. 2022. A systematic review of metabolomic studies of childhood obesity: State of the evidence for metabolic determinants and consequences. *Obesity Reviews,* 23**,** e13384.

HARA, K., HIROWATARI, Y., YOSHIKA, M., KOMIYAMA, Y., TSUKA, Y. & TAKAHASHI, H. 2004. The ratio of plasma to whole-blood serotonin may be a novel marker of atherosclerotic cardiovascular disease. *Journal of Laboratory and Clinical Medicine,* 144**,** 31-37.

HARNO, E., GALI RAMAMOORTHY, T., COLL, A. P. & WHITE, A. 2018. POMC: the physiological power of hormone processing. *Physiological reviews,* 98**,** 2381-2430.

HARPER, M.-E., GREEN, K. & BRAND, M. D. 2008. The efficiency of cellular energy transduction and its implications for obesity. *Annu. Rev. Nutr.,* 28**,** 13-33.

HASSAN, A. M., MANCANO, G., KASHOFER, K., FRÖHLICH, E. E., MATAK, A., MAYERHOFER, R., REICHMANN, F., OLIVARES, M., NEYRINCK, A. M. & DELZENNE, N. M. 2018. High-fat

diet induces depression-like behaviour in mice associated with changes in microbiome, neuropeptide Y, and brain metabolome. *Nutritional neuroscience*, 1-17.

HASSAN, A. M., MANCANO, G., KASHOFER, K., FRÖHLICH, E. E., MATAK, A., MAYERHOFER, R., REICHMANN, F., OLIVARES, M., NEYRINCK, A. M. & DELZENNE, N. M. 2019. High-fat diet induces depression-like behaviour in mice associated with changes in microbiome, neuropeptide Y, and brain metabolome. *Nutritional neuroscience,* 22**,** 877-893.

HAYDEN, M. R. & BANKS, W. A. 2021. Deficient leptin cellular signaling plays a key role in brain ultrastructural remodeling in obesity and type 2 diabetes mellitus. *International Journal of Molecular Sciences,* 22**,** 5427.

HE, Y., LIU, H., YIN, N., YANG, Y., WANG, C., YU, M., LIU, H., LIANG, C., WANG, J. & TU, L. 2021. Barbadin potentiates long-term effects of lorcaserin on POMC neurons and weight loss. *Journal of Neuroscience,* 41**,** 5734-5746.

HEBRAS, J., MARTY, V., PERSONNAZ, J., MERCIER, P., KROGH, N., NIELSEN, H., AGUIRREBENGOA, M., SEITZ, H., PRADERE, J.-P. & GUIARD, B. P. 2020. Reassessment of the involvement of Snord115 in the serotonin 2c receptor pathway in a genetically relevant mouse model. *Elife,* 9**,** e60862.

HEISLER, L. K., COWLEY, M. A., KISHI, T., TECOTT, L. H., FAN, W., LOW, M. J., SMART, J. L., RUBINSTEIN, M., TATRO, J. B. & ZIGMAN, J. M. 2003. Central serotonin and melanocortin pathways regulating energy homeostasis. *Annals of the New York Academy of Sciences,* 994**,** 169-174.

HEISLER, L. K., JOBST, E. E., SUTTON, G. M., ZHOU, L., BOROK, E., THORNTON-JONES, Z., LIU, H. Y., ZIGMAN, J. M., BALTHASAR, N. & KISHI, T. 2006. Serotonin reciprocally regulates melanocortin neurons to modulate food intake. *Neuron,* 51**,** 239-249.

HEKSCH, R., KAMBOJ, M., ANGLIN, K. & OBRYNBA, K. 2017. Review of Prader-Willi syndrome: the endocrine approach. *Transl Pediatr,* 6**,** 274-285.

HERRICK-DAVIS, K., GRINDE, E. & MAZURKIEWICZ, J. E. 2004. Biochemical and biophysical characterization of serotonin 5-HT2C receptor homodimers on the plasma membrane of living cells. *Biochemistry,* 43**,** 13963-13971.

HESS, M. E. & BRÜNING, J. C. 2014. The fat mass and obesity-associated (FTO) gene: Obesity and beyond? *Biochimica et Biophysica Acta (BBA)-Molecular Basis of Disease,* 1842**,** 2039-2047.

HEYMSFIELD, S. B., AVENA, N. M., BAIER, L., BRANTLEY, P., BRAY, G. A., BURNETT, L. C., BUTLER, M. G., DRISCOLL, D. J., EGLI, D. & ELMQUIST, J. 2014. Hyperphagia: current concepts and future directions proceedings of the 2nd international conference on hyperphagia. *Obesity,* 22**,** S1-S17.

HIGGINS, G. A., ZEEB, F. D. & FLETCHER, P. J. 2017. Role of impulsivity and reward in the anti-obesity actions of 5-HT2C receptor agonists. *Journal of Psychopharmacology,* 31**,** 1403-1418.

HIGGS, S., COOPER, A. J. & BARNES, N. M. 2011. Reversal of sibutramine-induced anorexia with a selective 5-HT2C receptor antagonist. *Psychopharmacology,* 214**,** 941-947.

HILL, J. O., WYATT, H. R. & PETERS, J. C. 2012. Energy balance and obesity. *Circulation,* 126**,** 126-132.

HOLST, J. J., VILSBØLL, T. & DEACON, C. F. 2009. The incretin system and its role in type 2 diabetes mellitus. *Molecular and cellular endocrinology,* 297**,** 127-136.

HUANG, X. F., WESTON‐GREEN, K. & YU, Y. 2018. Decreased 5‐HT2cR and GHSR1a interaction in antipsychotic drug‐induced obesity. *Obesity Reviews,* 19**,** 396-405.

HUMMON, A. B., LIM, S. R., DIFILIPPANTONIO, M. J. & RIED, T. 2007. Isolation and solubilization of proteins after TRIzol® extraction of RNA and DNA from patient material following prolonged storage. *Biotechniques,* 42**,** 467-472.

HWA, J. J., WITTEN, M. B., WILLIAMS, P., GHIBAUDI, L., GAO, J., SALISBURY, B. G., MULLINS, D., HAMUD, F., STRADER, C. D. & PARKER, E. M. 1999. Activation of the NPY Y5 receptor regulates both feeding and energy expenditure. *American Journal of Physiology-Regulatory, Integrative and Comparative Physiology,* 277**,** R1428-R1434.

ILLUMINA 2017.

INUI, A., ASAKAWA, A., Y. BOWERS, C., MANTOVANI, G., LAYLANO, A., M. MEGUID, M. & FUJIMIYA, M. 2004. Ghrelin, appetite, and gastric motility: the emerging role of the stomach as an endocrine organ. *The FASEB Journal,* 18**,** 439-456.

IRIZARRY, K. A., MILLER, M., FREEMARK, M. & HAQQ, A. M. 2016. Prader Willi syndrome: genetics, metabolomics, hormonal function, and new approaches to therapy. *Advances in pediatrics,* 63**,** 47.

JAIS, A. & BRÜNING, J. C. 2017. Hypothalamic inflammation in obesity and metabolic disease. *The Journal of clinical investigation,* 127**,** 24-32.

JAIS, A. & BRÜNING, J. C. 2021. Arcuate Nucleus-Dependent Regulation of Metabolism—Pathways to Obesity and Diabetes Mellitus. *Endocrine Reviews*.

JAIS, A. & BRÜNING, J. C. 2022. Arcuate Nucleus-Dependent Regulation of Metabolism—Pathways to Obesity and Diabetes Mellitus. *Endocrine Reviews,* 43**,** 314-328.

JAMES, W. P. T., CATERSON, I. D., COUTINHO, W., FINER, N., VAN GAAL, L. F., MAGGIONI, A. P., TORP-PEDERSEN, C., SHARMA, A. M., SHEPHERD, G. M. & RODE, R. A. 2010. Effect of sibutramine on cardiovascular outcomes in overweight and obese subjects. *New England Journal of Medicine,* 363**,** 905-917.

JANG, J. W., KIM, M. S., CHO, Y. S., CHO, A. E. & PAE, A. N. 2012. Identification of structural determinants of ligand selectivity in 5-HT2 receptor subtypes on the basis of protein–ligand interactions. *Journal of Molecular Graphics and Modelling,* 38**,** 342-353.

JANSSON, J.-O., PALSDOTTIR, V., HÄGG, D. A., SCHÉLE, E., DICKSON, S. L., ANESTEN, F., BAKE, T., MONTELIUS, M., BELLMAN, J. & JOHANSSON, M. E. 2018. Body weight homeostat that regulates fat mass independently of leptin in rats and mice. *Proceedings of the National Academy of Sciences,* 115**,** 427-432.

JIMENEZ-MUNOZ, C. M., LÓPEZ, M., ALBERICIO, F. & MAKOWSKI, K. 2021. Targeting Energy Expenditure—Drugs for Obesity Treatment. *Pharmaceuticals,* 14**,** 435.

JIN, S., ZHAO, Y., JIANG, Y., WANG, Y., LI, C., ZHANG, D., LIAN, B., DU, Z., SUN, H. & SUN, L. 2018. Anxiety-like behaviour assessments of adolescent rats after repeated maternal separation during early life. *Neuroreport,* 29**,** 643.

JOAO, A., REIS, F. & FERNANDES, R. 2016. The incretin system ABCs in obesity and diabetes–novel therapeutic strategies for weight loss and beyond. *Obesity Reviews,* 17**,** 553-572.

JUHASZ, G., CHASE, D., PEGG, E., DOWNEY, D., TOTH, Z. G., STONES, K., PLATT, H., MEKLI, K., PAYTON, A. & ELLIOTT, R. 2009. CNR1 gene is associated with high neuroticism and low agreeableness and interacts with recent negative life events to predict current depressive symptoms. *Neuropsychopharmacology,* 34**,** 2019-2027.

KAIYALA, K. J., WISSE, B. E. & LIGHTON, J. R. 2019. Validation of an equation for energy expenditure that does not require the respiratory quotient. *PLoS One,* 14**,** e0211585.

KAMALAKKANNAN, S., RAJENDRAN, R., VENKATESH, R. V., CLAYTON, P. & AKBARSHA, M. A. 2010. Antiobesogenic and antiatherosclerotic properties of Caralluma fimbriata extract. *Journal of nutrition and metabolism,* 2010.

KANSHANA, J. S., MATTILA, P. E., EWING, M. C., WOOD, A. N., SCHOISWOHL, G., MEYER, A. C., KOWALSKI, A., ROSENTHAL, S. L., GINGRAS, S. & KAUFMAN, B. A. 2021. A murine model of the human CREBRFR457Q obesity-risk variant does not influence energy or glucose homeostasis in response to nutritional stress. *Plos one,* 16**,** e0251895.

KAZAK, L., CHOUCHANI, E. T., JEDRYCHOWSKI, M. P., ERICKSON, B. K., SHINODA, K., COHEN, P., VETRIVELAN, R., LU, G. Z., LAZNIK-BOGOSLAVSKI, D. & HASENFUSS, S. C. 2015. A creatine-driven substrate cycle enhances energy expenditure and thermogenesis in beige fat. *Cell,* 163**,** 643-655.

KERAMAT, S. A., ALAM, K., AL-HANAWI, M. K., GOW, J., BIDDLE, S. J. & HASHMI, R. 2021. Trends in the prevalence of adult overweight and obesity in Australia, and its association with geographic remoteness. *Scientific reports,* 11**,** 1-9.

KHAN, S. S., NING, H., WILKINS, J. T., ALLEN, N., CARNETHON, M., BERRY, J. D., SWEIS, R. N. & LLOYD-JONES, D. M. 2018. Association of body mass index with lifetime risk of cardiovascular disease and compression of morbidity. *JAMA cardiology,* 3**,** 280-287.

KHANSARI, M. R., PANAHI, N., HOSSEINZADEH, S. & ZENDEHDEL, M. 2020. Effect of cannabinoid-serotonin interactions in the regulation of neuropeptide Y1 receptors expression in rats: the role of CB1 and 5-HT2C receptor. *Comparative Clinical Pathology,* 29**,** 561-571.

KILLION, E. A., WANG, J., YIE, J., SHI, S. D.-H., BATES, D., MIN, X., KOMOROWSKI, R., HAGER, T., DENG, L. & ATANGAN, L. 2018. Anti-obesity effects of GIPR antagonists alone and in combination with GLP-1R agonists in preclinical models. *Science Translational Medicine,* 10**,** eaat3392.

KIM, J. K. 2010. Inflammation and insulin resistance: an old story with new ideas. *Korean diabetes journal,* 34**,** 137-145.

KIM, S.-J., NIAN, C. & MCINTOSH, C. H. 2010. GIP increases human adipocyte LPL expression through CREB and TORC2-mediated trans-activation of the LPL gene. *Journal of lipid research,* 51**,** 3145-3157.

KIRCHNER, H., GUTIERREZ, J. A., SOLENBERG, P. J., PFLUGER, P. T., CZYZYK, T. A., WILLENCY, J. A., SCHÜRMANN, A., JOOST, H.-G., JANDACEK, R. J. & HALE, J. E. 2009. GOAT links dietary lipids with the endocrine control of energy balance. *Nature medicine,* 15**,** 741-745.

KIRWAN, P., KAY, R. G., BROUWERS, B., HERRANZ-PÉREZ, V., JURA, M., LARRAUFIE, P., JERBER, J., PEMBROKE, J., BARTELS, T. & WHITE, A. 2018. Quantitative mass spectrometry for human melanocortin peptides in vitro and in vivo suggests prominent roles for β-MSH and desacetyl α-MSH in energy homeostasis. *Molecular metabolism,* 17**,** 82-97.

KISHORE, S., KHANNA, A., ZHANG, Z., HUI, J., BALWIERZ, P. J., STEFAN, M., BEACH, C., NICHOLLS, R. D., ZAVOLAN, M. & STAMM, S. 2010. The snoRNA MBII-52 (SNORD 115) is processed into smaller RNAs and regulates alternative splicing. *Human molecular genetics,* 19**,** 1153-1164.

KISHORE, S. & STAMM, S. Regulation of alternative splicing by snoRNAs. Cold Spring Harbor symposia on quantitative biology, 2006. Cold Spring Harbor Laboratory Press, 329-334.

KITCHENER, S. & DOURISH, C. 1994. An examination of the behavioural specificity of hypophagia induced by 5-HT1B, 5-HT1C and 5-HT2 receptor agonists using the post-prandial satiety sequence in rats. *Psychopharmacology,* 113**,** 369-377.

KLEMENT, J., OTT, V., RAPP, K., BREDE, S., PICCININI, F., COBELLI, C., LEHNERT, H. & HALLSCHMID, M. 2017. Oxytocin improves β-cell responsivity and glucose tolerance in healthy men. *Diabetes,* 66**,** 264-271.

KLEYN, P. W., FAN, W., KOVATS, S. G., LEE, J. J., PULIDO, J. C., WU, Y., BERKEMEIER, L. R., MISUMI, D. J., HOLMGREN, L. & CHARLAT, O. 1996. Identification and characterization of the mouse obesity gene tubby: a member of a novel gene family. *Cell,* 85**,** 281-290.

KNIGHT, P., CHELLIAN, R., WILSON, R., BEHNOOD-ROD, A., PANUNZIO, S. & BRUIJNZEEL, A. W. 2021. Sex differences in the elevated plus-maze test and large open field test in adult Wistar rats. *Pharmacology Biochemistry and Behavior,* 204**,** 173168.

KOMARNYTSKY, S., ESPOSITO, D., POULEV, A. & RASKIN, I. 2013a. Pregnane glycosides interfere with steroidogenic enzymes to down‐regulate corticosteroid production in human adrenocortical H295R cells. *Journal of cellular physiology,* 228**,** 1120-1126.

KOMARNYTSKY, S., ESPOSITO, D., RATHINASABAPATHY, T., POULEV, A. & RASKIN, I. 2013b. Effects of pregnane glycosides on food intake depend on stimulation of the melanocortin pathway and BDNF in an animal model. *Journal of agricultural and food chemistry,* 61**,** 1841-1849.

KOOB, G. F. & VOLKOW, N. D. 2010. Neurocircuitry of addiction. *Neuropsychopharmacology,* 35**,** 217-238.

KRAEUTER, A.-K., GUEST, P. C. & SARNYAI, Z. 2019a. The elevated plus maze test for measuring anxiety-like behavior in rodents. *Pre-clinical models.* Springer.

KRAEUTER, A.-K., GUEST, P. C. & SARNYAI, Z. 2019b. The Y-maze for assessment of spatial working and reference memory in mice. *Pre-clinical models.* Springer.

KRISHNADAS, R., COOPER, S.-A., NICOL, A., PIMLOTT, S., SONI, S., HOLLAND, A. J., MCARTHUR, L. & CAVANAGH, J. 2018. Brain-stem serotonin transporter availability in maternal uniparental disomy and deletion Prader–Willi syndrome. *The British Journal of Psychiatry,* 212**,** 57-58.

KUMMERFELD, D.-M., SKRYABIN, B. V., BROSIUS, J., VAKHRUSHEV, S. Y. & ROZHDESTVENSKY, T. S. 2022. Reference Genes across Nine Brain Areas of Wild Type and Prader-Willi Syndrome Mice: Assessing Differences in Igfbp7, Pcsk1, Nhlh2 and Nlgn3 Expression. *International journal of molecular sciences,* 23**,** 8729.

KUREBAYASHI, N., SATO, M., FUJISAWA, T., FUKUSHIMA, K. & TAMURA, M. 2013. Regulation of neuropeptide Y Y1 receptor expression by bone morphogenetic protein 2 in C2C12 myoblasts. *Biochemical and Biophysical Research Communications,* 439**,** 506-510.

KURIYAN, R., RAJ, T., SRINIVAS, S., VAZ, M., RAJENDRAN, R. & KURPAD, A. V. 2007. Effect of Caralluma fimbriata extract on appetite, food intake and anthropometry in adult Indian men and women. *Appetite,* 48**,** 338-344.

KWON, J., REEVE, E., MANN, D., SWINBURN, B. & SACKS, G. 2022. Benchmarking for accountability on obesity prevention: evaluation of the Healthy Food Environment Policy Index (Food-EPI) in Australia (2016–2020). *Public health nutrition,* 25**,** 488-497.

LA FLEUR, S. E. & SERLIE, M. J. 2014. The interaction between nutrition and the brain and its consequences for body weight gain and metabolism; studies in rodents and men. *Best practice & research Clinical endocrinology & metabolism,* 28**,** 649-659.

LAFERRERE, B., SWERDLOW, N., BAWA, B., ARIAS, S., BOSE, M., OLIVAN, B., TEIXEIRA, J., MCGINTY, J. & ROTHER, K. I. 2010. Rise of oxyntomodulin in response to oral glucose

after gastric bypass surgery in patients with type 2 diabetes. *The Journal of Clinical Endocrinology & Metabolism,* 95**,** 4072-4076.

LALL, S., TUNG, L. Y., OHLSSON, C., JANSSON, J.-O. & DICKSON, S. L. 2001. Growth hormone (GH)-independent stimulation of adiposity by GH secretagogues. *Biochemical and biophysical research communications,* 280**,** 132-138.

LAM, D. D., PRZYDZIAL, M. J., RIDLEY, S. H., YEO, G. S., ROCHFORD, J. J., O'RAHILLY, S. & HEISLER, L. K. 2008. Serotonin 5-HT2C receptor agonist promotes hypophagia via downstream activation of melanocortin 4 receptors. *Endocrinology,* 149**,** 1323-1328.

LAMA, A., PIROZZI, C., SEVERI, I., MORGESE, M. G., SENZACQUA, M., ANNUNZIATA, C., COMELLA, F., DEL PIANO, F., SCHIAVONE, S. & PETROSINO, S. 2022a. Palmitoylethanolamide dampens neuroinflammation and anxiety-like behavior in obese mice. *Brain, Behavior, and Immunity,* 102**,** 110-123.

LAMA, A., PIROZZI, C., SEVERI, I., MORGESE, M. G., SENZACQUA, M., ANNUNZIATA, C., COMELLA, F., DEL PIANO, F., SCHIAVONE, S. & PETROSINO, S. 2022b. Palmitoylethanolamide dampens neuroinflammation and anxiety-like behavior in obese mice. *Brain, Behavior, and Immunity*.

LANG, P., HASSELWANDER, S., LI, H. & XIA, N. 2019. Effects of different diets used in diet-induced obesity models on insulin resistance and vascular dysfunction in C57BL/6 mice. *Scientific reports,* 9**,** 1-14.

LANTZ, K. A., HART, S. G. E., PLANEY, S. L., ROITMAN, M. F., RUIZ‐WHITE, I. A., WOLFE, H. R. & MCLANE, M. P. 2010. Inhibition of PTP1B by trodusquemine (MSI‐1436) causes fat‐specific weight loss in diet‐induced obese mice. *Obesity,* 18**,** 1516-1523.

LAROSE, M., BOUCHARD, C. & CHAGNON, Y. 2001. A new gene related to human obesity identified by suppression subtractive hybridization. *International journal of obesity,* 25**,** 770-776.

LAW, C. W., CHEN, Y., SHI, W. & SMYTH, G. K. 2014. voom: Precision weights unlock linear model analysis tools for RNA-seq read counts. *Genome biology,* 15**,** 1-17.

LAWSON, E. A., OLSZEWSKI, P. K., WELLER, A. & BLEVINS, J. E. 2020. The role of oxytocin in regulation of appetitive behaviour, body weight and glucose homeostasis. *Journal of neuroendocrinology,* 32**,** e12805.

LEE, J. H., REED, D. R., LI, W.-D., XU, W., JOO, E.-J., KILKER, R. L., NANTHAKUMAR, E., NORTH, M., SAKUL, H. & BELL, C. 1999. Genome scan for human obesity and linkage to markers in 20q13. *The American Journal of Human Genetics,* 64**,** 196-209.

LEE, K., JIN, H., CHEI, S., OH, H.-J., LEE, J.-Y. & LEE, B.-Y. 2020. Effect of dietary silk peptide on obesity, hyperglycemia, and skeletal muscle regeneration in high-fat diet-fed mice. *Cells,* 9**,** 377.

LEIGHTON, L. J., ZHAO, Q., MARSHALL, P. R., MADUGALLE, S. U., CHAN, A. H., MUSGROVE, M. R. B., REN, H., PERIYAKARUPPIAH, A., EDSON, J. & WEI, W. 2022. Orphan C/D box snoRNAs modulate fear-related memory processes in mice. *bioRxiv*.

LEVINE, L. R., ROSENBLATT, S. & BOSOMWORTH, J. 1987. Use of a serotonin re-uptake inhibitor, fluoxetine, in the treatment of obesity. *International journal of obesity,* 11**,** 185-190.

LI, H., BOAKYE, D., CHEN, X., JANSEN, L., CHANG-CLAUDE, J., HOFFMEISTER, M. & BRENNER, H. 2022. Associations of body mass index at different ages with early-onset colorectal cancer. *Gastroenterology,* 162**,** 1088-1097. e3.

LIAO, Y., SMYTH, G. K. & SHI, W. 2014. featureCounts: an efficient general purpose program for assigning sequence reads to genomic features. *Bioinformatics,* 30**,** 923-930.

LINDBERG, I. & FRICKER, L. D. 2021. Obesity, POMC, and POMC-processing enzymes: surprising results from animal models. *Endocrinology,* 162**,** bqab155.

LLORET LINARES, C., HAJJ, A., POITOU, C., SIMONEAU, G., CLEMENT, K., LAPLANCHE, J. L., LÉPINE, J.-P., BERGMANN, J. F., MOULY, S. & PEOC'H, K. 2011. Pilot study examining the frequency of several gene polymorphisms involved in morphine pharmacodynamics and pharmacokinetics in a morbidly obese population. *Obesity surgery,* 21**,** 1257-1264.

LÖFFLER, M. C., BETZ, M. J., BLONDIN, D. P., AUGUSTIN, R., SHARMA, A. K., TSENG, Y.-H., SCHEELE, C., ZIMDAHL, H., MARK, M. & HENNIGE, A. M. 2021. Challenges in tackling energy expenditure as obesity therapy: From preclinical models to clinical application. *Molecular Metabolism,* 51**,** 101237.

LOOS, R. J. & YEO, G. S. 2021. The genetics of obesity: From discovery to biology. *Nature Reviews Genetics***,** 1-14.

LUQUET, S., PEREZ, F. A., HNASKO, T. S. & PALMITER, R. D. 2005. NPY/AgRP neurons are essential for feeding in adult mice but can be ablated in neonates. *Science,* 310**,** 683-685.

LYNCH, M. 2012. From food to fuel: Perceptions of exercise and food in a community of food bloggers. *Health Education Journal,* 71**,** 72-79.

MACHT, M. 2008. How emotions affect eating: A five-way model. *Appetite,* 50**,** 1-11.

MALIK, S., MCGLONE, F., BEDROSSIAN, D. & DAGHER, A. 2008. Ghrelin modulates brain activity in areas that control appetitive behavior. *Cell metabolism,* 7**,** 400-409.

MANOCHA, M. & KHAN, W. I. 2012. Serotonin and GI disorders: an update on clinical and experimental studies. *Clinical and translational gastroenterology,* 3**,** e13.

MARENNE, G., HENDRICKS, A. E., PERDIKARI, A., BOUNDS, R., PAYNE, F., KEOGH, J. M., LELLIOTT, C. J., HENNING, E., PATHAN, S. & ASHFORD, S. 2020. Exome sequencing identifies genes and gene sets contributing to severe childhood obesity, linking PHIP variants to repressed POMC transcription. *Cell metabolism,* 31**,** 1107-1119. e12.

MARIN, P., BECAMEL, C., CHAUMONT-DUBEL, S., VANDERMOERE, F., BOCKAERT, J. & CLAEYSEN, S. 2020. Classification and signaling characteristics of 5-HT receptors: toward the concept of 5-HT receptosomes. *Handbook of Behavioral Neuroscience.* Elsevier.

MARTI, A. & MARTINEZ, J. 2004. Obesity studies in candidate genes. *Medicina clinica,* 122**,** 542-551.

MARTIN, C., RAMOND, F., FARRINGTON, D., AGUIAR JR, A., CHEVARIN, C., BERTHIAU, A., CAUSSANEL, S., LANFUMEY, L., HERRICK-DAVIS, K. & HAMON, M. 2013a. RNA splicing and editing modulation of 5-HT 2C receptor function: relevance to anxiety and aggression in VGV mice. *Molecular psychiatry,* 18**,** 656.

MARTIN, C. B., HAMON, M., LANFUMEY, L. & MONGEAU, R. 2014. Controversies on the role of 5-HT2C receptors in the mechanisms of action of antidepressant drugs. *Neuroscience & Biobehavioral Reviews,* 42**,** 208-223.

MARTIN, C. B. P., RAMOND, F., FARRINGTON, D. T., AGUIAR, A. S., CHEVARIN, C., BERTHIAU, A. S., CAUSSANEL, S., LANFUMEY, L., HERRICK-DAVIS, K., HAMON, M., MADJAR, J. J. & MONGEAU, R. 2013b. RNA splicing and editing modulation of 5-HT2C receptor function: relevance to anxiety and aggression in VGV mice. *Molecular Psychiatry,* 18**,** 656-665.

MARTÍNEZ-MARTÍNEZ, E., SOUZA-NETO, F. V., JIMÉNEZ-GONZÁLEZ, S. & CACHOFEIRO, V. 2021. Oxidative stress and vascular damage in the context of obesity: The hidden guest. *Antioxidants,* 10**,** 406.

MATHAI, M. L. 2021. Has the bloom gone out of lorcaserin following the CAMELLIA-TIMI61 trial? : Taylor & Francis.

MAVANJI, V., POMONIS, B. & KOTZ, C. M. 2021. Orexin, serotonin, and energy balance. *WIREs Mechanisms of Disease***,** e1536.

MAVANJI, V., POMONIS, B. & KOTZ, C. M. 2022. Orexin, serotonin, and energy balance. *WIREs Mechanisms of Disease,* 14**,** e1536.

MCANINCH, E. A. & BIANCO, A. C. 2014. Thyroid hormone signaling in energy homeostasis and energy metabolism. *Annals of the New York Academy of Sciences,* 1311**,** 77-87.

MCCORMACK, S. E., BLEVINS, J. E. & LAWSON, E. A. 2020. Metabolic effects of oxytocin. *Endocrine reviews,* 41**,** 121-145.

MCEWEN, B. S. 2022. Structural plasticity of the adult brain: how animal models help us understand brain changes in depression and systemic disorders related to depression. *Dialogues in clinical neuroscience*.

MCLEAN, F. H., GRANT, C., MORRIS, A. C., HORGAN, G. W., POLANSKI, A. J., ALLAN, K., CAMPBELL, F. M., LANGSTON, R. F. & WILLIAMS, L. M. 2018. Rapid and reversible impairment of episodic memory by a high-fat diet in mice. *Scientific reports,* 8**,** 1-9.

MECHANICK, J. I., FARKOUH, M. E., NEWMAN, J. D. & GARVEY, W. T. 2020. Cardiometabolic-based chronic disease, adiposity and dysglycemia drivers: JACC state-of-the-art review. *Journal of the American College of Cardiology,* 75**,** 525-538.

MEES, B., WAGNER, S., NINCI, E., TRIBULOVA, S., MARTIN, S., VAN HAPEREN, R., KOSTIN, S., HEIL, M., DE CROM, R. & SCHAPER, W. 2007. Endothelial nitric oxide synthase activity is essential for vasodilation during blood flow recovery but not for arteriogenesis. *Arteriosclerosis, thrombosis, and vascular biology,* 27**,** 1926-1933.

MELLO, A. D. A. F. D., MELLO, M. F. D., CARPENTER, L. L. & PRICE, L. H. 2003. Update on stress and depression: the role of the hypothalamic-pituitary-adrenal (HPA) axis. *Brazilian Journal of Psychiatry,* 25**,** 231-238.

MEMON, R. A., TECOTT, L. H., NONOGAKI, K., BEIGNEUX, A., MOSER, A. H., GRUNFELD, C. & FEINGOLD, K. R. 2000. Up-regulation of peroxisome proliferator-activated receptors (PPAR-α) and PPAR-γ messenger ribonucleic acid expression in the liver in murine obesity: troglitazone induces expression of PPAR-γ-responsive adipose tissue-specific genes in the liver of obese diabetic mice. *Endocrinology,* 141**,** 4021-4031.

MENG, Y., GROTH, S. W., HODGKINSON, C. A. & MARIANI, T. J. 2021. Serotonin system genes contribute to the susceptibility to obesity in Black adolescents. *Obesity science & practice,* 7**,** 441-449.

MERCER, J. G., HOGGARD, N., WILLIAMS, L. M., LAWRENCE, C. B., HANNAH, L. T. & TRAYHURN, P. 1996. Localization of leptin receptor mRNA and the long form splice variant (Ob-Rb) in mouse hypothalamus and adjacent brain regions by in situ hybridization. *FEBS letters,* 387**,** 113-116.

MILLER, K. J. 2005. Serotonin 5-ht2c receptor agonists: potential for the treatment of obesity. *Molecular interventions,* 5**,** 282.

MILLER, S., MOLINO, J. A., KENNEDY, J. F., EMO, A. K. & DO, A. 2008. Segway rider behavior: speed and clearance distance in passing sidewalk objects. *Transportation Research Record,* 2073**,** 125-132.

MISRA, A. & VERMA, S. 2013. An Overview of pharmacotherapy of obesity: AN Update. *International Journal of Pharmaceutical Sciences and Research,* 4**,** 881.

MIYAMOTO, J., WATANABE, K., TAIRA, S., KASUBUCHI, M., LI, X., IRIE, J., ITOH, H. & KIMURA, I. 2018. Barley β-glucan improves metabolic condition via short-chain fatty acids produced by gut microbial fermentation in high fat diet fed mice. *PLoS One,* 13**,** e0196579.

MONCHAUX DE OLIVEIRA, C., POURTAU, L., VANCASSEL, S., POUCHIEU, C., CAPURON, L., GAUDOUT, D. & CASTANON, N. 2021. Saffron extract-induced improvement of depressive-like behavior in mice is associated with modulation of monoaminergic neurotransmission. *Nutrients,* 13**,** 904.

MONIAN, P., SHIVALILA, C., LU, G., SHIMIZU, M., BOULAY, D., BUSSOW, K., BYRNE, M., BEZIGIAN, A., CHATTERJEE, A. & CHEW, D. 2022. Endogenous ADAR-mediated RNA editing in non-human primates using stereopure chemically modified oligonucleotides. *Nature Biotechnology***,** 1-10.

MONTÉGUT, L., LOPEZ-OTIN, C., MAGNAN, C. & KROEMER, G. 2021a. Old Paradoxes and New Opportunities for Appetite Control in Obesity. *Trends in Endocrinology & Metabolism*.

MONTÉGUT, L., LOPEZ-OTIN, C., MAGNAN, C. & KROEMER, G. 2021b. Old paradoxes and new opportunities for appetite control in obesity. *Trends in Endocrinology & Metabolism,* 32**,** 264-294.

MORABITO, M. V., ABBAS, A. I., HOOD, J. L., KESTERSON, R. A., JACOBS, M. M., KUMP, D. S., HACHEY, D. L., ROTH, B. L. & EMESON, R. B. 2010. Mice with altered serotonin 2C receptor RNA editing display characteristics of Prader–Willi syndrome. *Neurobiology of disease,* 39**,** 169-180.

MORLEY, J. E. 1987. Neuropeptide regulation of appetite and weight. *Endocrine reviews,* 8**,** 256-287.

MOULIN, T. C., COVILL, L. E., ITSKOV, P. M., WILLIAMS, M. J. & SCHIÖTH, H. B. 2021. Rodent and fly models in behavioral neuroscience: an evaluation of methodological advances, comparative research, and future perspectives. *Neuroscience & Biobehavioral Reviews,* 120**,** 1-12.

MOURA-ASSIS, A., FRIEDMAN, J. M. & VELLOSO, L. A. 2021. Gut-to-brain signals in feeding control. *American Journal of Physiology-Endocrinology and Metabolism,* 320**,** E326-E332.

MOY, S. S., NADLER, J. J., YOUNG, N. B., PEREZ, A., HOLLOWAY, L. P., BARBARO, R. P., BARBARO, J. R., WILSON, L. M., THREADGILL, D. W., LAUDER, J. M., MAGNUSON, T. R. & CRAWLEY, J. N. 2007. Mouse behavioral tasks relevant to autism: phenotypes of 10 inbred strains. *Behav Brain Res,* 176**,** 4-20.

MUST, A., SPADANO, J., COAKLEY, E. H., FIELD, A. E., COLDITZ, G. & DIETZ, W. H. 1999. The disease burden associated with overweight and obesity. *Jama,* 282**,** 1523-1529.

NAKAMURA, Y. & NAKAMURA, K. 2018. Central regulation of brown adipose tissue thermogenesis and energy homeostasis dependent on food availability. *Pflügers Archiv-European Journal of Physiology,* 470**,** 823-837.

NEEDHAM, B. D., FUNABASHI, M., ADAME, M. D., WANG, Z., BOKTOR, J. C., HANEY, J., WU, W.-L., RABUT, C., LADINSKY, M. S. & HWANG, S.-J. 2022. A gut-derived metabolite alters brain activity and anxiety behaviour in mice. *Nature***,** 1-7.

NEMES, A., HOMOKI, J. R., KISS, R., HEGEDŰS, C., KOVÁCS, D., PEITL, B., GÁL, F., STÜNDL, L., SZILVÁSSY, Z. & REMENYIK, J. 2019. Effect of anthocyanin-rich tart cherry extract on

inflammatory mediators and adipokines involved in type 2 diabetes in a high fat diet induced obesity mouse model. *Nutrients,* 11**,** 1966.

NESELILER, S., HAN, J.-E. & DAGHER, A. 2017. The use of functional magnetic resonance imaging in the study of appetite and obesity. *Appetite and Food Intake: Central Control***,** 117-134.

NIES, V. J., STRUIK, D., WOLFS, M., RENSEN, S., SZALOWSKA, E., UNMEHOPA, U., FLUITER, K., VAN DER MEER, T., HAJMOUSA, G. & BUURMAN, W. A. 2018. TUB gene expression in hypothalamus and adipose tissue and its association with obesity in humans. *International Journal of Obesity,* 42**,** 376-383.

NIETO‐MARTÍNEZ, R., GONZÁLEZ‐RIVAS, J. P. & MECHANICK, J. I. 2021. Cardiometabolic risk: New chronic care models. *Journal of Parenteral and Enteral Nutrition,* 45**,** S85-S92.

NOGUEIRAS, R., VEYRAT-DUREBEX, C., SUCHANEK, P. M., KLEIN, M., TSCHOP, J., CALDWELL, C., WOODS, S. C., WITTMANN, G., WATANABE, M. & LIPOSITS, Z. 2008. Peripheral, but Not Central, CB1 Antagonism Provides Food Intake–Independent Metabolic Benefits in Diet-Induced Obese Rats. *Diabetes,* 57**,** 2977-2991.

NONOGAKI, K. 1999. Obesity: autonomic circuits versus feeding. *Nature medicine,* 5**,** 742-743.

NONOGAKI, K. 2012. Serotonin Conflict in Sleep–Feeding. *Vitamins & Hormones,* 89**,** 223-239.

NONOGAKI, K. 2022. The Regulatory Role of the Central and Peripheral Serotonin Network on Feeding Signals in Metabolic Diseases. *International journal of molecular sciences,* 23**,** 1600.

NONOGAKI, K., OHBA, Y., SUMII, M. & OKA, Y. 2008. Serotonin systems upregulate the expression of hypothalamic NUCB2 via 5-HT2C receptors and induce anorexia via a leptin-independent pathway in mice. *Biochemical and biophysical research communications,* 372**,** 186-190.

NONOGAKI, K., STRACK, A. M., DALLMAN, M. F. & TECOTT, L. H. 1998. Leptin-independent hyperphagia and type 2 diabetes in mice with a mutated serotonin 5-HT2C receptor gene. *Nature medicine,* 4**,** 1152-1156.

NORDSBORG, N. B., ESPINOSA, H. G. & THIEL, D. V. 2014. Estimating Energy Expenditure During Front Crawl Swimming Using Accelerometers. *Procedia Engineering,* 72**,** 132-137.

NOVOSELOVA, T. V., HUSSAIN, M., KING, P. J., GUASTI, L., METHERELL, L. A., CHARALAMBOUS, M., CLARK, A. J. & CHAN, L. F. 2018. MRAP deficiency impairs adrenal progenitor cell differentiation and gland zonation. *The FASEB Journal,* 32**,** 6186-6196.

OLLMANN, M. M., WILSON, B. D., YANG, Y.-K., KERNS, J. A., CHEN, Y., GANTZ, I. & BARSH, G. S. 1997. Antagonism of central melanocortin receptors in vitro and in vivo by agouti-related protein. *Science,* 278**,** 135-138.

ONG-PÅLSSON, E., NJAVRO, J. R., WILSON, Y., PIGONI, M., SCHMIDT, A., MÜLLER, S. A., MEYER, M., HARTMANN, J., BUSCHE, M. A. & GUNNERSEN, J. M. 2022. The β-Secretase Substrate Seizure 6–Like Protein (SEZ6L) Controls Motor Functions in Mice. *Molecular neurobiology,* 59**,** 1183-1198.

ORGANIZATION, W. H. 2020. Overweight and obesity.

OSHLACK, A., ROBINSON, M. D. & YOUNG, M. D. 2010. From RNA-seq reads to differential expression results. *Genome biology,* 11**,** 1-10.

OSMAN, J. L. & SOBAL, J. 2006. Chocolate cravings in American and Spanish individuals: Biological and cultural influences. *Appetite,* 47**,** 290-301.

PALACIOS, J. M., PAZOS, A. & HOYER, D. 2017. A short history of the 5-HT 2C receptor: from the choroid plexus to depression, obesity and addiction treatment. *Psychopharmacology,* 234**,** 1395-1418.

PANAGIOTOU, M., MEIJER, J. H. & DEBOER, T. 2018. Chronic high‐caloric diet modifies sleep homeostasis in mice. *European Journal of Neuroscience,* 47**,** 1339-1352.

PARANDE, F., DAVE, A., PARK, E.-J., MCALLISTER, C. & PEZZUTO, J. M. 2022. Effect of Dietary Grapes on Female C57BL6/J Mice Consuming a High-Fat Diet: Behavioral and Genetic Changes. *Antioxidants,* 11**,** 414.

PARE, D., HILOU, A., N'DO, J. Y.-P., SOMBIE, N. E., GUENNE, S. & OUEDRAOGO, N. 2019. Caralluma dalzielii Ethanolic Extract Prevents High-fat-diet-induced Obesity in Mice.

PARK, B. S., KANG, D., KIM, K. K., JEONG, B., LEE, T. H., PARK, J. W., KIMURA, S., YEH, J.-Y., ROH, G. S. & LEE, C.-J. 2022. Hypothalamic TTF-1 orchestrates the sensitivity of leptin. *Molecular Metabolism***,** 101636.

PARK, H. S., KIM, Y. & LEE, C. 2005. Single nucleotide variants in the β2-adrenergic and β3-adrenergic receptor genes explained 18.3% of adolescent obesity variation. *Journal of human genetics,* 50**,** 365-369.

PATEL, H., KERNDT, C. C. & BHARDWAJ, A. 2018. Physiology, respiratory quotient.

PATEL, V., JOHARAPURKAR, A., KSHIRSAGAR, S., PATEL, M., SAVSANI, H., BAHEKAR, R. & JAIN, M. 2020. Combination of Lorcaserin and GLP-1/glucagon Coagonist Improves Metabolic Dysfunction in Diet Induced-Obese Mice. *Drug Research,* 70**,** 376-384.

PAVLOVSKA, I., POLCROVA, A., MECHANICK, J. I., BROŽ, J., INFANTE-GARCIA, M. M., NIETO-MARTÍNEZ, R., MARANHAO NETO, G. A., KUNZOVA, S., SKLADANA, M. & NOVOTNY, J. S. 2021. Dysglycemia and abnormal adiposity drivers of cardiometabolic-based chronic disease in the Czech population: biological, behavioral, and cultural/social determinants of health. *Nutrients,* 13**,** 2338.

PEARCE, L. R., ATANASSOVA, N., BANTON, M. C., BOTTOMLEY, B., VAN DER KLAAUW, A. A., REVELLI, J.-P., HENDRICKS, A., KEOGH, J. M., HENNING, E. & DOREE, D. 2013. KSR2 mutations are associated with obesity, insulin resistance, and impaired cellular fuel oxidation. *Cell,* 155**,** 765-777.

PÉREZ-MACEIRA, J. J., OTERO-RODIÑO, C., MANCEBO, M. J., SOENGAS, J. L. & ALDEGUNDE, M. 2016. Food intake inhibition in rainbow trout induced by activation of serotonin 5-HT2C receptors is associated with increases in POMC, CART and CRF mRNA abundance in hypothalamus. *Journal of Comparative Physiology B,* 186**,** 313-321.

PERREAULT, L. 2018. Obesity in adults: drug therapy. *Waltham: UpToDate*.

PÉRUSSE, L. & BOUCHARD, C. 2000. Gene-diet interactions in obesity. *The American journal of clinical nutrition,* 72**,** 1285s-1290s.

PETRIDOU, A., SIOPI, A. & MOUGIOS, V. 2019. Exercise in the management of obesity. *Metabolism,* 92**,** 163-169.

PETRILLI, C. M., JONES, S. A., YANG, J., RAJAGOPALAN, H., O'DONNELL, L., CHERNYAK, Y., TOBIN, K. A., CERFOLIO, R. J., FRANCOIS, F. & HORWITZ, L. I. 2020. Factors associated with hospital admission and critical illness among 5279 people with coronavirus disease 2019 in New York City: prospective cohort study. *bmj,* 369.

PHILLIPS, B. U., DEWAN, S., NILSSON, S. R., ROBBINS, T. W., HEATH, C. J., SAKSIDA, L. M., BUSSEY, T. J. & ALSIÖ, J. 2018. Selective effects of 5-HT2C receptor modulation on performance of a novel valence-probe visual discrimination task and probabilistic reversal learning in mice. *Psychopharmacology,* 235**,** 2101-2111.

POGORELOV, V. M., RODRIGUIZ, R. M., CHENG, J., HUANG, M., SCHMERBERG, C. M., MELTZER, H. Y., ROTH, B. L., KOZIKOWSKI, A. P. & WETSEL, W. C. 2017. 5-HT 2C agonists modulate schizophrenia-like behaviors in mice. *Neuropsychopharmacology,* 42**,** 2163.

POLLACK, A. 2010. Panel urges denial of diet drug. *New York Times*.

PONDUGULA, S. R., MAJRASHI, M., ALMAGHRABI, M., RAMESH, S., ABBOTT, K. L., GOVINDARAJULU, M., GILL, K., FAHOURY, E., NARAYANAN, N. & DESAI, D. 2021. Oroxylum Indicum ameliorates chemotherapy induced cognitive impairment. *Plos one,* 16**,** e0252522.

POWELL, T. M. & KHERA, A. 2010. Therapeutic approaches to obesity. *Current Treatment Options in Cardiovascular Medicine,* 12**,** 381-395.

POWELL-WILEY, T. M., POIRIER, P., BURKE, L. E., DESPRÉS, J.-P., GORDON-LARSEN, P., LAVIE, C. J., LEAR, S. A., NDUMELE, C. E., NEELAND, I. J. & SANDERS, P. 2021. Obesity and cardiovascular disease: a scientific statement from the American Heart Association. *Circulation,* 143**,** e984-e1010.

PRICE, A. E., ANASTASIO, N. C., STUTZ, S. J., HOMMEL, J. D. & CUNNINGHAM, K. A. 2018. Serotonin 5-HT2C receptor activation suppresses binge intake and the reinforcing and motivational properties of high-fat food. *Frontiers in Pharmacology,* 9**,** 821.

PRICE, R. A., LI, W.-D. & KILKER, R. 2002. An X-chromosome scan reveals a locus for fat distribution in chromosome region Xp21–22. *Diabetes,* 51**,** 1989-1991.

PURKAYASTHA, S., ZHANG, G. & CAI, D. 2011. Uncoupling the mechanisms of obesity and hypertension by targeting hypothalamic IKK-β and NF-κB. *Nature medicine,* 17**,** 883-887.

QARADAKHI, T., GADANEC, L. K., TACEY, A. B., HARE, D. L., BUXTON, B. F., APOSTOLOPOULOS, V., LEVINGER, I. & ZULLI, A. 2019. The effect of recombinant undercarboxylated osteocalcin on endothelial dysfunction. *Calcified tissue international,* 105**,** 546-556.

QUARTA, C., CLARET, M., ZELTSER, L. M., WILLIAMS, K. W., YEO, G. S., TSCHÖP, M. H., DIANO, S., BRÜNING, J. C. & COTA, D. 2021. POMC neuronal heterogeneity in energy balance and beyond: an integrated view. *Nature metabolism,* 3**,** 299-308.

QUATELA, A., CALLISTER, R., PATTERSON, A. & MACDONALD-WICKS, L. 2016. The energy content and composition of meals consumed after an overnight fast and their effects on diet induced thermogenesis: a systematic review, meta-analyses and meta-regressions. *Nutrients,* 8**,** 670.

RAMOS-MOLINA, B., MARTIN, M. G. & LINDBERG, I. 2016. PCSK1 variants and human obesity. *Progress in molecular biology and translational science,* 140**,** 47-74.

RAMOS-MOLINA, B., MOLINA-VEGA, M., FERNÁNDEZ-GARCÍA, J. & CREEMERS, J. 2018. Hyperphagia and Obesity in Prader–Willi Syndrome: PCSK1 Deficiency and Beyond? *Genes,* 9**,** 288.

RAO, A., BRISKEY, D., DOS REIS, C. & MALLARD, A. R. 2021. The effect of an orally-dosed Caralluma Fimbriata extract on appetite control and body composition in overweight adults. *Scientific Reports,* 11**,** 1-9.

RASK-ANDERSEN, M., ALMÉN, M. S., OLAUSEN, H. R., OLSZEWSKI, P. K., ERIKSSON, J., CHAVAN, R. A., LEVINE, A. S., FREDRIKSSON, R. & SCHIÖTH, H. B. 2011. Functional coupling analysis suggests link between the obesity gene FTO and the BDNF-NTRK2 signaling pathway. *BMC neuroscience,* 12**,** 1-9.

RATNER, C., HE, Z., GRUNDDAL, K. V., SKOV, L. J., HARTMANN, B., ZHANG, F., FEUCHTINGER, A., BJERREGAARD, A., CHRISTOFFERSEN, C. & TSCHÖP, M. H. 2019. Long-acting

neurotensin synergizes with liraglutide to reverse obesity through a melanocortin-dependent pathway. *Diabetes,* 68**,** 1329-1340.

RATNER, C., SKOV, L. J., RAIDA, Z., BÄCHLER, T., BELLMANN-SICKERT, K., LE FOLL, C., SIVERTSEN, B., DALBØGE, L. S., HARTMANN, B. & BECK-SICKINGER, A. G. 2016. Effects of peripheral neurotensin on appetite regulation and its role in gastric bypass surgery. *Endocrinology,* 157**,** 3482-3492.

REBAI, R., JASMIN, L. & BOUDAH, A. 2021. Agomelatine effects on fat-enriched diet induced neuroinflammation and depression-like behavior in rats. *Biomedicine & Pharmacotherapy,* 135**,** 111246.

RELKOVIC, D. & ISLES, A. R. 2013. Behavioural and cognitive profiles of mouse models for Prader-Willi syndrome. *Brain Res Bull,* 92**,** 41-8.

REN, D., ZHOU, Y., MORRIS, D., LI, M., LI, Z. & RUI, L. 2007. Neuronal SH2B1 is essential for controlling energy and glucose homeostasis. *The Journal of clinical investigation,* 117**,** 397-406.

REN, J., WU, N. N., WANG, S., SOWERS, J. R. & ZHANG, Y. 2021. Obesity cardiomyopathy: evidence, mechanisms, and therapeutic implications. *Physiological reviews,* 101**,** 1745-1807.

REYNOLDS, G. P., ZHANG, Z. & ZHANG, X. 2003. Polymorphism of the promoter region of the serotonin 5-HT2C receptor gene and clozapine-induced weight gain. *American Journal of Psychiatry,* 160**,** 677-679.

RÍOS-HOYO, A. & GUTIÉRREZ-SALMEÁN, G. 2016. New dietary supplements for obesity: What we currently know. *Current obesity reports,* 5**,** 262-270.

RODRIGUEZ, J. A. & ZIGMAN, J. M. 2018. Hypothalamic loss of Snord116 and Prader-Willi syndrome hyperphagia: the buck stops here? *The Journal of clinical investigation,* 128**,** 900-902.

ROSS, R. & BRADSHAW, A. J. 2009. The future of obesity reduction: beyond weight loss. *Nature Reviews Endocrinology,* 5**,** 319-325.

ROUAULT, A. A., SRINIVASAN, D. K., YIN, T. C., LEE, A. A. & SEBAG, J. A. 2017. Melanocortin receptor accessory proteins (MRAPs): functions in the melanocortin system and beyond. *Biochimica et Biophysica Acta (BBA)-Molecular Basis of Disease,* 1863**,** 2462-2467.

RUIZ-VILLALBA, A., VAN PELT-VERKUIL, E., GUNST, Q. D., RUIJTER, J. M. & VAN DEN HOFF, M. J. 2017. Amplification of nonspecific products in quantitative polymerase chain reactions (qPCR). *Biomolecular detection and quantification,* 14**,** 7-18.

RYAN, D. H. 2000. Use of sibutramine and other noradrenergic and serotonergic drugs in the management of obesity. *Endocrine,* 13**,** 193-199.

SAINSBURY, A., ROHNER-JEANRENAUD, F., CUSIN, I., ZAKRZEWSKA, K., HALBAN, P. A., GAILLARD, R. & JEANRENAUD, B. 1997. Chronic central neuropeptide Y infusion in normal rats: status of the hypothalamo-pituitary-adrenal axis, and vagal mediation of hyperinsulinaemia. *Diabetologia,* 40**,** 1269-1277.

SAKORE, S., PATIL, S. & SURANA, S. 2012. Hypolipidemic activity of Caralluma adscendens on triton and methimazole induced hyperlipidemic rats. *Pharmtechmedica,* 1**,** 49-52.

SAMPEY, B. P., VANHOOSE, A. M., WINFIELD, H. M., FREEMERMAN, A. J., MUEHLBAUER, M. J., FUEGER, P. T., NEWGARD, C. B. & MAKOWSKI, L. 2011. Cafeteria diet is a robust model of human metabolic syndrome with liver and adipose inflammation: comparison to high‐fat diet. *Obesity,* 19**,** 1109-1117.

SARGENT, P., SHARPLEY, A., WILLIAMS, C., GOODALL, E. & COWEN, P. 1997. 5-HT2C receptor activation decreases appetite and body weight in obese subjects. *Psychopharmacology,* 133**,** 309-312.

SARMA, S., SOCKALINGAM, S. & DASH, S. 2021. Obesity as a multisystem disease: Trends in obesity rates and obesity‐related complications. *Diabetes, Obesity and Metabolism,* 23**,** 3-16.

SATTAR, N. & VALABHJI, J. 2021. Obesity as a Risk Factor for Severe COVID-19: Summary of the Best Evidence and Implications for Health Care. *Current Obesity Reports***,** 1-8.

SCHACHTER, J., MARTEL, J., LIN, C.-S., CHANG, C.-J., WU, T.-R., LU, C.-C., KO, Y.-F., LAI, H.-C., OJCIUS, D. M. & YOUNG, J. D. 2018. Effects of obesity on depression: a role for inflammation and the gut microbiota. *Brain, Behavior, and Immunity,* 69**,** 1-8.

SCHELLEKENS, H., DE FRANCESCO, P. N., KANDIL, D., THEEUWES, W. F., MCCARTHY, T., VAN OEFFELEN, W. E., PERELLÓ, M., GIBLIN, L., DINAN, T. G. & CRYAN, J. F. 2015. Ghrelin's orexigenic effect is modulated via a serotonin 2C receptor interaction. *ACS chemical neuroscience,* 6**,** 1186-1197.

SEKAR, R., WANG, L. & CHOW, B. K. C. 2017. Central control of feeding behavior by the secretin, PACAP, and glucagon family of peptides. *Frontiers in endocrinology,* 8**,** 18.

SHARF, R., SARHAN, M. & DILEONE, R. J. 2010. Role of orexin/hypocretin in dependence and addiction. *Brain research,* 1314**,** 130-138.

SHI, Y. & BURN, P. 2004. Lipid metabolic enzymes: emerging drug targets for the treatment of obesity. *Nature reviews Drug discovery,* 3**,** 695-710.

SHI, Y. & CHENG, D. 2009. Beyond triglyceride synthesis: the dynamic functional roles of MGAT and DGAT enzymes in energy metabolism. *American Journal of Physiology-Endocrinology and Metabolism,* 297**,** E10-E18.

SHI, Y.-C., LAU, J., LIN, Z., ZHANG, H., ZHAI, L., SPERK, G., HEILBRONN, R., MIETZSCH, M., WEGER, S. & HUANG, X.-F. 2013. Arcuate NPY controls sympathetic output and BAT function via a relay of tyrosine hydroxylase neurons in the PVN. *Cell metabolism,* 17**,** 236-248.

SHI, Y.-C., LIN, S., WONG, I. P., BALDOCK, P. A., ALJANOVA, A., ENRIQUEZ, R. F., CASTILLO, L., MITCHELL, N. F., YE, J.-M. & ZHANG, L. 2010. NPY neuron-specific Y2 receptors regulate adipose tissue and trabecular bone but not cortical bone homeostasis in mice. *PloS one,* 5**,** e11361.

SHI, Z., PELLETIER, N. E., WONG, J., LI, B., SDRULLA, A. D., MADDEN, C. J., MARKS, D. L. & BROOKS, V. L. 2020. Leptin increases sympathetic nerve activity via induction of its own receptor in the paraventricular nucleus. *Elife,* 9.

SHIMOGORI, T., LEE, D. A., MIRANDA-ANGULO, A., YANG, Y., WANG, H., JIANG, L., YOSHIDA, A. C., KATAOKA, A., MASHIKO, H. & AVETISYAN, M. 2010. A genomic atlas of mouse hypothalamic development. *Nature neuroscience,* 13**,** 767-775.

SHIPLEY, M. M., MANGOLD, C. A., KUNY, C. V. & SZPARA, M. L. 2017. Differentiated human SH-SY5Y cells provide a reductionist model of herpes simplex virus 1 neurotropism. *Journal of virology,* 91**,** e00958-17.

SHIPLEY, M. M., MANGOLD, C. A. & SZPARA, M. L. 2016. Differentiation of the SH-SY5Y human neuroblastoma cell line. *JoVE (Journal of Visualized Experiments)***,** e53193.

SHUTTER, J. R., GRAHAM, M., KINSEY, A. C., SCULLY, S., LÜTHY, R. & STARK, K. L. 1997. Hypothalamic expression of ART, a novel gene related to agouti, is up-regulated in obese and diabetic mutant mice. *Genes & development,* 11**,** 593-602.

SIGURGEIRSSON, B., EMANUELSSON, O. & LUNDEBERG, J. 2014. Sequencing degraded RNA addressed by 3'tag counting. *PloS one,* 9**,** e91851.

SILVENTOINEN, K., JELENKOVIC, A., SUND, R., HUR, Y.-M., YOKOYAMA, Y., HONDA, C., HJELMBORG, J. V., MÖLLER, S., OOKI, S. & AALTONEN, S. 2016. Genetic and environmental effects on body mass index from infancy to the onset of adulthood: an individual-based pooled analysis of 45 twin cohorts participating in the COllaborative project of Development of Anthropometrical measures in Twins (CODATwins) study. *The American journal of clinical nutrition,* 104**,** 371-379.

SIMÕES, A. E., PEREIRA, D. M., AMARAL, J. D., NUNES, A. F., GOMES, S. E., RODRIGUES, P. M., LO, A. C., D'HOOGE, R., STEER, C. J. & THIBODEAU, S. N. 2013. Efficient recovery of proteins from multiple source samples after trizol® or trizol® LS RNA extraction and long-term storage. *BMC genomics,* 14**,** 181.

SINGH, A. K. & SINGH, R. 2020. Efficacy and safety of lorcaserin in obesity: a systematic review and meta-analysis of randomized controlled trials. *Expert review of clinical pharmacology,* 13**,** 183-190.

SINGH, M. 2014. Mood, food, and obesity. *Frontiers in psychology,* 5**,** 925.

SMITH, H. C., GOTT, J. M. & HANSON, M. R. 1997. A guide to RNA editing. *Rna,* 3**,** 1105.

SOLOMON, O., OREN, S., SAFRAN, M., DESHET-UNGER, N., AKIVA, P., JACOB-HIRSCH, J., CESARKAS, K., KABESA, R., AMARIGLIO, N. & UNGER, R. 2013. Global regulation of alternative splicing by adenosine deaminase acting on RNA (ADAR). *Rna,* 19**,** 591-604.

SOUNDARARAJAN, K., RAMASWAMY, R., RAMASAMY V, V. & PAUL, C. 2011. Effect of Caralluma fimbriata extract on 3T3-L1 pre-adipocyte cell division. *Food and Nutrition Sciences,* 2011.

SPANSWICK, D., SMITH, M., GROPPI, V., LOGAN, S. & ASHFORD, M. 1997. Leptin inhibits hypothalamic neurons by activation of ATP-sensitive potassium channels. *Nature,* 390**,** 521-525.

SPEAKMAN, J. R. 2013. Measuring energy metabolism in the mouse–theoretical, practical, and analytical considerations. *Frontiers in physiology,* 4**,** 34.

STAM, N. J., VANDERHEYDEN, P., VAN ALEBEEK, C., KLOMP, J., DE BOER, T., VAN DELFT, A. M. & OLIJVE, W. 1994. Genomic organisation and functional expression of the gene encoding the human serotonin 5-HT2C receptor. *European Journal of Pharmacology: Molecular Pharmacology,* 269**,** 339-348.

STAMM, S., GRUBER, S. B., RABCHEVSKY, A. G. & EMESON, R. B. 2017. The activity of the serotonin receptor 2C is regulated by alternative splicing. *Human genetics,* 136**,** 1079-1091.

STASI, C., BELLINI, M., BASSOTTI, G., BLANDIZZI, C. & MILANI, S. 2014. Serotonin receptors and their role in the pathophysiology and therapy of irritable bowel syndrome. *Techniques in coloproctology,* 18**,** 613-621.

STIJNEN, P., RAMOS-MOLINA, B., O'RAHILLY, S. & CREEMERS, J. W. 2016. PCSK1 mutations and human endocrinopathies: from obesity to gastrointestinal disorders. *Endocrine reviews,* 37**,** 347-371.

STOCK, S., GRANSTRÖM, L., BACKMAN, L., MATTHIESEN, A. & UVNÄS-MOBERG, K. 1989. Elevated plasma levels of oxytocin in obese subjects before and after gastric banding. *International journal of obesity,* 13**,** 213-222.

STRASSER, B., GOSTNER, J. M. & FUCHS, D. 2016. Mood, food, and cognition: role of tryptophan and serotonin. *Current Opinion in Clinical Nutrition & Metabolic Care,* 19**,** 55-61.

SULTAN, M., AMSTISLAVSKIY, V., RISCH, T., SCHUETTE, M., DÖKEL, S., RALSER, M., BALZEREIT, D., LEHRACH, H. & YASPO, M.-L. 2014. Influence of RNA extraction methods and library selection schemes on RNA-seq data. *BMC genomics,* 15**,** 675.

SUN, J. 2020. Supplementary Materials Supplementary Methods B cell Transcriptome Analysis Cells. 79**,** 1-7.

SUN, X., HAN, F., LU, Q., LI, X., REN, D., ZHANG, J., HAN, Y., XIANG, Y. K. & LI, J. 2020. Empagliflozin ameliorates obesity-related cardiac dysfunction by regulating Sestrin2-mediated AMPK-mTOR signaling and redox homeostasis in high-fat diet–induced obese mice. *Diabetes,* 69**,** 1292-1305.

SUTTON, A. K. & KRASHES, M. J. 2020. Integrating hunger with rival motivations. *Trends in Endocrinology & Metabolism,* 31**,** 495-507.

SUZUKI, K., SIMPSON, K. A., MINNION, J. S., SHILLITO, J. C. & BLOOM, S. R. 2010. The role of gut hormones and the hypothalamus in appetite regulation. *Endocrine journal,* 57**,** 359-372.

TABARÉS SEISDEDOS, R. 2017. Health effects of overweight and obesity in 195 countries over 25 years. *New England Journal of Medicine, 2017, vol. 377, num. 1, p. 13-27*.

TACK, J., CAMILLERI, M., CHANG, L., CHEY, W. D., GALLIGAN, J., LACY, B., MÜLLER‐LISSNER, S., QUIGLEY, E. M., SCHUURKES, J. & DE MAEYER, J. 2012. Systematic review: cardiovascular safety profile of 5‐HT 4 agonists developed for gastrointestinal disorders. *Alimentary pharmacology & therapeutics,* 35**,** 745-767.

TAICHER, G. Z., TINSLEY, F. C., REIDERMAN, A. & HEIMAN, M. L. 2003. Quantitative magnetic resonance (QMR) method for bone and whole-body-composition analysis. *Analytical and bioanalytical chemistry,* 377**,** 990-1002.

TAKAO, K., KOBAYASHI, K., HAGIHARA, H., OHIRA, K., SHOJI, H., HATTORI, S., KOSHIMIZU, H., UMEMORI, J., TOYAMA, K. & NAKAMURA, H. K. 2013. Deficiency of schnurri-2, an MHC enhancer binding protein, induces mild chronic inflammation in the brain and confers molecular, neuronal, and behavioral phenotypes related to schizophrenia. *Neuropsychopharmacology,* 38**,** 1409-1425.

TAMURA, Y., HAYASHI, K., OMORI, N., NISHIURA, Y., WATANABE, K., TANAKA, N., FUJIOKA, M., KOUYAMA, N., YUKIMASA, A. & TANAKA, Y. 2013. Identification of a novel benzimidazole derivative as a highly potent NPY Y5 receptor antagonist with an anti-obesity profile. *Bioorganic & medicinal chemistry letters,* 23**,** 90-95.

TAMURA, Y., OMORI, N., KOUYAMA, N., NISHIURA, Y., HAYASHI, K., WATANABE, K., TANAKA, Y., CHIBA, T., YUKIOKA, H. & SATO, H. 2012. Design, synthesis and identification of novel benzimidazole derivatives as highly potent NPY Y5 receptor antagonists with attractive in vitro ADME profiles. *Bioorganic & medicinal chemistry letters,* 22**,** 5498-5502.

TCHANG, B. G., ABEL, B., ZECCA, C., SAUNDERS, K. H. & SHUKLA, A. P. 2020. An up-to-date evaluation of lorcaserin hydrochloride for the treatment of obesity. *Expert Opinion on Pharmacotherapy,* 21**,** 21-28.

TECOTT, L. H., SUN, L. M., AKANA, S. F., STRACK, A. M., LOWENSTEIN, D. H., DALLMAN, M. F. & JULIUS, D. 1995. Eating disorder and epilepsy in mice lacking 5-HT2c serotonin receptors. *Nature,* 374**,** 542-546.

TESKE, J. A., LEVINE, A. S., KUSKOWSKI, M., LEVINE, J. A. & KOTZ, C. M. 2006. Elevated hypothalamic orexin signaling, sensitivity to orexin A, and spontaneous physical activity in obesity-resistant rats. *American Journal of Physiology-Regulatory, Integrative and Comparative Physiology,* 291**,** R889-R899.

THEILADE, S., CHRISTENSEN, M. B., VILSBØLL, T. & KNOP, F. K. 2021. An overview of obesity mechanisms in humans: Endocrine regulation of food intake, eating behaviour and common determinants of body weight. *Diabetes, Obesity and Metabolism,* 23**,** 17-35.

TIDMAN, M. M., WHITE, D. & WHITE, T. 2022. Effects of an low carbohydrate/healthy fat/ketogenic diet on biomarkers of health and symptoms, anxiety and depression in Parkinson's disease: a pilot study. *Neurodegenerative Disease Management*.

TIERNEY, A. 2001. Structure and function of invertebrate 5-HT receptors: a review. *Comparative Biochemistry and Physiology Part A: Molecular & Integrative Physiology,* 128**,** 791-804.

TOLETE, P., KNUPP, K., KARLOVICH, M., DECARLO, E., BLUVSTEIN, J., CONWAY, E., FRIEDMAN, D., DUGAN, P. & DEVINSKY, O. 2018. Lorcaserin therapy for severe epilepsy of childhood onset: A case series. *Neurology,* 91**,** 837-839.

TRAN, L. T., PARK, S., KIM, S. K., LEE, J. S., KIM, K. W. & KWON, O. 2022a. Hypothalamic control of energy expenditure and thermogenesis. *Experimental & Molecular Medicine,* 54**,** 358-369.

TRAN, L. T., PARK, S., KIM, S. K., LEE, J. S., KIM, K. W. & KWON, O. 2022b. Hypothalamic control of energy expenditure and thermogenesis. *Experimental & Molecular Medicine***,** 1-12.

TRAN, P. V., TAMURA, Y., PHAM, C. V., ELHUSSINY, M. Z., HAN, G., CHOWDHURY, V. S. & FURUSE, M. 2021. Neuropeptide Y modifies a part of diencephalic catecholamine but not indolamine metabolism in chicks depending on feeding status. *Neuropeptides,* 89**,** 102169.

TSENG, Y.-H., CYPESS, A. M. & KAHN, C. R. 2010. Cellular bioenergetics as a target for obesity therapy. *Nature reviews Drug discovery,* 9**,** 465-482.

TSYGANOV, K., JAMES PERRY, A., KENNETH ARCHER, S. & POWELL, D. 2018. RNAsik: A Pipeline for complete and reproducible RNA-seq analysis that runs anywhere with speed and ease. *Journal of Open Source Software,* 3**,** 583.

UGWAH-OGUEJIOFOR, C. J., OKOLI, C. O., UGWAH, M. O., UMARU, M. L., OGBULIE, C. S., MSHELIA, H. E., UMAR, M. & NJAN, A. A. 2019. Acute and sub-acute toxicity of aqueous extract of aerial parts of Caralluma dalzielii NE Brown in mice and rats. *Heliyon,* 5**,** e01179.

VAISSE, C., CLEMENT, K., DURAND, E., HERCBERG, S., GUY-GRAND, B. & FROGUEL, P. 2000. Melanocortin-4 receptor mutations are a frequent and heterogeneous cause of morbid obesity. *The Journal of clinical investigation,* 106**,** 253-262.

VALENCIA-TORRES, L., OLARTE-SÁNCHEZ, C. M., LYONS, D. J., GEORGESCU, T., GREENWALD-YARNELL, M., MYERS JR, M. G., BRADSHAW, C. M. & HEISLER, L. K. 2017. Activation of Ventral Tegmental Area 5-HT 2C Receptors Reduces Incentive Motivation. *Neuropsychopharmacology,* 42**,** 1511.

VALENTINO, M. A. 2012. *An intestinal prouroguanylin-hypothalamic GUCY2C axis mediates nutrient-induced satiety*, Thomas Jefferson University.

VALSAMAKIS, G., KONSTANTAKOU, P. & MASTORAKOS, G. 2017. New targets for drug treatment of obesity. *Annual Review of Pharmacology and Toxicology,* 57**,** 585-605.

VAN GALEN, K. A., TER HORST, K. W. & SERLIE, M. J. 2021. Serotonin, food intake, and obesity. *Obesity Reviews,* 22**,** e13210.

VARELA, L. & HORVATH, T. L. 2012. Leptin and insulin pathways in POMC and AgRP neurons that modulate energy balance and glucose homeostasis. *EMBO reports,* 13**,** 1079-1086.

VASDEKI, D., KOUFAKIS, T., TSAMOS, G., BUSETTO, L., ZEBEKAKIS, P. & KOTSA, K. 2022. Remission as an Emerging Therapeutic Target in Type 2 Diabetes in the Era of New Glucose-Lowering Agents: Benefits, Challenges, and Treatment Approaches. *Nutrients,* 14**,** 4801.

VERMAAK, I., HAMMAN, J. H. & VILJOEN, A. M. 2011. Hoodia gordonii: an up-to-date review of a commercially important anti-obesity plant. *Planta medica,* 77**,** 1149-1160.

VITALONE, A., DI SOTTO, A., MAMMOLA, C. L., HEYN, R., MIGLIETTA, S., MARIANI, P., SCIUBBA, F., PASSARELLI, F., NATIVIO, P. & MAZZANTI, G. 2017. Phytochemical analysis and effects on ingestive behaviour of a Caralluma fimbriata extract. *Food and Chemical Toxicology,* 108**,** 63-73.

VLAARDINGERBROEK, H., VAN DEN AKKER, E. & HOKKEN-KOELEGA, A. 2021. Appetite-and weight-inducing and-inhibiting neuroendocrine factors in Prader–Willi syndrome, Bardet–Biedl syndrome and craniopharyngioma versus anorexia nervosa. *Endocrine connections,* 10**,** R175-R188.

VOHRA, M. S., BENCHOULA, K., SERPELL, C. J. & HWA, W. E. 2021. AgRP/NPY and POMC neurons in the arcuate nucleus and their potential role in treatment of obesity. *European journal of pharmacology***,** 174611.

WAGNER, S., BRIERLEY, D. I., LEESON-PAYNE, A., JIANG, W., CHIANESE, R., LAM, B. Y., DOWSETT, G., CRISTIANO, C., LYONS, D. & REIMANN, F. 2022. Obesity medication lorcaserin requires brainstem GLP-1 neurons to reduce food intake in mice. *bioRxiv*.

WALLACE, C. W. & FORDAHL, S. C. 2021. Obesity and dietary fat influence dopamine neurotransmission: Exploring the convergence of metabolic state, physiological stress, and inflammation on dopaminergic control of food intake. *Nutrition research reviews***,** 1-16.

WAN, X. Q., ZENG, F., HUANG, X. F., YANG, H. Q., WANG, L., SHI, Y. C., ZHANG, Z. H. & LIN, S. 2020. Risperidone stimulates food intake and induces body weight gain via the hypothalamic arcuate nucleus 5‐HT2c receptor–NPY pathway. *CNS neuroscience & therapeutics,* 26**,** 558-566.

WANG, C.-Y. & LIAO, J. K. 2012. A mouse model of diet-induced obesity and insulin resistance. *mTOR.* Springer.

WANG, R., WANG, Y., MU, N., LOU, X., LI, W., CHEN, Y., FAN, D. & TAN, H. 2017. Activation of NLRP3 inflammasomes contributes to hyperhomocysteinemia-aggravated inflammation and atherosclerosis in apoE-deficient mice. *Laboratory Investigation,* 97**,** 922-934.

WANG, S., TIAN, M., YANG, R., JING, Y., CHEN, W., WANG, J., ZHENG, X. & WANG, F. 2018. 6-Gingerol ameliorates behavioral changes and atherosclerotic lesions in ApoE−/− mice exposed to chronic mild stress. *Cardiovascular Toxicology,* 18**,** 420-430.

WANG, Z., KHOR, S. & CAI, D. 2020. Regulation of muscle and metabolic physiology by hypothalamic erythropoietin independently of its peripheral action. *Molecular Metabolism,* 32**,** 56-68.

WANHAINEN, A., VERZINI, F., VAN HERZEELE, I., ALLAIRE, E., BOWN, M., COHNERT, T., DICK, F., VAN HERWAARDEN, J., KARKOS, C. & KOELEMAY, M. 2019. Editor's choice–European Society for Vascular Surgery (ESVS) 2019 clinical practice guidelines on the management of abdominal aorto-iliac artery aneurysms. *European Journal of Vascular and Endovascular Surgery,* 57**,** 8-93.

WEBSTER, E., CHO, M. T., ALEXANDER, N., DESAI, S., NAIDU, S., BEKHEIRNIA, M. R., LEWIS, A., RETTERER, K., JUUSOLA, J. & CHUNG, W. K. 2016. De novo PHIP-predicted deleterious

variants are associated with developmental delay, intellectual disability, obesity, and dysmorphic features. *Molecular Case Studies,* 2**,** a001172.

WEI, Y., XIAO, L., FAN, W., ZOU, J., YANG, H., LIU, B., YE, Y., WEN, D. & LIAO, L. 2022. Astrocyte Activation, but not Microglia, Is Associated with the Experimental Mouse Model of Schizophrenia Induced by Chronic Ketamine. *Journal of Molecular Neuroscience,* 72**,** 1902-1915.

WEINSIER, R., NELSON, K., HENSRUD, D., DARNELL, B., HUNTER, G. & SCHUTZ, Y. 1995. Metabolic predictors of obesity. Contribution of resting energy expenditure, thermic effect of food, and fuel utilization to four-year weight gain of post-obese and never-obese women. *The Journal of clinical investigation,* 95**,** 980-985.

WHO 2020. Overweight and obesity.

WREN, A. & BLOOM, S. 2007. Gut hormones and appetite control. *Gastroenterology,* 132**,** 2116-2130.

WU, H., LV, W., PAN, Q., KALAVAGUNTA, P. K., LIU, Q., QIN, G., CAI, M., ZHOU, L., WANG, T. & XIA, Z. 2019. Simvastatin therapy in adolescent mice attenuates HFD-induced depression-like behavior by reducing hippocampal neuroinflammation. *Journal of Affective Disorders,* 243**,** 83-95.

WU, H., WANG, R., QIN, X., LIU, D., WANG, W., XU, J., JIANG, H. & PAN, F. 2021. Effects of chronic stress on depressive-like behaviors and JMJD3 expression in the prefrontal cortex and hippocampus of C57BL/6 and ob/ob mice. *Journal of Psychiatric Research,* 133**,** 142-155.

XIAO, F. & GUO, F. 2021. Impacts of essential amino acids on energy balance. *Molecular metabolism***,** 101393.

XIE, C., HUA, W., ZHAO, Y., RUI, J., FENG, J., CHEN, Y., LIU, Y., LIU, J., YANG, X. & XU, X. 2020. The ADRB3 rs4994 polymorphism increases risk of childhood and adolescent overweight/obesity for East Asia's population: an evidence-based meta-analysis. *Adipocyte,* 9**,** 77-86.

XIE, K. Y., CHIEN, S. J., TAN, B. C. M. & CHEN, Y. W. 2021. RNA editing of 5‐HT2CR impairs insulin secretion of pancreatic beta cells via altered store‐operated calcium entry. *The FASEB Journal,* 35**,** e21929.

XU, Y., JONES, J. E., LAUZON, D. A., ANDERSON, J. G., BALTHASAR, N., HEISLER, L. K., ZINN, A. R., LOWELL, B. B. & ELMQUIST, J. K. 2010. A serotonin and melanocortin circuit mediates D-fenfluramine anorexia. *Journal of Neuroscience,* 30**,** 14630-14634.

YAN, L. & LI, J. 2022. The central nervous system control of energy homeostasis: high fat diet induced hypothalamic microinflammation and obesity. *Brain Research Bulletin*.

YAO, F. & MACKENZIE, R. G. 2010. Obesity drug update: The lost decade? *Pharmaceuticals,* 3**,** 3494-3521.

YAZDI, F. T., CLEE, S. M. & MEYRE, D. 2015. Obesity genetics in mouse and human: back and forth, and back again. *PeerJ,* 3**,** e856.

YOON, G., CHO, K. A., SONG, J. & KIM, Y.-K. 2019. Transcriptomic analysis of high fat diet fed mouse brain cortex. *Frontiers in genetics,* 10**,** 83.

YOSHIZAKI, K., ASAI, M. & HARA, T. 2020. High-fat diet enhances working memory in the Y-maze test in male C57BL/6J mice with less anxiety in the elevated plus maze test. *Nutrients,* 12**,** 2036.

YU, B., BATTAGLIA, D. M., FOSTER, T. P. & NICHOLS, C. D. 2021. Serotonin 5-HT2A receptor activity mediates adipocyte differentiation through control of adipogenic gene expression. *Scientific Reports,* 11**,** 19714.

YUAN, J., ZHANG, R., WU, R., GU, Y. & LU, Y. 2020. The effects of oxytocin to rectify metabolic dysfunction in obese mice are associated with increased thermogenesis. *Molecular and Cellular Endocrinology,* 514**,** 110903.

YUAN, M., PICKERING, R. T., SINGER, M. & MOORE, L. 2019. Dietary Saturated Fat Is Associated with Larger LDL Particle Size and Reduced CVD Risk in Framingham Offspring Study (P08-128-19). *Current Developments in Nutrition,* 3**,** nzz044. P08-128-19.

YUN, K. U., RYU, C. S., OH, J. M., KIM, C. H., LEE, K. S., LEE, C.-H., LEE, H.-S., KIM, B.-H. & KIM, S. K. 2013. Plasma homocysteine level and hepatic sulfur amino acid metabolism in mice fed a high-fat diet. *European journal of nutrition,* 52**,** 127-134.

ZEENI, N., DAGHER-HAMALIAN, C., DIMASSI, H. & FAOUR, W. H. 2015. Cafeteria diet-fed mice is a pertinent model of obesity-induced organ damage: a potential role of inflammation. *Inflammation Research,* 64**,** 501-512.

ZHANG, F., LAVAN, B. & GREGOIRE, F. M. 2004. Peroxisome proliferator-activated receptors as attractive antiobesity targets. *Drug News & Perspectives,* 17**,** 661-669.

ZHANG, G., WU, X., ZHANG, Y.-M., LIU, H., JIANG, Q., PANG, G., TAO, X., DONG, L. & STACKMAN JR, R. W. 2016a. Activation of serotonin 5-HT2C receptor suppresses behavioral sensitization and naloxone-precipitated withdrawal symptoms in morphine-dependent mice. *Neuropharmacology,* 101**,** 246-254.

ZHANG, H., WU, C., CHEN, Q., CHEN, X., XU, Z., WU, J. & CAI, D. 2013. Treatment of obesity and diabetes using oxytocin or analogs in patients and mouse models. *PloS one,* 8**,** e61477.

ZHANG, S., TAKANO, J., MURAYAMA, N., TOMINAGA, M., ABE, T., PARK, I., SEOL, J., ISHIHARA, A., TANAKA, Y. & YAJIMA, K. 2020. Subacute ingestion of caffeine and oolong tea increases fat oxidation without affecting energy expenditure and sleep architecture: A randomized, placebo-controlled, double-blinded cross-over trial. *Nutrients,* 12**,** 3671.

ZHANG, Z., SHEN, M., GRESCH, P. J., GHAMARI‐LANGROUDI, M., RABCHEVSKY, A. G., EMESON, R. B. & STAMM, S. 2016b. Oligonucleotide‐induced alternative splicing of serotonin 2C receptor reduces food intake. *EMBO molecular medicine,* 8**,** 878-894.

ZHENG, J., ZHANG, J., GUO, Y., CUI, H., LIN, A., HU, B., GAO, Q., CHEN, Y. & LIU, H. 2020. Improvement on metabolic syndrome in high fat diet-induced obese mice through modulation of gut microbiota by sangguayin decoction. *Journal of Ethnopharmacology,* 246**,** 112225.

ZHOU, J. & AUSTIN, R. C. 2009. Contributions of hyperhomocysteinemia to atherosclerosis: Causal relationship and potential mechanisms. *Biofactors,* 35**,** 120-129.

ZOU, T., WANG, B., LI, S., LIU, Y. & YOU, J. 2020. Dietary apple polyphenols promote fat browning in high‐fat diet‐induced obese mice through activation of adenosine monophosphate‐activated protein kinase α. *Journal of the Science of Food and Agriculture,* 100**,** 2389-2398.

ZULLI, A. & HARE, D. L. 2009. High dietary methionine plus cholesterol stimulates early atherosclerosis and late fibrous cap development which is associated with a decrease in GRP78 positive plaque cells. *International journal of experimental pathology,* 90**,** 311-320.

ZULLI, A., LAU, E., WIJAYA, B. P., JIN, X., SUTARGA, K., SCHWARTZ, G. D., LEARMONT, J., WOOKEY, P. J., ZINELLU, A. & CARRU, C. 2009. High dietary taurine reduces apoptosis and atherosclerosis in the left main coronary artery: association with reduced

CCAAT/enhancer binding protein homologous protein and total plasma homocysteine but not lipidemia. *Hypertension,* 53**,** 1017-1022.

ZULLI, A., WIDDOP, R. E., HARE, D. L., BUXTON, B. F. & BLACK, M. J. 2003. High methionine and cholesterol diet abolishes endothelial relaxation. *Arteriosclerosis, thrombosis, and vascular biology,* 23**,** 1358-1363.